



Structures ordonnées dans des écoulements géophysiques

Coralie Renault

► To cite this version:

| Coralie Renault. Structures ordonnées dans des écoulements géophysiques. Equations aux dérivées partielles [math.AP]. Université de Rennes, 2018. Français. NNT : 2018REN1S053 . tel-02044540

HAL Id: tel-02044540

<https://theses.hal.science/tel-02044540>

Submitted on 21 Feb 2019

HAL is a multi-disciplinary open access archive for the deposit and dissemination of scientific research documents, whether they are published or not. The documents may come from teaching and research institutions in France or abroad, or from public or private research centers.

L'archive ouverte pluridisciplinaire **HAL**, est destinée au dépôt et à la diffusion de documents scientifiques de niveau recherche, publiés ou non, émanant des établissements d'enseignement et de recherche français ou étrangers, des laboratoires publics ou privés.

THÈSE / UNIVERSITÉ DE RENNES 1

sous le sceau de l'Université Bretagne Loire

pour le grade de

DOCTEUR DE L'UNIVERSITÉ DE RENNES 1

Mention : Mathématiques et leurs interactions

Ecole doctorale MathSTIC

présentée par

Coralie Renault

Préparée à l'unité de recherche UMR 6625 du CNRS : IRMAR

Institut de Recherche de Mathématiques de Rennes

U.F.R. De Mathématiques

**Structures ordonnées
dans des
écoulements
géophysiques.**

**Thèse soutenue à Rennes
le 16/05/2018**

devant le jury composé de :

Angel CASTRO

Cientifica Titular, Univ. Madrid/ *rapporteur*

Didier BRESCH

Directeur de recherche, CNRS/ *rapporteur*

Valeria BANICA

Professeur, Univ. Pierre et Marie Curie/
examinateur

Dragos IFTIMIE

Professeur, Univ. Lyon 1 / *examinateur*

Thierry GALLAY

Professeur, Univ. Grenoble Alpes / *examinateur*

Christophe CHEVERRY

Professeur, Univ. Rennes 1/ *examinateur*

Mohammed LEMOU

Directeur de recherche, Univ. Rennes 1/
examinateur

Taoufik HMIDI

Maître de conférence, Univ. Rennes 1/ *directeur de thèse*

Structures ordonnées dans des écoulements géophysiques.

Coralie Renault

May 2, 2018

Contents

1	Introduction	7
1.1	Contexte	8
1.2	Présentation des résultats	17
1.2.1	Le théorème de Crandall-Rabinowitz	17
1.2.2	Existence de V-states doublement connexes pour les équations quasi-géostrophiques	19
1.2.3	Existence de petites boucles dans le diagramme de bifurcation près des valeurs propres dégénérées.	23
1.2.4	Existence de V-states pour les équations shallow water quasi-géostrophiques et étude des perturbations du diagramme de bifurcation.	26
2	Relative equilibria with holes for the surface quasi-geostrophic equations	33
2.1	Introduction	34
2.2	Boundary equations	37
2.3	Tools	38
2.3.1	Crandall-Rabinowitz's theorem	38
2.3.2	Function spaces	39
2.3.3	Hypergeometric functions	40
2.4	Regularity of the nonlinear functional	41
2.4.1	Existence	41
2.4.2	Regularity	47
2.5	Study of the linearized operator	54
2.5.1	Linearized operator	54
2.5.2	Monotonicity of the eigenvalues	61
2.5.3	Proof of Theorem 4.5.1	63
3	Existence of small loops in the bifurcation diagram near the degenerate eigenvalues	69
3.1	Introduction	70
3.2	Reminder and preliminaries	74
3.2.1	Hölder spaces	74
3.2.2	Boundary equations	74
3.2.3	Reduced bifurcation equation.	75
3.3	Taylor expansion	78
3.3.1	General formulae	78
3.3.2	Explicit formulae for the quadratic form	79
3.4	Proof of the main theorem	93
4	Imperfect bifurcation for the quasi-geostrophic shallow-water equations	99
4.1	Introduction	100
4.2	Numerical approach	101
4.3	Numerical results	105

4.3.1	2-fold vortex patch equilibria	105
4.3.2	3-fold vortex patch equilibria	106
4.4	Tools used for the mathematical analysis	111
4.4.1	Notation	111
4.4.2	Modified Bessel functions	112
4.4.3	Boundary equations	114
4.5	Bifurcation to m -fold symmetric vortex patch equilibria	115
4.5.1	Main result	115
4.5.2	Crandall-Rabinowitz's Theorem with a parameter	116
4.5.3	Function spaces I	118
4.5.4	Regularity of the functional I	119
4.5.5	Spectral study	120
4.6	Imperfect bifurcation close to the branch of Kirchhoff ellipses	125
4.6.1	Function spaces II	126
4.6.2	Summary of the bifurcations from Kirchhoff ellipses	126
4.6.3	Regularity of the functional II	127
4.6.4	Bifurcation diagram far from the resonant set	129
4.6.5	Breakdown of the bifurcation diagram close to the resonant set	133
4.7	Conclusions	148

Bibliography	149
---------------------	------------

Remerciements

En premier lieu, je tiens à remercier mon directeur de thèse, Taoufik Hmidi. Sa bienveillance, ses encouragements et sa patience n'ont jamais fait défaut au cours de ces trois dernières années. Le sujet qu'il m'a donné correspondait à mes attentes et j'ai appris énormément à ses côtés. Il a été à mon écoute tout au long de ma thèse et m'a soutenu pendant les périodes difficiles notamment celles impliquant quelques os cassés. Je pense que je n'aurais pas pu trouver un meilleur directeur.

J'adresse mes remerciements à Ángel Castro et Didier Bresch pour avoir accepté de rapporter ma thèse et pour l'intérêt qu'ils ont montré pour mon travail.

Je tiens à remercier Valeria Banica, Christophe Cheverry, Thierry Gallay, Dragos Iftimie et Mohammed Lemou d'avoir accepter de faire partie de mon jury et d'avoir fait le déplacement jusqu'à Rennes.

Je remercie David Dritschel pour avoir passé du temps sur les simulations numériques au cours de ma deuxième année de thèse.

Un grand merci à l'administration de l'UFR mathématiques et de l'IRMAR pour leur disponibilité et leur réactivité. Je pense notamment à Marie-Annick, Marie-Aude, Chantal, Florian et Carole qui ont été mes principaux interlocuteurs et qui m'ont souvent tenu par la main.

Je tiens à remercier les personnes qui m'ont fait découvrir le monde des EDP et de la recherche. Je n'oublierai jamais le cours de François Castella et le contrôle de ses solutions pour "éviter quelles nous explosent à la gueule". Ceux de Florian Méhats sont les plus propres et les plus rigoureux que j'ai pu suivre à l'université. Enfin, je remercie Benjamin Boutin pour m'avoir encadré pendant mon séminaire de M2 et m'avoir fait découvrir les solutions faibles de Riemann.

Au cours de cette thèse j'ai eu l'occasion d'enseigner avec des personnes formidables. Je pense notamment à Virginie et Anne qui m'ont entendu pester contre Xcas pendant deux ans. Je garderai malgré tout un bon souvenir de mes enseignements à l'IUT. Merci à Matthieu et Benjamin de m'avoir laissé l'occasion d'enseigner aux agrégés. Mes Tds du lundi matin resteront de bons souvenirs, j'ai beaucoup aimé échanger avec eux. Enfin, merci à Christophe Dupont pour son organisation pour le TD en L1 bio et sa patience devant mes réponses parfois tardives à ses mails.

Tout au long de mon cursus j'ai eu la chance d'être entourée d'enseignants extraordinaires. Je pense notamment à Philippe Dehais et Catherine Masclet, "ma mère", qui ont énormément influencé ma manière d'enseigner et qui ont eu une patience légendaire pour gérer notre formidable promo de S. Les voyages à Briançon et à Cley resteront de très bons souvenirs. Je me souviens de la réplique de mon professeur de physique de sup, David Lasne, qui m'aura appris "qu'enseigner c'est répéter", son mantra m'aura pas mal aidé durant mes enseignements auprès des L1 bio cette année :-). Merci à Myriam Verdure pour m'avoir fais découvrir la géométrie et pour m'avoir coaché, avec Michel, pour les oraux du magistère de Rennes. J'ai pu éviter quelques écueils grâce à eux. Bien évidemment, je voudrais aussi remercier Michel Schweitzer pour le soutien qu'il m'a apporté depuis que je l'ai eu en sup et le rôle de maître Jedi qu'il a pu jouer. Un de mes

meilleurs souvenirs de thèse restera la semaine que j'ai pu passer en prépa à Caen avec toi durant laquelle tu m'as convaincu d'aller jusqu'au bout.

Mes amis ont été d'un grand soutien pendant ma thèse. Je pense notamment à mes amis havrais : Michmich pour m'avoir ramené un nombre incalculable de fois en sortant du bar, Mélissa pour les goûters et les pintes au Macday's et Aymerick pour m'avoir vendu que la prépa c'est cool =). Merci aussi à Godzi pour m'avoir aidé avec mon placard! Durant ma prépa j'ai eu la chance de rencontrer deux piliers qui ont toujours répondu présents quand j'en avais besoin. Merci à Thomy et Diane pour les soirées au cool caf! Malheureusement nous n'aurons pas réussi à tester tous les restauraux de Rennes =(. Je n'oublie pas les heures passées dans les rues du Havre avec toi Oumi. La distance n'a pas été un frein à notre amitié et j'ai adoré les moments passés à Paris avec Erwan et Ryad. Mes amis Rennais ne sont pas en reste, je pense notamment aux soirées chez Flo, au concours de 5 fruits et légumes avec Blandine qui restera gravé dans ma mémoire et aux soirees Ti-punch avec Cricri et Paul à discuter d'Indochine et d'enseignement. Merci à Greg pour les pauses cafés qui m'ont parfois motivées à venir au bureau, j'étais contente de retrouver un autre boulet. Nos discussions sur la recherche, notre avenir et nos "bobos" sportifs me manqueront. Au passage, je tiens à remercier Servane pour avoir passer un an et demi à me remettre sur pied et pour ne pas avoir râlé devant ma mémoire défaillante ! JJ et Tristan vos remarques me manquent, une pensée pour Pied de biche et Cocyclique ! Merci à Adrien et Axel de m'avoir donner envie de faire du triathlon. Malgré les quelques plumes que j'y ai laissées ce fut une belle découverte! Et encore désolé Adrien pour le coup du canapé :-).

Durant ma thèse j'ai eu l'occasion de rencontrer de nombreux doctorants. Une pensée pour Tristan, Camille et Florian et le test de la salle de sport, les repas interminables avec Charles, Damien et Nestor au RU, les discussions enseignement avec Cyril, Ti et Valentin, les gâteaux de crêpes de Julie, la soirée dans le Poitou avec Arnaud et Ophélie, Aurélien et sa lampe frontale pour lire Grothendieck à 5h du matin, le soutien de Mac pour nos articles respectifs et les meringues de Thom-Thom.

Les quelques mois passés avec Salomé dans le bureau resteront des bons souvenirs. Je me rappelle notamment qu'elle avait parié que je ne tiendrais pas le 8H-17H pendant 3 ans....je pense qu'elle a gagné son pari !

Le reste de ma thèse fut marqué par ma cohabitation avec Marine. En tant que deux normandes fraîchement débarquées en terre bretonne à notre arrivée à l'ENS nous nous sommes tout de suite bien entendues. Je n'oublie pas les heures passées à la bu, le poussage du fauteuil roulant jusqu'au RU, la manière élégante que tu as de démonter les gens avec le sourire et qui a fait ta réputation ainsi que les concours de qui soufflera le plus dans le bureau! Ces dernières années m'ont permis de rencontrer une amie sur laquelle je peux compter en toutes circonstances et avec qui j'ai partagé de nombreux bons moments ! J'ai hâte de rencontrer votre mini-vous =) !

Une autre personne a joué un rôle particulier pendant mes années rennaises. Basile je te remercie de m'avoir épauler et encourager durant toutes ces années ! Je pense que tu mérites une médaille pour avoir supporter mon caractère de cochon ! Cette thèse te doit beaucoup (c'est quoi une fonction analytique ?) et je ne pense pas que j'aurai pu aller jusqu'au bout si tu n'avais pas été là ! Je te souhaite le meilleur à Orléans ! (Et un sub 5H au marathon vert ?)

Je souhaite remercier mes parents et Gillou pour m'avoir encouragé dans mes études et soutenu dans mes choix ! Un merci à Mami et Papi Campagne pour répondre présent au moindre soucis, je ne compte plus vos aller-retour sur Rennes pour venir m'aider ainsi qu'à Mami Renault pour les parties de Ramy voleurs et de Yams ! Je n'oublie pas les après-midi passées chez Michèle et Marco dans les framboisières ni celle chez Valé à vider ton stock de café caramel. Enfin, un énorme merci à mon frère et ma soeur pour leur présence ! Les après-midis Columbus et les soirées chez les parents avec Kévin étaient de véritables bols d'air !

Enfin, ma dernière année de thèse fut marquée par l'arrivée de Petit Ours dans ma vie, merci d'avoir illuminé ces derniers mois.

Chapter 1

Introduction

*Il n'est pas nécessaire d'aller vite,
le tout est de ne pas s'arrêter.*

CONFUCIUS

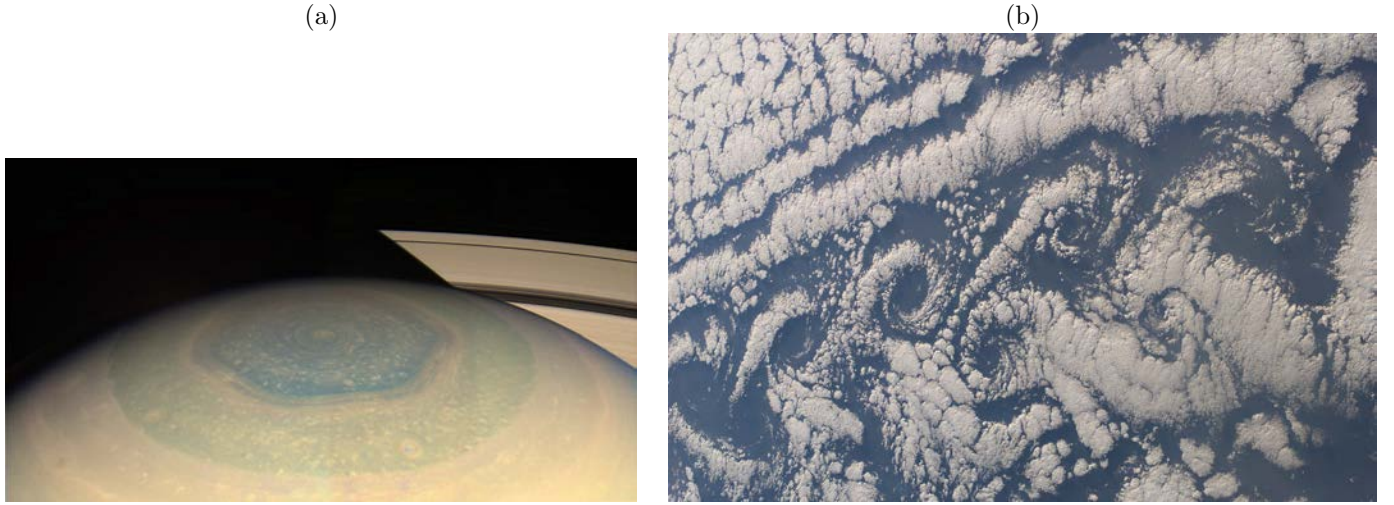


Figure 1.1: Hexagone de la planète Saturne (a) et ligne de tourbillon de Kàrmàn (b).

1.1 Contexte

Dans cette thèse, on s'est intéressé principalement à la dynamique des poches de tourbillon pour des équations issues de la mécanique des fluides posées dans le plan. Le point commun de toutes ces équations est que le tourbillon vérifie une équation de transport et qu'on retrouve la vitesse en convolant le tourbillon avec un noyau spécifique à chaque équation. Plus généralement, l'étude de la dynamique du tourbillon est un sujet ancien pour les équations d'Euler et est toujours en vogue. Les tourbillons se manifestent dans différents phénomènes géophysiques, par exemple avec l'hexagone sur la planète Saturne et les tourbillons de Von Kàrmàn (voir figure 1.1). De nombreuses études ont été menées que ce soit d'un point de vue théorique, numérique et expérimentale et le sujet est trop vaste pour que nous puissions faire une synthèse regroupant tous les résultats existants. Nous nous contenterons donc de ne citer que quelques résultats du domaine. Pour commencer, on rappelle les équations d'Euler qui permettent de décrire l'évolution d'un fluide parfait incompressible homogène et non visqueux dans l'espace tout entier \mathbb{R}^d .

$$\begin{cases} \partial_t v + v \cdot \nabla v + \nabla p = 0, & (t, x) \in \mathbb{R}_+ \times \mathbb{R}^d, \\ \operatorname{div}(v) = 0, \\ v|_{t=0} = v_0. \end{cases} \quad (1.1.1)$$

Dans ce cas, v désigne le champ des vitesses et le scalaire p désigne la pression en tout point du fluide. Physiquement, ces équations traduisent les conservations du moment et de la masse. Dans cette thèse où ne s'est intéressé qu'à des modèles posés dans le plan donc par la suite nous nous attacherons au cas où $d = 2$. On tient quand même à souligner que ce cas est particulier comparé au cas de la dimension trois. En effet, dans le plan, les normes L^p du tourbillon seront conservées ce qui permet de construire des solutions classiques globales en temps. Malheureusement, pour les dimensions supérieurs ce n'est plus le cas et l'existence de solutions globales reste une question ouverte dans le cas général. On sait cependant que le système est localement bien posé pour des données initiales régulières. On peut par exemple citer les travaux de Wolibner et de Kato qui le montrent pour des espaces de Hölder et de Sobolev. Pour ces solutions, la vitesse est nécessairement lipschitzienne. Nous verrons qu'en dimension deux on peut construire des solutions avec une vitesse moins régulière.

Nous allons maintenant nous concentrer sur la dynamique des tourbillons. Physiquement, le tourbillon va représenter la rotation locale de la particule. Le premier à s'y être intéressé est Helmholtz en 1858. Dans [32],

il étudie les tourbillons en dimensions deux et trois. Il montre en particulier que dans le plan, le tourbillon peut s'identifier à un scalaire $\omega = \partial_1 v_2 - \partial_2 v_1$ et que son évolution est régit par une équation de transport,

$$\frac{D\omega}{dt} = \partial_t \omega + v \cdot \nabla \omega = 0. \quad (1.1.2)$$

Cette équation est typique de la dimension deux, en effet, dans ce cas la vitesse est orthogonale en tout temps et en tout point au tourbillon. Ce n'est plus le cas en dimension trois et on obtient un terme en plus qui vient représenter l'étirement du tourbillon dans le fluide tridimensionnel. Ce terme ne permet pas d'obtenir les lois de conservations sur les normes L^p . Cependant, dans notre cas nous avons une infinité de lois de conservation données par

$$\forall p \in [1, +\infty], \|\omega(t)\|_{L^p} = \|\omega_0\|_{L^p}.$$

Ce sont ces lois de conservation qui nous permettent de construire des solutions à la Yudovich avec une vitesse sous la régularité lipschitzienne. L'équation (1.1.2) à elle seule n'est pas équivalente au système (1.1.1). Pour pouvoir retrouver la vitesse, il nous faut rajouter une équation que l'on obtient sous des hypothèses raisonnables de décroissance à l'infini qui nous permettent de retrouver la loi de Biot-Savart

$$v(t, x) = \nabla^\perp \Psi(t, x) = \frac{1}{2\pi} \int_{\mathbb{R}^2} \frac{(x-y)^\perp}{|x-y|^2} \omega(t, y) dy.$$

La fonction de courant Ψ est donnée par

$$\Psi(t, x) = \frac{1}{2\pi} \int_{\mathbb{R}^2} \log(|x-y|) \omega(t, y) dy.$$

On obtient sous ces hypothèses deux systèmes équivalents, dont le deuxième est

$$\begin{cases} \partial_t \omega + v \cdot \nabla \omega = 0, & (t, x) \in \mathbb{R}_+ \times \mathbb{R}^2, \\ v = -\nabla^\perp (-\Delta)^{-1} \omega, \\ \omega|_{t=0} = \omega_0 \end{cases} \quad (1.1.3)$$

Cette reformulation a permis à Yudovich de démontrer le théorème suivant [72].

Theorem 1.1.1. *Soit $\omega_0 \in L^2 \cap L^\infty$ alors le système (1.1.3) admet une unique solution faible globale $\omega \in L^\infty(\mathbb{R}^+; L^2 \cap L^\infty)$. De plus la vitesse v admet un flot ψ continue dans les deux variables et qui est l'unique solution de l'équation:*

$$\psi(t, x) = x + \int_0^t v(s, \psi(s, x)) ds.$$

Très récemment, un résultat similaire a été démontré dans [23] où la condition d'intégrabilité a été remplacée par une condition de symétrie. Le théorème de Yudovich nous permet aussi d'affirmer que le tourbillon est transporté par le flot c'est-à-dire que

$$\omega(t, x) = \omega_0(\psi_t^{-1}(x)).$$

On verra par la suite que si l'on prend comme donnée initiale une poche de tourbillon alors cette structure perdurera dans le temps. Nous allons d'abord aborder un cas limite des poches de tourbillon qui est les points-vortex. Helmholtz a introduit dans son papier la notion de lignes de tourbillons dans l'espace, c'est une ligne tangente en chaque point au vecteur tourbillon en ce point, et tubes de tourbillon, l'ensemble des lignes de tourbillon s'appuyant sur une courbe fermée infiniment petite. Si maintenant on considère des tubes de tourbillons de direction parallèle à l'axe des z et que l'on regarde la coupe dans un plan orthogonal à cet axe, on remarque que le mouvement des points obtenus est le même dans tous les plans. Ces points sont appelés points-vortex et c'est ce qui va nous intéresser pour le moment. Il explique un résultat bien connu maintenant qui affirme que si l'on considère deux points vortex de même intensités alors ils vont être en

rotation uniforme autour de leur centre de gravité et si leurs intensités sont de signes opposés alors ils vont être animés d'un mouvement de translation. Ces points-vortex se retrouvent dans la nature notamment dans les plasmas et les superfluides, on pourra consulter [3, 71, 22, 66, 25] pour quelques exemples ainsi que [52, 2, 1] pour plus de détails que ceux donnés par la suite. Plus précisément, si l'on considère un tourbillon constitué de N points vortex situés dans le plan et ayant comme position $X_i(t) = (x_i(t), y_i(t))$ alors

$$w_0(x) = \sum_{i=0}^N \Gamma_i \delta(x - X_i(0)),$$

avec Γ_i la circulation du i-ème vortex. On fait maintenant appel au théorème de la circulation de Kelvin qui nous dit que pour un fluide parfait incompressible n'étant soumis à aucune force extérieure, la circulation le long d'une courbe matériel fermée $C(t)$ qui se déplace avec le fluide est constante, voir par exemple [63]. Cela implique que le tourbillon à tout instant va rester concentré selon N points-vortex, autrement dit

$$\omega(t, x) = \sum_{i=0}^N \Gamma_i \delta(x - X_i(t)).$$

Quitte à négliger les effets induits, on peut montrer que l'évolution du i-ème point-vortex est régit par l'équation

$$\Gamma_i \frac{dX_i}{dt} = \nabla^\perp H(x_i, y_i)$$

avec

$$H(x_i, y_i) = -\frac{1}{4\pi} \sum_{i \neq j} \Gamma_i \Gamma_j \log(|X_i - X_j|).$$

On obtient donc un système hamiltonien. Pour savoir si celui est intégrable ou non, on peut s'intéresser aux quantités globalement conservées. On peut montrer que l'hamiltonien est une intégrale première du mouvement et qu'il représente l'énergie cinétique du mouvement du fluide entourant les vortex. De plus, comme l'hamiltonien est invariant par translation et rotation on peut montrer que les deux composantes de l'impulsion linéaire ainsi que l'impulsion angulaire vont être conservées. Ainsi si l'on considère un système à $N \leq 3$ points, celui-ci est intégrable. Ce problème est à rapprocher de celui de la mécanique céleste et notamment de celui des trois corps. Dans ce cas, le satellite de masse négligeable serait apparenté à un point-vortex d'intensité nulle et pour des raisons de dimensions, il faudrait considérer trois autres points-vortex (voir par exemple [12]). Ce domaine est assez riche et permet de faire le lien avec d'autres branches des mathématiques. Par exemple, des résultats ont été obtenus en faisant un lien avec des polynômes. Si l'on considère $N = N_1 + N_2$ vortex de même intensités en valeurs absolues avec N_1 positives et N_2 négatives, on peut introduire les polynômes

$$P(z) = (z - z_1)(z - z_2) \cdots (z - z_{N_1})$$

et

$$Q(z) = (z - z_1)(z - z_2) \cdots (z - z_{N_2}).$$

Au début, cette approche a été utilisée pour étudier les points-vortex qui étaient en équilibres relatifs, c'est-à-dire en mouvement de rotation ou translation uniforme ou qui restaient à l'équilibre. De nombreux résultats ont été prouvés, pour plus d'exemples que ceux donnés on pourra consulter [1] par exemple. On peut citer que N points-vortex identiques alignés sont en équilibres relatifs si et seulement si ils correspondent aux racines du N-ème polynôme de Hermite. Si l'on considère maintenant N vortex identiques situés sur un cercle avec un vortex au centre ou non alors ils sont en position d'équilibres relatifs si et seulement si ils sont situés sur les sommets du polygone régulier à N côtés.

Les points-vortex peuvent être vues comme les objets limites d'une autre structure, les tourbillons concentrés. Si la donnée initiale est de la forme

$$\omega_0(x) = \frac{1}{\varepsilon^2} \chi_{D_\varepsilon} \text{ avec } D_\varepsilon = \varepsilon D$$

avec D un domaine borné alors l'objet limite lorsque ε tend vers zéro est un point-vortex. Nous allons maintenant nous intéresser aux poches de tourbillon. On considère une donnée initiale qui est une poche de tourbillon, $\omega_0 = \chi_D$ avec D comme précédemment. Dans ce cas, on sait que la solution va garder en tout temps cette structure de poche. De plus, le domaine à l'instant t est le transporté du domaine D par le flot et la compréhension de notre solution dépend uniquement de la connaissance du bord du domaine à tout instant. Cependant, le flot n'est pas assez régulier pour s'assurer que la régularité du bord soit toujours transportée. Quelques résultats de persistance existent, par exemple dans [13], Chemin a montré que si l'on part d'un bord ayant une régularité höldérienne $C^{1+\varepsilon}$ avec $0 < \varepsilon < 1$ alors il n'y a pas formation de singularité en temps fini et la régularité est bien propagée. On peut aussi lier ces objets aux points-vortex. Par exemple, dans [36], ils partent de la connaissance du mouvements de deux points-vortex pour montrer que le résultat persiste pour deux poches de tourbillon et les points-vortex sont dans ce cas vues comme une limite de ces poches. On va maintenant s'intéresser à un type particulier de poches de tourbillon dont le mouvement est périodique en temps appelés V-states ou équilibres relatives en mouvement de rotation uniforme. On impose en plus la condition de rotation du domaine autour de l'origine à vitesse angulaire constante. Cela se traduit par $D_t = e^{i\Omega t}D$ avec Ω une constante réelle. De plus, on dira qu'une V-state est m-symétrique si son domaine est invariant par le groupe diédral d'ordre $2m$. Le principal avantage de ces solutions est qu'on connaît leurs dynamiques exactes à tout instant. Le pionnier du domaine est Kirchhoff qui a découvert qu'une ellipse de demi-axes a et b tourne uniformément à la vitesse $\Omega = \frac{ab}{a^2+b^2}$, voir [43]. Des résultats numériques sont venus compléter l'étude, Deem et Zabusky ont construit numériquement des V-states m-symétriques dans [17] pour $m \in \{3, 4, 5\}$. La première preuve analytique de l'existence des V-states est due à Burbea et s'appuie sur une technique perturbative. Pour résumer sa preuve en quelques mots, on commence par reformuler l'équation vérifiée par le bord de la V-state. Pour l'obtenir, on se place dans le référentiel de la poche qui tourne. On peut montrer que la vitesse d'un point du bord et celle de la particule de fluide qui occupe la même position ont les mêmes composantes normales ce qui se traduit par

$$(v(t, x) - \Omega x^\perp) \cdot n = 0, \forall x \in \partial D_t \quad (1.1.4)$$

avec n un vecteur normal unitaire sortant à la frontière. Une autre équation équivalente à (1.1.4) est obtenue en considérant plutôt la fonction de courant Ψ . Dans le référentiel en rotation, le bord est fixe donc c'est une ligne de niveau de la fonction de courant relative, autrement dit

$$\Psi(x) - \frac{1}{2}\Omega x^2 - \mu = 0, \forall x \in \partial D,$$

avec μ une constante. En utilisant la dynamique prescrite de la solution, on peut se ramener à une équation statique où nos inconnues sont le bord de D et la vitesse de rotation Ω . On commence par paramétriser le bord de D à l'aide de son application conforme Φ et on montre que l'équation que l'on doit résoudre se ramène à $G(\Omega, \Phi) = 0$ avec G une fonctionnelle non linéaire. On montre ensuite que le disque va être une poche tournante pour n'importe quelle vitesse, c'est-à-dire

$$G(\Omega, \text{Id}) = 0, \forall \Omega \in \mathbb{R}.$$

Enfin, on construit de nouvelles solutions en perturbant cet ensemble de solutions à l'aide d'un théorème de bifurcation. Ce théorème est appelé théorème de Crandall-Rabinowitz et sa démonstration sera présentée dans la section suivante. La preuve de Burbea a été reprise avec plus de détails dans [37]. Ils ont en même temps prouvé que les V-states étaient convexes et que le bord possédait une régularité C^∞ . On obtient donc avec ces résultats une famille de solutions faibles globales en temps dont la dynamique est explicite. On peut citer deux autres résultats en lien avec ceux-ci. Récemment, Córdoba et al ont exhibé, en utilisant une technique perturbative, des solutions fortes globales pour (1.1.3) dans [9]. Ces solutions sont des régularisations des V-states obtenues précédemment. Pour le deuxième résultat, on rappelle que Kirchhoff a montré que les solutions deux-symétriques sont des ellipses et qu'il obtient une formule explicite de ces solutions. Comme la technique employée par Burbea et revisitée dans [37] s'appuie sur le fait qu'on connaît une famille explicite de solutions triviales, Hmidi et Mateu ont donc pu perturber ces ellipses pour créer d'autres solutions dans [34].

Enfin, nous allons nous intéresser à un dernier objet qui est de nature topologique un peu différent, les V-states "avec un trou". Dans ce cas, $D = D_1 \setminus D_2$ avec D_1 et D_2 deux domaines bornés simplement connexes tel que $\overline{D_2} \subset D_1$. Leurs existences ont été prouvées dans [33] en perturbant l'anneau $\mathbb{A}_b = \{z, b < |z| < 1\}$. Cependant il a été nécessaire d'imposer quelques conditions pour pouvoir appliquer le théorème de Crandall-Rabinowitz. Le troisième chapitre de cette thèse vient compléter l'étude menée dans [33, 35]. Leurs résultats sont les suivants

Theorem 1.1.2. *Soit $b \in (0, 1)$ et $m \geq 3$ un entier tel que*

$$1 + b^m - \frac{(1 - b^2)}{2}m < 0. \quad (1.1.5)$$

Alors il existe deux courbes de V-states doublement connexes m-symétriques obtenues en bifurquant de l'anneau \mathbb{A}_b aux vitesses angulaires

$$\Omega_m^\pm = \frac{1 - b^2}{4} \pm \frac{1}{2m} \sqrt{\Delta_m}$$

avec

$$\Delta_m = \left(\frac{1 - b^2}{2}m - 1 \right)^2 - b^{2m}.$$

La condition donnée par (1.1.5) assure une valeur propre Ω_m simple et un discriminant Δ_m non nul. Si cette condition n'est pas vérifiée, la valeur propre est double et nous sommes dans un cas dégénéré où le théorème de Crandall-Rabinowitz ne s'applique plus. Pour pallier à ce problème, Hmidi et Mateu ont utilisé la réduction de Lyapunov-Schmidt dans [35]. Cette technique permet de réduire un problème de dimension infinie à un problème de dimension finie et ils ont montré que

Theorem 1.1.3. *Pour $m \geq 3$, on note b_m l'unique solution dans $(0, 1)$ de*

$$1 + b^m - \frac{(1 - b^2)}{2}m = 0. \quad (1.1.6)$$

- *Soit $b \in (0, 1) \setminus \{b_{2m}, m \geq 2\}$ alors il existe une courbe de V-states doublement connexes 2-symétriques qui bifurque de l'anneau \mathbb{A}_b à la vitesse angulaire $\frac{1-b^2}{4}$. Dans ce cas, la bifurcation est transcritique.*
- *Si $b = b_m$ avec $m \geq 3$ alors il n'existe pas de V-states m-symétriques qui bifurquent de l'anneau \mathbb{A}_b .*

Ces travaux ont été accompagnés d'études numériques obtenues dans [33]. Ils ont remarqué que pour b proche de b_m , il y avait des petites boucles qui apparaissaient dans le diagramme de bifurcation. L'objectif du troisième chapitre a donc été de venir valider ce qui était observé de numériquement. Il a été nécessaire d'aller plus loin que le théorème de bifurcation de Crandall-Rabinowitz. Sa démonstration revient à développer la fonctionnelle à l'ordre un autour d'une solution triviale après avoir utiliser la réduction de Lyapunov-Schmidt. Ici, nous avons dû aller jusqu'à l'ordre deux dans le développement comme nous le verrons par la suite avec plus de détails.

Dans les chapitres 2 et 4 de cette thèse nous avons cherché à prouver l'existence de V-states en rotation uniforme pour d'autres équations issues de la mécanique des fluides. Le modèle est toujours de la forme suivante

$$\begin{cases} \partial_t \omega + v \cdot \nabla \omega = 0, & (t, x) \in \mathbb{R}_+ \times \mathbb{R}^2, \\ v(t, x) = \nabla^\perp \Psi(t, x), \\ \omega|_{t=0} = \omega_0 \end{cases} \quad (1.1.7)$$

où $v = (v_1, v_2)$ est le champ des vitesses du fluide, $\nabla^\perp = (-\partial_2, \partial_1)$ et Ψ est la fonction de courant. Elle est donnée par

$$\Psi(t, x) = \int_{\mathbb{R}^2} K(|x - y|)w(t, y)dy$$

avec K un opérateur spécifique à l'équation considérée. Par la suite, on va considérer deux modèles

$$K(x) = \begin{cases} \frac{\Gamma(\alpha/2)}{2^{1-\alpha}\Gamma(\frac{2-\alpha}{2})} \frac{1}{2\pi} \frac{1}{|x|^\alpha}, & \text{SQG} \\ \frac{1}{2\pi} K_0(|\varepsilon|x), & \text{SWQG} \end{cases} \quad (1.1.8)$$

avec $\alpha \in]0, 1]$ et $\varepsilon \in \mathbb{R}$. En prenant la limite en zéro dans la variable ε ou α , on peut montrer qu'on retrouve les équations d'Euler. Le modèle avec le paramètre α permet d'interpoler les équations d'Euler incompressibles ($\alpha = 0$) et les équations pour les surfaces quasi-géostrophiques appelées par la suite SQG qui correspondent au cas $\alpha = 1$. Le modèle SQG est un modèle asymptotique obtenu dans certains régimes du modèle quasi-géostrophique général. On suppose que les nombres de Rossby et de Ekman sont petits et que le tourbillon potentiel est constant, voir [54]. Il permet de décrire l'évolution de la température θ pour certains flux atmosphériques et océaniques. Dans la littérature, ce n'est d'ailleurs pas le tourbillon qui vérifie l'équation (1.1.7) mais θ . Les équations SQG ont été utilisées par Juckes et Held et al dans respectivement [39] et [27] pour modéliser la circulation atmosphérique près de la tropopause. Lapeyre et Klein s'en sont servies pour décrire la dynamique des couches océaniques supérieures dans [45]. De plus, ce modèle a l'intérêt de montrer des analogies mathématiques et physiques avec les équations d'Euler en trois dimensions (voir [14]). En effet, on montre que le champ de vecteur $\nabla^\perp \theta$ solution de SQG est analogue au tourbillon puis que les lignes de niveaux de θ sont analogues aux lignes de tourbillon pour Euler 3D. On retrouve aussi des critères d'explosions analogues. Le deuxième modèle est appelé modèle quasi-géostrophique shallow-water. Notre but est de donner quelques explications sur la dérivation du modèle.

Développons la dérivation formelle du modèle shallow water quasi-géostrophique (SWQG), voir [67] pour plus de détails. Nous commençons par mettre en place les équations de shallow water. Pour se faire on considère un fluide de densité constante et tel que l'échelle de la variation de la hauteur du flot soit petite devant la profondeur du fluide. Avec cette hypothèse nous pouvons considérer que l'approximation hydrostatique est valide. La courbure de la Terre sera aussi négligée et le fond rigide sera supposé plan et à une altitude nulle. De plus, on fera l'hypothèse que la vitesse angulaire de la Terre est constante et on la notera f . Introduisons maintenant quelques notations, la vitesse dans l'espace sera notée $\mathbf{v} = u\mathbf{i} + v\mathbf{j} + w\mathbf{k}$ avec \mathbf{k} qui désigne la direction verticale et la vitesse dans le plan sera $\mathbf{u} = u\mathbf{i} + v\mathbf{j}$. L'épaisseur de la couche de fluide au point (x, y) sera notée h et la hauteur moyenne du fluide H . On applique le principe fondamental de la dynamique pour obtenir l'équation suivante

$$\frac{\partial \mathbf{u}}{\partial t} + \mathbf{u} \cdot \nabla \mathbf{u} + f \times \mathbf{u} = -g \nabla h. \quad (1.1.9)$$

D'autre part, le fluide étant incompressible, on a l'équation classique de conservation de la masse

$$\operatorname{div}(\mathbf{v}) = 0.$$

On peut réécrire cette équation en coordonnée

$$\frac{\partial w}{\partial z} = -\operatorname{div}_h(\mathbf{u}).$$

On intègre cette équation entre le fond rigide et la surface libre et on obtient

$$w(h) - w(0) = -h \operatorname{div}_h(\mathbf{u}).$$

Or à la surface la vitesse verticale correspond à la dérivée matérielle de la position de la particule de fluide

$$w(h) = \frac{Dh}{dt} = \frac{\partial h}{\partial t} + \mathbf{u} \cdot \nabla h.$$

On obtient une autre version de l'équation de la conservation de la masse

$$\frac{\partial h}{\partial t} + \mathbf{u} \cdot \nabla h + h \operatorname{div}_h(\mathbf{u}) = 0. \quad (1.1.10)$$

Le principe est maintenant d'adimensionner nos équations et de voir sous certains régimes asymptotiques quels sont les termes principaux. Pour se faire, on a besoin d'introduire des échelles, notamment celle de la longueur et celle de la vitesse caractéristiques notées respectivement L et U et qui seront supposées horizontalement isotropes. On a donc

$$(x, y) = \mathcal{O}(L) \text{ et } (u, v) = \mathcal{O}(U).$$

On notera par la suite les valeurs adimensionnées avec un chapeau, par exemple,

$$\hat{x} = \frac{x}{L}.$$

On introduit aussi le paramètre de Rossby $R_0 = \frac{U}{fL}$ et le rayon de déformation $L_d = \frac{\sqrt{gH}}{f}$. Dans les océans, les valeurs typiques de L_d sont situées entre 25 km et 100 km. Dans l'atmosphère terrestre à des latitudes moyennes et aux pôles, les valeurs sont plutôt comprises entre 1000 km et 1500 km (voir [55]). Physiquement, le nombre de Rossby représente le rapport entre le terme d'advection et le terme de rotation dans l'équation de conservation du moment. Dans les océans comme dans l'atmosphère pour des grandes valeurs de L il est petit (respectivement $R_0 = 0,01$ et $R_0 = 0,1$). Enfin on peut écrire que la hauteur est une perturbation de la hauteur moyenne,

$$h(x, y) = H + \Delta h(x, y)$$

avec l'échelle suivante

$$\frac{\Delta h}{H} \sim R_0 \left(\frac{L^2}{L_d^2} \right).$$

On a donc

$$h = H \left(1 + R_0 \frac{L^2}{L_d^2} \hat{h} \right) \text{ et } \Delta h = R_0 \frac{L^2}{L_d^2} H \hat{h}.$$

On suppose par la suite que l'advection est prédominante et que l'échelle de temps peut être choisie de la manière suivante

$$T = \frac{L}{U}.$$

Enfin la vitesse angulaire adimensionnée vaut un. On obtient après adimensionnement des équations (1.1.9) et (1.1.10) les équations suivantes

$$R_0 \left[\frac{\partial \hat{u}}{\partial \hat{t}} + (\hat{u} \cdot \nabla) \hat{u} \right] + \hat{f} \times \hat{u} = -\nabla \hat{h} \quad (1.1.11)$$

et

$$R_0 \left(\frac{L^2}{L_d^2} \right) \left[\frac{\partial \hat{h}}{\partial \hat{t}} + \hat{u} \cdot \nabla \hat{h} \right] + \left[1 + R_0 \left(\frac{L^2}{L_d^2} \right) \right] \nabla \cdot \hat{u} = 0. \quad (1.1.12)$$

On se place à présent sous les hypothèses quasi-géostrophiques. Elles consistent à supposer que R_0 est petit et que les variations de la hauteur sont petites dans le sens où

$$R_0 \left(\frac{L^2}{L_d^2} \right) = \mathcal{O}(R_0).$$

On peut développer toutes nos grandeurs en série suivant le paramètre de Rossby

$$\hat{u} = \hat{u}_0 + R_0 \hat{u}_1 + R_0^2 \hat{u}_2 + \dots$$

En regardant les termes d'ordre zéro obtenus de (1.1.12) et (1.1.11), on obtient

$$\hat{f}_0 \hat{u}_0 = -\frac{\partial \hat{h}_0}{\partial \hat{y}}, \quad (1.1.13)$$

$$\hat{f}_0 \hat{v}_0 = \frac{\partial \hat{h}_0}{\partial \hat{x}} \quad (1.1.14)$$

et

$$\operatorname{div}(\hat{u}_0) = 0. \quad (1.1.15)$$

En considérant les termes obtenus à l'ordre un, on trouve les équations suivantes

$$\left(\frac{L}{L_d} \right)^2 \frac{\partial \hat{h}_0}{\partial \hat{t}} + \left(\frac{L}{L_d} \right)^2 \hat{u}_0 \cdot \nabla \hat{h}_0 + \operatorname{div}(\hat{u}_1) = 0 \quad (1.1.16)$$

et

$$\frac{\partial \hat{u}_0}{\partial \hat{t}} + (\hat{u}_0 \cdot \nabla) \hat{u}_0 + \hat{f}_0 \mathbf{k} \times \hat{u}_1 = -\nabla \hat{h}_1. \quad (1.1.17)$$

On note ξ la composante verticale du vecteur tourbillon et on applique le rotationnel à (1.1.17) pour obtenir

$$\frac{\partial \hat{\xi}_0}{\partial \hat{t}} + (\hat{u}_0 \cdot \nabla) \hat{\xi}_0 = -\hat{f}_0 \operatorname{div}(\hat{u}_1). \quad (1.1.18)$$

On introduit la fonction de courant $\hat{\psi}_0 = \frac{\hat{h}_0}{\hat{f}_0}$ et grâce à (1.1.13) et (1.1.14) on obtient

$$\hat{u}_0 = -\frac{\partial \hat{\psi}_0}{\partial \hat{x}}, \hat{v}_0 = \frac{\partial \hat{\psi}_0}{\partial \hat{y}} \text{ et } \hat{\xi}_0 = \nabla^2 \hat{\psi}_0. \quad (1.1.19)$$

En injectant (1.1.19) dans (1.1.18) et en redimensionnant l'équation, on obtient finalement

$$\frac{\partial q}{\partial t} + u \cdot \nabla q = 0$$

avec q le potentiel du tourbillon pour l'équation shallow water quasi-géostrophique. Il est donné par

$$q \triangleq \nabla^2 \psi - \frac{1}{L_d^2} \psi.$$

On retrouve ainsi le modèle avec le paramètre ε en posant $\varepsilon = \frac{1}{L_d}$.

La théorie pour les équations d'Euler posées dans le plan est bien connue. Malheureusement, pour les autres équations ce n'est pas le cas. Le modèle shallow water quasi-géostrophique a été très peu étudié mathématiquement, nous citerons donc majoritairement les résultats concernant le modèle avec le paramètre α . On va d'abord se concentrer sur le modèle SQG dont les équations sont données dans la littérature sous la forme suivante et qui permettent de décrire le potentiel de température noté θ

$$\begin{cases} \partial_t \theta + u \cdot \nabla \theta = 0, (t, x) \in \mathbb{R}_+ \times \mathbb{R}^2, \\ u = -\nabla^\perp (-\Delta)^{-\frac{1}{2}} \theta, \\ \theta|_{t=0} = \theta_0 \end{cases} \quad (1.1.20)$$

avec u le champ des vitesses et $\nabla^\perp = (-\partial_2, \partial_1)$. L'opérateur $(-\Delta)^{-\frac{1}{2}}$ est défini de la manière suivante

$$(-\Delta)^{-\frac{1}{2}} \theta(x) = \frac{1}{2\pi} \int_{\mathbb{R}^2} \frac{\theta(y)}{|x-y|} dy.$$

Pour $\alpha > 0$, le noyau est plus singulier que le logarithme et il n'existe pas de résultats équivalents au théorème de Yudovich. Les premiers résultats pour SQG ont été obtenus dans [14]. Ils ont prouvé analytiquement l'existence locale de solutions dans les espaces de Sobolev $H^s(\mathbb{R}^2)$ avec $s \geq 3$. L'existence et l'unicité locale ont ensuite été prouvées dans d'autres espaces, par exemple pour $\theta_0 \in C^r \cap L^q$ avec $r > 1$ et $q > 1$ dans [70]. Quelques résultats existent pour des données initiales moins régulières. L'existence de solutions faibles globales a été prouvée dans L^2 par Resnick dans [61] puis dans L^p avec $p > \frac{4}{3}$ par Marchand dans [51]. La

question de l'unicité pour des solutions L^2 est toujours ouverte, cependant pour des espaces moins réguliers, Buckmaster et al ont apporté une réponse négative dans [5].

Jusqu'à très récemment, l'existence de solutions fortes globales était aussi une question sans réponse. Córdoba et al ont exhibé des solutions fortes globales pour SGQ dans [9] en régularisant des V-states.

On peut obtenir plus d'informations si on impose à la condition initiale d'être une poche de tourbillon, dans ce cas $\theta_0(x) = \chi_D$ avec D un domaine borné. Dans ces conditions, la solution existe au moins localement en temps et garde cette structure de poche. Des existences locales ont été démontrées pour un front C^∞ par Rodrigo en utilisant le théorème de Nash-Moser et pour un bord dans un espace de Sobolev par Gancedo dans [62, 26] pour SQG .On considère maintenant des V-states en imposant en plus la rotation à vitesse uniforme. Quelques résultats existent pour ces objets.

Dans [29, 8] l'existence de V-states bifurquant du disque a été prouvée pour $0 \leq \alpha \leq 1$ et ils ont montré que le bord était analytique. Pour ce qui est des V-states avec un trou, leurs existences ont été prouvées pour $0 \leq \alpha < 1$ dans [33, 30] en perturbant l'anneau $\mathbb{A}_b = \{z, b < |z| < 1\}$. Le théorème de Yudovich n'étant plus vrai pour $\alpha > 0$, le caractère global en temps de ces solutions est aussi intéressant. Le cas $\alpha = 1$ posait problème car l'espace fonctionnel proposé dans [30] ne permettait pas de gérer la croissance logarithmique du spectre non linéaire. L'objectif du chapitre 2 est de venir compléter l'étude en palliant à ce problème. On s'est inspiré de l'espace fonctionnel proposé dans [8]. Quelques difficultés sont apparues notamment dans le calcul du linéarisé pour le cas limite $\alpha = 1$. En effet, dans [33], le calcul n'avait pas été prouvé mais obtenu par passage à la limite. Pour vérifier les hypothèses du théorème de bifurcation, il nous a fallu trouver une forme compacte du linéarisé et nous avons dû faire appel à la théorie des fonctions spéciales. De plus, chercher les valeurs propres qui induisent un noyau unidimensionnel n'était pas non plus une chose aisée et a demandé quelques efforts. Nous avons aussi montré que l'application conforme qui définit notre V-state pouvait être étendue en une fonction analytique sur une couronne. Des résultats similaires avaient été prouvés uniquement pour la bifurcation depuis le disque dans [8].

Dans le dernier chapitre, on s'intéresse au modèle SWQG. A ce jour, il n'existe pas de résultat théorique. Cependant, le noyau a une singularité logarithmique donc le théorème de Yudovich devrait être aussi valide dans ce cas. On peut citer quelques résultats numériques. Dans [55], Plotka et Dritschel s'intéressent aux V-states 2-symétriques pour différents paramètres γ et λ où λ correspond au ratio des deux demi-axes. Ils étudient entre autres les valeurs pour lesquelles des instabilités apparaissent. Dans [57], Polvani et all étudient l'existence de V-states et de deux poches de tourbillon en mouvement de translation.

Dans le chapitre 4, on a commencé par prouver l'existence de V-states m-symétriques obtenues en perturbant le disque. Ensuite, on a étudié comment le diagramme de bifurcation est perturbé en fonction de ε en s'intéressant notamment à la branche 2-symétrique. Les résultats obtenus s'inscrivent dans des travaux plus généraux liés à la bifurcation imparfaite qui consiste à étudier comment la structure géométrique du diagramme de bifurcation varie en fonction d'un paramètre. Les pionniers du domaine sont Golubitsky et Schaeffer [28] qui ont classifié différents cas possibles en utilisant la théorie des singularités. On peut trouver des travaux en lien avec nos résultats dans [47, 65] par exemple. Le point qui a posé problème dans la preuve de l'existence des V-states m-symétriques est le calcul du linéarisé qui était plus complexe que dans le cas d'Euler. En effet, le noyau n'étant plus explicite, nous avons dû faire appel aux fonctions de Bessel pour obtenir une forme compacte du linéarisé. De plus, quelques estimations sur ces mêmes fonctions ont été nécessaires pour valider les hypothèses du théorème de bifurcation. Pour les autres résultats, nous avons voulu perturber les solutions existantes pour les équations d'Euler. En effet, nous savons que les solutions pour $m = 2$ correspondent aux ellipses de Kirchhoff et dans [34] les auteurs ont montré que cette famille d'ellipses pouvait être perturbée pour créer de nouvelles solutions. Nous avons prouvé que pour ε petit on peut construire des solutions 2-symétriques qui sont des perturbations des ellipses de Kirchhoff. Ensuite on a bifurqué de cette famille pour certains paramètres. Enfin nous avons aussi montré qu'une singularité présente pour $\varepsilon = 0$ dans le diagramme de bifurcation était éclatée . Pour cela, nous avons du développer la fonctionnelle jusqu'à l'ordre deux. Pour finir, le dernier chapitre comporte aussi des résultats numériques concernant les V-states ayant une symétrie deux et trois. On regarde notamment l'éclatement de certaines parties de la branche quand le paramètre ε est non nul et les V-states limites obtenues au bout des branches.

Les résultats obtenus seront présentés de manière plus précise dans la partie suivante.

1.2 Présentation des résultats

1.2.1 Le théorème de Crandall-Rabinowitz

L'objectif de cette partie est de rappeler la preuve du théorème de Crandall-Rabinowitz, on pourra voir par exemple [42]. Les différentes preuves que nous avons élaborées au cours de cette thèse sont intrinsèquement liées à la démonstration de ce théorème. Dans le chapitre 2, nous avons utilisé le théorème pour obtenir un résultat global vis-à-vis du diagramme de bifurcation. Cependant pour les deux derniers chapitres, ils nous a fallu comprendre la preuve du théorème de bifurcation et aller au delà pour obtenir des résultats plus précis.

Tous les problèmes que nous avons rencontrés peuvent se ramener à la résolution d'une équation de type

$$F(\Omega, f) = 0 \quad (1.2.1)$$

avec

$$\begin{aligned} F : \mathbb{R} \times X &\longrightarrow Y \\ (\Omega, f) &\longmapsto F(\Omega, f) \end{aligned}$$

où X et Y sont des espaces de Banach et on demandera à la fonctionnelle F d'avoir une certaine régularité. A chaque fois, nous connaitrons un ensemble de solutions triviales, c'est-à-dire que nous aurons

$$F(\Omega, 0) = 0, \forall \Omega \in \mathbb{R}. \quad (1.2.2)$$

Dans les chapitres qui vont suivre, le paramètre f correspond à une déformation d'un objet géométrique. On considérera des déformations d'anneaux, de disques et d'ellipses qui vivront dans un espace de dimension infinie. L'équation (1.2.2) signifie que ces formes géométriques seront des poches tournantes pour n'importe quelle vitesse de rotation uniforme. L'idée est maintenant de venir perturber ces formes pour créer de nouvelles solutions. Moralement, si le disque est solution pour n'importe quelle vitesse, on se dit qu'en tordant un peu son bord, on pourra trouver une vitesse pour laquelle la forme obtenue sera une solution. En vertu du théorème des fonctions implicites, on voit qu'une condition pour espérer avoir des solutions non triviales est que le noyau du linéarisé autour de $(0, 0)$ ne soit pas réduit à zéro. Plus précisément on va demander au linéarisé de vérifier les conditions suivantes

$$\dim(\text{Ker}(D_f F(0, 0))) = 1 \text{ avec } \text{Ker}(D_f F(0, 0)) = \text{Vect}(f_0) \quad (1.2.3)$$

et

$$\dim\left(Y/\text{Im}\left(D_f F(0, 0)\right)\right) = 1. \quad (1.2.4)$$

Autrement dit, on demande à $D_f F(0, 0)$ d'être un opérateur de type Fredholm d'indice zéro. La prochaine étape est d'utiliser ces hypothèses pour ramener notre problème de dimension infinie à un problème de dimension finie en faisant appel à la réduction de Lyapunov-Schmidt. Tout d'abord, grâce à (1.2.3) on peut trouver un sous-espace fermé \mathcal{X} de X tel que

$$X = \text{Vect}(f_0) \oplus \mathcal{X}.$$

Si \mathcal{Y} désigne l'image de $D_f F(0, 0)$ que l'on suppose fermée dans Y , d'après (1.2.4) on peut écrire la décomposition suivante

$$Y = \mathcal{Y} \oplus \text{Vect}(W).$$

La réduction de Lyapunov-Schmidt permet d'isoler la partie dimension infinie de la perturbation et de l'exprimer en fonction des autres paramètres en utilisant le théorème des fonctions implicites. Cette technique repose sur l'utilisation de deux projecteurs,

$$P : X \rightarrow \text{Vect}(f_0) \text{ et } Q : Y \rightarrow \text{Vect}(W).$$

Pour $f \in X$ on peut donc écrire la décomposition suivante,

$$f = g + k \text{ avec } g = Pf \text{ et } k = (Id - P)f.$$

L'équation (1.2.1) est donc équivalente au système

$$F_1(\Omega, g, k) \triangleq (Id - Q)F(\Omega, g + k) = 0 \text{ et } QF(\Omega, g + k) = 0. \quad (1.2.5)$$

On remarque que

$$F_1(0, 0, 0) = 0,$$

F_1 est régulière et $D_k F_1(0, 0, 0) : \mathcal{X} \rightarrow \mathcal{Y}$ est inversible. On peut donc appliquer le théorème des fonctions implicites et les solutions de $F_1(\Omega, g, k) = 0$ sont localement autour du point $(0, 0, 0)$ paramétrisées par $k = \varphi(\Omega, g)$ avec

$$\varphi : \mathbb{R} \times \text{Vect}(f_0) \rightarrow \mathcal{X}$$

qui est régulière. Le système (1.2.5) est donc localement autour de $(0, 0, 0)$ équivalent à l'équation posée en dimension finie

$$F_2(\Omega, t) \triangleq QF(\Omega, tf_0 + \varphi(\Omega, tf_0)) = 0. \quad (1.2.6)$$

Comme on a

$$F_2(0, 0) = 0,$$

en utilisant un développement de Taylor à l'ordre un, on montre que (1.2.6) est équivalente à l'équation suivante qui porte le nom d'équation de bifurcation réduite

$$\hat{F}_2(\Omega, t) \triangleq \int_0^1 QD_f F(\Omega, stf_0 + \varphi(\Omega, stf_0))(f_0 + \partial_g \varphi(\Omega, stf_0)f_0)ds = 0.$$

On a toujours

$$\hat{F}_2(0, 0) = 0$$

et notre but maintenant est d'appliquer le théorème des fonctions implicites à la fonctionnelle \hat{F}_2 . Pour cela on va supposer que la condition dite de transversalité est vérifiée

$$\partial_\Omega D_f F(0, 0)f_0 \notin \text{Im}(D_f F(0, 0)). \quad (1.2.7)$$

Cette hypothèse nous assure la bijectivité du linéarisé

$$\partial_\Omega \hat{F}_2(0, 0) = Q\partial_\Omega D_f F(0, 0) \neq 0.$$

On peut donc appliquer le théorème des fonctions implicites pour obtenir localement autour de $(0, 0)$ que

$$\Omega = \psi(t).$$

Finalement, pour t dans un voisinage de zéro on a

$$F(\psi(t), tf_0 + \varphi(\psi(t), tf_0)) = 0.$$

Ceci achève la démonstration du théorème de Crandall-Rabinowitz dont l'énoncé précis sera donné par exemple dans le chapitre 2.

Dans les chapitres 3 et 4 notre but était d'obtenir plus de précisions sur l'ensemble décrit par le couple (Ω, t) et le théorème de Crandall-Rabinowitz n'était plus suffisant. On a prouvé que cet ensemble est une ellipse déformée et une hyperbole déformée et pour le démontrer ils nous a fallu développer la fonctionnelle jusqu'à l'ordre deux. Nous allons maintenant donner plus de détails sur les résultats démontrés au cours de cette thèse.

1.2.2 Existence de V-states doublement connexes pour les équations quasi-géostrophiques

Dans ce chapitre, on s'est intéressé au modèle quasi-géostrophique dont les équations sont

$$\begin{cases} \partial_t \theta + v \cdot \nabla \theta = 0, & (t, x) \in \mathbb{R}_+ \times \mathbb{R}^2, \\ v = -\nabla^\perp (-\Delta)^{-\frac{1}{2}} \theta, \\ \theta|_{t=0} = \theta_0 \end{cases} \quad (1.2.8)$$

L'opérateur $(-\Delta)^{-\frac{1}{2}}$ est défini de la manière suivante

$$(-\Delta)^{-\frac{1}{2}} \theta = \frac{1}{2\pi} \int_{\mathbb{R}^2} \frac{\theta(y)}{|x-y|} dy.$$

On remarque qu'il est plus singulier que dans le cas quasi-géostrophique généralisé avec $\alpha \in [0, 1]$. Cette singularité avait posé problème à Hassania, Hmidi et de la Hoz dans [29, 30] pour étendre leurs résultats d'existence de V-states simplement et doublement connexes jusqu'à $\alpha = 1$. En effet, l'espace fonctionnel proposé ne permettait pas de gérer cette singularité. Il a fallu attendre le papier [8] de Castro et ses collaborateurs pour obtenir un espace fonctionnel satisfaisant. Ils ont prouvé l'existence de V-states simplement connexes en déformant un disque. D'un point de vue technique, la différence entre la preuve dans le cas simplement connexe et doublement connexe apparaît surtout dans le calcul du linéarisé et la recherche des valeurs propres qui conduisent à un opérateur de noyau unidimensionnel. Cependant, les espaces fonctionnels restent similaires pour les deux preuves. Pour prouver l'existence de V-states doublement connexes, je me suis inspirée de leurs espaces mais j'ai dû les adapter pour pouvoir les utiliser avec le formalisme des applications conformes. On rappelle que pour ces objets, notre donnée initiale est de la forme $\theta_0 = \chi_D$ avec $D = D_1 \setminus D_2$ où D_1 et D_2 sont deux domaines bornés simplement connexes avec $\overline{D_2} \subset D_1$. Notre but est de construire de nouvelles solutions en perturbant l'anneau $\mathbb{A}_b = \{z \in \mathbb{C}, b < |z| < 1\}$ avec $b \in (0, 1)$. La preuve de l'existence de ces solutions suit les idées introduites par Burbea dans [6] et reprises dans [33, 30] dans le cadre des V-states doublement connexes. La première étape consiste à réécrire les équations, on pourra voir par exemple [29, 30]. On a vu précédemment que le bord du domaine était transporté par le flot. Si l'on part d'un domaine ayant un bord régulier, au moins de classe C^1 , alors il peut être défini de manière implicite à l'aide d'une fonction de classe au moins C^1 , $\varphi_0 : \mathbb{R}^2 \rightarrow \mathbb{R}$,

$$\partial D = \{x \in \mathbb{R}^2; \varphi_0(x) = 0\},$$

avec les hypothèses suivantes: $\forall x \in \partial D, \nabla \varphi_0(x) \neq 0$,

$$\varphi_0 < 0 \text{ sur } D \text{ et } \varphi_0 > 0 \text{ sur } \mathbb{R}^2 \setminus \overline{D}.$$

On introduit maintenant

$$F(t, x) = \varphi(\psi^{-1}(t, x)),$$

où ψ désigne le flot associé à la vitesse v et qui est donné par

$$\psi(t, x) = x + \int_0^t v(s, \psi(s, x)) ds.$$

Dans ce cas, $F(t, \cdot)$ permet de décrire implicitement le bord à l'instant t donné par $\partial D_t = \psi(t, \partial D)$ et elle vérifie l'équation de transport

$$\partial_t F + v \cdot \nabla F = 0.$$

Soit $\sigma \in [0, 2\pi] \mapsto \gamma_t(\sigma)$ une paramétrisation de ∂D_t , continument différentiable en t et \vec{n}_t un vecteur normal unitaire sortant à ∂D_t . En dérivant par rapport à t l'équation $F(t, \gamma_t(\sigma)) = 0$ on arrive à

$$\partial_t F + \partial_t \gamma_t \cdot \nabla F = 0.$$

Or pour un point du bord, le vecteur $\nabla F(t, x)$ est colinéaire au vecteur normal \vec{n}_t donc on obtient

$$(\partial_t \gamma_t - v(t, \gamma_t)) \cdot \vec{n}_t = 0. \quad (1.2.9)$$

L'équation (1.2.9) signifie que le transport du bord par le flot implique que la vitesse d'un point du bord et celle de la particule de fluide qui occupe la même position ont le même vecteur normal. On commence par reformuler cette équation en utilisant les notations complexes pour obtenir

$$\operatorname{Im} \left\{ \left(\partial_t \gamma_t - v(t, \gamma_t) \right) \overline{\gamma'_t} \right\} = 0,$$

où le prime désigne la dérivée en la variable σ . On peut maintenant exprimer la vitesse à l'instant t en fonction de la vitesse initiale via la formule

$$v(t, x) = e^{i\Omega t} v_0(e^{-i\Omega t} x).$$

On obtient donc la relation suivante

$$\operatorname{Im} \left\{ v(t, \gamma_t) \overline{\gamma'_t} \right\} = \operatorname{Im} \left\{ v_0(\gamma_0) \overline{\gamma'_0} \right\}.$$

Comme un point du bord à l'instant t est un point du domaine initial qui a subi une rotation d'angle Ωt , alors on a la relation $\gamma_t = e^{i\Omega t} \gamma_0$. On obtient ainsi l'équation suivante

$$\Omega \operatorname{Re} \{ z \bar{z}' \} = \operatorname{Im} \{ v_0(z) \bar{z}' \}, \forall z \in \partial D_1 \cup \partial D_2 \quad (1.2.10)$$

où z' est un vecteur tangent au bord ∂D_1 ou ∂D_2 . La vitesse v_0 est donnée grâce à la loi de Biot-Savart,

$$v_0(z) = \frac{1}{2\pi} \int_{\partial D_1} \frac{1}{|z - \xi|} d\xi - \frac{1}{2\pi} \int_{\partial D_2} \frac{1}{|z - \xi|} d\xi$$

où $d\xi$ désigne l'intégration complexe sur les bords respectifs de D_1 et D_2 orientés dans le sens trigonométrique. Utilisons maintenant les applications conformes pour paramétriser nos bords. Pour cela, on commence par énoncer deux théorèmes sur ces applications. Le premier est le théorème des applications conformes de Riemann.

Theorem 1.2.1. *On désigne par \mathbb{D} la boule unité ouverte et $K \subset \mathbb{C}$ un domaine borné simplement connexe. Alors il existe une unique application bi-holomorphe appelée aussi application conforme, $\Phi : \mathbb{C} \setminus \overline{\mathbb{D}} \rightarrow \mathbb{C} \setminus \overline{K}$ qui s'écrit de la manière suivante*

$$\Phi(z) = az + \sum_{n \in \mathbb{N}} \frac{a_n}{z^n} \text{ avec } a > 0.$$

De plus, si le bord est assez régulier on peut prolonger l'application conforme jusqu'au bord. Plus précisément si la frontière $\Phi(\mathbb{T})$ est une courbe de Jordan de classe $C^{n+1+\beta}$ avec $n \in \mathbb{N}$ et $0 < \beta < 1$ alors Φ peut être prolongée continuellement jusqu'au bord par une application de classe $C^{n+1+\beta}$. On paramétrise nos bords avec nos deux applications conformes extérieures $\Phi_j : \mathbb{T} \rightarrow \partial D_j$ avec $j \in \{1, 2\}$. Ensuite on réécrit (1.2.10) sur chaque bord avec celles-ci pour arriver au système d'équations suivant: Pour $j \in \{1, 2\}$ et $w \in \mathbb{T}$

$$\begin{aligned} G_j(\Omega, \Phi_1, \Phi_2)(w) &\triangleq \operatorname{Im} \left\{ \left(\Omega \Phi'_j(w) - S(\Phi_1, \Phi_j)(w) + S(\Phi_2, \Phi_j)(w) \right) \overline{\Phi'_j(w)} \overline{w} \right\} \\ &= 0 \end{aligned}$$

avec

$$S(\Phi_i, \Phi_j)(w) = \oint_{\mathbb{T}} \frac{\tau \Phi'_i(\tau) - w \Phi'_j(w)}{|\Phi_i(\tau) - \Phi_j(w)|} \frac{d\tau}{\tau}$$

où le terme en $\Phi'_j(w)$ rajouté dans $S(\Phi_i, \Phi_j)$ ne change rien à l'équation car orthogonal au vecteur normal mais permet de mieux contrôler la singularité. On cherche maintenant notre ensemble de solutions triviales. On peut remarquer que l'anneau est une poche tournante pour n'importe quelle vitesse angulaire Ω , c'est-à-dire que pour tout $\Omega \in \mathbb{R}$ et pour $j \in \{1, 2\}$ on a

$$\forall w \in \mathbb{T}, G_j(\Omega, \text{Id}, b\text{Id})(w) = 0.$$

Nous allons donc essayer de trouver de nouvelles solutions en perturbant l'anneau \mathbb{A}_b avec $b \in (0, 1)$ en utilisant le théorème de Crandall-Rabinowitz. Dans ce cas, les applications conformes ont la forme suivante,

$$\forall |z| \geq 1, \Phi_1(z) = z + f_1(z) = z + \sum_{n=1}^{+\infty} \frac{a_n}{z^n}$$

et

$$\Phi_2(z) = bz + f_2(z) = bz + \sum_{n=1}^{+\infty} \frac{b_n}{z^n}.$$

Les coefficients de Fourier sont supposés réels ce qui signifie que l'on cherche des V-states symétriques par rapport à l'axe des abscisses. Dans un premier temps, on a besoin de vérifier que la fonctionnelle est bien définie. Un des points délicats est de montrer l'analyticité. Plus précisément, considérons $\varepsilon \in (0, 1)$ on introduit les deux ensembles suivants

$$C_\varepsilon = \left\{ z \in \mathbb{C} \mid \varepsilon < |z| < \frac{1}{\varepsilon} \right\} \quad \text{et} \quad \Delta_\varepsilon = \left\{ z \in \mathbb{C} \mid \varepsilon < |z| \right\}.$$

On désigne par \mathcal{A}_ε l'ensemble des fonctions holomorphes h sur Δ_ε et telle que

$$\forall z \in \Delta_\varepsilon, h(z) = \sum_{n \geq 1} h_n z^{-n} \quad \text{avec} \quad h_n \in \mathbb{R}.$$

et par $\widehat{\mathcal{A}}_\varepsilon$ l'ensemble des fonctions holomorphes h sur C_ε qui vérifient

$$\forall z \in C_\varepsilon, h(z) = i \sum_{n=1}^{+\infty} h_n (z^n - z^{-n}), h_n \in \mathbb{R}.$$

Moralement, pour prouver l'analyticité, on a besoin d'abord de s'assurer que

$$\begin{aligned} G_j : \mathbb{R} \times V \times V &\longrightarrow \widehat{\mathcal{A}}_\varepsilon \\ (\Omega, f_1, f_2) &\longmapsto G_j(\Omega, f_1, f_2) \end{aligned}$$

est bien définie avec V un voisinage de zéro dans \mathcal{A}_ε . La partie technique consiste à prouver que le terme $S(\Phi_i, \Phi_i)$ avec $i \in \{1, 2\}$ peut être étendu analytiquement sur C_ε . Les termes croisés sont plus simples à gérer car moins singuliers. On va expliquer les points clés sur un exemple type

$$K(w) = \int_{\mathbb{T}} \frac{\tau \partial_\tau h(\tau) - w \partial_\tau h(w)}{|W(\tau) - W(w)|} \frac{d\tau}{\tau}$$

avec $h \in V$ et $W = b^{j-1} \text{Id} + f$ avec $f \in V$ et on va expliquer comment étendre cette fonction. Tout d'abord, nous devons comprendre comment nous pouvons prolonger le module. Pour se faire, on remarque que

$$|W(\tau w) - W(w)|^2 = b^{2(j-1)} |\tau - 1|^2 g(\tau, w) g(\bar{\tau}, w^{-1})$$

avec la fonction g qui peut être étendu de la manière suivante

$$\forall z \in \overline{\Delta_\varepsilon}, g(\tau, z) = 1 + \frac{f(\tau z) - f(z)}{b^{j-1} z(\tau - 1)}.$$

En utilisant le théorème des accroissements finis et le principe du maximum, on arrive à montrer que pour f assez petit dans une certaine norme, la fonction $z \in C_\varepsilon \rightarrow g(\tau, z)g(\bar{\tau}, z^{-1})$ est holomorphe et n'intersecte pas le demi-axe réel négatif, ceci nous permet de définir la racine carrée de cette fonction qui va être holomorphe sur le même ensemble. On doit finalement montrer que la fonction

$$\tilde{K}(z) = z \int_{\mathbb{T}} \frac{\tau \partial_\tau h(\tau) - w \partial_\tau h(w)}{b^{j-1} |\tau - 1|} g(\tau, z)^{-\frac{1}{2}} g(\bar{\tau}, z^{-1})^{-\frac{1}{2}} \frac{d\tau}{\tau}$$

est holomorphe sur \mathbb{C}_ε . Pour le prouver on utilise le théorème d'holomorphie sous le signe intégral. Ceci montre que la fonctionnelle est bien définie. Ensuite, on doit prouver que les solutions existent en vérifiant les différentes hypothèses du théorème de bifurcation.

Nous devons donc nous intéresser à l'opérateur linéarisé calculé autour de la solution triviale. Pour implémenter le théorème de Crandall-Rabinowitz, nous avons besoin de trouver les valeurs de Ω associées à un noyau unidimensionnel pour l'opérateur linéarisé. On commence par calculer l'opérateur linéarisé autour de l'anneau. Le calcul est long et technique et pour obtenir une forme adéquate pour la suite, il nous faut faire appel aux fonctions hypergéométriques de Gauss. On a aussi eu besoin d'utiliser les fonctions de Bessel de première espèces J_m avec $m \in \mathbb{N}$ données par

$$\forall z \in \mathbb{C}; J_m(z) = \sum_{k=0}^{+\infty} \frac{(-1)^k}{k!(n+k)!} \left(\frac{z}{2}\right)^{2k+n}.$$

Pour prendre en compte la symétrie m avec m un entier plus grand que un, on considère

$$h_1(w) = \sum_{n=1}^{+\infty} a_n \bar{w}^{nm-1} \text{ et } h_2(w) = \sum_{n=1}^{+\infty} c_n \bar{w}^{nm-1}, w \in \mathbb{T}.$$

Dans ce cas, on obtient

$$DG(\Omega, \text{Id}, b\text{Id})(h_1, h_2)(w) = \frac{i}{2} \sum_{n \geq 1} nm M_{nm} \begin{pmatrix} a_n \\ c_n \end{pmatrix} (w^{nm} - \bar{w}^{nm})$$

où la matrice M_n est donné pour tout $n \geq 2$ par

$$M_n \triangleq \begin{pmatrix} \Omega - S_n + b^2 \Lambda_1(b) & -b^2 \Lambda_n(b) \\ b \Lambda_n(b) & b \Omega + S_n - b \Lambda_1(b) \end{pmatrix}$$

avec

$$S_n = \frac{2}{\pi} \sum_{k=1}^{n-1} \frac{1}{2k+1}$$

et

$$\lambda_n(b) \triangleq \frac{1}{b} \int_0^{+\infty} J_n(bt) J_n(t) dt.$$

Avec cette expression, nous pouvons trouver les valeurs de Ω tel que le noyau de $DG(\Omega, \text{Id}, b\text{Id})$ est unidimensionnel. On commence par chercher quelles sont les valeurs de λ qui conduisent à un noyau de dimension un pour M_n avec $\lambda \triangleq 1 - 2\Omega$. On s'intéresse donc à son déterminant qui est un polynôme du second degré

$$\det(M_n) = \frac{b}{4} (\lambda^2 - 2C_n + D_n)$$

et dont le discriminant réduit associé est

$$\Delta_n = \left(\frac{1}{b} + 1\right) S_n - (1 + b^2) \lambda_1(b)^2 - 4b^2 \lambda_n^2(b).$$

Pour des raisons techniques, une restriction sur la symétrie m est imposée afin de s'assurer que λ soit une valeur propre simple pour la matrice M_n . En effet, si la valeur propre est double, on n'est plus confronté à un opérateur de type Fredholm d'indice zéro et le théorème de bifurcation ne s'applique plus. Ensuite, on montre la stricte monotonie des valeurs propres en fonction de n pour conclure sur la dimension du noyau de la fonctionnelle, la preuve s'appuie sur celle développée dans [30]. Nous pouvons ensuite vérifier les autres conditions du théorème de Crandall-Rabinowitz. La condition de transversalité est vérifiée car nous avons évité le cas où la valeur propre était double. On peut donc appliquer le théorème de bifurcation et établir l'existence de nos V-states. Le résultat démontré est le suivant

Theorem 1.2.2. *Soit $b \in (0, 1)$ alors il existe $N \in \mathbb{N}^* \setminus \{1\}$ tel que pour tout entier $m \geq N$ il existe deux courbes de V-states doublement connexes m -symétriques solutions de l'équation (1.2.8) ayant un bord analytique qui bifurquent de l'anneau $\mathbb{A}_b = \{z \in \mathbb{C}, b < |z| < 1\}$ aux vitesses angulaires*

$$\Omega_m^\pm = \frac{1}{2} \left[\left(1 - \frac{1}{b} \right) S_m + (1 - b^2) \lambda_1(b) \right] \pm \sqrt{\Delta_m(b)}$$

avec

$$\lambda_m(b) \triangleq \frac{1}{b} \int_0^{+\infty} J_m(bt) J_m(t) dt$$

et

$$S_m \triangleq \frac{2}{\pi} \sum_{k=1}^{m-1} \frac{1}{2k+1}$$

où J_m désigne la fonction de Bessel de première ordre.

Remark 1.2.3. *Dans [30], Hmidi et al avaient démontré l'existence de V-states doublement connexes pour $\alpha \in (0, 1)$. En passant à la limite lorsque α tend vers un dans leurs résultats, ils avaient prédit ce que j'ai démontré.*

1.2.3 Existence de petites boucles dans le diagramme de bifurcation près des valeurs propres dégénérées.

Le but de ce chapitre est d'étudier quelques propriétés locales du diagramme de bifurcation des poches doublement connexes en rotation uniforme pour les équations d'Euler. On redonne les équations du tourbillon pour le modèle Euler incompressible dans le plan

$$\begin{cases} \partial_t \omega + v \cdot \nabla \omega = 0, & (t, x) \in \mathbb{R}_+ \times \mathbb{R}^2, \\ v = -\nabla^\perp (-\Delta)^{-1} \omega, \\ \omega|_{t=0} = \omega_0 \end{cases} \quad (1.2.11)$$

L'existence de V-states m -symétriques doublement connexes obtenues en bifurquant de l'anneau \mathbb{A}_b est connue. On a vu que pour chaque symétrie, on pouvait bifurquer si $b < b_m$ où b_m est l'unique solution dans $(0, 1)$ de (1.1.6) et correspond à un cas dégénéré. Notre but est de comprendre ce qui se passe dans le diagramme de bifurcation près des cas dégénérés où l'opérateur n'est plus de type Fredholm d'indice zéro. Un étude numérique a été faite dans [33]. Ils ont analyser les différentes structure du diagramme de bifurcation qui apparaissent lorsque le paramètre b varie. L'étude qu'ils ont mené a été faite pour $m = 4$ et deux cas sont apparues. Ils ont montré dans un premier temps que si l'on choisi un b proche de b_4 alors on peut construire des solutions pour tout $\Omega \in (\Omega_4^-, \Omega_4^+)$, il n'y a pas de "trou" dans le diagramme de bifurcation et les deux branches issues des valeurs Ω_4^- et Ω_4^+ se rejoignent pour former des petites boucles dans le diagramme de bifurcation, voir figure 1.2. De plus, les solutions construites pour les valeurs extrêmes de Ω sont proches de l'anneau et se sont entre temps déformées de la manière suivante, les deux frontières sont passées du cercle à un carré arrondi puis se sont déformées en un cercle avec un décalage de $\Pi/4$ entre les deux. Cependant lorsqu'ils considèrent des valeurs de b assez éloignées du cas dégénéré, ils n'arrivent à construire des solutions que pour $\Omega \in (\Omega_4^-, \Omega_4^- + \varepsilon_-]$ et $\Omega \in [\Omega_4^+ - \varepsilon_+, \Omega_4^+)$, avec ε_- et ε_+ des constantes positives. Il y a donc un

trou dans le diagramme de bifurcation. Dans ce cas, la frontière extérieure reste proche du cercle tandis que la frontière intérieure se transforme en un carré légèrement arrondi non convexe avec des singularités qui semblent apparaître aux coins. Ces observations numériques rentrent dans les résultats connues sur la bifurcation globale, voir [42], où sous certaines hypothèses, on peut montrer que les branches se rejoignent ou qu'elles sont non bornées.

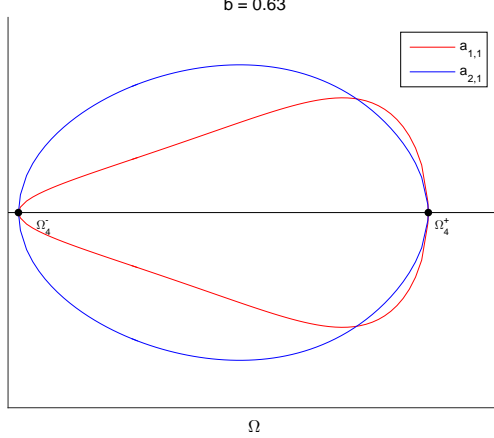


Figure 1.2: Courbes de bifurcation des premiers coefficients de Fourier des deux applications conformes $a_{1,1}$ and $a_{2,1}$ par rapport à Ω .

Notre but est de prouver analytiquement l'existence des petites boucles dans le diagramme de bifurcation pour b proche de b_m^* . Plus précisément, nous allons montrer que

Theorem 1.2.4. *Soit $m \geq 3$ et b_m^* l'unique solution dans $(0, 1)$ de l'équation (1.1.6). Alors il existe $b_m \in (0, b_m^*)$ tel que pour tout b dans (b_m, b_m^*) les deux courbes de V-states m -symétriques données par le Théorème 1.1.5 se rencontrent et forment une boucle.*

Comme pour le résultat précédent, nous pouvons réécrire les équations (1.2.11) avec les applications conformes et montrer qu'elles sont équivalentes à: pour $j \in \{1, 2\}$ et $w \in \mathbb{T}$

$$\begin{aligned} G_j(\lambda, f_1, f_2)(w) &\triangleq \operatorname{Im}\left\{\left(\Omega \Phi_j(w) - S(\Phi_1, \Phi_j)(w) + S(\Phi_2, \Phi_j)(w)\right) \overline{\Phi'_j(w)} \bar{w}\right\} \\ &= 0 \end{aligned} \quad (1.2.12)$$

avec

$$\lambda = 1 - 2\Omega, \Phi_j(w) = b_j w + f_j(w) \text{ où } b_1 = 1 \text{ et } b_2 = b$$

et

$$S(\Phi_i, \Phi_j)(w) = \int_{\mathbb{T}} \frac{\overline{\Phi_i(w)} - \overline{\Phi_j(\tau)}}{\overline{\Phi_i(w)} - \overline{\Phi_j(\tau)}} \Phi'_i(\tau) d\tau.$$

On définit pour $j \in \{1, 2\}$

$$h_j(w) = \sum_{n \geq 1} \frac{a_{j,n}}{w^{nm-1}}.$$

On peut calculer l'opérateur linéarisé autour de la solution triviale pour la fonctionnelle $G = (G_1, G_2)$

$$DG(\lambda, 0, 0)(h_1, h_2)(w) = \sum_{n \geq 1} M_{nm}(\lambda) \begin{pmatrix} a_{1,n} \\ a_{2,n} \end{pmatrix} e_{nm}$$

où $e_n = \text{Im}(\bar{w}^n)$ et pour tout $n \geq 1$ on a

$$M_n(\lambda) = \begin{pmatrix} n\lambda - 1 - nb^2 & b^{n+1} \\ -b^n & b(n\lambda - n + 1) \end{pmatrix}.$$

Soit $m \geq 3$, on rappelle que b_m^* désigne l'unique solution dans $(0, 1)$ de l'équation (1.1.6) et que dans ce cas la valeur propre est double. Pour tout $b \in [0, b_m^*)$, les valeurs propres de M_n sont simples et sont données par

$$\lambda_n^\pm = \frac{1+b^2}{2} \pm \frac{1}{n}\sqrt{\Delta_n(b)}$$

avec

$$\Delta_n(b) = \left(\frac{1-b^2}{2}n - 1 \right)^2 - b^{2n} > 0.$$

Notre stratégie est de reprendre la preuve du théorème de Crandall-Rabinowitz qui a été développée dans la section 1.2.1 en effectuant un développement de la fonctionnelle autour de la solution triviale. Cependant pour pouvoir prouver l'existence de la boucle dans le diagramme de bifurcation nous aurons besoin d'aller à l'ordre deux. En effet, le terme linéaire dégénère pour le cas critique et on ne peut pas espérer un résultat d'existence uniforme en b si l'on se contente de l'ordre un. On introduit maintenant les notations dans notre cas. Tout d'abord, on peut montrer que

$$\text{Ker}(\partial_f G(\lambda_m^\pm, 0, 0)) = \langle v_m \rangle.$$

Si G est définie sur $\mathbb{R} \times X_m$ et que son espace d'arrivé est Y_m , on peut montrer qu'il existe \mathcal{X}_m un sous-espace fermé de X_m tel que

$$X_m = \langle v_m \rangle \oplus \mathcal{X}_m.$$

De plus si on note \mathcal{Y}_m l'image de $\partial_f G(\lambda_m^\pm, 0, 0)$, on peut montrer qu'elle est de codimension un dans Y_m et qu'on peut écrire la décomposition suivante

$$Y_m = \langle \mathbb{W}_m \rangle \oplus \mathcal{Y}_m.$$

On introduit donc nos deux projecteurs utilisés dans la réduction de Lyapunov-Schmidt

$$P : X_m \mapsto \langle v_m \rangle \quad \text{et} \quad Q : Y_m \mapsto \langle \mathbb{W}_m \rangle.$$

Maintenant, pour $f = (f_1, f_2) \in X_m$, on utilise la décomposition

$$f = g + k \quad \text{avec} \quad g = Pf \quad \text{et} \quad k = (Id - P)f.$$

L'équation de la V-state (1.2.12) est donc équivalente au système

$$F_1(\lambda, g, k) \triangleq (Id - Q)G(\lambda, g + k) = 0 \quad \text{et} \quad QG(\lambda, g + k) = 0.$$

On montre qu'on peut appliquer le théorème des fonctions implicites à F_1 et que les solutions de l'équation $F_1(\lambda, g, k) = 0$ sont localement décrites autour du point $(\lambda_m^\pm, 0)$ par la paramétrisation $k = \varphi(\lambda, g)$ avec

$$\varphi : \mathbb{R} \times \langle v_m \rangle \rightarrow \mathcal{X}_m$$

qui est régulière. Finalement résoudre l'équation de la V-state près de $(\lambda_m^\pm, 0)$ est équivalent à résoudre

$$QG(\lambda, tv_m + \varphi(\lambda, tv_m)) = 0. \tag{1.2.13}$$

En utilisant un développement de Taylor à l'ordre un, on montre que résoudre (1.2.13) est équivalent à résoudre l'équation réduite de bifurcation

$$F_2(\lambda, t) \triangleq \int_0^1 Q\partial_f G(\lambda, stv_m + \varphi(\lambda, stv_m))(v_m + \partial_g \varphi(\lambda, stv_m)v_m)ds = 0.$$

Contrairement à la preuve de Crandall-Rabnowitz où un développement de F_2 à l'ordre un autour de $(\lambda^\pm, 0)$ suffit, nous avons eu besoin de calculer le développement à l'ordre deux. Après de nombreux calculs techniques nous obtenons

$$F_2(\lambda, t) = a_m(b)(\lambda - \lambda_m^+) + c_m(b)(\lambda - \lambda_m^+)^2 + d_m(b)t^2 + ((\lambda - \lambda_m^+)^2 + t^2)\varepsilon(\lambda, t)$$

avec

$$\lim_{(\lambda, t) \rightarrow (\lambda_m^+, 0)} \varepsilon(\lambda, t) = 0.$$

On peut montrer qu'il existe b_m tel que pour tout $b \in (b_m, b_m*)$ on a

$$a_m(b) < 0, c_m(b) > 0 \text{ et } d_m(b) > 0.$$

Finalement, les zéros de F_2 sont sur une ellipse perturbée. On montre qu'ils peuvent être paramétrisés par une courbe de Jordan régulière en appliquant le théorème des fonctions implicites et qu cette courbe possède deux points d'intersections avec l'axe des réels. Ces points d'intersections correspondent à des V-states m-symétriques donc on en déduit que le deuxième point d'intersection correspond à la solution triviale $(\lambda_m^-, 0)$ ce qui implique la formation de boucles dans le diagramme de bifurcation.

1.2.4 Existence de V-states pour les équations shallow water quasi-géostrophiques et étude des perturbations du diagramme de bifurcation.

L'objectif de ce chapitre est de prouver l'existence de V-states pour le modèle shallow water quasi-géostrophique dont on rappelle les équations

$$\begin{cases} \partial_t q + v \cdot \nabla q = 0, \quad (t, x) \in \mathbb{R}_+ \times \mathbb{R}^2, \\ v = -\nabla^\perp (-\Delta + \varepsilon^2)^{-1} q, \\ q|_{t=0} = q_0 \end{cases} \quad (1.2.14)$$

avec $\varepsilon \in \mathbb{R}$. On va de plus étudier le comportement local du diagramme de bifurcation pour des faibles amplitudes en ε et voir les différences par rapport au diagramme obtenu pour Euler. Dans un premier temps nous avons prouvé l'existence de V-states simplement connexes obtenues en bifurquant du disque à ε fixé. Nous avons également montré un résultat d'existence uniforme en ε pour ε dans un voisinage de zéro. Pour montrer l'existence à ε fixé on utilise le théorème de Crandall-Rabinowitz classique tandis que l'existence uniforme requiert une version modifiée où le paramètre est pris en compte. Dans tous les cas, nous devons réécrire les équations (1.2.14) comme précédemment et on montre qu'elles sont équivalentes à: pour tout $w \in \mathbb{T}$

$$\begin{aligned} G(\varepsilon, \Omega, f)(w) &\triangleq \operatorname{Im} \left\{ \Omega \Phi(w) \overline{\Phi'(w)} \bar{w} - \overline{\Phi'(w)} \bar{w} \int_{\mathbb{T}} \Phi'(\tau) K_0^\varepsilon(|\Phi(w) - \Phi(\tau)|) d\tau \right\} \\ &= 0 \end{aligned} \quad (1.2.15)$$

avec

$$K_0^\varepsilon(x) \triangleq K_0(|\varepsilon|x) + \log(|\varepsilon|/2)$$

où K_0 désigne la fonction de Bessel modifiée de deuxième espèce d'ordre zéro. Son expression est la suivante, voir [69, p. 79-80],

$$K_0(z) = -\log\left(\frac{z}{2}\right) I_0(z) + \sum_{m=0}^{\infty} \frac{(\frac{z}{2})^{2m}}{(m!)^2} \psi(m+1), \quad K'_0(z) = -K_1(z), \quad (1.2.16)$$

avec

$$\psi(1) = -\gamma \quad \text{and} \quad \forall m \in \mathbb{N}^*, \quad \psi(m+1) = \sum_{k=1}^m \frac{1}{k} - \gamma.$$

Le noyau a été additionné d'une constante pour tuer la singularité en ε et obtenir une meilleure régularité en cette variable mais cette astuce ne change rien aux équations. On peut montrer que pour toute valeur de ε , le disque est une poche tournante pour n'importe quelle vitesse, en effet, pour tout $\Omega \in \mathbb{R}$ et pour tout $w \in \mathbb{T}$ on a

$$G(\varepsilon, \Omega, 0)(w) = 0.$$

On va donc considérer des perturbations du disques,

$$\Phi(w) = w + f(w) = w + \sum_{n=0}^{+\infty} a_n \bar{w}^n.$$

Il nous a fallu calculer l'opérateur linéarisé autour du disque et trouver une expression compacte. Contrairement au modèle d'Euler, le noyau n'est pas explicite et nous avons dû faire appel aux fonctions de Bessels modifiées de deuxième espèce d'ordre m , I_m et K_m , pour $m \in \mathbb{N}^*$. On rappelle leurs expressions,

$$I_m(z) = \sum_{n=0}^{+\infty} \frac{\left(\frac{z}{2}\right)^{m+2n}}{n! \Gamma(m+n+1)}, \quad |\arg(z)| < \pi$$

et

$$\begin{aligned} K_n(z) &= (-1)^{n+1} \sum_{m=0}^{+\infty} \frac{\left(\frac{z}{2}\right)^{n+2m}}{m!(n+m)!} \left(\log\left(\frac{z}{2}\right) - \frac{1}{2}\psi(m+1) - \frac{1}{2}\psi(n+m+1) \right) \\ &\quad + \frac{1}{2} \sum_{m=0}^{n-1} \frac{(-1)^m (n-m-1)!}{m! \left(\frac{z}{2}\right)^{n-2m}}. \end{aligned}$$

L'identité clé pour trouver une forme sympathique de l'opérateur linéarisé est la représentation intégrale de Nicholson pour $I_n(z)K_n(z)$, voir [69, p. 441] : pour $n \in \mathbb{N}$

$$I_n(z)K_n(z) = \frac{2(-1)^n}{\pi} \int_0^{\frac{\pi}{2}} K_0(2z \cos \theta) \cos(2n\theta) d\theta. \quad (1.2.17)$$

On considère maintenant

$$h(w) = \sum_{n=0}^{+\infty} a_n \bar{w}^n$$

et on obtient que

$$D_f G(\varepsilon, \Omega, 0)(h)(w) = \sum_{n=0}^{+\infty} a_n (n+1) (\Omega_{n+1}(\varepsilon) - \Omega) e_{n+1}, \quad \text{avec } e_n = \text{Im}(w^n)$$

avec

$$\Omega_m(\varepsilon) = I_1(|\varepsilon|)K_1(|\varepsilon|) - I_m(|\varepsilon|)K_m(|\varepsilon|).$$

On montre que la suite $(I_m(|\varepsilon|)K_m(|\varepsilon|))_{m \geq 0}$ est strictement décroissante et on en déduit la stricte monotonie de la suite $(\Omega_m)_{m \geq 2}$ qui nous permet de conclure sur les valeurs de Ω qui induisent un noyau unidimensionnel. Les autres conditions du théorème de bifurcation sont vérifiées. Pour l'existence uniforme en ε , il suffit de vérifier que la fonctionnelle a une certaine régularité en la variable ε . Le résultat que l'on a démontré est le suivant

Theorem 1.2.5. *Soit $\varepsilon \in \mathbb{R}$ and $\alpha \in (0, 1)$. Alors pour tout entier $m \geq 1$ il existe une courbe de V-states m-symétriques obtenue en bifurquant du disque unité à la vitesse angulaire*

$$\Omega_m(\varepsilon) = I_1(|\varepsilon|)K_1(|\varepsilon|) - I_m(|\varepsilon|)K_m(|\varepsilon|).$$

De plus, l'existence est uniforme en ε , pour ε assez petit, au sens suivant. Il existe $a > 0$ et des fonctions continues $\varphi : (-a, a)^2 \rightarrow \mathbb{R}$, $\psi : (-a, a)^2 \rightarrow C^{1+\alpha}(\mathbb{T})$ qui vérifient

$$\varphi(0, 0) = \Omega_m(0) = \frac{m-1}{2m}, \quad \psi(0, 0) = 0$$

tel que

$$\Omega = \varphi(\varepsilon, t), \quad \psi(\varepsilon, t, w) = \sum_{n \geq 2} a_{nm-1}(\varepsilon, t) \bar{w}^{nm-1}$$

et

$$G(\varepsilon, \varphi(\varepsilon, t), w + t\bar{w}^{m-1} + t\psi(\varepsilon, t, w)) = 0, \quad \forall (\varepsilon, t) \in (-a, a)^2, \quad \forall w \in \mathbb{T}.$$

Remark 1.2.6. On peut commencer par remarquer que le cas $m = 1$ est trivial, il correspond à la translation du disque unité. De plus, la régularité démontrée n'est pas optimale. Le noyau considéré étant une perturbation régulière du logarithme, on suppose que l'on peut montrer l'analyticité de l'application conforme comme dans le cas d'Euler, voir [8].

Remark 1.2.7. On sait que pour les équations d'Euler, le diagramme de bifurcation dans le cas des V-states simplement connexes est constituée de courbes pitchforks obtenues en bifurquant des disques de Rankine pour chaque symétrie m . Notre théorème montre que localement cette structure est préservée pour n'importe quelle perturbation en ε et on ne perd pas de symétries. On verra plus loin que ce n'est plus le cas lorsqu'on essaye de construire de nouvelles solutions en perturbant les ellipses de Kirchhoff.

Dans une deuxième partie, nous nous sommes intéressées à la branche des solutions 2-symétriques et nous avons chercher à comprendre comment cette branche allait être perturbée lorsque l'on fait varier ε . Nos résultats sont en liens avec des travaux plus généraux liés à la bifurcation imparfaite qui consiste à étudier comment la structure géométrique du diagramme de bifurcation varie en fonction d'un paramètre. C'est un sujet nouveau dans l'étude des V-states et on a montré quelques résultats intéressants. On connaît explicitement la branche 2-symétrique pour Euler qui est constituée des ellipses de Kirchhoff. D'autres branches de V-states bifurquent à partir des ellipses avec de manière alternée la symétrie deux et la symétrie un. Numériquement, on observe que pour de faibles valeurs de ε la branche 2-symétrique pert son caractère connexe et devient fragmentée en une famille dénombrables de composantes connexes. Nous avons réussi à prouver partiellement ce résultat. Pour commencer, nous avons montré que pour ε suffisamment petit nous pouvions fabriquer des solutions qui allaient être des perturbations des ellipses de Kirchhoff. Pour se faire on commence par utiliser que les ellipses sont des solutions triviales pour le modèle d'Euler, c'est-à-dire que

$$G\left(0, \frac{1-Q^2}{4}, \alpha_Q\right) = 0, \quad \forall Q \in (0, 1)$$

où $\alpha_Q : w \in \mathbb{T} \mapsto w + Q\bar{w}$ est la paramétrisation conforme de l'ellipse centrée en zéro de demi-axes $\pm Q$ avec $Q \in [0, 1]$. On sait que l'on peut construire des solutions pour ε nul en perturbant l'ellipse, c'est-à-dire que notre application conforme prends la forme suivante

$$\Phi(w) = \alpha_Q(w) + f(w) = w + \sum_{n=2}^{+\infty} f_n w^n, \quad \text{avec } f_n \in \mathbb{R}$$

et on voudrait savoir si le résultat persiste pour ε non nul. Pour se faire on introduit maintenant

$$F(\varepsilon, Q, f) \triangleq G\left(\varepsilon, \frac{1-Q^2}{4}, \alpha_Q + f\right).$$

Notre but est de résoudre

$$F(\varepsilon, Q, f) = 0 \tag{1.2.18}$$

en appliquant le théorème des fonctions implicites. On sait que

$$F(0, Q, 0) = 0, \quad \forall Q \in [0, 1].$$

Soit $m \geq 3$ un entier et on désigne par Q_m l'unique solution dans $[0, 1)$ de l'équation

$$1 + Q^m - \frac{1 - Q^2}{4}m = 0.$$

Ils ont montré dans [34] que la suite $(Q_m)_{m \geq 3}$ est strictement croissante avec

$$\lim_{m \rightarrow +\infty} Q_m = 1.$$

Nous allons introduire deux ensembles distincts,

$$\mathcal{S}_{reso} \triangleq \{Q_{2m}, m \geq 2\} \text{ et } \mathcal{S}_{Nreso} \triangleq \{Q_{2m+1}, m \geq 1\}$$

qui sont appelés ensemble de résonnance et de non résonnance et qui vont avoir des comportements différents par la suite. Le calcul de l'opérateur linéarisé pour Euler autour de l'ellipse a été fait dans [34], on rappelle sa forme ici. Si $h(w) = \sum_{n \geq 2} a_n w^n$ alors

$$\mathcal{L}_Q h \triangleq D_f F(0, Q, 0)h = \frac{1}{2} \sum_{n \geq 1} g_{n+1} e_n; \quad e_n(w) = \text{Im}(w^n),$$

avec

$$\begin{aligned} g_2 &= \frac{1}{2}(1 + Q)^2 a_2, \\ g_3 &= 2Q^2 a_3, \\ g_{n+1} &= \left(1 + Q^n - \frac{1 - Q^2}{2}n\right)(a_{n+1} - Qa_{n-1}), \quad \forall n \geq 3. \end{aligned}$$

De plus, le noyau de \mathcal{L}_Q est non trivial si et seulement si $Q = Q_m \in \mathcal{S}_{reso} \cup \mathcal{S}_{Nreso}$ et dans ce cas il est unidimensionnel engendré par le vecteur

$$v_m(w) = \frac{w^{m+1}}{1 - Qw^2}.$$

Nous avons étudié la structure du diagramme de bifurcation loin de l'ensemble \mathcal{S}_{reso} . Plus précisément, soit $m \in \mathbb{N}$, on fixe $\delta < \frac{Q_{2m+2} - Q_{2m}}{2}$ et on considère $I_{m,\delta} = [Q_{2m} + \delta, Q_{2m+2} - \delta]$. Nous avons commencé par prouver la stabilité de la branche des ellipses de Kirchhoff en montrant qu'il existe une branche de solution, pour ε assez petit, qui vit près de cette branche. On commence par choisir l'espace dans lequel vit la perturbation pour obtenir une solution 2-symétrique de telle sorte que le noyau du linéarisé autour du point $(0, Q, 0)$ pour Q dans l'ensemble $I_{m,\delta}$ est filtré. Pour tout $Q \in I_{m,\delta}$, le noyau de $D_f F(0, Q, 0)$ est trivial si $Q \neq Q_{2m+1}$ et pour $Q = Q_{2m+1}$ il est engendré par $v_{2m+1}(w)$. On choisit donc un espace pour la perturbation qui ne contient pas ce vecteur en la prenant sous la forme

$$f(w) = \sum_{n \geq 2} h_n w^{2n+1}.$$

Dans ce cas, pour tout $Q \in I_{m,\delta}$, \mathcal{L}_Q est injective. Ensuite, on montre la surjectivité de la différentielle et on peut appliquer le théorème des fonctions implicites pour construire nos solutions. Le théorème que nous avons démontré est le suivant

Theorem 1.2.8. *On considère l'équation de la V-state (1.2.18) et soit $m \in \mathbb{N}^*$ et $\delta < \frac{Q_{2m+2} - Q_{2m}}{2}$. On définit $I_{m,\delta} = [Q_{2m} + \delta, Q_{2m+2} - \delta]$. Alors il existe $\varepsilon_0 > 0$ et une fonction*

$$\begin{aligned} f: [-\varepsilon_0, \varepsilon_0] \times I_{m,\delta} &\longrightarrow X_2 \\ (\varepsilon, Q) &\longmapsto f(\varepsilon, Q). \end{aligned}$$

de classe C^1 tel que

$$F(\varepsilon, Q, f(\varepsilon, Q)) = 0, \quad \forall (\varepsilon, Q) \in [-\varepsilon_0, \varepsilon_0] \times I_{m,\delta}.$$

En particulier, la courbe $Q \in I_{m,\delta} \mapsto \alpha_Q + f(\varepsilon, Q)$ paramétrise des V-states deux-symétriques qui vivent près des ellipses de Kirchhoff

Maintenant que nous avons prouvé l'existence d'une branche 2-symétrique pour ε petit qui est proche de celle d'Euler, on va prouver qu'on peut bifurquer de cette branche de solutions constituées d'ellipses perturbées pour construire des solutions un-symétrique près de l'ensemble \mathcal{S}_{reso} . Pour le prouver, nous avons une nouvelle fois utilisé la réduction de Lyapuno-Schmidt pour construire nos solutions. On sait que

$$\text{Ker}(\partial_f F(0, Q_m, 0)) = \langle v_m \rangle \text{ avec } v_m(w) = \frac{w^{m+1}}{1 - Qw^2}.$$

Si X désigne l'espace dans lequel vit la perturbation et que l'espace d'arrivé de F est Y , on peut montrer qu'il existe \mathcal{X} un sous-espace fermé de X tel que

$$X = \langle v_m \rangle \oplus \mathcal{X}.$$

De plus si on note \mathcal{Y} l'image de $D_f F(0, Q_m, 0)$, on peut montrer qu'elle est de codimension un dans Y et qu'on peut écrire la décomposition suivante

$$Y = \langle \mathbb{W}_m \rangle \oplus \mathcal{Y}.$$

On introduit donc nos deux projecteurs utilisés dans la réduction de Lyapunov-Schmidt

$$P : X \mapsto \langle v_m \rangle \text{ et } \Pi : Y \mapsto \langle \mathbb{W}_m \rangle.$$

Maintenant, pour $f \in X$, on utilise la décomposition

$$f = sv_m + g \text{ avec } g \in \mathcal{X} \text{ et } Pf = sv_m.$$

On montre que (1.2.18) est équivalente au système

$$F_1(\varepsilon, Q, s, g) \triangleq (Id - \Pi)F(\varepsilon, Q, sv_m + g) = 0 \quad (1.2.19)$$

et

$$F_2(\varepsilon, Q, s, g) \triangleq \Pi F(\varepsilon, Q, sv_m + g) = 0. \quad (1.2.20)$$

Comme pour les preuves précédentes, on applique le théorème des fonctions implicites à F_1 autour du point $(0, Q_m, 0, 0)$ et on obtient une paramétrisation de g par une application φ qui est de classe \mathcal{C}^1 ,

$$g = \varphi(\varepsilon, Q, s) \text{ et par unicité } \varphi(\varepsilon, Q, 0) = f(\varepsilon, Q).$$

On montre ensuite que l'équation (1.2.20) est équivalente à

$$\hat{g}(\varepsilon, Q, s) = 0$$

avec

$$\hat{g}(\varepsilon, Q, s) \triangleq \begin{cases} \frac{F_2(\varepsilon, Q, s, \varphi(\varepsilon, Q, s))}{s}, & s \neq 0 \\ \Pi \partial_f F(\varepsilon, Q, \varphi(\varepsilon, Q, 0))(v_m + \partial_s \varphi(\varepsilon, Q, 0)), & s = 0. \end{cases} \quad (1.2.21)$$

puis on applique le théorème des fonctions implicites à \hat{g} pour obtenir nos solutions. Plus précisément, le théorème démontré est le suivant,

Theorem 1.2.9. *Soit $m \geq 3$ un entier impair. Alors il existe ε_0 tel que pour tout $\varepsilon \in [-\varepsilon_0, \varepsilon_0]$, il existe une courbe de V-states un-symétriques obtenue en bifurquant au point $Q_{\varepsilon, m}$ proche de Q_m de la branche deux-symétrique construite au théorème 1.2.8.*

Le dernier résultat que nous avons démontré est l'éclatement de la branche deux-symétrique en plusieurs composantes connexes dans le diagramme de bifurcation pour un ε petit non nul qui a été observé numériquement, voir figure 1.2.4

L'éclatement des singularités semble être vrai pour l'ensemble \mathcal{S}_{reso} mais nous ne le montrons analytiquement que pour Q_4 . De plus nous avons réussi à prouver la séparation des deux branches uniquement localement autour de Q_4 . Le résultat est le suivant,

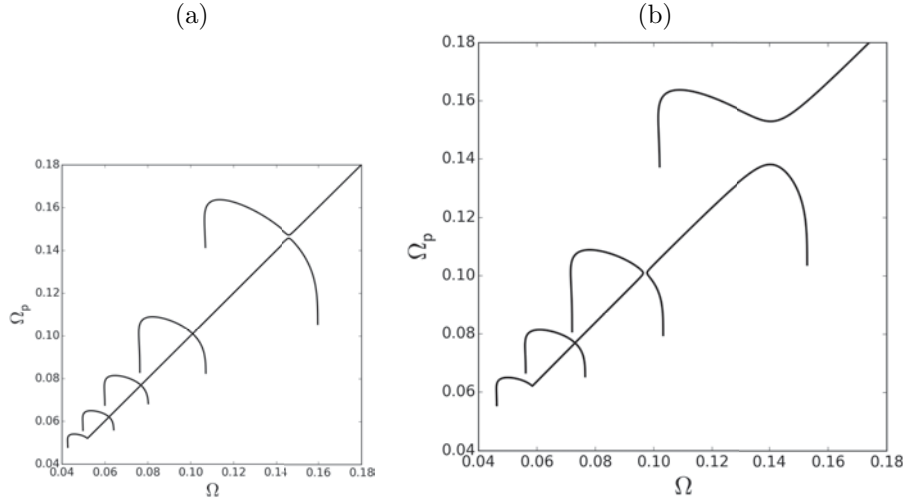


Figure 1.3: Eclatement de la branche deux-fold quand $\varepsilon = 0.01$ dans (a) et $\varepsilon = 0.1$ dans (b)

Theorem 1.2.10. *On considère l'équation de la V-state donnée par (1.2.18). Alors il existe $\varepsilon_0 > 0$ tel que pour tout $\varepsilon \in (-\varepsilon_0, \varepsilon_0) \setminus \{0\}$ il existe r_ε tel que l'ensemble*

$$\{F(\varepsilon, Q, f) = 0, |Q - Q_4| < r_\varepsilon, f \in X_2, \|f\|_{C^{1+\alpha}} < r_\varepsilon\}$$

est donné par l'union de deux courbes unidimensionnelles disjointes.

Pour démontrer ce théorème on va faire un développement de l'équation (1.2.18) jusqu'à l'ordre deux. La première subtilité est de faire disparaître la singularité logarithmique en ε au second ordre en le faisant rentrer dans le terme de rotation et il n'a donc plus de contribution en tant que terme non linéaire. Pour cela on commence par réécrire le noyau de la manière suivante pour tout $x > 0$

$$K_0^\varepsilon(x) = \psi(1) - \log(x) - \frac{\varepsilon^2}{4}x^2 \log(x) + \frac{\varepsilon^2}{4}(\psi(2) - \log(|\varepsilon|/2))x^2 + \varepsilon^4 \log \varepsilon \mathcal{R}^\varepsilon(x)$$

avec \mathcal{R}^ε qui est au moins de classe C^3 dans la variable x et analytique en ε . On note de plus

$$G_E(\Omega, \Phi) = G(0, \Omega, \Phi)$$

avec G qui est défini par (1.1.20). On utilise la nouvelle forme du noyau pour obtenir une nouvelle expression pour $G(\varepsilon, \Omega, \Phi)$.

$$G(\varepsilon, \Omega, \Phi) = -G_E(\Omega_\varepsilon, \Phi) + \frac{\varepsilon^2}{4} \operatorname{Im}\{G_1(\Phi)\} + \varepsilon^4 \log |\varepsilon| \operatorname{Im}\{G_2(\varepsilon, \Phi)\}$$

avec

$$\Omega_\varepsilon \triangleq \Omega + \frac{\varepsilon^2}{4}(\psi(2) - \log(|\varepsilon|/2)) \int_{\mathbb{T}} \overline{\Phi(\tau)} \Phi'(\tau) d\tau,$$

$$G_1(\Phi) \triangleq \overline{w} \overline{\Phi'(w)} \int_{\mathbb{T}} \log(|\Phi(\tau) - \Phi(w)|) |\Phi(\tau) - \Phi(w)|^2 \Phi'(\tau) d\tau$$

et

$$G_2(\varepsilon, \Phi) \triangleq -\overline{w} \overline{\Phi'(w)} \int_{\mathbb{T}} \Phi'(\tau) \mathcal{R}^\varepsilon(|\Phi(\tau) - \Phi(w)|) d\tau.$$

Comme avant, on cherche des solutions qui sont des perturbations de l'ellipse

$$\Phi = \alpha_Q + f, f \in X_2,$$

et on impose la condition

$$\Omega_\varepsilon = \frac{1 - Q^2}{4}.$$

Finalement l'équation de la V-state est équivalente à

$$\hat{F}(\varepsilon, \Omega, \Phi) \triangleq F_E(Q, f) + \frac{\varepsilon^2}{4} \operatorname{Im}\{F_1(Q, f)\} + \varepsilon^4 \log |\varepsilon| \operatorname{Im}\{F_2(\varepsilon, Q, f)\} = 0$$

avec

$$F_E(Q, f) \triangleq -G_E((1 - Q^2)/4, \alpha_Q + f), \quad F_1(Q, f) \triangleq G_1(\alpha_Q + f)$$

et

$$F_2(\varepsilon, Q, f) \triangleq G_2(\varepsilon, \alpha_Q + f).$$

Après cette modification faîte, notre fonctionnelle est plus régulière en ε et on développe notre équation à l'ordre deux après avoir une nouvelle fois utilisé la réduction de Lyapunov-Schmidt. On écrit notre perturbation sous la forme $f = sv_4 + g$ comme précédemment, g est obtenue en appliquant le théorème des fonctions implicites et on se ramène à devoir résoudre une équation du type

$$\psi(\varepsilon, Q, s) = [a\varepsilon^2 + bs(Q - Q_4) + cs^2 + \tilde{\varepsilon}(\varepsilon, Q, s)] e_4$$

avec

$$a > 0, b > 0 \text{ et } c < 0.$$

Quitte à faire des changements de variables, cela revient à résoudre

$$a\varepsilon^2 - \tilde{c}X^2 + \tilde{b}\mathbf{Q}^2 + \hat{\varepsilon}(\varepsilon, \mathbf{Q}, X) = 0$$

avec tous les paramètres positifs. Nos solutions sont cherchées sous la forme d'une perturbation de la solution sans le petit terme,

$$X = \pm \sqrt{\frac{a}{\tilde{c}}\varepsilon^2 + \frac{\tilde{b}}{\tilde{c}}\mathbf{Q}^2 + y}$$

et la perturbation est obtenue dans les deux cas en montrant qu'elle est solution d'un problème de point fixe. Pour obtenir la contraction de l'application, on va devoir utiliser que notre fonctionnelle possède une certaine régularité en ε . C'est pour cela que la partie singulière en ε a dû être masquée. Ensuite on montre que nos deux courbes $\mathbf{Q} \mapsto \sqrt{\frac{a}{\tilde{c}}\varepsilon^2 + \frac{\tilde{b}}{\tilde{c}}\mathbf{Q}^2 + y_1(\mathbf{Q})}$ et $\mathbf{Q} \mapsto -\sqrt{\frac{a}{\tilde{c}}\varepsilon^2 + \frac{\tilde{b}}{\tilde{c}}\mathbf{Q}^2 + y_2(\mathbf{Q})}$ ne s'intersectent jamais ce qui montre la séparation de la branche en deux parties distinctes.

Chapter 2

Relative equilibria with holes for the surface quasi-geostrophic equations

*Rendre l'âme? D'accord, mais à
qui?*

— *Pensées, provoc et autres
volutes,*
Serge GAINSBOURG

This chapter is the subject of the following publication:

Renault, Coralie, *Relative equilibria with holes for the surface quasi-geostrophic equations.*

Journal of Differential Equations, 263, 2017, no. 1, 567-614.

Abstract. We study the existence of doubly connected rotating patches for the inviscid surface quasi-geostrophic equation left open by de la Hoz, Hassainia and Hmidi in 2016 in [30]. By using the approach proposed in 2016 by Castro, Córdoba and Gómez-Serrano in [8] we also prove that close to the annulus the boundaries are actually analytic curves.

2.1 Introduction

In this paper we investigate the surface quasi-geostrophic (SQG) model which describes the evolution of the potential temperature θ according to the transport equation,

$$\begin{cases} \partial_t \theta + u \cdot \nabla \theta = 0, & (t, x) \in \mathbb{R}_+ \times \mathbb{R}^2, \\ u = -\nabla^\perp (-\Delta)^{-\frac{1}{2}} \theta, \\ \theta|_{t=0} = \theta_0 \end{cases} \quad (2.1.1)$$

where u refers to the velocity field and $\nabla^\perp = (-\partial_2, \partial_1)$. The operator $(-\Delta)^{-\frac{1}{2}}$ is defined as follows

$$(-\Delta)^{-\frac{1}{2}} \theta(x) = \frac{1}{2\pi} \int_{\mathbb{R}^2} \frac{\theta(y)}{|x-y|} dy.$$

This model is used to study the atmospheric circulations near the tropopause and the ocean dynamics in the upper layers, see for instance [27, 39, 45]. This nonlinear transport equation is more singular than the vorticity equation for the 2D Euler equations where the connection between the velocity and the vorticity is given by the Biot-Savart law

$$u = -\nabla^\perp (-\Delta)^{-1} \theta.$$

Another model appearing in the literature which interpolates between the (SQG) and Euler equations is the $(\text{SQG})_\alpha$ model, see [15], where the velocity is given by

$$u = -\nabla^\perp (-\Delta)^{-1+\frac{\alpha}{2}} \theta, \quad \alpha \in (0, 2).$$

These equations have been intensively studied during the past few decades and abundant results have been established in different topics such as the well-posedness problem or the vorticity dynamics. For instance, it is well-known that for Euler equations when the initial data θ_0 belongs to $L^\infty \cap L^1$ then there is a unique global weak solution $\theta \in L^\infty(\mathbb{R}^+; L^\infty \cap L^1)$. This result is due to Yudovich, see for instance [72]. This theory fails for $\alpha > 0$ due to the singularity of the kernel. However, the local well-posedness can be elaborated in the sub-class of the vortex patches as it was shown in [11] and [26]. Recall that an initial datum is a vortex patch when it takes the form χ_D , which is the characteristic function of a smooth bounded domain D . The solutions keep this structure for a short time, that is, $\theta(t) = \chi_{D_t}$ where D_t is another domain describing the deformation of the initial one in the complex plane. The global existence of these solutions is an outstanding open problem except for Euler equations in which case Chemin proved in [13] the persistence of smooth regularity globally in time. Note that a significant progress towards settling this problem, for α enough close to zero, has been done recently in [44]. Another direction related to the construction of periodic global solutions through the bifurcation theory has been recently investigated. They correspond to rotating patches also called V-states or relative equilibria. In this setting the domain of the patch is explicitly given by a pure rotation with uniform angular velocity, that is, $D_t = R_{x_0, \Omega t} D$ where $R_{x_0, \Omega t}$ is the planar rotation with the center x_0 and the angle Ωt ; the parameter Ω is the angular velocity. The first example of rotating patches goes back for Euler equation to Kirchhoff who discovered that an ellipse of semi-axes a and b rotates uniformly with the angular velocity $\Omega = \frac{ab}{(a^2+b^2)}$; see for instance [4, p304] and [46, p 232]. One century later,

Deem and Zabusky gave in [17] numerical evidence of the existence of the V-states with m -fold symmetry for each integer $m \in \{2, 3, 4, 5\}$ and afterwards Burbea gave an analytically proof in [6]. The main idea of the demonstration is to reformulate the V-states equations with the contour dynamics equations, using the conformal parametrization Φ , and to implement some bifurcation arguments. The bifurcation from the ellipses to countable curves of non symmetric rotating patches was discussed numerically and analytically in [8, 37, 40]. On the other hand we point out that the extension of this study to the $(\text{SQG})_\alpha$ was successfully carried out in [7, 29]. Moreover the boundary regularity was achieved in [7, 8, 37].

The existence of V-states with one hole, also called doubly connected V-states, has been recently explored in [30, 33]. To fix the terminology, a patch $\theta_0 = \chi_D$ is said to be doubly connected if the domain $D = D_1 \setminus D_2$ with D_1 and D_2 being two simply connected bounded domains such that the closure $\overline{D_2}$ is strictly embedded in D_1 . The first result on the existence of m -fold symmetric V-states bifurcating from the annulus $\mathbb{A}_b = \{z; b < |z| < 1\}$ is established in [30]. Roughly speaking, it is shown that for higher modes m there exist two branches of m -fold symmetric doubly connected V-states bifurcating from the annulus at explicit eigenvalues Ω_m^\pm . Similar result with more involved computations was obtained for $(\text{SQG})_\alpha$ model with $\alpha \in [0, 1)$, see [33]. Actually, it is shown that for given $\alpha \in [0, 1)$ and $b \in (0, 1)$, there exists $N \in \mathbb{N}$ such that for each $m \geq N$ there exists two curves of m -fold doubly connected V-states bifurcating from the annulus \mathbb{A}_b at the angular velocities

$$\Omega_m^\pm = \frac{1}{2} ((1 - b^{-\alpha}) S_m + (1 - b^2) \Lambda_1(b)) \pm \frac{1}{2} \sqrt{\Delta_m(\alpha, b)}$$

with

$$\Delta_m(\alpha, b) = ((b^{-\alpha} + 1) S_m - (1 + b^2) \Lambda_1(b))^2 - 4b^2 \Lambda_m^2(b),$$

$$\Lambda_m(b) \triangleq \frac{1}{b} \int_0^{+\infty} J_m(bt) J_m(t) \frac{dt}{t^{1-\alpha}}$$

and

$$S_m \triangleq \Lambda_1(1) - \Lambda_m(1).$$

Where J_m refers to the Bessel function of the first kind.

The main goal of this paper is to study the same problem for the SQG equation (4.1.1) corresponding to $\alpha = 1$. Our aim is twofolds. First we shall establish the existence of doubly connected V-states and second we shall prove that the boundary is analytic. The main result of this paper reads as follows.

Theorem 2.1.1. *Let $b \in (0, 1)$, there exists $N \in \mathbb{N}^* \setminus \{1\}$ with the following property: For any integer $m \geq N$ there exist two curves of m -fold doubly connected V-states with analytic boundaries for (4.1.1) bifurcating from the annulus $\mathbb{A}_b = \{z \in \mathbb{C}, b < |z| < 1\}$ at the angular velocities*

$$\Omega_m^\pm = \frac{1}{2} \left[\left(1 - \frac{1}{b} \right) S_m + (1 - b^2) \Lambda_1(b) \right] \pm \frac{1}{2} \sqrt{\Delta_m(b)} \quad (2.1.2)$$

where S_m, Λ_m and Δ_m are defined above by taking $\alpha = 1$.

- For $\alpha = 1$, the expression of S_m can be simplified and takes the form

$$S_n = \frac{2}{\pi} \sum_{k=1}^{n-1} \frac{1}{2k+1}.$$

- As we shall see later in the proofs, the number N is defined as the smallest integer such that

$$S_N > b \left(\frac{1+b^2}{1+b} \Lambda_1(b) + \frac{2b}{1+b} \Lambda_N(b) \right).$$

- Our results are in line with results foretold in [30].

Now we shall sketch the proof of Theorem 4.5.1 which relies on Crandall-Rabinowitz's theorem applied in suitable Banach spaces that capture the analyticity of the boundary. We mention that these spaces were introduced in [8] in order to study the simply connected V-states. The first step is to write the boundary equations using the exterior conformal parametrization of the domains D_1 and D_2 . These conformal mappings $\Phi_j : \mathbb{D}^c \rightarrow D_j^c$ have the following structure

$$\forall |z| > 1, \Phi_1(z) = z + \sum_{n \in \mathbb{N}} \frac{a_n}{z^n} \quad \text{and} \quad \Phi_2(z) = bz + \sum_{n \in \mathbb{N}} \frac{c_n}{z^n}.$$

with \mathbb{D} being the unit closed disc. The Fourier coefficients are supposed to be real meaning that we look only for the V-states which are symmetric with respect to the real axis. Notice also that when the boundaries are assumed to be enough smooth then the Φ_j admit unique univalent extension up the boundary. We recall from Section 4.4.3 that the boundaries of the V-states are subject to the equations: For $j \in \{1, 2\}$ and $\omega \in \mathbb{T}$

$$\begin{aligned} G_j(\Omega, \Phi_1, \Phi_2)(\omega) &\triangleq \operatorname{Im} \left\{ \left(\Omega \Phi_j(\omega) - S(\Phi_1, \Phi_j)(\omega) + S(\Phi_2, \Phi_j)(\omega) \right) \overline{\Phi'_j(\omega)} \bar{\omega} \right\} \\ &= 0 \end{aligned}$$

with

$$S(\Phi_i, \Phi_j)(\omega) = \int_{\mathbb{T}} \frac{\tau \Phi'_i(\tau) - \omega \Phi'_j(\omega)}{|\Phi_i(\tau) - \Phi_j(\omega)|} \frac{d\tau}{\tau}.$$

To apply the bifurcation arguments we make use of the Banach spaces $X^{k+\log}$ and Y^{k-1} that will be fully described in the subsection 2.3.2. The main difficulty is to show that the functionals G_j send a small neighborhood in $X^{k+\log}$ of the trivial solution $(\operatorname{Id}, b\operatorname{Id})$ to the space Y^{k-1} . This will be done carefully in Section 2.4 where additional regularity properties will also be established. The second step is to compute explicitly the linearized operator of the vectorial functional $G = (G_1, G_2)$ at the annular solution $(\operatorname{Id}, b\operatorname{Id})$. This part is very computational and after using special structures of the Gauss hypergeometric functions we obtain the following compact expression: Given

$$h_1(\omega) = \sum_{n=1}^{+\infty} a_n \bar{\omega}^n \quad \text{and} \quad h_2(\omega) = \sum_{n=1}^{+\infty} c_n \bar{\omega}^n, \quad \omega \in \mathbb{T}$$

we get

$$DG(\Omega, \operatorname{Id}, b\operatorname{Id})(h_1, h_2)(\omega) = \frac{i}{2} \sum_{n \geq 1} (n+1) M_{n+1} \begin{pmatrix} a_n \\ c_n \end{pmatrix} (\omega^{n+1} - \bar{\omega}^{n+1})$$

where the matrix M_n is given for $n \geq 2$ by

$$M_n \triangleq \begin{pmatrix} \Omega - S_n + b^2 \Lambda_1(b) & -b^2 \Lambda_n b \\ b \Lambda_n(b) & b \Omega + S_n - b \Lambda_1(b) \end{pmatrix}.$$

With this explicit formula in hand we find the values of Ω leading to a one dimensional kernel operator. We say throughout this paper that Ω is an eigenvalue if for some n the matrix $M_n(\Omega)$ is not invertible. We also check the full conditions required by the Crandall-Rabinowitz's theorem. This discussion will be investigated in detail in Section 2.5.

In what follows, we will need some notations:

- The unit disc and its boundary will be denoted respectively by \mathbb{D} and \mathbb{T} .
- The disc of r radius and centered in 0 and its boundary will be denoted by \mathbb{D}_r and \mathbb{T}_r .
- We denote by C any positive constant that may change from line to line.

- Let $f : \mathbb{T} \rightarrow \mathbb{C}$ be a continuous function. We define its mean value by,

$$\oint_{\mathbb{T}} f(\tau) d\tau \triangleq \frac{1}{2i\pi} \int_{\mathbb{T}} f(\tau) d\tau,$$

where $d\tau$ stands for the complex integration.

- Let X and Y be two normed spaces. We denote by $\mathcal{L}(X, Y)$ the space of all continuous linear maps $T : X \rightarrow Y$ endowed with its usual strong topology.
- Let Y be a vector space and R be a subspace, then Y/R denotes the quotient space.

2.2 Boundary equations

We intend in this section to write down the equations governing the V-states in the doubly connected case. But before doing that we shall recall the Riemann mapping theorem. To restate this result we need to recall the definition of *simply connected* domains. Let $\widehat{\mathbb{C}} \triangleq \mathbb{C} \cup \{\infty\}$ denote the Riemann sphere, we say that a domain $U \subset \widehat{\mathbb{C}}$ is *simply connected* if the sets U and $\widehat{\mathbb{C}} \setminus U$ are connected.

Theorem 2.2.1 (Riemann Mapping Theorem). *Let \mathbb{D} denote the unit open ball and $U \subset \mathbb{C}$ be a simply connected bounded domain. Then there is a unique bi-holomorphic map called also conformal, $\Phi : \mathbb{C} \setminus \overline{\mathbb{D}} \rightarrow \mathbb{C} \setminus \overline{U}$ taking the form*

$$\Phi(z) = az + \sum_{n \in \mathbb{N}} \frac{a_n}{z^n} \quad \text{with } a > 0.$$

Notice that in this theorem the regularity of the boundary has no effect regarding the existence of the conformal mapping but it contributes in the boundary behavior of the conformal mapping, see for instance [60, 68].

Next, we shall move to the equations governing the boundary of the doubly connected V-states. This can be done in the spirit of the paper [30]. Assume that $\theta_0 = \chi_D$ is a rotating patch with an angular velocity Ω and such that $D = D_1 \setminus D_2$ is a doubly connected domain meaning that D_1 and D_2 are two simply connected bounded domains with $D_2 \subset D_1$. Denote by Γ_1 and Γ_2 their boundaries, respectively. Then following the same lines of [30] we find that the exterior conformal mappings Φ_1 and Φ_2 associated to D_1 and D_2 satisfy the coupled nonlinear equations: For $j \in \{1, 2\}, \omega \in \mathbb{T}$,

$$\begin{aligned} \tilde{G}_j(\Omega, \Phi_1, \Phi_2)(\omega) &\triangleq \operatorname{Im} \left\{ \left(\Omega \Phi_j(\omega) - S(\Phi_1, \Phi_j)(\omega) + S(\Phi_2, \Phi_j)(\omega) \right) \overline{\Phi'_j(\omega)} \bar{\omega} \right\} \\ &= 0 \end{aligned} \tag{2.2.1}$$

with

$$S(\Phi_i, \Phi_j)(\omega) = \oint_{\mathbb{T}} \frac{\tau \Phi'_i(\tau) - \omega \Phi'_j(\omega)}{|\Phi_i(\tau) - \Phi_j(\omega)|} \frac{d\tau}{\tau}.$$

Notice that we aim at finding V-states which are small perturbation of the annulus \mathbb{A}_b with $b \in (0, 1)$ and therefore the conformal mappings take the form,

$$\forall |z| \geq 1, \quad \Phi_1(z) = z + f_1(z) = z + \sum_{n=1}^{+\infty} \frac{a_n}{z^n}$$

and

$$\Phi_2(z) = bz + f_2(z) = bz + \sum_{n=1}^{+\infty} \frac{b_n}{z^n}.$$

We shall introduce the functionals

$$G_j(\Omega, f_1, f_2) \triangleq \tilde{G}_j(\Omega, \Phi_1, \Phi_2) \quad j = 1, 2. \tag{2.2.2}$$

Then equations of the V-states become,

$$\forall \omega \in \mathbb{T}, G_j(\Omega, f_1, f_2)(\omega) = 0, j = 1, 2.$$

Now we can check that the annulus is a rotating patch for any $\Omega \in \mathbb{R}$. Indeed,

$$G_1(\Omega, 0, 0)(\omega) = \text{Im} \left\{ -\bar{\omega} \int_{\mathbb{T}} \frac{\tau - \omega}{|\tau - \omega|} \frac{d\tau}{\tau} + \bar{\omega} \int_{\mathbb{T}} \frac{b\tau - \omega}{|b\tau - \omega|} \frac{d\tau}{\tau} \right\}.$$

Using the change of variable $\tau = \omega\xi$ in the last equation we obtain:

$$G_1(\Omega, 0, 0)(\omega) = \text{Im} \left\{ - \int_{\mathbb{T}} \frac{\xi - 1}{|\xi - 1|} \frac{d\xi}{\xi} + \int_{\mathbb{T}} \frac{b\xi - 1}{|b\xi - 1|} \frac{d\xi}{\xi} \right\}.$$

Now we just observe that each integral is real. In fact using the parametrization $\xi = e^{i\eta}$ one gets,

$$\forall a \in (0, 1], \int_{\mathbb{T}} \frac{a\xi - 1}{|a\xi - 1|} \frac{d\xi}{\xi} = \frac{1}{2\pi} \int_0^{2\pi} \frac{ae^{-i\eta} - 1}{|ae^{-i\eta} - 1|} d\eta.$$

It suffices now to make again the change of variables $\eta \mapsto -\eta$. Hence we find,

$$\forall \omega \in \mathbb{T}, G_1(\Omega, 0, 0)(\omega) = 0.$$

Arguing similarly we also get

$$\forall \omega \in \mathbb{T}, G_2(\Omega, 0, 0)(\omega) = 0.$$

2.3 Tools

In this section, we shall gather some useful results that we shall use throughout the paper. First, we will recall the Crandall-Rabinowitz's theorem which is the key tool of the proof of our main result. Second, we shall introduce different basic Banach spaces needed in the bifurcation. Last, we shall collect some important properties on special functions and which are helpful in the subsection 2.5.1 to get compact formula for the linearized operator.

2.3.1 Crandall-Rabinowitz's theorem

We intend now to recall Crandall-Rabinowitz's theorem which is an important tool in the bifurcation theory and will be used in the proof of Theorem 4.5.1. Let $F : \mathbb{R} \times X \rightarrow Y$ be a continuous function with X and Y being two Banach spaces. Assume that $F(\lambda, 0) = 0$ for any $\lambda \in \mathbb{R}$. Whether or not close to a trivial solution $(\lambda_0, 0)$ one may find a branch of non trivial solutions of the equation $F(\lambda, x) = 0$ is the main concern of the bifurcation theory. The following theorem provides sufficient conditions for the bifurcation based on the structure of the linearized operator at the point $(\lambda_0, 0)$. For more details we refer to [16, 42].

Theorem 2.3.1. *Let X, Y be two Banach spaces, V a neighborhood of 0 in X and let $F : \mathbb{R} \times X \rightarrow Y$ with the following properties:*

- 1 $F(\lambda, 0) = 0$ for any $\lambda \in \mathbb{R}$.
- 2 The partial derivatives F_λ , F_x and $F_{\lambda x}$ exist and are continuous.
- 3 $\text{Ker}(\mathcal{L}_0)$ and $Y/\text{Im}(\mathcal{L}_0)$ are one-dimensional.
- 4 Transversality assumption: $\partial_\lambda \partial_x F(0, 0)x_0 \notin \text{Im}(\mathcal{L}_0)$, where

$$\text{Ker}(\mathcal{L}_0) = \text{span}(x_0), \mathcal{L}_0 \triangleq \partial_x F(0, 0).$$

If Z is any complement of $\text{Ker}(\mathcal{L}_0)$ in X , then there is a neighborhood U of $(0, 0)$ in $\mathbb{R} \times X$, an interval $(-a, a)$, and continuous functions $\phi : (-a, a) \rightarrow \mathbb{R}$, $\psi : (-a, a) \rightarrow Z$ such that $\phi(0) = 0, \psi(0) = 0$ and

$$F^{-1}(0) \cap U = \left\{ (\phi(\xi), \xi x_0 + \xi \psi(\xi)); |\xi| < a \right\} \cup \left\{ (\lambda, 0); (\lambda, 0) \in U \right\}.$$

2.3.2 Function spaces

We shall see later the spaces that we shall introduce in this paragraph will play a central role in the proof of our main theorem. They were first devised in [7] but with a different representation. Let $\varepsilon \in (0, 1)$ and introduce the sets

$$C_\varepsilon = \left\{ z \in \mathbb{C} \mid \varepsilon < |z| < \frac{1}{\varepsilon} \right\} \quad \text{and} \quad \Delta_\varepsilon = \left\{ z \in \mathbb{C} \mid \varepsilon < |z| \right\}.$$

We denote by \mathcal{A}_ε the set of holomorphic functions h on Δ_ε and such that

$$\forall z \in \Delta_\varepsilon, \quad h(z) = \sum_{n \geq 1} h_n z^{-n} \quad \text{with} \quad h_n \in \mathbb{R}.$$

For $m \in \mathbb{N}$ we define $\mathcal{A}_\varepsilon^m$ as the set of functions $h \in \mathcal{A}_\varepsilon$ such that

$$\forall z \in \Delta_\varepsilon, \quad h(z) = \sum_{n \geq 1} h_n z^{-nm+1}.$$

Let $\widehat{\mathcal{A}}_\varepsilon$ be the set of holomorphic functions h on C_ε with the property

$$\forall z \in C_\varepsilon, \quad h(z) = i \sum_{n=1}^{+\infty} h_n (z^n - z^{-n}), \quad h_n \in \mathbb{R}.$$

For $m \in \mathbb{N}$ we define $\widehat{\mathcal{A}}_\varepsilon^m$ as the set of functions $h \in \widehat{\mathcal{A}}_\varepsilon$ such that,

$$\forall z \in C_\varepsilon, \quad h(z) = i \sum_{n=1}^{+\infty} h_n (z^{nm} - z^{-nm}), \quad h_n \in \mathbb{R}.$$

Finally we denote by \tilde{A}_ε the set of holomorphic functions on C_ε and such that,

$$\forall z \in C_\varepsilon, \quad h(z) = \sum_{n \in \mathbb{Z}} h_n z^n \quad \text{with} \quad h_n \in \mathbb{R}.$$

For $k \in \mathbb{N}$ we introduce the spaces,

$$X^{k+\log} = \left\{ h \in \mathcal{A}_\varepsilon, \quad \int_0^{2\pi} |h(\varepsilon e^{i\theta})|^2 d\theta < +\infty, \int_0^{2\pi} |(\partial_z^k h)(\varepsilon e^{i\theta})|^2 d\theta < +\infty, \right. \\ \left. \left\| \int_{\mathbb{T}} \frac{(\partial_z^k h)(\varepsilon \tau) - (\partial_z^k h)(\varepsilon \cdot)}{|\tau - \cdot|} \frac{d\tau}{\tau} \right\|_{L^2(\mathbb{T})} < +\infty \right\}$$

and

$$X_m^{k+\log} = X^{k+\log} \cap \mathcal{A}_\varepsilon^m.$$

We also define the spaces,

$$Y^{k-1} = \left\{ h \in \widehat{\mathcal{A}}_\varepsilon, \quad \int_0^{2\pi} |h(\varepsilon e^{i\theta})|^2 d\theta < +\infty, \quad \int_0^{2\pi} |(\partial_z^{k-1} h)(\varepsilon e^{i\theta})|^2 d\theta < +\infty \right\},$$

$$Y_m^{k-1} = Y^{k-1} \cap \widehat{\mathcal{A}}_\varepsilon^m$$

and

$$\tilde{Y}^{k-1} = \left\{ h \in \tilde{A}_\varepsilon, \quad \int_0^{2\pi} |h(\varepsilon e^{i\theta})|^2 d\theta < +\infty, \quad \int_0^{2\pi} |h(\varepsilon^{-1} e^{i\theta})|^2 d\theta < +\infty, \right. \\ \left. \int_0^{2\pi} |(\partial_z^{k-1} h)(\varepsilon e^{i\theta})|^2 d\theta < +\infty, \quad \int_0^{2\pi} |(\partial_z^{k-1} h)(\varepsilon^{-1} e^{i\theta})|^2 d\theta < +\infty \right\}.$$

Next we shall be concerned with a characterization of the space $X^{k+\log}$ space in terms of the Fourier coefficients.

Lemma 2.3.2. *Let $k \in \mathbb{N}$ and $h \in \mathcal{A}_\varepsilon$ with $h(z) = \sum_{n \in \mathbb{N}^*} h_n z^{-n}$. Then $h \in X^{k+\log}$ if and only if*

$$\forall \omega \in \mathbb{T}, h(\omega) = \sum_{n=1}^{+\infty} h_n \bar{\omega}^n \quad \text{and} \quad \|h\|_{X^{k+\log}}^2 \approx \sum_{n=1}^{+\infty} \frac{h_n^2}{\varepsilon^{2(n+k)}} n^{2k} (1 + \log(n))^2.$$

Proof. It is easy to see that for $z \in \Delta_\varepsilon$

$$(\partial_z^k h)(z) = \sum_{n=1}^{+\infty} (-1)^k h_n \frac{(n+k-1)!}{(n-1)!} \frac{1}{z^{n+k}}.$$

Hence using the identity (2.5.1) we get for $\omega \in \mathbb{T}$

$$\begin{aligned} \int_{\mathbb{T}} \frac{(\partial_z^k h)(\varepsilon\tau) - (\partial_z^k h)(\varepsilon\omega)}{|\tau - \omega|} \frac{d\tau}{\tau} &= \sum_{n=1}^{+\infty} (-1)^k \frac{h_n}{\varepsilon^{n+k}} \frac{(n+k-1)!}{(n-1)!} \int_{\mathbb{T}} \frac{\bar{\tau}^{n+k} - \bar{\omega}^{n+k}}{|\tau - \omega|} \frac{d\tau}{\tau} \\ &= \sum_{n=1}^{+\infty} (-1)^k \frac{h_n}{\varepsilon^{n+k}} \frac{(n+k-1)!}{(n-1)!} \bar{\omega}^{n+k} \left[-\frac{2}{\pi} - S_{n+k} \right]. \end{aligned}$$

Therefore we may obtain the equivalence between the norms since $S_n \sim \log(n)$. \square

2.3.3 Hypergeometric functions

We shall give basic results on the Gauss hypergeometric functions. The formulae listed below will be crucial in the computations of the linearized operator associated to the V-state equations. Recall that $\forall (a, b, c) \in \mathbb{R} \times \mathbb{R} \times \mathbb{R} \setminus (-\mathbb{N})$ the hypergeometric function $z \mapsto F(a, b, c; z)$ is defined on the open unit disc \mathbb{D} by the power series

$$F(a, b, c; z) = \sum_{n=0}^{+\infty} \frac{(a)_n (b)_n}{(c)_n} \frac{z^n}{n!}, \quad \forall z \in \mathbb{D}.$$

Here, $(x)_n$ is the Pochhammer symbol defined by,

$$(x)_n = \begin{cases} 1 & n = 0 \\ x(x+1) \cdots (x+n-1) & n \geq 1. \end{cases}$$

One may easily see that

$$(x)_n = x(1+x)_{n-1}, \quad (x)_{n+1} = (x+n)(x)_n.$$

For a future use we recall an integral representation of the hypergeometric function, for instance see [69]. Assume that $c > b > 0$, then

$$F(a, b, c; z) = \frac{\Gamma(c)}{\Gamma(b)\Gamma(c-b)} \int_0^1 x^{b-1} (1-x)^{c-b-1} (1-zx)^{-a} dx, \quad \forall z \in \mathbb{D}.$$

The function $\Gamma : \mathbb{C} \setminus (-\mathbb{N}) \rightarrow \mathbb{C}$ refers to the gamma function which is an analytic continuation to the negative half plane of the usual gamma function defined on the positive half-plane $\{\operatorname{Re}(z) > 0\}$ by the integral representation,

$$\Gamma(z) = \int_0^{+\infty} t^{z-1} e^{-t} dt.$$

Next, we recall some contiguous functions relations of the hypergeometric series, see [69].

$$cF(a, b, c; z) - cF(a+1, b, c; z) + bzF(a+1, b+1, c+1; z) = 0 \tag{2.3.1}$$

$$cF(a, b, c; z) - cF(a, b + 1, c; z) + azF(a + 1, b + 1, c + 1; z) = 0 \quad (2.3.2)$$

$$bF(a, b + 1, c; z) - aF(a + 1, b, c; z) + (a - b)(a, b, c; z) = 0 \quad (2.3.3)$$

$$cF(a, b, c; z) - (c - b)F(a, b, c + 1; z) - bF(a, b + 1, c + 1; z) = 0 \quad (2.3.4)$$

We end this discussion with recalling Bessel function J_n of the first kind with $n \in \mathbb{N}$,

$$\forall z \in \mathbb{C}, \quad J_n(z) = \sum_{k \geq 0} \frac{(-1)^k}{k!(n+k)!} \left(\frac{z}{2}\right)^{2k+n}.$$

We recall the Sonine-Schafheitlin's formula which hold provided that $0 < b < a$ and the integral is convergent, see for example [69, p. 401],

$$\begin{aligned} \int_0^{+\infty} \frac{J_\mu(at)J_\nu(bt)}{t^\lambda} dt &= \frac{a^{\lambda-\nu-1}b^\nu\Gamma(\frac{1}{2}\mu+\frac{1}{2}\nu-\frac{1}{2}\lambda+\frac{1}{2})}{2^\lambda\Gamma(\nu+1)\Gamma(\frac{1}{2}\mu+\frac{1}{2}\lambda-\frac{1}{2}\nu+\frac{1}{2})} \\ &\times F\left(\frac{\mu+\nu-\lambda+1}{2}, \frac{\nu-\lambda-\mu+1}{2}, \nu+1; \frac{b^2}{a^2}\right). \end{aligned}$$

2.4 Regularity of the nonlinear functional

In this section we are going to check that the functionals G_j seen in (3.2.3) are well-defined and satisfy the regularity assumption required by Crandall-Rabinowitz's theorem. Recall that the exterior domains $\mathbb{C} \setminus D_j$ are parametrized by the conformal mappings Φ_j whose extension to the boundaries enjoy the following structure,

$$\forall \omega \in \mathbb{T}, \quad \Phi_1(\omega) = \omega + \sum_{n \in \mathbb{N}^*} a_n \bar{\omega}^n = \omega + f_1(\omega) \text{ with } a_n \in \mathbb{R}.$$

$$\Phi_2(\omega) = b\omega + \sum_{n \in \mathbb{N}^*} c_n \bar{\omega}^n = b\omega + f_2(\omega) \text{ with } c_n \in \mathbb{R}.$$

The parameter b belongs to $(0, 1)$ which means that we are looking for V-states which are perturbation of the annulus centered at zero and of radius b and 1. Recall that the equations of the V-states are given by,

$$\forall \omega \in \mathbb{T}, \quad G_j(\Omega, f_1, f_2)(\omega) = 0, \quad j = 1, 2,$$

where

$$G_j(\Omega, f_1, f_2)(\omega) = \operatorname{Im} \left\{ (\Omega\Phi_j(\omega) - S(\Phi_1, \Phi_j)(\omega) + S(\Phi_2, \Phi_j)(\omega)) \overline{\Phi'_j(\omega)} \bar{\omega} \right\} \quad (2.4.1)$$

with

$$S(\Phi_i, \Phi_j)(\omega) = \oint_{\mathbb{T}} \frac{\tau\Phi'_i(\tau) - \omega\Phi'_j(\omega)}{|\Phi_i(\tau) - \Phi_j(\omega)|} \frac{d\tau}{\tau}.$$

The study of the regularity of these functionals will be done in several steps. In the first step we shall analyze the existence of the functionals and in the second one establish some strong regularity.

2.4.1 Existence

The main result of this section reads as follows.

Proposition 2.4.1. *For $j \in \{1, 2\}$ and for any $k \geq 3$, there exists $r \in (0, 1)$ such that,*

$$\begin{aligned} G_j : \quad \mathbb{R} \times V_r \times V_r &\longrightarrow Y^{k-1} \\ (\Omega, f_1, f_2) &\longmapsto G_j(\Omega, f_1, f_2) \end{aligned}$$

is well-defined. Where $V_r = \{f \in X^{k+\log}, \|f\|_{X^{k+\log}} \leq r\}$.

The proof of this result is postponed later and is founded on the following lemma.

Lemma 2.4.2. *Let $\varepsilon \in (0, 1)$, $j \in \{1, 2\}$, $V = b^{j-1}\text{Id} + \tilde{V}$ with $\tilde{V} \in V_r$ and r small enough. Let $h \in V_r$, then the function*

$$K : \omega \in \mathbb{T} \mapsto \int_{\mathbb{T}} \frac{\tau \partial_{\tau} h(\tau) - \omega \partial_{\tau} h(\omega)}{|V(\tau) - V(\omega)|} \frac{d\tau}{\tau}$$

can be extended analytically in C_{ε} to a function \tilde{K} with $\tilde{K} \in \tilde{Y}^{k-1}$. In addition,

$$\|\tilde{K}\|_{\tilde{Y}^{k-1}} \leq C \left(\|V\|_{H^k(\varepsilon\mathbb{T})} + \|V\|_{H^k(\varepsilon^{-1}\mathbb{T})} \right) \|h\|_{X^{k+\log}}.$$

Before giving details of the proof we need to make a comment.

Remark 2.4.3. *Take*

$$\begin{aligned} h : \mathbb{T} &\longrightarrow \mathbb{C} \\ \tau &\longmapsto \sum_{n=1}^{+\infty} a_n \bar{\tau}^n \end{aligned} \quad \text{and} \quad \begin{aligned} \tilde{h} : C_{\varepsilon} &\longrightarrow \mathbb{C} \\ z &\longmapsto \sum_{n=1}^{+\infty} \frac{a_n}{z^n} \end{aligned}$$

then for any $\tau \in \mathbb{T}$, $z \in C_{\varepsilon}$

$$\partial_{\tau} h(\tau) = - \sum_{n=1}^{+\infty} n a_n \bar{\tau}^{n+1} \quad \text{and} \quad \partial_z \tilde{h}(z) = - \sum_{n=1}^{+\infty} n \frac{a_n}{z^{n+1}}.$$

Thus,

$$\partial_{\tau} h = \partial_z \tilde{h} \Big|_{\mathbb{T}}.$$

Proof. By change of variables, we may write

$$K(\omega) = \omega \int_{\mathbb{T}} \frac{\tau \partial_{\tau} h(\tau\omega) - \partial_{\tau} h(\omega)}{|V(\tau\omega) - V(\omega)|} \frac{d\tau}{\tau}.$$

Our next task is to get a holomorphic extension of $\omega \mapsto |V(\tau\omega) - V(\omega)|$. For this aim we write for any $\tau, \omega \in \mathbb{T}$,

$$\begin{aligned} |V(\tau\omega) - V(\omega)|^2 &= (V(\tau\omega) - V(\omega)) (V(\bar{\tau}\omega^{-1}) - V(\omega^{-1})) \\ &= b^{2(j-1)} |\tau - 1|^2 g(\tau, \omega) g(\bar{\tau}, \omega^{-1}), \end{aligned}$$

where g can be extended in a usual way as follows,

$$\forall z \in \overline{\Delta_{\varepsilon}}, \quad g(\tau, z) = 1 + \frac{\tilde{V}(\tau z) - \tilde{V}(z)}{b^{j-1} z(\tau - 1)}. \quad (2.4.2)$$

Therefore we get as a by-product,

$$\exists C > 0, \forall \tau \in \mathbb{T}, \forall z \in \overline{\Delta_{\varepsilon}}, \quad C^{-1} \leq |g(\tau, z)| \leq C. \quad (2.4.3)$$

Now we shall use the following estimate,

$$|\tilde{V}(\tau z) - \tilde{V}(z)| \leq \varepsilon |\tau - 1| \|\partial_z \tilde{V}\|_{L^{\infty}(\varepsilon\mathbb{T})}.$$

This follows from the mean value theorem combined with the maximum principle for holomorphic functions. Indeed, setting $\widehat{V}(z) = \tilde{V}(\frac{1}{z})$, which is holomorphic in the disc $D_{\frac{1}{\varepsilon}} = \{z \in \mathbb{C}, |z| < \frac{1}{\varepsilon}\}$, we deduce by the mean value theorem that for any $z_1, z_2 \in D_{\frac{1}{\varepsilon}}$,

$$|\widehat{V}(z_1) - \widehat{V}(z_2)| \leq |z_1 - z_2| \|\partial_z \widehat{V}\|_{L^{\infty}(\overline{D_{\frac{1}{\varepsilon}}})}. \quad (2.4.4)$$

According to the maximum principle one readily gets

$$\begin{aligned}\|\partial_z \widehat{V}\|_{L^\infty(\overline{D_{\frac{1}{\varepsilon}}})} &= \|\partial_z \widehat{V}\|_{L^\infty(\varepsilon^{-1}\mathbb{T})} \\ &= \varepsilon^2 \|\partial_z \tilde{V}\|_{L^\infty(\varepsilon\mathbb{T})},\end{aligned}$$

Applying this inequality with $z_1 = \frac{1}{\tau z}$ and $z_2 = \frac{1}{z}$ for $z \in C_\varepsilon$ we deduce

$$|\tilde{V}(\tau z) - \tilde{V}(z)| \leq \varepsilon |\tau - 1| \|\partial_z \tilde{V}\|_{L^\infty(\varepsilon\mathbb{T})}$$

which is the desired inequality. Using Sobolev embedding $X^{k+\log} \hookrightarrow \text{Lip}(\varepsilon\mathbb{T})$ for $k \geq 2$ we find

$$|\tilde{V}(\tau z) - \tilde{V}(z)| \leq C |\tau - 1| \|\partial_z \tilde{V}\|_{X^{k-1+\log}} \leq C |\tau - 1| \|\tilde{V}\|_{X^{k+\log}} \quad (2.4.5)$$

with C a constant depending on ε .

Consequently, one may find small r such that for $\tilde{V} \in V_r$ the function $z \in C_\varepsilon \mapsto g(\tau, z)g(\tau, z^{-1})$ is holomorphic and does not cross the negative real axis \mathbb{R}_- . This allows to define the square root of this latter function, which remains in turn holomorphic in the same set C_ε . Finally, the holomorphic extension of K to C_ε could be

$$\begin{aligned}\tilde{K}(z) &= z \int_{\mathbb{T}} \frac{\tau(\partial_z h)(\tau z) - (\partial_z h)(z)}{b^{j-1}|\tau - 1|} g(\tau, z)^{-\frac{1}{2}} g(\bar{\tau}, \frac{1}{z})^{-\frac{1}{2}} \frac{d\tau}{\tau} \\ &\triangleq z \int_{\mathbb{T}} k(z, \tau) d\tau.\end{aligned}$$

It remains to check the holomorphic structure of this integral with respect to the complex parameter. Observe that for fixed $\tau \in \mathbb{T} \setminus \{1\}$ the function $z \in C_\varepsilon \mapsto k(\tau, z)$ is holomorphic. We also note that the mapping $\tau \in \mathbb{T} \setminus \{1\} \mapsto k(\tau, z)$ is bounded uniformly in $z \in C_\varepsilon$. This follows from the estimate

$$\begin{aligned}|\partial_z h(\tau z) - \partial_z h(z)| &\leq \varepsilon |\tau - 1| \|\partial_z^2 h\|_{L^\infty(\varepsilon\mathbb{T})} \\ &\leq C |\tau - 1| \|h\|_{H^3(\varepsilon\mathbb{T})} \\ &\leq C |\tau - 1| \|h\|_{X^{k+\log}}.\end{aligned}$$

Therefore in view of (2.4.3), we find a constant C such that for any $(z, \tau) \in \overline{C_\varepsilon} \times \mathbb{T}$

$$|k(z, \tau)| \leq C. \quad (2.4.6)$$

Consequently \tilde{K} is analytic in the annulus C_ε and therefore it belongs to the class \tilde{A}_ε . Hence, it remains to check that \tilde{K} has finite norm in \tilde{Y}^{k-1} . We shall start with the L^2 norm of the inner restriction $\omega \in \mathbb{T} \mapsto \tilde{K}(\varepsilon\omega)$. We observe that

$$\tilde{K}(\varepsilon\omega) = \varepsilon\omega \int_{\mathbb{T}} k(\varepsilon\omega, \tau) d\tau.$$

It is obvious from (2.4.6) that

$$\tilde{K}(\varepsilon \cdot) \in L^\infty(\mathbb{T}) \subset L^2(\mathbb{T})$$

with

$$\|\tilde{K}(\varepsilon \cdot)\|_{L^2(\mathbb{T})} \leq C \|V\|_{H^2(\varepsilon\mathbb{T})} \|h\|_{H^3(\varepsilon\mathbb{T})}.$$

As to the estimate over the exterior boundary we proceed in the same way as before and we get

$$\|\tilde{K}(\frac{1}{\varepsilon} \cdot)\|_{L^2(\mathbb{T})} \leq C \|V\|_{H^2(\varepsilon\mathbb{T})} \|h\|_{H^3(\varepsilon\mathbb{T})}.$$

Now, we want to control the L^2 norm of $\partial_z^{k-1}\tilde{K}(\varepsilon^\pm \cdot)$. In what follows, we just give details about $\partial_z^{k-1}\tilde{K}(\varepsilon \cdot)$, we deal with the other term with similar ideas. The computations are very long and we shall focus only on the leading term of $\partial_z^{k-1}\tilde{K}$. From Leibniz formula we may write

$$\begin{aligned}\partial_z^{k-1}\tilde{K}(z) &= z \int_{\mathbb{T}} \frac{(\partial_z^k h)(\tau z) - (\partial_z^k h)(z)}{b^{j-1}|\tau - 1|} g(\tau, z)^{-\frac{1}{2}} g(\bar{\tau}, \frac{1}{z})^{-\frac{1}{2}} \frac{d\tau}{\tau} \\ &+ z \int_{\mathbb{T}} \frac{(\tau^k - 1)(\partial_z^k h)(\tau z)}{b^{j-1}|\tau - 1|} g(\tau, z)^{-\frac{1}{2}} g(\bar{\tau}, \frac{1}{z})^{-\frac{1}{2}} \frac{d\tau}{\tau} \\ &+ z \int_{\mathbb{T}} \frac{\tau(\partial_z h)(\tau z) - (\partial_z h)(z)}{b^{j-1}|\tau - 1|} \partial_z^{k-1} \left[g(\tau, z)^{-\frac{1}{2}} g(\bar{\tau}, \frac{1}{z})^{-\frac{1}{2}} \right] \frac{d\tau}{\tau} + l.o.t. \\ &\triangleq z K_1(z) + z K_2(z) + z K_3(z) + l.o.t.\end{aligned}$$

We shall now check that the terms K_2 and K_3 can actually be included to the low order terms. Indeed, for K_2 we write according to (2.4.3),

$$\|K_2(\varepsilon \cdot)\|_{L^\infty(\mathbb{T})} \leq C \|\partial_z^k h(\varepsilon \cdot)\|_{L^2(\mathbb{T})}.$$

As to the third term K_3 we shall only extract some significant terms and the other ones are treated in a similar way. First, it is easy to get

$$\partial_z \left[g(\tau, z)^{-\frac{1}{2}} g(\bar{\tau}, \frac{1}{z})^{-\frac{1}{2}} \right] = -\frac{1}{2} \partial_z \left(g(\tau, z) g(\bar{\tau}, \frac{1}{z}) \right) g(\tau, z)^{-\frac{3}{2}} g(\bar{\tau}, \frac{1}{z})^{-\frac{3}{2}}$$

and

$$\begin{aligned}\partial_z \left(g(\tau, z) g(\bar{\tau}, \frac{1}{z}) \right) &= \frac{z(\tau - 1) \partial_z \tilde{V}(\tau z) + z \left(\partial_z \tilde{V}(\tau z) - \partial_z \tilde{V}(z) \right) - \left(\tilde{V}(\tau z) - \tilde{V}(z) \right)}{z^2 b^{j-1}(\tau - 1)} g(\bar{\tau}, \frac{1}{z}) \\ &+ \frac{z \left(\tilde{V}(\frac{\bar{\tau}}{z}) - \tilde{V}(\frac{1}{z}) \right) - (\bar{\tau} - 1) \partial_z \tilde{V}(\frac{\bar{\tau}}{z}) - \left(\partial_z \tilde{V}(\frac{\bar{\tau}}{z}) - \partial_z \tilde{V}(\frac{1}{z}) \right)}{b^{j-1} z (\bar{\tau} - 1)} g(\tau, z).\end{aligned}$$

Thus

$$\begin{aligned}z \partial_z \left(g(\tau, z)^{-\frac{1}{2}} g(\bar{\tau}, \frac{1}{z})^{-\frac{1}{2}} \right) &= -\frac{1}{2b^{j-1}} \frac{\partial_z \tilde{V}(\tau z) - \partial_z \tilde{V}(z)}{(\tau - 1)} g(\tau, z)^{-\frac{3}{2}} g(\bar{\tau}, \frac{1}{z})^{-\frac{1}{2}} \\ &+ \frac{1}{2b^{j-1}} \frac{\partial_z \tilde{V}(\frac{\bar{\tau}}{z}) - \partial_z \tilde{V}(\frac{1}{z})}{(\bar{\tau} - 1)} g(\tau, z)^{-\frac{1}{2}} g(\bar{\tau}, \frac{1}{z})^{-\frac{3}{2}} + l.o.t.\end{aligned}$$

Iterating this procedure we find

$$\begin{aligned}z \partial_z^{k-1} \left(g(\tau, z)^{-\frac{1}{2}} g(\bar{\tau}, \frac{1}{z})^{-\frac{1}{2}} \right) &= -\frac{1}{2b^{j-1}} \frac{\partial_z^{k-1} \tilde{V}(\tau z) - \partial_z^{k-1} \tilde{V}(z)}{(\tau - 1)} g(\tau, z)^{-\frac{3}{2}} g(\bar{\tau}, \frac{1}{z})^{-\frac{1}{2}} \\ &+ \frac{1}{2b^{j-1}} \frac{\partial_z^{k-1} \tilde{V}(\frac{\bar{\tau}}{z}) - \partial_z^{k-1} \tilde{V}(\frac{1}{z})}{(\bar{\tau} - 1)} g(\tau, z)^{-\frac{1}{2}} g(\bar{\tau}, \frac{1}{z})^{-\frac{3}{2}} + l.o.t.\end{aligned}$$

It follows that

$$\begin{aligned}K_3(\varepsilon \omega) &= -\frac{1}{2b^{j-1}} \int_{\mathbb{T}} \frac{\tau \partial_z h(\varepsilon \tau \omega) - \partial_z h(\varepsilon \omega)}{|\tau - 1|} \frac{\partial_z^{k-1} \tilde{V}(\varepsilon \tau \omega) - \partial_z^{k-1} \tilde{V}(\varepsilon \omega)}{\tau - 1} g(\tau, \varepsilon \omega)^{-\frac{3}{2}} g(\bar{\tau}, \frac{1}{\varepsilon \omega})^{-\frac{1}{2}} \frac{d\tau}{\tau} \\ &+ \frac{1}{2b^{j-1}} \int_{\mathbb{T}} \frac{\tau \partial_z h(\varepsilon \tau \omega) - \partial_z h(\varepsilon \omega)}{|\tau - 1|} \frac{\partial_z^{k-1} \tilde{V}(\frac{\bar{\tau}}{\varepsilon \omega}) - \partial_z^{k-1} \tilde{V}(\frac{1}{\varepsilon \omega})}{\bar{\tau} - 1} g(\tau, \varepsilon \omega)^{-\frac{1}{2}} g(\bar{\tau}, \frac{1}{\varepsilon \omega})^{-\frac{3}{2}} \frac{d\tau}{\tau} + l.o.t.\end{aligned}$$

By the definition of Hölder spaces

$$|\partial_z^{k-1}\tilde{V}(\varepsilon^{\pm 1}\tau\omega) - \partial_z^{k-1}\tilde{V}(\varepsilon^{\pm 1}\omega)| \leq \varepsilon^{\pm \frac{1}{2}} \|\partial_z^{k-1}\tilde{V}\|_{C^{\frac{1}{2}}(\varepsilon^{\pm 1}\mathbb{T})} |\tau - 1|^{\frac{1}{2}}.$$

Thanks to

$$\int_{\mathbb{T}} \frac{1}{|\tau - 1|^{\frac{1}{2}}} |d\tau| < +\infty$$

combined with (2.4.3) we obtain

$$\|K_3(\varepsilon \cdot)\|_{L^\infty(\mathbb{T})} \leq C \left(\|\partial_z h\|_{L^\infty(\varepsilon\mathbb{T})} + \|\partial_z^2 h\|_{L^\infty(\varepsilon\mathbb{T})} \right) \left(\|\partial_z^{k-1}\tilde{V}\|_{C^{\frac{1}{2}}(\varepsilon\mathbb{T})} + \|\partial_z^{k-1}\tilde{V}\|_{C^{\frac{1}{2}}(\varepsilon^{-1}\mathbb{T})} \right) + \dots$$

Hence, using Sobolev embedding we get

$$\|K_3(\varepsilon \cdot)\|_{L^\infty(\mathbb{T})} \leq C \left(\|V\|_{H^k(\varepsilon\mathbb{T})} + \|V\|_{H^k(\varepsilon^{-1}\mathbb{T})} \right) \|h\|_{H^3(\varepsilon\mathbb{T})}.$$

Now let us move to the estimate of the term K_1 which is the most singular one. For this goal we need the following lemma.

Lemma 2.4.4. *Let be $\varepsilon \in (0, 1)$, $\tilde{V} \in \tilde{V}_r$ and r be small enough. Define for any $\tau \in \mathbb{T}$ and $z \in \varepsilon\mathbb{T} \cup \varepsilon^{-1}\mathbb{T}$*

$$g(\tau, z) = 1 + \frac{\tilde{V}(\tau z) - \tilde{V}(z)}{b^{j-1}z(\tau - 1)}.$$

Then

$$g(\tau, z)^{-\frac{1}{2}} = \left(1 + \frac{\partial_z \tilde{V}(z)}{b^{j-1}} \right)^{-\frac{1}{2}} + (\tau - 1)H(\tau, z)$$

where $H(\cdot, \varepsilon^{\pm 1}\cdot) \in L^\infty(\mathbb{T} \times \mathbb{T})$ and

$$\|H(\cdot, \varepsilon^{\pm 1}\cdot)\|_{L^\infty(\mathbb{T} \times \mathbb{T})} \leq C \|\tilde{V}\|_{H^3(\varepsilon^{\pm 1}\mathbb{T})}.$$

Proof. We shall only prove the result for $z \in \varepsilon\mathbb{T}$. Similar computations can be done for $z \in \varepsilon^{-1}\mathbb{T}$. From Taylor expansion at the second order we find,

$$\forall z \in \varepsilon\mathbb{T}, g(\tau, z) = 1 + \frac{\partial_z \tilde{V}(z)}{b^{j-1}} + (\tau - 1)H_1(\tau, z),$$

such that

$$|H_1(\tau, z)| \leq C \|\partial_z^2 \tilde{V}\|_{L^\infty(\varepsilon\mathbb{T})}.$$

Using Sobolev embeddings we get for $k \geq 3$ and $(\tau, z) \in \mathbb{T} \times \varepsilon\mathbb{T}$

$$|H_1(\tau, z)| \leq C \|\tilde{V}\|_{X^{k+\log}}.$$

Finally, from standard computations we obtain the identity

$$g(\tau, z)^{-\frac{1}{2}} = \left(1 + \frac{\partial_z \tilde{V}(z)}{b^{j-1}} \right)^{-\frac{1}{2}} + (\tau - 1)H(\tau, z)$$

with

$$H(\tau, z) = -\frac{H_1(\tau, z) \left(\sqrt{1 + \frac{\partial_z \tilde{V}(z)}{b^{j-1}}} + \sqrt{1 + \frac{\partial_z \tilde{V}(z)}{b^{j-1}} + (\tau - 1)H_1(\tau, z)} \right)^{-1}}{\sqrt{1 + \frac{\partial_z \tilde{V}(z)}{b^{j-1}}} \sqrt{1 + \frac{\partial_z \tilde{V}(z)}{b^{j-1}} + (\tau - 1)H_1(\tau, z)}}.$$

One may easily check that

$$H(\cdot, \cdot) \in L^\infty(\mathbb{T} \times \varepsilon\mathbb{T})$$

and the desired result follows immediately by choosing the radius r small enough. \square

Let us now see how to use the preceding lemma for estimating K_1 . According to this lemma one may obtain a constant C depending on ε and b such that

$$\begin{aligned} \|K_1(\varepsilon \cdot)\|_{L^2(\mathbb{T})} &\leq C \left\| \left(1 + \frac{\partial_z \tilde{V}(\varepsilon \cdot)}{b^{j-1}}\right)^{-\frac{1}{2}} \left(1 + \frac{\partial_z \tilde{V}(\frac{1}{\varepsilon \cdot})}{b^{j-1}}\right)^{-\frac{1}{2}} \right\|_{L^\infty(\mathbb{T})} \left\| \int_{\mathbb{T}} \frac{\partial_z^k h(\varepsilon \tau \cdot) - \partial_z^k h(\varepsilon \cdot)}{|\tau - 1|} \frac{d\tau}{\tau} \right\|_{L^2(\mathbb{T})} \\ &+ C \|\partial_z^k h(\varepsilon \cdot)\|_{L^2(\mathbb{T})} \leq C \|h\|_{X^{k+\log}}. \end{aligned}$$

This concludes the proof of the Lemma 2.4.2. \square

Now, we are in position to give the proof of the Proposition 4.6.2.

Proof. Note that for any $\omega \in \mathbb{T}$ one has

$$G_j(\Omega, f_1, f_2)(\omega) = \frac{F_j(\omega) - F_j(\frac{1}{\omega})}{2i},$$

with

$$\begin{aligned} F_j(\omega) &= \Omega \Phi_j(\omega) \Phi'_j \left(\frac{1}{\omega} \right) \frac{1}{\omega} - \Phi'_j \left(\frac{1}{\omega} \right) \frac{1}{\omega} \int_{\mathbb{T}} \frac{\tau \partial_\tau \Phi_1(\tau) - \omega \partial_\tau \Phi_j(\omega)}{|\Phi_1(\tau) - \Phi_j(\omega)|} \frac{d\tau}{\tau} \\ &+ \Phi'_j \left(\frac{1}{\omega} \right) \frac{1}{\omega} \int_{\mathbb{T}} \frac{\tau \partial_\tau \Phi_2(\tau) - \omega \partial_\tau \Phi_j(\omega)}{|\Phi_2(\tau) - \Phi_j(\omega)|} \frac{d\tau}{\tau}. \end{aligned}$$

We shall prove that F_j belongs to \tilde{Y}^{k-1} . The first term of the right-hand side describing the rotation term belongs to that space. The remaining terms are of two kinds: the self-induced terms and the interaction terms. For the first ones we simply use Lemma 2.4.2 with $h = V = \Phi_j$. As to the interaction terms, the integrand is nowhere singular because the interfaces do not intersect and therefore they are well estimated. We shall briefly give more explanation about this fact. Take the term

$$\hat{K}(\omega) \triangleq \int_{\mathbb{T}} \frac{\tau \Phi'_2(\tau) - \omega \Phi'_1(\omega)}{|\Phi_2(\tau) - \Phi_1(\omega)|} \frac{d\tau}{\tau} = \omega \int_{\mathbb{T}} \frac{\tau \Phi'_2(\tau \omega) - \Phi'_1(\omega)}{|\Phi_2(\tau \omega) - \Phi_1(\omega)|} \frac{d\tau}{\tau}.$$

As before we write, for any $\tau, \omega \in \mathbb{T}$,

$$|\Phi_2(\tau \omega) - \Phi_1(\omega)| = |b\tau - 1| \left(\tilde{g}(\tau, \omega) \tilde{g}(\bar{\tau}, \omega^{-1}) \right)^{\frac{1}{2}}$$

where

$$\forall z \in \overline{\Delta_\varepsilon}, \tilde{g}(\tau, z) = 1 + \frac{f_2(\tau z) - f_1(z)}{(b\tau - 1)z}.$$

From the maximum principle,

$$\left| \frac{f_2(\tau z) - f_1(z)}{(b\tau - 1)z} \right| \leq \varepsilon \frac{\|f_2(\varepsilon \cdot)\|_{L^\infty(\mathbb{T})} + \|f_1(\varepsilon \cdot)\|_{L^\infty(\mathbb{T})}}{1 - b} \leq \varepsilon \frac{2r}{1 - b}.$$

Hence

$$\hat{K}(z) = z \int_{\mathbb{T}} \frac{\tau \Phi'_2(\tau z) - \Phi'_1(z)}{|b\tau - 1|} \tilde{g}(\tau, z)^{-\frac{1}{2}} \tilde{g}(\bar{\tau}, \frac{1}{z})^{-\frac{1}{2}} \frac{d\tau}{\tau}.$$

Note that

$$0 < 1 - b \leq |b\tau - 1| \leq 1 + b$$

and consequently the integrand is less singular than those of the self-induced terms and thus one can find that \hat{K} is analytic in C_ε and belongs to \tilde{Y}^{k-1} . At this stage we have shown that F_j belongs to the space \tilde{Y}^{k-1} and to achieve the proof of the proposition it remains to check that the Fourier coefficients of $G_j(\Omega, f_1, f_2)$ belong to $i\mathbb{R}$. By the assumptions, the Fourier coefficients of $\Phi_j = b^{j-1} Id + f_j$ are real and thus the coefficient of

$\overline{\Phi'_j}$ are real too. From the stability of this property under the multiplication and the conjugation we deduce that the Fourier coefficients of $\omega \mapsto \Omega\Phi_j(\omega)\overline{\Phi'_j(\omega)}\bar{\omega}$ are real. To end the proof we shall check that the Fourier coefficients of $S(\Phi_i, \Phi_j)$ for $i, j \in \{1, 2\}$ are real. We have

$$S(\Phi_i, \Phi_j)(\omega) = \sum_{n \in \mathbb{Z}} a_n \omega^n, \quad a_n = \int_{\mathbb{T}} \frac{S(\Phi_i, \Phi_j)(\omega)}{\omega^{n+1}} d\omega = \int_{\mathbb{T}} \int_{\mathbb{T}} \frac{\tau \Phi'_i(\tau) - \omega \Phi'_j(\omega)}{|\Phi_i(\tau) - \Phi_j(\omega)|} \frac{d\tau}{\tau} \frac{d\omega}{\omega^{n+1}}.$$

The coefficient can also be written in the form

$$a_n = \frac{1}{4\pi^2} \int_0^{2\pi} \int_0^{2\pi} \frac{e^{i\theta} \Phi'_i(e^{i\theta}) - e^{i\eta} \Phi'_j(e^{i\eta})}{|\Phi_i(e^{i\theta}) - \Phi_j(e^{i\eta})|} e^{-in\eta} d\theta d\eta.$$

By taking the conjugate of a_n and using the properties:

$$\overline{\Phi_i(e^{i\theta})} = \Phi_i(e^{-i\theta}), \quad \overline{\Phi'_i(e^{i\theta})} = \Phi'_i(e^{-i\theta}) \text{ and } |z| = |\bar{z}|.$$

One may obtain by change of variable

$$\begin{aligned} \overline{a_n} &= \frac{1}{4\pi^2} \int_0^{2\pi} \int_0^{2\pi} \frac{e^{-i\theta} \Phi'_i(e^{-i\theta}) - e^{-i\eta} \Phi'_j(e^{-i\eta})}{|\Phi_i(e^{-i\theta}) - \Phi_j(e^{-i\eta})|} e^{in\eta} d\theta d\eta \\ &= \frac{1}{4\pi^2} \int_0^{2\pi} \int_0^{2\pi} \frac{e^{i\theta} \Phi'_i(e^{i\theta}) - e^{i\eta} \Phi'_j(e^{i\eta})}{|\Phi_i(e^{i\theta}) - \Phi_j(e^{i\eta})|} e^{-in\eta} d\theta d\eta = a_n. \end{aligned}$$

Consequently the Fourier coefficients of $S(\Phi_i, \Phi_j)$ are real and therefore $G_j(\Omega, \Phi_1, \Phi_2)$ belongs to the space Y^{k-1} and the proof of Proposition 4.6.2 is now achieved. \square

2.4.2 Regularity

The goal of this section is to study the strong regularity of G_j and the main result reads as follows.

Proposition 2.4.5. *For $j \in \{1, 2\}$ and for any $k \geq 3$, there exists $r \in (0, 1)$ such that,*

$$\begin{aligned} G_j : \quad \mathbb{R} \times V_r \times V_r &\longrightarrow Y^{k-1} \\ (\Omega, f_1, f_2) &\longmapsto G_j(\Omega, f_1, f_2) \end{aligned}$$

is of class C^1 , where $V_r = \{f \in X^{k+\log} \mid \|f\|_{X^{k+\log}} \leq r\}$.

Proof. To prove that G_j is of class C^1 we shall first check the existence of its Gâteaux derivative. Second, we will show that this derivative is strongly continuous, and therefore it will necessarily coincide with the Fréchet derivative. This will answer the C^1 regularity. We split G_j into two terms, the self-induced term and the interaction term,

$$G_j(\Omega, f_1, f_2) = O_j(\Omega, f_j) + N_j(f_1, f_2), \quad j \in \{1, 2\}$$

with

$$\forall \omega \in \mathbb{T}, \quad O_j(\Omega, f_j)(\omega) \triangleq \operatorname{Im} \left\{ (\Omega\Phi_j(\omega) + (-1)^j S(\Phi_j, \Phi_j)(\omega)) \overline{\omega \Phi'_j(\omega)} \right\}$$

and

$$N_j(f_1, f_2)(\omega) \triangleq (-1)^{j-1} \operatorname{Im} \left\{ S(\Phi_i, \Phi_j)(\omega) \overline{\omega \Phi'_j(\omega)} \right\}, \quad i \neq j.$$

The Gâteaux derivative of G_j at (f_1, f_2) in the direction (h_1, h_2) is given by the formula:

$$\begin{aligned} DG_j(\Omega, f_1, f_2)(h_1, h_2) &= DO_j(\Omega, f_j)h_j + DN_j(f_1, f_2)(h_1, h_2) \\ &\triangleq \lim_{t \rightarrow 0} \frac{1}{t} [O_j(\Omega, f_j + th_j) - O_j(\Omega, f_j)] + \lim_{t \rightarrow 0} \frac{1}{t} [N_j(f_1 + th_1, f_2 + th_2) - N_j(f_1, f_2)] \\ &= \frac{d}{dt} \Big|_{t=0} O_j(\Omega, f_j + th_j) + \frac{d}{dt} \Big|_{t=0} N_j(f_1 + th_1, f_2 + th_2), \end{aligned} \tag{2.4.7}$$

where the limits are taken in the strong topology of Y^{k-1} . Once we have checked the existence of these quantities, it remains to verify that the functions,

$$F_1(t, \omega) \triangleq \frac{1}{t} \left[O_j(\Omega, f_j + th_j)(\omega) - O_j(\Omega, f_j)(\omega) \right] - \frac{d}{dt} \Big|_{t=0} O_j(\Omega, f_j + th_j)(\omega)$$

and

$$F_2(t, \omega) \triangleq \frac{1}{t} \left[N_j(\Omega, f_1 + th_1, f_2 + th_2)(\omega) - N_j(\Omega, f_1, f_2)(\omega) \right] - \frac{d}{dt} \Big|_{t=0} N_j(\Omega, f_1 + th_1, f_2 + th_2)(\omega)$$

can be analytically extended on C_ε , and their extension, still denoted by F_j , satisfy

$$\lim_{t \rightarrow 0} \|F_j(t)\|_{Y^{k-1}} = 0.$$

The existence of Gâteaux derivative can be done in a straightforward way and one readily gets

$$\begin{aligned} DO_j(\Omega, f_j)h_j(\omega) &= \operatorname{Im} \left\{ \Omega \left(\Phi_j(\omega) \overline{h'_j(\omega)} + \overline{\Phi'_j(\omega)} h_j(\omega) \right) \bar{\omega} + (-1)^j \overline{h'_j(\omega)} \bar{\omega} \int_{\mathbb{T}} \frac{\tau \Phi'_j(\tau) - \omega \Phi'_j(\omega)}{|\Phi_j(\omega) - \Phi_j(\tau)|} \frac{d\tau}{\tau} \right\} \\ &+ (-1)^{j-1} \operatorname{Im} \left\{ \overline{\Phi'_j(\omega)} \bar{\omega} \int_{\mathbb{T}} \frac{(\tau \Phi'_j(\tau) - \omega \Phi'_j(\omega)) \operatorname{Re} \left((\overline{h_j(\tau)} - \overline{h_j(\omega)}) (\Phi_j(\tau) - \Phi_j(\omega)) \right)}{|\Phi_j(\tau) - \Phi_j(\omega)|^3} \frac{d\tau}{\tau} \right\} \\ &+ (-1)^j \operatorname{Im} \left\{ \overline{\Phi'_j(\omega)} \bar{\omega} \int_{\mathbb{T}} \frac{\tau h'_j(\tau) - \omega h'_j(\omega)}{|\Phi_j(\omega) - \Phi_j(\tau)|} \frac{d\tau}{\tau} \right\} \end{aligned} \quad (2.4.8)$$

and

$$\begin{aligned} DN_j(\Omega, f_1, f_2)(h_1, h_2)(\omega) &= (-1)^{j-1} \operatorname{Im} \left\{ \overline{h'_j(\omega)} \bar{\omega} \int_{\mathbb{T}} \frac{\tau \Phi'_i(\tau) - \omega \Phi'_j(\omega)}{|\Phi_i(\omega) - \Phi_j(\tau)|} \frac{d\tau}{\tau} \right. \\ &- \overline{\Phi'_j(\omega)} \bar{\omega} \int_{\mathbb{T}} \frac{[\tau \Phi'_i(\tau) - \omega \Phi'_j(\omega)] \operatorname{Re} \left((\overline{h_i(\tau)} - \overline{h_j(\omega)}) (\Phi_i(\tau) - \Phi_j(\omega)) \right)}{|\Phi_i(\tau) - \Phi_j(\omega)|^3} \frac{d\tau}{\tau} \\ &\left. + \overline{\Phi'_j(\omega)} \bar{\omega} \int_{\mathbb{T}} \frac{\tau h'_i(\tau) - \omega h'_j(\omega)}{|\Phi_i(\omega) - \Phi_j(\tau)|} \frac{d\tau}{\tau} \right\} \end{aligned} \quad (2.4.9)$$

First we note that $F_1(t, \omega)$ can be written in the form

$$F_1(t, \omega) = \sum_{l=1}^5 \frac{I_l(t, \omega) - I_l(t, \omega^{-1})}{2i}$$

with

$$\begin{aligned} I_1(t, \omega) &= \frac{\overline{\Phi'_j(\omega)} \bar{\omega}}{t} \int_{\mathbb{T}} [\tau \Phi'_j(\tau) - \omega \Phi'_j(\omega)] \left[\frac{1}{\Delta_{\Phi_j}^t(h_j)(\tau, \omega)} - \frac{1}{\Delta \Phi_j(\tau, \omega)} \right] \frac{d\tau}{\tau} \\ &+ \overline{\Phi'_j(\omega)} \bar{\omega} \int_{\mathbb{T}} [\tau \Phi'_j(\tau) - \omega \Phi'_j(\omega)] \left[\frac{\operatorname{Re} \left((\overline{h_j(\tau)} - \overline{h_j(\omega)}) (\Phi_j(\tau) - \Phi_j(\omega)) \right)}{[\Delta \Phi_j(\tau, \omega)]^3} \right] \frac{d\tau}{\tau}, \end{aligned}$$

$$\begin{aligned}
I_2(t, \omega) &= \overline{\Phi'_j(\omega)} \bar{\omega} \int_{\mathbb{T}} [\tau h'_j(\tau) - \omega h'_j(\omega)] \left[\frac{1}{\Delta_{\Phi_j}^t(h_j)(\tau, \omega)} - \frac{1}{\Delta\Phi_j(\tau, \omega)} \right] \frac{d\tau}{\tau}, \\
I_3(t, \omega) &= \overline{h'_j(\omega)} \bar{\omega} \int_{\mathbb{T}} [\tau \Phi'_j(\tau) - \omega \Phi'_j(\omega)] \left[\frac{1}{\Delta_{\Phi_j}^t(h_j)(\tau, \omega)} - \frac{1}{\Delta\Phi_j(\tau, \omega)} \right] \frac{d\tau}{\tau}, \\
I_4(t, \omega) &= t \overline{h'_j(\omega)} \bar{\omega} \int_{\mathbb{T}} \frac{\tau h'_j(\tau) - \omega h'_j(\omega)}{\Delta_{\Phi_j}^t(h_j)(\tau, \omega)} \frac{d\tau}{\tau}, \\
I_5(t, \omega) &= t \Omega \bar{\omega} \overline{h'_j(\omega)} h_j(\omega).
\end{aligned}$$

We have use the following notations,

$$\Delta\Phi_j(\tau, \omega) = |\Phi_j(\tau) - \Phi_j(\omega)|$$

and

$$\Delta_{\Phi_j}^t(h_j)(\tau, \omega) = |\Phi_j(\tau) + th_j(\tau) - \Phi_j(\omega) - th_j(\omega)|.$$

First, it is not difficult to check the following limit

$$\lim_{t \rightarrow 0} \|I_5(t)\|_{\tilde{Y}^{k-1}} = 0$$

Moreover, if t is small enough, one may use the Lemma 2.4.2 with $h = h_j$ and $V = \Phi_j + th_j$ to establish

$$\lim_{t \rightarrow 0} \|I_4(t)\|_{\tilde{Y}^{k-1}} = 0$$

We have to rewrite the terms I_1, I_2 and I_3 to compute theirs limits. We begin to rewrite one part of the integrand term:

$$\frac{1}{\Delta_{\Phi_j}^t(h_j)(\tau, \omega)} - \frac{1}{\Delta\Phi_j(\tau, \omega)} = \frac{\left(\Delta\Phi_j(\tau, \omega)\right)^2 - \left(\Delta_{\Phi_j}^t(h_j)(\tau, \omega)\right)^2}{\left(\Delta\Phi_j(\tau, \omega)\right) \left(\Delta_{\Phi_j}^t(h_j)(\tau, \omega)\right) \left(\Delta_{\Phi_j}^t(h_j)(\tau, \omega) + \Delta\Phi_j(\tau, \omega)\right)}. \quad (2.4.10)$$

Then we display the dependency on t in the numerator

$$\left(\Delta\Phi_j(\tau, \omega)\right)^2 - \left(\Delta_{\Phi_j}^t(h_j)(\tau, \omega)\right)^2 = -t \left[2\text{Re}\left(\left(\overline{h_j(\tau) - h_j(\omega)}\right) \left(\Phi_j(\tau) - \Phi_j(\omega)\right)\right) \right] - t^2 |h_j(\tau) - h_j(\omega)|^2. \quad (2.4.11)$$

Moreover, straightforward manipulations lead to the following identity usefull for the term I_3

$$\begin{aligned}
&\frac{1}{(\Delta\Phi_j(\tau, \omega))^3} - \frac{2}{(\Delta\Phi_j(\tau, \omega)) \left(\Delta_{\Phi_j}^t(h_j)(\tau, \omega)\right) \left(\Delta_{\Phi_j}^t(h_j)(\tau, \omega) + \Delta\Phi_j(\tau, \omega)\right)} = \\
&\frac{\left[\Delta_{\Phi_j}^t(h_j)(\tau, \omega)\right]^2 - [\Delta\Phi_j(\tau, \omega)]^2}{[\Delta\Phi_j(\tau, \omega)]^3 \left[\Delta_{\Phi_j}^t(h_j)(\tau, \omega)\right] \left[\Delta_{\Phi_j}^t(h_j)(\tau, \omega) + \Delta\Phi_j(\tau, \omega)\right]} + \frac{\left[\Delta_{\Phi_j}^t(h_j)(\tau, \omega)\right]^2 - [\Delta\Phi_j(\tau, \omega)]^2}{\left(\Delta_{\Phi_j}^t(h_j)(\tau, \omega)\right) (\Delta\Phi_j(\tau, \omega))^2 \left(\Delta_{\Phi_j}^t(h_j)(\tau, \omega) + \Delta\Phi_j(\tau, \omega)\right)} \quad (2.4.12)
\end{aligned}$$

Thanks to (2.4.10), (2.4.11), we rewrite the terms I_2 and I_3 .

$$\begin{aligned} I_2(t, \omega) &= -t^2 \overline{\Phi'_j(\omega)} \bar{\omega} \int_{\mathbb{T}} \frac{[\tau h'_j(\tau) - \omega h'_j(\omega)] |h_j(\tau) - h_j(\omega)|^2}{(\Delta\Phi_j(\tau, \omega)) (\Delta_{\Phi_j}^t(h_j)(\tau, \omega)) (\Delta_{\Phi_j}^t(h_j)(\tau, \omega) + \Delta\Phi_j(\tau, \omega))} \frac{d\tau}{\tau}, \\ &\quad -t \overline{\Phi'_j(\omega)} \bar{\omega} \int_{\mathbb{T}} \frac{[\tau h'_j(\tau) - \omega h'_j(\omega)] \left[2\operatorname{Re} \left(\overline{(h_j(\tau) - h_j(\omega))} (\Phi_j(\tau) - \Phi_j(\omega)) \right) \right]}{(\Delta\Phi_j(\tau, \omega)) (\Delta_{\Phi_j}^t(h_j)(\tau, \omega)) (\Delta_{\Phi_j}^t(h_j)(\tau, \omega) + \Delta\Phi_j(\tau, \omega))} \frac{d\tau}{\tau}, \\ I_3(t, \omega) &= -t^2 \overline{h'_j(\omega)} \bar{\omega} \int_{\mathbb{T}} \frac{[\tau \Phi'_j(\tau) - \omega \Phi'_j(\omega)] |h_j(\tau) - h_j(\omega)|^2}{(\Delta\Phi_j(\tau, \omega)) (\Delta_{\Phi_j}^t(h_j)(\tau, \omega)) (\Delta_{\Phi_j}^t(h_j)(\tau, \omega) + \Delta\Phi_j(\tau, \omega))} \frac{d\tau}{\tau} \\ &\quad -t \overline{h'_j(\omega)} \bar{\omega} \int_{\mathbb{T}} \frac{[\tau \Phi'_j(\tau) - \omega \Phi'_j(\omega)] \left[2\operatorname{Re} \left(\overline{(h_j(\tau) - h_j(\omega))} (\Phi_j(\tau) - \Phi_j(\omega)) \right) \right]}{(\Delta\Phi_j(\tau, \omega)) (\Delta_{\Phi_j}^t(h_j)(\tau, \omega)) (\Delta_{\Phi_j}^t(h_j)(\tau, \omega) + \Delta\Phi_j(\tau, \omega))} \frac{d\tau}{\tau} \end{aligned}$$

Moreover, using in addition 2.4.12 we can also rewrite I_1 .

$$\begin{aligned} I_1(t, \omega) &= -t \overline{\Phi'_j(\omega)} \bar{\omega} \int_{\mathbb{T}} \frac{[\tau \Phi'_j(\tau) - \omega \Phi'_j(\omega)] |h_j(\tau) - h_j(\omega)|^2}{(\Delta\Phi_j(\tau, \omega)) (\Delta_{\Phi_j}^t(h_j)(\tau, \omega)) (\Delta_{\Phi_j}^t(h_j)(\tau, \omega) + \Delta\Phi_j(\tau, \omega))} \frac{d\tau}{\tau} \\ &\quad -t^2 \overline{\Phi'_j(\omega)} \bar{\omega} \int_{\mathbb{T}} \frac{[\tau \Phi'_j(\tau) - \omega \Phi'_j(\omega)] \left[\operatorname{Re} \left(\overline{(h_j(\tau) - h_j(\omega))} (\Phi_j(\tau) - \Phi_j(\omega)) \right) \right] |h_j(\tau) - h_j(\omega)|^2}{(\Delta\Phi_j(\tau, \omega))^3 (\Delta_{\Phi_j}^t(h_j)(\tau, \omega)) (\Delta_{\Phi_j}^t(h_j)(\tau, \omega) + \Delta\Phi_j(\tau, \omega))} \frac{d\tau}{\tau} \\ &\quad -t^2 \overline{\Phi'_j(\omega)} \bar{\omega} \int_{\mathbb{T}} \frac{[\tau \Phi'_j(\tau) - \omega \Phi'_j(\omega)] \left[\operatorname{Re} \left(\overline{(h_j(\tau) - h_j(\omega))} (\Phi_j(\tau) - \Phi_j(\omega)) \right) \right] |h_j(\tau) - h_j(\omega)|^2}{(\Delta_{\Phi_j}^t(h_j)(\tau, \omega)) (\Delta\Phi_j(\tau, \omega))^2 (\Delta_{\Phi_j}^t(h_j)(\tau, \omega) + \Delta\Phi_j(\tau, \omega))^2} \frac{d\tau}{\tau} \\ &\quad -2t \overline{\Phi'_j(\omega)} \bar{\omega} \int_{\mathbb{T}} \frac{[\tau \Phi'_j(\tau) - \omega \Phi'_j(\omega)] \left[\operatorname{Re} \left(\overline{(h_j(\tau) - h_j(\omega))} (\Phi_j(\tau) - \Phi_j(\omega)) \right) \right]^2}{(\Delta\Phi_j(\tau, \omega))^3 (\Delta_{\Phi_j}^t(h_j)(\tau, \omega)) (\Delta_{\Phi_j}^t(h_j)(\tau, \omega) + \Delta\Phi_j(\tau, \omega))} \frac{d\tau}{\tau} \\ &\quad -2t \overline{\Phi'_j(\omega)} \bar{\omega} \int_{\mathbb{T}} \frac{[\tau \Phi'_j(\tau) - \omega \Phi'_j(\omega)] \left[\operatorname{Re} \left(\overline{(h_j(\tau) - h_j(\omega))} (\Phi_j(\tau) - \Phi_j(\omega)) \right) \right]^2}{(\Delta_{\Phi_j}^t(h_j)(\tau, \omega)) (\Delta\Phi_j(\tau, \omega))^2 (\Delta_{\Phi_j}^t(h_j)(\tau, \omega) + \Delta\Phi_j(\tau, \omega))^2} \frac{d\tau}{\tau} \end{aligned}$$

One may see that we just need to check that the integral term of $I_i(t, \omega)$ belongs to \tilde{Y}^{k-1} . We introduce a model integral term, the others term are controled in a similarly way. For any $\omega \in \mathbb{T}$,

$$\begin{aligned} P(\omega) &\triangleq \int_{\mathbb{T}} \frac{(\tau \Phi'_j(\tau) - \omega \Phi'_j(\omega)) (h(\tau) - h(\omega)) (h(\bar{\tau}) - h(\bar{\omega}))}{(\Delta_{\Phi_j}^t(h_j)(\tau, \omega) + \Delta\Phi_j(\tau, \omega)) (\Delta\Phi_j(\tau, \omega)) (\Delta_{\Phi_j}^t(h_j)(\tau, \omega))} \frac{d\tau}{\tau} \\ &= \omega \int_{\mathbb{T}} \frac{((\tau - 1)\Phi'_j(\tau\omega) + \Phi'_j(\tau\omega) - \Phi'_j(\omega)) (h_j(\tau\omega) - h_j(\omega)) (h_j(\frac{\bar{\tau}}{\omega}) - h_j(\frac{1}{\omega}))}{(\Delta_{\Phi_j}^t(h_j)(\tau\omega, \omega) + \Delta\Phi_j(\tau\omega, \omega)) (\Delta\Phi_j(\tau\omega, \omega)) (\Delta_{\Phi_j}^t(h_j)(\tau\omega, \omega))} \frac{d\tau}{\tau} \end{aligned}$$

Following the same idea of the Lemma 2.4.2, we can write

$$\frac{1}{\Delta\Phi_j(\tau\omega, \omega) + \Delta_{\Phi_j}^t(h_j)(\tau\omega, \omega)} = \frac{1}{b^{j-1}|\tau - 1|} \frac{1}{\sqrt{g_j(\tau, \omega)g_j(\bar{\tau}, \frac{1}{\omega})} + \sqrt{\tilde{g}_j(\tau, \omega)\tilde{g}_j(\bar{\tau}, \frac{1}{\omega})}}.$$

Where g_j and \tilde{g}_j can be extended in the usual ways as follows,

$$\forall z \in \overline{\Delta_\varepsilon}, g_j(\tau, z) = 1 + \frac{f_j(\tau z) - f_j(z)}{b^{j-1}z(\tau - 1)} \text{ and } \tilde{g}_j(\tau, z) = g_j(\tau, z) + t \frac{h_j(\tau z) - h_j(z)}{b^{j-1}z(\tau - 1)}.$$

As before we can extend P analytically in C_ε and control the L^2 norm of the inner restriction $\omega \in \mathbb{T} \mapsto P(\varepsilon^{\pm 1}\omega)$. We just give few details to control the L^2 norm of the leading term of $\partial_z^{k-1}P(\varepsilon \cdot)$, the proof for the control of $\partial_z^{k-1}P(\varepsilon^{-1} \cdot)$ is similar. Using the same arguments than before we may write for $z \in \overline{\mathcal{C}_\varepsilon}$

$$\partial_z^{k-1}P(z) = z \int_{\mathbb{T}} \frac{\left((\partial_z^k \Phi_j)(\tau z) - (\partial_z^k \Phi_j)(z) \right) \left(h_j(\tau z) - h_j(z) \right) \left(h_j(\bar{\tau}) - h_j(\frac{1}{z}) \right) g_j(\tau, z)^{-\frac{1}{2}} g_j(\bar{\tau}, \frac{1}{z})^{-\frac{1}{2}}}{b^{3(j-1)} |\tau - 1|^3 \left(\sqrt{g_j(\tau, z) g_j(\bar{\tau}, \frac{1}{z})} + \sqrt{\tilde{g}_j(\tau, z) \tilde{g}_j(\bar{\tau}, \frac{1}{z})} \right) \sqrt{\tilde{g}_j(\tau, z) \tilde{g}_j(\bar{\tau}, \frac{1}{z})}} \frac{d\tau}{\tau} + l.o.t$$

Applying the Lemma 2.4.4 with $\tilde{V}_1 = f_j$ and $\tilde{V}_2 = f_j + th_j$ we can establish for $z \in \varepsilon \mathbb{T} \cup \varepsilon^{-1} \mathbb{T}$ the following identity

$$\begin{aligned} \frac{\left(\sqrt{g(\tau, z) g(\bar{\tau}, \frac{1}{z})} + \sqrt{\tilde{g}(\tau, z) \tilde{g}(\bar{\tau}, \frac{1}{z})} \right)^{-1}}{|\tau - 1|} &= \frac{(\tau - 1)}{|\tau - 1|} H(\tau, z) \\ &+ \frac{\left(\sqrt{(1 + \frac{(\partial_z f_j)(z)}{b^{j-1}})(1 + \frac{(\partial_z f_j)(\frac{1}{z})}{b^{j-1}})} + \sqrt{(1 + \frac{(\partial_z(f_j + th_j))(z)}{b^{j-1}})(1 + \frac{(\partial_z(f_j + th_j))(\frac{1}{z})}{b^{j-1}})} \right)^{-1}}{|\tau - 1|}. \end{aligned}$$

With $H(\cdot, \varepsilon^\pm \cdot) \in L^\infty(\mathbb{T} \times \mathbb{T})$.

Consequently, this identity allows us to deal with the leading term of $\partial_z^{k-1}P$. It follows for $l \in \{1, 2, 3\}$

$$\lim_{t \rightarrow 0} \|I_l\|_{\tilde{Y}^{k-1}} = 0.$$

Eventually, we have proved than F_1 can be extended analytically on C_ε and

$$\lim_{t \rightarrow 0} \|F_1\|_{Y^{k-1}} = 0.$$

Moreover, the interaction term F_2 is dealed with the same arguments than the regularity of the interaction term. Our next task is to prove that

$$DG_j : \mathbb{R} \times V_r \times V_r \rightarrow \mathcal{L}(\mathbb{R} \times X^{k+\log} \times X^{k+\log}, Y^{k-1})$$

is well-defined and continuous.

For the first part, the non trivial point is that $\forall (\Omega, f_1, f_2) \in \mathbb{R} \times V_r \times V_r$, $DG_j(\Omega, f_1, f_2) \in \mathcal{L}(\mathbb{R} \times X^{k+\log} \times X^{k+\log}, Y^{k-1})$. The linearity is obvious.

As before, we just give details about the continuity of the self-induced term $DO_j(\Omega, f_j)$. To begin we rewrite

$$DO_j(\Omega, f_j)(h_j)(\omega) = \sum_{i=1}^4 \frac{\hat{I}_i(\omega) - \hat{I}_i(\frac{1}{\omega})}{2i}$$

with

$$\begin{aligned} \hat{I}_1(\omega) &= \Omega \frac{1}{\omega} \left[\Phi_j(\omega) h'_j(\frac{1}{\omega}) + h_j(\omega) \Phi'_j(\frac{1}{\omega}) \right], \\ \hat{I}_2(\omega) &= (-1)^j h'_j(\frac{1}{\omega}) \frac{1}{\omega} \int_{\mathbb{T}} \frac{\tau \Phi'_j(\tau) - \omega \Phi'_j(\omega)}{\Delta \Phi_j(\tau, \omega)} \frac{d\tau}{\tau}, \\ \hat{I}_3(\omega) &= (-1)^j \Phi'_j(\frac{1}{\omega}) \frac{1}{\omega} \int_{\mathbb{T}} \frac{\tau h'_j(\tau) - \omega h'_j(\omega)}{\Delta \Phi_j(\tau, \omega)} \frac{d\tau}{\tau}, \end{aligned}$$

and

$$\hat{I}_4(\omega) = -(-1)^j \Phi'_j\left(\frac{1}{\omega}\right) \frac{1}{\omega} \int_{\mathbb{T}} \frac{(\tau \Phi'_j(\tau) - \omega \Phi'_j(\omega)) \operatorname{Re} \left((\overline{h_j(\tau)} - h_j(\omega)) (\Phi_j(\tau) - \Phi_j(\omega)) \right)}{(\Delta \Phi_j(\tau, \omega))^3} \frac{d\tau}{\tau}.$$

Using the Lemma 2.4.2 and an adaptation, one may find a constant C such that for $p \in \{1, 2, 3, 4\}$ the following estimate is checked

$$\|\hat{I}_p\|_{\tilde{Y}^{k-1}} \leq C \|\Phi_j\|_{X^{k+\log}} \|h_j\|_{X^{k+\log}}.$$

Consequently, DG_j is well-defined. The continuity of DG_j is the final point of the proof. We just explain the continuity of $DO_j(\Omega, \cdot)$. Let be $f_j, \tilde{f}_j \in V_r \times V_r$ and $h_j \in X^{k+\log}$ with $\|h_j\|_{X^{k+\log}} = 1$, we have for any $\omega \in \mathbb{T}$

$$DO_j(\Omega, f_j)(h_j)(\omega) - DO_j(\Omega, \tilde{f}_j)(h_j)(\omega) = \sum_{i=1}^9 \frac{\tilde{I}_i(\omega) - \tilde{I}_i\left(\frac{1}{\omega}\right)}{2i}$$

with

$$\begin{aligned} \tilde{I}_1(\omega) &= \frac{\Omega}{\omega} \left(\Phi_j(\omega) - \tilde{\Phi}_j(\omega) \right) h'_j\left(\frac{1}{\omega}\right) + \frac{\Omega}{\omega} \left(\Phi'_j\left(\frac{1}{\omega}\right) - \tilde{\Phi}'_j\left(\frac{1}{\omega}\right) \right) h_j(\omega), \\ \tilde{I}_2(\omega) &= \frac{(-1)^j}{\omega} h'_j\left(\frac{1}{\omega}\right) \int_{\mathbb{T}} \frac{\tau \left(\Phi'_j(\tau) - \tilde{\Phi}'_j(\tau) \right) - \omega \left(\Phi'_j(\omega) - \tilde{\Phi}'_j(\omega) \right)}{\Delta \Phi_j(\tau, \omega)} \frac{d\tau}{\tau}, \\ \tilde{I}_3(\omega) &= \frac{(-1)^j}{\omega} h'_j\left(\frac{1}{\omega}\right) \int_{\mathbb{T}} \left[\tau \tilde{\Phi}'_j(\tau) - \omega \tilde{\Phi}'_j(\omega) \right] \left[\frac{1}{\Delta \Phi_j(\tau, \omega)} - \frac{1}{\Delta \tilde{\Phi}_j(\tau, \omega)} \right] \frac{d\tau}{\tau}, \\ \tilde{I}_4(\omega) &= \frac{(-1)^j}{\omega} \left(\Phi'_j\left(\frac{1}{\omega}\right) - \tilde{\Phi}'_j\left(\frac{1}{\omega}\right) \right) \int_{\mathbb{T}} \frac{\tau h'_j(\tau) - \omega h'_j(\omega)}{\Delta \Phi_j(\tau, \omega)} \frac{d\tau}{\tau}, \\ \tilde{I}_5(\omega) &= \frac{(-1)^j}{\omega} \tilde{\Phi}'_j\left(\frac{1}{\omega}\right) \int_{\mathbb{T}} \left(\tau h'_j(\tau) - \omega h'_j(\omega) \right) \left[\frac{1}{\Delta \Phi_j(\tau, \omega)} - \frac{1}{\Delta \tilde{\Phi}_j(\tau, \omega)} \right] \frac{d\tau}{\tau}, \\ \tilde{I}_6(\omega) &= \frac{(-1)^j}{\omega} \left(\tilde{\Phi}'_j\left(\frac{1}{\omega}\right) - \Phi'_j\left(\frac{1}{\omega}\right) \right) \int_{\mathbb{T}} \frac{\left(\tau \tilde{\Phi}'_j(\tau) - \omega \tilde{\Phi}'_j(\omega) \right) \operatorname{Re} \left((\overline{h_j(\omega)} - h_j(\tau)) (\tilde{\Phi}_j(\omega) - \tilde{\Phi}_j(\tau)) \right)}{(\Delta \tilde{\Phi}_j(\tau, \omega))^3} \frac{d\tau}{\tau}, \\ \tilde{I}_7(\omega) &= \frac{(-1)^j}{\omega} \Phi'_j\left(\frac{1}{\omega}\right) \int_{\mathbb{T}} \frac{\left(\tau (\tilde{\Phi}'_j(\tau) - \Phi'_j(\tau)) - \omega (\tilde{\Phi}'_j(\omega) - \Phi'_j(\omega)) \right) \operatorname{Re} \left((\overline{h_j(\omega)} - h_j(\tau)) (\tilde{\Phi}_j(\omega) - \tilde{\Phi}_j(\tau)) \right)}{(\Delta \tilde{\Phi}_j(\tau, \omega))^3} \frac{d\tau}{\tau}, \\ \tilde{I}_8(\omega) &= \frac{(-1)^j}{\omega} \Phi'_j\left(\frac{1}{\omega}\right) \int_{\mathbb{T}} \frac{\left(\tau \Phi'_j(\tau) - \omega \Phi'_j(\omega) \right) \operatorname{Re} \left((\overline{h_j(\omega)} - h_j(\tau)) ((\tilde{\Phi}_j(\omega) - \Phi_j(\omega)) - (\tilde{\Phi}_j(\tau) - \Phi_j(\tau))) \right)}{(\Delta \tilde{\Phi}_j(\tau, \omega))^3} \frac{d\tau}{\tau} \end{aligned}$$

and

$$\begin{aligned} \tilde{I}_9(\omega) &= \frac{(-1)^j}{\omega} \Phi'_j\left(\frac{1}{\omega}\right) \int_{\mathbb{T}} \left(\tau \Phi'_j(\tau) - \omega \Phi'_j(\omega) \right) \operatorname{Re} \left((\overline{h_j(\omega)} - h_j(\tau)) (\Phi_j(\omega) - \Phi_j(\tau)) \right) \times \\ &\quad \left[\frac{1}{(\Delta \tilde{\Phi}_j(\tau, \omega))^3} - \frac{1}{(\Delta \Phi_j(\tau, \omega))^3} \right] \frac{d\tau}{\tau}. \end{aligned}$$

For $p \in \{1, 2, 4, 6, 7, 8\}$, one may extend \tilde{I}_p as before. The control of the \tilde{Y}^{k-1} norm leads on the lemma 2.4.2 and an adaptation, we can find a constant C such that

$$\|\tilde{I}_p\|_{\tilde{Y}^{k-1}} \leq C \|\Phi_j - \tilde{\Phi}_j\|_{X^{k+\log}}.$$

We give few details for the integral term of \tilde{I}_3 . As

$$\frac{1}{\Delta\Phi_j(\tau, \omega)} - \frac{1}{\Delta\tilde{\Phi}_j(\tau, \omega)} = \frac{\left(\tilde{\Phi}_j(\tau) - \tilde{\Phi}_j(\omega)\right)\left(\left(\tilde{\Phi}_j(\bar{\tau}) - \Phi_j(\bar{\tau})\right) - \left(\tilde{\Phi}_j(\frac{1}{\omega}) - \Phi_j(\frac{1}{\omega})\right)\right)}{(\Delta\Phi_j(\tau, \omega))(\Delta\tilde{\Phi}_j(\tau, \omega))(\Delta\Phi_j(\tau, \omega) + \Delta\tilde{\Phi}_j(\tau, \omega))} \\ + \frac{\left(\Phi_j(\bar{\tau}) - \Phi_j(\frac{1}{\omega})\right)\left(\tilde{\Phi}_j(\tau) - \Phi_j(\tau) - \tilde{\Phi}_j(\omega) + \Phi_j(\omega)\right)}{(\Delta\Phi_j(\tau, \omega))(\Delta\tilde{\Phi}_j(\tau, \omega))(\Delta\Phi_j(\tau, \omega) + \Delta\tilde{\Phi}_j(\tau, \omega))}.$$

The integral can be split in two terms and we just give few details for one. We deal with the other in the same way. After a change of variable, we shall extend and control the term

$$\tilde{I}_3(\omega) \triangleq \omega \oint_{\mathbb{T}} \frac{\left(\tau\tilde{\Phi}'_j(\tau\omega) - \tilde{\Phi}'_j(\omega)\right)\left(\tilde{\Phi}_j(\tau\omega) - \tilde{\Phi}_j(\omega)\right)\left(\left(\tilde{\Phi}_j(\frac{\bar{\tau}}{\omega}) - \Phi_j(\frac{\bar{\tau}}{\omega})\right) - \left(\tilde{\Phi}_j(\frac{1}{\omega}) - \Phi_j(\frac{1}{\omega})\right)\right)}{(\Delta\Phi_j(\tau\omega, \omega))(\Delta\tilde{\Phi}_j(\tau\omega, \omega))(\Delta\Phi_j(\tau\omega, \omega) + \Delta\tilde{\Phi}_j(\tau\omega, \omega))} \frac{d\tau}{\tau}.$$

As before, we can write

$$\Delta\Phi_j(\tau\omega, \omega) = b^{j-1}|\tau - 1| \sqrt{g(\tau, \omega)g(\bar{\tau}, \frac{1}{\omega})}, \\ \Delta\tilde{\Phi}_j(\tau\omega, \omega) = b^{j-1}|\tau - 1| \sqrt{\tilde{g}(\tau, \omega)\tilde{g}(\bar{\tau}, \frac{1}{\omega})},$$

and

$$\Delta\Phi_j(\tau\omega, \omega) + \Delta\tilde{\Phi}_j(\tau\omega, \omega) = b^{j-1}|\tau - 1| \left(\sqrt{g(\tau, \omega)g(\bar{\tau}, \frac{1}{\omega})} + \sqrt{\tilde{g}(\tau, \omega)\tilde{g}(\bar{\tau}, \frac{1}{\omega})} \right).$$

where we can extend g and \tilde{g} as usual,

$$\forall z \in \overline{\Delta_\varepsilon}, g(\tau, z) = 1 + \frac{f_j(\tau z) - f_j(z)}{b^{j-1}\omega(\tau - 1)} \text{ and } \tilde{g}(\tau, z) = 1 + \frac{\tilde{f}_j(\tau z) - \tilde{f}_j(z)}{b^{j-1}\omega(\tau - 1)}.$$

Thus the holomorphic extension of \tilde{I}_3 on C_ε is given by

$$\tilde{I}_3(z) = z \oint_{\mathbb{T}} \frac{\left(\tau\partial_z\tilde{\Phi}_j(\tau z) - \partial_z\tilde{\Phi}_j(z)\right)\left(\tilde{\Phi}_j(\tau z) - \tilde{\Phi}_j(z)\right)\left(\tilde{\Phi}_j(\frac{\bar{\tau}}{z}) - \Phi_j(\frac{\bar{\tau}}{z}) - \tilde{\Phi}_j(\frac{1}{z}) + \Phi_j(\frac{1}{z})\right)}{b^{3(j-1)}|\tau - 1|^3 \sqrt{\tilde{g}(\tau, z)\tilde{g}(\bar{\tau}, \frac{1}{z})} \sqrt{g(\tau, z)g(\bar{\tau}, \frac{1}{z})} \left(\sqrt{g(\tau, z)g(\bar{\tau}, \frac{1}{z})} + \sqrt{\tilde{g}(\tau, z)\tilde{g}(\bar{\tau}, \frac{1}{z})}\right)} \frac{d\tau}{\tau}.$$

Concerning the \tilde{Y}^{k-1} norm, we just give some details for the L^2 norm of the leading term of $\partial_z^{k-1}\tilde{I}_3(\varepsilon\cdot)$. For $z \in \overline{C_\varepsilon}$, one may write

$$\partial_z^{k-1}\tilde{I}_3(z) = \oint_{\mathbb{T}} \frac{\left(\partial_z\tilde{\Phi}_j(\tau z) - \partial_z\tilde{\Phi}_j(z)\right)\left(\tilde{\Phi}_j(\tau z) - \tilde{\Phi}_j(z)\right)\left(\tilde{\Phi}_j(\frac{\bar{\tau}}{z}) - \Phi_j(\frac{\bar{\tau}}{z}) - \tilde{\Phi}_j(\frac{1}{z}) + \Phi_j(\frac{1}{z})\right)}{|\tau - 1|^3 \sqrt{\tilde{g}(\tau, z)\tilde{g}(\bar{\tau}, \frac{1}{z})} \sqrt{g(\tau, z)g(\bar{\tau}, \frac{1}{z})} \left(\sqrt{g(\tau, z)g(\bar{\tau}, \frac{1}{z})} + \sqrt{\tilde{g}(\tau, z)\tilde{g}(\bar{\tau}, \frac{1}{z})}\right)} \frac{d\tau}{\tau} + l.o.t$$

The control of the L^2 norm of the inner restriction ($\omega \mapsto \partial_z^{k-1}\tilde{I}_3(\varepsilon\omega)$) must ensure the continuity. First, one may obtain the following identity for $z \in \varepsilon\mathbb{T} \cup \varepsilon^{-1}\mathbb{T}$:

$$\frac{\left(\tilde{\Phi}_j(\tau z) - \tilde{\Phi}_j(z)\right)\left(\tilde{\Phi}_j(\frac{\bar{\tau}}{z}) - \Phi_j(\frac{\bar{\tau}}{z}) - \tilde{\Phi}_j(\frac{1}{z}) + \Phi_j(\frac{1}{z})\right)}{|\tau - 1|^3 \sqrt{\tilde{g}(\tau, z)\tilde{g}(\bar{\tau}, \frac{1}{z})} \sqrt{g(\tau, z)g(\bar{\tau}, \frac{1}{z})} \left(\sqrt{g(\tau, z)g(\bar{\tau}, \frac{1}{z})} + \sqrt{\tilde{g}(\tau, z)\tilde{g}(\bar{\tau}, \frac{1}{z})}\right)} = \frac{K(z)}{|\tau - 1|} + \frac{(\tau - 1)}{|\tau - 1|} H(\tau, z)$$

with the estimations

$$\|K\|_{L^\infty(\varepsilon^\pm\mathbb{T})} \leq C\|\Phi_j - \tilde{\Phi}_j\|_{X^{k+\log}}, \|H\|_{L^\infty(\mathbb{T} \times \varepsilon^\pm\mathbb{T})} \leq C\|\Phi_j - \tilde{\Phi}_j\|_{X^{k+\log}}. \quad (2.4.13)$$

The proof leads on the lemma 2.4.4 and an adaptation. Hence, we can estimate for $p \in \{3, 5\}$:

$$\|\tilde{I}_p\|_{\tilde{Y}^{k-1}} \leq C\|\Phi_j - \tilde{\Phi}_j\|_{X^{k+\log}}$$

For \tilde{I}_9 we just need to notice this decomposition

$$\begin{aligned} \frac{1}{(\Delta\Phi_j(\tau, \omega))^3} - \frac{1}{(\Delta\tilde{\Phi}_j(\tau, \omega))^3} &= \frac{1}{(\Delta\Phi_j(\tau, \omega))^2} \left[\frac{1}{\Delta\Phi_j(\tau, \omega)} - \frac{1}{\Delta\tilde{\Phi}_j(\tau, \omega)} \right] \\ &+ \frac{1}{(\Delta\Phi_j(\tau, \omega))(\Delta\tilde{\Phi}_j(\tau, \omega))} \left[\frac{1}{\Delta\Phi_j(\tau, \omega)} - \frac{1}{\Delta\tilde{\Phi}_j(\tau, \omega)} \right] \\ &+ \frac{1}{(\Delta\tilde{\Phi}_j(\tau, \omega))^2} \left[\frac{1}{\Delta\Phi_j(\tau, \omega)} - \frac{1}{\Delta\tilde{\Phi}_j(\tau, \omega)} \right]. \end{aligned}$$

With this writing and the same arguments than for \tilde{I}_3 , we get

$$\|\tilde{I}_9\|_{\tilde{Y}^{k-1}} \leq C\|\Phi_j - \tilde{\Phi}_j\|_{X^{k+\log}}.$$

Finally, DG_j is continuous. \square

2.5 Study of the linearized operator

The main task of this section is to perform a spectral study of the linearized operator of the functional G introduced in (3.2.3) at the annular solution $(\text{Id}, b\text{Id})$. The first subsection is dedicated to an explicit computation of this operator and to get a more user-friendly expression through some basic identities on hypergeometric functions. In the second part, we want to find the values of Ω leading to a one-dimensional kernel for the linearized operator. We show that for each frequency mode this study reduces to a second degree equation on the variable Ω . The dimension of the kernel is achieved through the strict monotonicity of the eigenvalues with respect to the frequency. Lastly, we check the full assumptions of the Crandall-Rabinowitz's theorem especially the transversality condition which holds only when the eigenvalues are simple.

2.5.1 Linearized operator

The primary purpose of this section is to compute the linearized operator of G at the trivial solution $(\text{Id}, b\text{Id})$ and to reach a more simplified and compact expression. Since $G = (G_1, G_2)$ then for given $(h_1, h_2) \in X^{k+\log} \times X^{k+\log}$, we have

$$DG(\Omega, 0, 0)(h_1, h_2) = \begin{pmatrix} D_{f_1}G_1(\Omega, 0, 0)h_1 + D_{f_2}G_1(\Omega, 0, 0)h_2 \\ D_{f_1}G_2(\Omega, 0, 0)h_1 + D_{f_2}G_2(\Omega, 0, 0)h_2 \end{pmatrix}.$$

Replacing in (2.4.7), (2.4.8) and (2.4.9) Φ_1 by Id and Φ_2 by $b\text{Id}$ yields

$$DG_1(\Omega, 0, 0)(h_1, h_2)(\omega) = \Omega \mathcal{L}_0(h_1)(\omega) + \mathcal{L}_1(h_1)(\omega) + \mathcal{L}_2(h_1, h_2)(\omega),$$

$$DG_2(\Omega, 0, 0)(h_1, h_2)(\omega) = \Omega b\mathcal{L}_0(h_2)(\omega) + \mathcal{L}_1(h_2)(\omega) + \mathcal{L}_3(h_1, h_2)(\omega)$$

with

$$\mathcal{L}_0(h_j)(\omega) = \text{Im} \{ h'_j(\bar{\omega}) + h_j(\omega)\bar{\omega} \},$$

$$\begin{aligned} \mathcal{L}_1(h_j)(\omega) &= \text{Im} \left\{ (-1)^j \overline{h'_j(\omega)} \bar{\omega} \int_{\mathbb{T}} \frac{\tau - \omega}{|\omega - \tau|} \frac{d\tau}{\tau} - (-1)^j \bar{\omega} \int_{\mathbb{T}} \frac{(\tau - \omega) \text{Re}((\bar{h}_j(\tau) - h_j(\omega))(\tau - \omega))}{|\tau - \omega|^3} \frac{d\tau}{\tau} \right\} \\ &+ \text{Im} \left\{ (-1)^j \bar{\omega} \int_{\mathbb{T}} \frac{\tau h'_j(\tau) - \omega h'_j(\omega)}{|\omega - \tau|} \frac{d\tau}{\tau} \right\}, \end{aligned}$$

$$\begin{aligned}\mathcal{L}_2(h_1, h_2)(\omega) &= \operatorname{Im} \left\{ \overline{h'_1(\omega)} \bar{\omega} \int_{\mathbb{T}} \frac{b\tau - \omega}{|b\tau - \omega|} \frac{d\tau}{\tau} \right\} - \operatorname{Im} \left\{ \bar{\omega} \int_{\mathbb{T}} \frac{\omega h'_1(\omega) - \tau h'_2(\tau)}{|\omega - b\tau|} \frac{d\tau}{\tau} \right\} \\ &+ \operatorname{Im} \left\{ -\bar{\omega} \int_{\mathbb{T}} \frac{(b\tau - \omega) \operatorname{Re}((h_1(\omega) - h_2(\tau))(\bar{\omega} - b\tau))}{|b\tau - \omega|^3} \frac{d\tau}{\tau} \right\}\end{aligned}$$

and

$$\begin{aligned}\mathcal{L}_3(h_1, h_2)(\omega) &= \operatorname{Im} \left(-\bar{\omega} h'_2(\bar{\omega}) \int_{\mathbb{T}} \frac{\tau - b\omega}{|\tau - b\omega|} \frac{d\tau}{\tau} + \bar{\omega} b \int_{\mathbb{T}} \frac{\omega h'_2(\omega) - \tau h'_1(\tau)}{|b\omega - \tau|} \frac{d\tau}{\tau} \right) \\ &+ \operatorname{Im} \left(b \bar{\omega} \int_{\mathbb{T}} \frac{(\tau - b\omega) \operatorname{Re}((h_1(\tau) - h_2(\omega))(\bar{\omega} - b\omega))}{|\tau - b\omega|^3} \frac{d\tau}{\tau} \right).\end{aligned}$$

We shall now compute the Fourier series of the mapping $\omega \mapsto DG(\Omega, 0, 0)(h_1, h_2)(\omega)$ with

$$h_1(\omega) = \sum_{n=1}^{+\infty} a_n \bar{\omega}^n \text{ and } h_2(\omega) = \sum_{n=1}^{+\infty} c_n \bar{\omega}^n, \quad \omega \in \mathbb{T}$$

where a_n and c_n are real for all the values $n \in \mathbb{N}^*$. This is summarized in the following proposition.

Proposition 2.5.1. *Let $b \in (0, 1)$, $n \in \mathbb{N}^*$ and define*

$$\Lambda_n(b) \triangleq \frac{1}{b} \int_0^{+\infty} J_n(bt) J_n(t) dt, \quad S_n \triangleq \frac{2}{\pi} \sum_{k=1}^{n-1} \frac{1}{2k+1}$$

with J_n refers to the Bessel function of the first kind. Then, we have

$$DG(\Omega, 0, 0)(h_1, h_2)(\omega) = \frac{i}{2} \sum_{n \geq 1} (n+1) M_{n+1} \begin{pmatrix} a_n \\ c_n \end{pmatrix} (\omega^{n+1} - \bar{\omega}^{n+1}), \quad \forall \omega \in \mathbb{T}$$

where the matrix M_n is given for $n \geq 2$ by:

$$M_n = \begin{pmatrix} \Omega - S_n + b^2 \Lambda_1(b) & -b^2 \Lambda_n(b) \\ b \Lambda_n(b) & b \Omega + S_n - b \Lambda_1(b) \end{pmatrix}.$$

Proof. We begin with the easier term $\mathcal{L}_0(h_j)(\omega)$. Thus by straightforward computations we obtain

$$\mathcal{L}_0(h_1)(\omega) = \frac{i}{2} \sum_{n=1}^{+\infty} (n+1) a_n (\omega^{n+1} - \bar{\omega}^{n+1}).$$

and

$$\mathcal{L}_0(h_2)(\omega) = \frac{i}{2} \sum_{n=1}^{+\infty} (n+1) c_n (\omega^{n+1} - \bar{\omega}^{n+1}).$$

The computation of $\mathcal{L}_1(h_1)(\omega)$ lies on the following identities whose proofs can be found in [?]. Let $n \in \mathbb{N}^*$ and $\omega \in \mathbb{T}$ then

$$\int_{\mathbb{T}} \frac{\tau^n - \omega^n}{|\omega - \tau|} \frac{d\tau}{\tau} = -\frac{2\omega^n}{\pi} \sum_{k=0}^{n-1} \frac{1}{2k+1} \tag{2.5.1}$$

and

$$\int_{\mathbb{T}} \frac{(\tau - \omega)^2 (\tau^n - \omega^n)}{|\omega - \tau|^3} \frac{d\tau}{\tau} = \frac{2\omega^{n+2}}{\pi} \sum_{k=1}^n \frac{1}{2k+1}. \tag{2.5.2}$$

Performing straightforward computations we obtain the result

$$\begin{aligned}\mathcal{L}_1(h_1)(\omega) &= \operatorname{Im} \left\{ \sum_{n=1}^{+\infty} n a_n \omega^n \int_{\mathbb{T}} \frac{\tau - \omega}{|\tau - \omega|} \frac{d\tau}{\tau} + \frac{1}{2\omega} \sum_{n=1}^{+\infty} a_n \int_{\mathbb{T}} \frac{(\tau^n - \omega^n)(\tau - \omega)^2}{|\tau - \omega|^3} \frac{d\tau}{\tau} \right\} \\ &\quad + \operatorname{Im} \left\{ \bar{\omega} \sum_{n=1}^{+\infty} n a_n \int_{\mathbb{T}} \frac{\bar{\tau}^n - \bar{\omega}^n}{|\tau - \omega|} \frac{d\tau}{\tau} + \frac{1}{2\omega} \sum_{n=1}^{+\infty} a_n \int_{\mathbb{T}} \frac{\bar{\tau}^n - \bar{\omega}^n}{|\tau - \omega|} \frac{d\tau}{\tau} \right\}.\end{aligned}$$

Noticing the following equality

$$\forall \tau \in \mathbb{T}, \forall \omega \in \mathbb{T}, \int_{\mathbb{T}} \frac{\bar{\tau}^n - \bar{\omega}^n}{|\omega - \tau|} \frac{d\tau}{\tau} = \overline{\int_{\mathbb{T}} \frac{\tau^n - \omega^n}{|\omega - \tau|} \frac{d\tau}{\tau}},$$

we obtain thanks to (2.5.1) and (2.5.2) the following identity

$$\mathcal{L}_1(h_1)(\omega) = - \sum_{n=1}^{+\infty} \alpha_n a_n \operatorname{Im} \{ \bar{\omega}^{n+1} \} + \sum_{n=1}^{+\infty} \beta_n a_n \operatorname{Im} \{ \omega^{n+1} \}$$

where

$$\alpha_n \triangleq \frac{2n+1}{\pi} \sum_{k=0}^{n-1} \frac{1}{2k+1}$$

and

$$\beta_n \triangleq -\frac{2n}{\pi} + \frac{1}{\pi} \sum_{k=1}^n \frac{1}{2k+1}.$$

As

$$\alpha_n + \beta_n = \frac{2(n+1)}{\pi} \sum_{k=1}^n \frac{1}{2k+1}.$$

Finally we get

$$\mathcal{L}_1(h_1)(\omega) = -\frac{i}{2} \sum_{n=1}^{+\infty} a_n (n+1) S_{n+1} (\omega^{n+1} - \bar{\omega}^{n+1}).$$

In the same way we obtain

$$\mathcal{L}_1(h_2)(\omega) = \frac{i}{2} \sum_{n=1}^{+\infty} c_n (n+1) S_{n+1} (\omega^{n+1} - \bar{\omega}^{n+1}).$$

To compute $\mathcal{L}_2(h_1, h_2)(\omega)$ we begin to rewrite

$$\begin{aligned}-\bar{\omega} \int_{\mathbb{T}} \frac{(b\tau - \omega) \operatorname{Re} (h_1(\omega) - h_2(\tau)) \overline{(\omega - b\tau)}}{|b\tau - \omega|^3} \frac{d\tau}{\tau} &= \frac{\bar{\omega}}{2} \int_{\mathbb{T}} \frac{h_1(\omega) - h_2(\tau)}{|b\tau - \omega|} \frac{d\tau}{\tau} \\ &\quad + \frac{\bar{\omega}}{2} \int_{\mathbb{T}} \frac{(b\tau - \omega)^2 \overline{(h_1(\omega) - h_2(\tau))}}{|b\tau - \omega|^3} \frac{d\tau}{\tau}.\end{aligned}$$

Replacing h_j and h'_j by their expressions, we obtain the following identity

$$\begin{aligned}\mathcal{L}_2(h_1, h_2)(\omega) &= \operatorname{Im} \left\{ - \sum_{n=1}^{+\infty} n a_n \int_{\mathbb{T}} \frac{b\tau - \omega}{|b\tau - \omega|} \frac{d\tau}{\tau} + \sum_{n=1}^{+\infty} n \bar{\omega} \int_{\mathbb{T}} \frac{a_n \bar{\omega}^n - c_n \bar{\tau}^n}{|\omega - b\tau|} \frac{d\tau}{\tau} \right\} \\ &\quad + \operatorname{Im} \left\{ \frac{b}{2} \sum_{n=1}^{+\infty} \bar{\omega} \frac{(b\omega - \tau)(a_n \omega^n - c_n \tau^n)}{|b\tau - \omega|^3} d\tau - \frac{1}{2} \sum_{n=1}^{+\infty} \frac{(b - \omega \bar{\tau})(a_n \omega^n - c_n \tau^n)}{|b\tau - \omega|^3} d\tau \right\} \\ &\quad + \operatorname{Im} \left\{ \frac{1}{2} \sum_{n=1}^{+\infty} \bar{\omega} \int_{\mathbb{T}} \frac{a_n \bar{\omega}^n - \bar{\tau}^n}{|b\tau - \omega|} \frac{d\tau}{\tau} \right\}.\end{aligned}$$

To compute these terms, we will use the identities proved in [30]: Let $b \in (0, 1)$ and $n \in \mathbb{N}$, then for any $\omega \in \mathbb{T}$ we have

$$\int_{\mathbb{T}} \frac{\tau^{n-1}}{|b\tau - \omega|} d\tau = \omega^n b^n \frac{(\frac{1}{2})_n}{n!} F\left(\frac{1}{2}, n + \frac{1}{2}, n + 1; b^2\right), \quad (2.5.3)$$

$$\begin{aligned} \int_{\mathbb{T}} \frac{\bar{\tau}^{n+1}}{|b\tau - \omega|} d\tau &= \overline{\int_{\mathbb{T}} \frac{\tau^{n-1}}{|b\tau - \omega|} d\tau} \\ &= \bar{\omega}^n b^n \frac{(\frac{1}{2})_n}{n!} F\left(\frac{1}{2}, n + \frac{1}{2}, n + 1; b^2\right), \end{aligned} \quad (2.5.4)$$

$$\int_{\mathbb{T}} \frac{\bar{\tau}^{n+1}}{|\omega - b\tau|^3} d\tau = \omega^n b^n \frac{(\frac{3}{2})_n}{n!} F\left(\frac{3}{2}, n + \frac{3}{2}, n + 1; b^2\right), \quad (2.5.5)$$

$$\int_{\mathbb{T}} \frac{\tau^{n-1}}{|\omega - b\tau|^3} d\tau = \omega^n b^n \frac{(\frac{3}{2})_n}{n!} F\left(\frac{3}{2}, n + \frac{3}{2}, n + 1; b^2\right), \quad (2.5.6)$$

$$\int_{\mathbb{T}} \frac{(b\tau - \omega)(a\omega^n - c\tau^n)}{|\omega - b\tau|^3} d\tau = -\omega^{n+2} b \left[\frac{3}{2} a F\left(\frac{1}{2}, \frac{5}{2}, 2; b^2\right) - cb^n \frac{(\frac{3}{2})_{n+1}}{(n+1)!} F\left(\frac{1}{2}, n + \frac{5}{2}, n + 2; b^2\right) \right], \quad (2.5.7)$$

and

$$\int_{\mathbb{T}} \frac{(b\omega - \tau)(c\omega^n - a\tau^n)}{|\omega - b\tau|^3} d\tau = -\omega^{n+2} b^2 \left[\frac{3}{8} c F\left(\frac{3}{2}, \frac{5}{2}, 3; b^2\right) - ab^n \frac{(\frac{1}{2})_{n+2}}{(n+2)!} F\left(\frac{3}{2}, n + \frac{5}{2}, n + 3; b^2\right) \right]. \quad (2.5.8)$$

We shall split the computation in many parts. By using (2.5.3) and (2.5.4) we find

$$-\sum_{n=1}^{+\infty} na_n \int_{\mathbb{T}} \frac{b\tau - \omega}{|b\tau - \omega|} \frac{d\tau}{\tau} = \sum_{n=1}^{+\infty} na_n \left[F\left(\frac{1}{2}, \frac{1}{2}, 1; b^2\right) - \frac{b^2}{2} F\left(\frac{1}{2}, \frac{3}{2}, 2; b^2\right) \right] \omega^{n+1}.$$

Moreover

$$\begin{aligned} \sum_{n=1}^{+\infty} \left(n + \frac{1}{2}\right) \bar{\omega} \int_{\mathbb{T}} \frac{a_n \bar{\omega}^n - c_n \bar{\tau}^n}{|\omega - b\tau|} \frac{d\tau}{\tau} &= \sum_{n=1}^{+\infty} \left(n + \frac{1}{2}\right) a_n F\left(\frac{1}{2}, \frac{1}{2}, 1; b^2\right) \bar{\omega}^{n+1} \\ &\quad - \sum_{n=1}^{+\infty} \left(n + \frac{1}{2}\right) c_n b^n \frac{(\frac{1}{2})_n}{n!} F\left(\frac{1}{2}, n + \frac{1}{2}, n + 1; b^2\right) \bar{\omega}^{n+1} \end{aligned}$$

Now, using (2.5.7) we obtain

$$\begin{aligned} \frac{b}{2} \sum_{n=1}^{+\infty} \bar{\omega} \int_{\mathbb{T}} \frac{(b\omega - \tau)(a_n \omega^n - c_n \tau^n)}{|\omega - b\tau|^3} d\tau &= \frac{b^{n+2}}{2} c_n \frac{(\frac{3}{2})_{n+1}}{(n+1)!} F\left(\frac{1}{2}, n + \frac{5}{2}, n + 2; b^2\right) \omega^{n+1} \\ &\quad - \frac{3b^2}{4} a_n F\left(\frac{1}{2}, \frac{5}{2}, 2; b^2\right) \omega^{n+1}. \end{aligned}$$

For the last term of $\mathcal{L}_2(h_1, h_2)$ we use (2.5.5) and (2.5.6)

$$\begin{aligned} -\frac{1}{2} \sum_{n=1}^{+\infty} \int_{\mathbb{T}} \frac{(b - \omega\bar{\tau})(a_n \omega^n - c_n \tau^n)}{|\omega - b\tau|^3} d\tau &= -\frac{1}{2} \sum_{n=1}^{+\infty} a_n \left[\frac{3}{2} b^2 F\left(\frac{3}{2}, \frac{5}{2}, 2; b^2\right) - F\left(\frac{3}{2}, \frac{3}{2}, 1; b^2\right) \right] \omega^{n+1} \\ &\quad + \frac{1}{2} \sum_{n=1}^{+\infty} c_n \frac{b^n}{n!} \left(\frac{3}{2}\right)_n \left[\frac{(n + \frac{3}{2})}{(n+1)} b^2 F\left(\frac{3}{2}, n + \frac{5}{2}, n + 2; b^2\right) - F\left(\frac{3}{2}, n + \frac{3}{2}, n + 1; b^2\right) \right] \omega^{n+1}. \end{aligned}$$

Now we shall apply (2.3.1) with $a = \frac{1}{2}$, $b = \tilde{n} + \frac{3}{2}$, $c = \tilde{n} + 1$ and $z = b^2$ where $\tilde{n} \in \{0, n\}$

$$-\frac{1}{2} \sum_{n=1}^{+\infty} \int_{\mathbb{T}} \frac{(b - \omega\bar{\tau})(a_n \omega^n - c_n \tau^n)}{|b\tau - \omega|^3} d\tau = \frac{1}{2} \sum_{n=1}^{+\infty} \left[a_n F\left(\frac{1}{2}, \frac{3}{2}, 1; b^2\right) - c_n \frac{b^n}{n!} \binom{3}{2}_n F\left(\frac{1}{2}, n + \frac{3}{2}, 1; b^2\right) \right] \omega^{n+1}.$$

Finally we get

$$\mathcal{L}_2(h_1, h_2)(\omega) = \frac{i}{2} \sum_{n=1}^{+\infty} \left[a_n (\tilde{\gamma}_n - \gamma_n) + (\tilde{\beta}_n - \beta_n) c_n \right] (\omega^{n+1} - \bar{\omega}^{n+1})$$

with

$$\begin{aligned} \gamma_n &= n \left[F\left(\frac{1}{2}, \frac{1}{2}, 1; b^2\right) - \frac{b^2}{2} F\left(\frac{1}{2}, \frac{3}{2}, 2; b^2\right) \right] - \frac{3}{4} b^2 F\left(\frac{1}{2}, \frac{5}{2}, 2; b^2\right) + \frac{1}{2} F\left(\frac{1}{2}, \frac{3}{2}, 1; b^2\right), \\ \tilde{\gamma}_n &= (n + \frac{1}{2}) F\left(\frac{1}{2}, \frac{1}{2}, 1; b^2\right), \\ \beta_n &= \frac{b^{n+2}}{2} \frac{(\frac{3}{2})_{n+1}}{(n+1)!} F\left(\frac{1}{2}, n + \frac{5}{2}, n + 2; b^2\right) - \frac{b^n}{2} \frac{(\frac{3}{2})_n}{n!} F\left(\frac{1}{2}, n + \frac{3}{2}, n + 1; b^2\right) \end{aligned}$$

and

$$\tilde{\beta}_n = -(n + \frac{1}{2}) b^n \frac{(\frac{1}{2})_n}{n!} F\left(\frac{1}{2}, n + \frac{1}{2}, n + 1; b^2\right).$$

Now, we want to simplify the expression of $\mathcal{L}_2(h_1, h_2)$ through the use of the identities (2.3.1)-(2.3.4). We begin with (2.3.2) with $a = \frac{1}{2}$, $b = \tilde{n} + \frac{1}{2}$, $c = \tilde{n} + 1$ and $z = b^2$ where $\tilde{n} \in \{0, n\}$ which implies

$$\gamma_n - \tilde{\gamma}_n = -n \frac{b^2}{2} F\left(\frac{1}{2}, \frac{3}{2}, 2; b^2\right) - \frac{3}{4} b^2 F\left(\frac{1}{2}, \frac{5}{2}, 2; b^2\right) + \frac{b^2}{4} F\left(\frac{3}{2}, \frac{3}{2}, 2; b^2\right)$$

and

$$\beta_n - \tilde{\beta}_n = \frac{b^{n+2}}{2(n+1)!} \binom{3}{2}_n \left[\left(n + \frac{3}{2} \right) F\left(\frac{1}{2}, n + \frac{5}{2}, n + 2; b^2\right) - \frac{1}{2} F\left(\frac{1}{2}, n + \frac{3}{2}, n + 1; b^2\right) \right].$$

Thus using (2.3.3), one may check the following expression

$$\begin{aligned} \mathcal{L}_2(h_1, h_2)(\omega) &= \frac{i}{2} \sum_{n=1}^{+\infty} (n+1) \frac{b^2}{2} F\left(\frac{1}{2}, \frac{3}{2}, 2; b^2\right) a_n (\omega^{n+1} - \bar{\omega}^{n+1}) \\ &\quad - \frac{i}{2} \sum_{n=1}^{+\infty} \frac{b^{n+2}}{n!} \left(\frac{1}{2} \right)_{n+1} F\left(\frac{1}{2}, n + \frac{3}{2}, n + 2; b^2\right) c_n (\omega^{n+1} - \bar{\omega}^{n+1}). \end{aligned}$$

Now we focus on $\mathcal{L}_3(h_1, h_2)$ given by

$$\begin{aligned} \mathcal{L}_3(h_1, h_2)(\omega) &= \text{Im} \left\{ -\bar{\omega} h'_2(\bar{\omega}) \int_{\mathbb{T}} \frac{\tau - b\omega}{|\tau - b\omega|} \frac{d\tau}{\tau} + \bar{\omega} b \int_{\mathbb{T}} \frac{\omega h'_2(\omega) - \tau h'_1(\tau)}{|b\omega - \tau|} \frac{d\tau}{\tau} \right\} \\ &\quad + \text{Im} \left\{ b\bar{\omega} \int_{\mathbb{T}} \frac{(\tau - b\omega) \text{Re}((h_1(\tau) - h_2(\omega))(\overline{\tau - b\omega}))}{|\tau - b\omega|^3} \frac{d\tau}{\tau} \right\}. \end{aligned}$$

Observe that

$$\begin{aligned} b\bar{\omega} \int_{\mathbb{T}} \frac{(\tau - b\omega) \text{Re}((h_1(\tau) - h_2(\omega))(\overline{\tau - b\omega}))}{|\tau - b\omega|^3} \frac{d\tau}{\tau} &= \frac{b}{2} \bar{\omega} \int_{\mathbb{T}} \frac{h_1(\tau) - h_2(\omega)}{|\tau - b\omega|} \frac{d\tau}{\tau} \\ &\quad + \frac{b}{2} \bar{\omega} \int_{\mathbb{T}} \frac{(\tau - b\omega)^2 (\overline{h_1(\tau) - h_2(\omega)})}{|\tau - b\omega|^3} \frac{d\tau}{\tau}. \end{aligned}$$

Replacing h_j and h'_j by their expressions we get

$$\begin{aligned}\mathcal{L}_3(h_1, h_2)(\omega) &= \operatorname{Im} \left\{ \sum_{n=1}^{+\infty} nc_n \omega^n \int_{\mathbb{T}} \frac{\tau - b\omega}{|\tau - b\omega|} \frac{d\tau}{\tau} - \bar{\omega}b \sum_{n=1}^{+\infty} \left(n + \frac{1}{2} \right) \int_{\mathbb{T}} \frac{c_n \bar{\omega}^n - a_n \bar{\tau}^n}{|b\omega - \tau|} \frac{d\tau}{\tau} \right\} \\ &\quad + \operatorname{Im} \left\{ \frac{b}{2} \bar{\omega} \sum_{n=1}^{+\infty} \int_{\mathbb{T}} \frac{(b\omega - \tau)(c_n \omega^n - a_n \tau^n)}{|\tau - b\omega|^3} d\tau + \frac{b^2}{2} \sum_{n=1}^{+\infty} \int_{\mathbb{T}} \frac{(1 - b\omega \bar{\tau})(c_n \omega^n - a_n \tau^n)}{|\tau - b\omega|^3} d\tau \right\}.\end{aligned}$$

As before, we shall split the computations in many parts. Thanks to (2.5.3) and (2.5.4), the first term takes the form

$$\begin{aligned}\sum_{n=1}^{+\infty} nc_n \omega^n \int_{\mathbb{T}} \frac{\tau - b\omega}{|\tau - b\omega|} \frac{d\tau}{\tau} &= \sum_{n=1}^{+\infty} nc_n \omega^n \int_{\mathbb{T}} \frac{\tau - b\omega}{|\tau b - \omega|} \frac{d\tau}{\tau} \\ &= \sum_{n=1}^{+\infty} nbc_n \left[\frac{1}{2} F\left(\frac{1}{2}, \frac{3}{2}, 2; b^2\right) - F\left(\frac{1}{2}, \frac{1}{2}, 1; b^2\right) \right] \omega^{n+1}.\end{aligned}$$

Note that we have used in the first line the identity

$$\forall \tau, \omega \in \mathbb{T}, \quad |\tau - b\omega| = |b\tau - \omega|$$

For the second term, we use (2.5.3) and (2.5.4) to obtain

$$\begin{aligned}-\bar{\omega}b \sum_{n=1}^{+\infty} \left(n + \frac{1}{2} \right) \int_{\mathbb{T}} \frac{c_n \bar{\omega}^n - a_n \bar{\tau}^n}{|b\omega - \tau|} \frac{d\tau}{\tau} &= - \sum_{n=1}^{+\infty} \left(n + \frac{1}{2} \right) bc_n F\left(\frac{1}{2}, \frac{1}{2}, 1; b^2\right) \bar{\omega}^{n+1} \\ &\quad + \sum_{n=1}^{+\infty} \left(n + \frac{1}{2} \right) a_n \frac{b^{n+1}}{n!} \left(\frac{1}{2}\right)_n F\left(\frac{1}{2}, n + \frac{1}{2}, n + 1; b^2\right) \bar{\omega}^{n+1}.\end{aligned}$$

The computation of the third term can be done in view of (2.5.8),

$$\begin{aligned}\frac{b}{2} \bar{\omega} \sum_{n=1}^{+\infty} \int_{\mathbb{T}} \frac{(b\omega - \tau)(c_n \omega^n - a_n \tau^n)}{|\tau - b\omega|^3} d\tau &= \sum_{n=1}^{+\infty} \frac{a_n}{2} \frac{b^{n+3}}{(n+2)!} \left(\frac{1}{2}\right)_{n+2} F\left(\frac{3}{2}, n + \frac{5}{2}, n + 3; b^2\right) \omega^{n+1} \\ &\quad - \sum_{n=1}^{+\infty} \frac{3b^3}{16} c_n F\left(\frac{3}{2}, \frac{5}{2}, 3; b^2\right) \omega^{n+1}.\end{aligned}$$

For the last term, we use (2.5.5) and (2.5.6)

$$\begin{aligned}\frac{b^2}{2} \sum_{n=1}^{+\infty} \int_{\mathbb{T}} \frac{(1 - b\omega \bar{\tau})(c_n \omega^n - a_n \tau^n)}{|\tau - b\omega|^3} d\tau &= \sum_{n=1}^{+\infty} \frac{b^3}{2} c_n \left[\frac{3}{2} F\left(\frac{3}{2}, \frac{5}{2}, 2; b^2\right) - F\left(\frac{3}{2}, \frac{3}{2}, 1; b^2\right) \right] \omega^{n+1} \\ &\quad - \sum_{n=1}^{+\infty} \frac{b^{n+3}}{2} a_n \left[\frac{(\frac{3}{2})_{n+1}}{(n+1)!} F\left(\frac{3}{2}, n + \frac{5}{2}, n + 2; b^2\right) - \frac{(\frac{3}{2})_n}{n!} F\left(\frac{3}{2}, n + \frac{3}{2}, n + 1; b^2\right) \right] \omega^{n+1}\end{aligned}$$

Finally, we obtain the following expression

$$\mathcal{L}_3(h_1, h_2)(\omega) = \frac{i}{2} \sum_{n=1}^{+\infty} \left[a_n (\tilde{\Delta}_n - \Delta_n) + c_n (\tilde{\theta}_n - \theta_n) \right] (\omega^{n+1} - \bar{\omega}^{n+1})$$

with

$$\begin{aligned}\Delta_n &= \frac{b^{n+3}}{2} \frac{(\frac{1}{2})_{n+2}}{(n+2)!} F\left(\frac{3}{2}, n + \frac{5}{2}, n+3; b^2\right) - \frac{b^{n+3}}{2} \frac{(\frac{3}{2})_{n+1}}{(n+1)!} F\left(\frac{3}{2}, n + \frac{5}{2}, n+2; b^2\right) \\ &\quad + \frac{b^{n+3}}{2} \frac{(\frac{3}{2})_n}{n!} F\left(\frac{3}{2}, n + \frac{3}{2}, n+1; b^2\right), \\ \tilde{\Delta}_n &= \left(n + \frac{1}{2}\right) b^{n+1} \frac{(\frac{1}{2})_n}{n!} F\left(\frac{1}{2}, n + \frac{1}{2}, n+1; b^2\right), \\ \theta_n &= bn \left[\frac{1}{2} F\left(\frac{1}{2}, \frac{3}{2}, 2; b^2\right) - F\left(\frac{1}{2}, \frac{1}{2}, 1; b^2\right) \right] - \frac{3b^3}{16} F\left(\frac{3}{2}, \frac{5}{2}, 3; b^2\right) \\ &\quad + \frac{b^3}{2} \left[\frac{3}{2} F\left(\frac{3}{2}, \frac{5}{2}, 2; b^2\right) - F\left(\frac{3}{2}, \frac{3}{2}, 1; b^2\right) \right]\end{aligned}$$

and

$$\tilde{\theta}_n = - \left(n + \frac{1}{2}\right) b F\left(\frac{1}{2}, \frac{1}{2}, 1; b^2\right).$$

We want to simplify the expression of $\mathcal{L}_3(h_1, h_2)$. First we note that

$$\begin{aligned}\theta_n - \tilde{\theta}_n &= \frac{nb}{2} F\left(\frac{1}{2}, \frac{3}{2}, 2; b^2\right) + \frac{b}{2} F\left(\frac{1}{2}, \frac{1}{2}, 1; b^2\right) - \frac{3b^3}{16} F\left(\frac{3}{2}, \frac{5}{2}, 3; b^2\right) \\ &\quad + \frac{b^3}{2} \left[\frac{3}{2} F\left(\frac{3}{2}, \frac{5}{2}, 2; b^2\right) - F\left(\frac{3}{2}, \frac{3}{2}, 1; b^2\right) \right].\end{aligned}$$

By using (2.3.2) we get

$$\begin{aligned}\theta_n - \tilde{\theta}_n &= \frac{b}{2} (n+1) F\left(\frac{1}{2}, \frac{3}{2}, 2; b^2\right) + \frac{b}{2} F\left(\frac{1}{2}, \frac{1}{2}, 1; b^2\right) - \frac{b}{2} F\left(\frac{1}{2}, \frac{3}{2}, 1; b^2\right) \\ &\quad + \frac{b^3}{2} \left[\frac{3}{2} F\left(\frac{3}{2}, \frac{5}{2}, 2; b^2\right) - F\left(\frac{3}{2}, \frac{3}{2}, 1; b^2\right) \right].\end{aligned}$$

Now combining (2.3.2) with $a = b = \frac{1}{2}$, $c = 1$ and $z = b^2$ as well as (2.3.4) with $a = b = \frac{3}{2}$, $c = 1$ and $z = b^2$, one may obtain the following identity

$$F\left(\frac{1}{2}, \frac{1}{2}, 1; b^2\right) - F\left(\frac{1}{2}, \frac{3}{2}, 1; b^2\right) + \frac{3}{2} b^2 F\left(\frac{3}{2}, \frac{5}{2}, 2; b^2\right) - b^2 F\left(\frac{3}{2}, \frac{3}{2}, 1; b^2\right) = 0.$$

Consequently,

$$\theta_n - \tilde{\theta}_n = \frac{b}{2} (n+1) F\left(\frac{1}{2}, \frac{3}{2}, 2; b^2\right).$$

On the other hand

$$\begin{aligned}\Delta_n - \tilde{\Delta}_n &= b^{n+1} \frac{(\frac{1}{2})_{n+1}}{(n+1)!} \left[\frac{b^2 (n+\frac{3}{2})}{2 (n+2)} F\left(\frac{3}{2}, n + \frac{5}{2}, n+3; b^2\right) - b^2 \left(n + \frac{3}{2}\right) F\left(\frac{3}{2}, n + \frac{5}{2}, n+2; b^2\right) \right. \\ &\quad \left. + b^2 (n+1) F\left(\frac{3}{2}, n + \frac{3}{2}, n+1; b^2\right) - (n+1) F\left(\frac{1}{2}, n + \frac{1}{2}, n+1; b^2\right) \right].\end{aligned}$$

Applying (2.3.2) with $a = \frac{1}{2}, b = n + \frac{1}{2}, c = n + 1$ and $z = b^2$ one gets,

$$\begin{aligned}\Delta_n - \tilde{\Delta}_n &= b^{n+1} \frac{(\frac{1}{2})_{n+1}}{(n+1)!} \left[\frac{b^2}{2} \frac{(n+\frac{3}{2})}{(n+2)} F\left(\frac{3}{2}, n + \frac{5}{2}, n+3; b^2\right) - b^2 \left(n + \frac{3}{2}\right) F\left(\frac{3}{2}, n + \frac{5}{2}, n+2; b^2\right) \right. \\ &\quad + b^2(n+1)F\left(\frac{3}{2}, n + \frac{3}{2}, n+1; b^2\right) - (n+1)F\left(\frac{1}{2}, n + \frac{3}{2}, n+1; b^2\right) \\ &\quad \left. + \frac{b^2}{2} F\left(\frac{3}{2}, n + \frac{3}{2}, n+2; b^2\right) \right].\end{aligned}$$

Again applying (2.3.2) with $a = \frac{1}{2}, b = n + \frac{3}{2}, c = n + 2$ and $z = b^2$, we deduce

$$\begin{aligned}\Delta_n - \tilde{\Delta}_n &= b^{n+1} \frac{(\frac{1}{2})_{n+1}}{(n+1)!} \left[(n + \frac{3}{2})F\left(\frac{1}{2}, n + \frac{5}{2}, n+2; b^2\right) - (n + \frac{3}{2})F\left(\frac{1}{2}, n + \frac{3}{2}, n+2; b^2\right) \right. \\ &\quad - b^2 \left(n + \frac{3}{2}\right) F\left(\frac{3}{2}, n + \frac{5}{2}, n+2; b^2\right) + b^2(n+1)F\left(\frac{3}{2}, n + \frac{3}{2}, n+1; b^2\right) \\ &\quad \left. - (n+1)F\left(\frac{1}{2}, n + \frac{3}{2}, n+1; b^2\right) + \frac{b^2}{2} F\left(\frac{3}{2}, n + \frac{3}{2}, n+2; b^2\right) \right].\end{aligned}$$

We use (2.3.4) with $a = \frac{3}{2}, b = n + \frac{3}{2}, c = n + 1$ and $z = b^2$ to cancel some terms

$$\begin{aligned}\Delta_n - \tilde{\Delta}_n &= b^{n+1} \frac{(\frac{1}{2})_{n+1}}{(n+1)!} \left[(n + \frac{3}{2})F\left(\frac{1}{2}, n + \frac{5}{2}, n+2; b^2\right) - (n + \frac{3}{2})F\left(\frac{1}{2}, n + \frac{3}{2}, n+2; b^2\right) \right. \\ &\quad \left. - (n+1)F\left(\frac{1}{2}, n + \frac{3}{2}, n+1; b^2\right) \right].\end{aligned}$$

Finally, using (2.3.4) with $a = \frac{1}{2}, b = n + \frac{3}{2}, c = n + 1$ and $z = b^2$, we obtain

$$\Delta_n - \tilde{\Delta}_n = -\frac{b^{n+1}}{(n+1)!} \left(\frac{1}{2}\right)_{n+1} (n+1)F\left(\frac{1}{2}, n + \frac{3}{2}, n+2; b^2\right).$$

Consequently, we have

$$\begin{aligned}\mathcal{L}_3(h_1, h_2)(\omega) &= \frac{i}{2} \sum_{n=1}^{+\infty} \frac{b^{n+1}}{(n+1)!} \left(\frac{1}{2}\right)_{n+1} (n+1)F\left(\frac{1}{2}, n + \frac{3}{2}, n+2; b^2\right) a_n (\omega^{n+1} - \bar{\omega}^{n+1}) \\ &\quad - \frac{i}{2} \sum_{n=1}^{+\infty} \frac{b}{2} (n+1)F\left(\frac{1}{2}, \frac{3}{2}, 2; b^2\right) c_n (\omega^{n+1} - \bar{\omega}^{n+1}).\end{aligned}$$

As we have (see [69])

$$\Lambda_n(b) = \frac{(\frac{1}{2})_n}{n!} b^{n-1} F\left(\frac{1}{2}, n + \frac{1}{2}, n+1, b^2\right).$$

the proof of the proposition is now achieved. \square

2.5.2 Monotonicity of the eigenvalues

In what follows we shall use the variable $\lambda \triangleq 1 - 2\Omega$ instead of Ω . The main task is to list the suitable conditions on the used parameters in order to guarantee a one-dimensional kernel. Recall from Proposition

[2.5.1](#) that the operator $DG(\Omega, 0, 0)$ acts as a Fourier matrix multiplier and the determinant of each matrix M_n is given by

$$\det(M_n) = \frac{b}{4}(\lambda^2 - 2C_n\lambda + D_n) \quad (2.5.9)$$

with

$$\begin{cases} C_n &= 1 + \left(\frac{1}{b} - 1\right)S_n - (1 - b^2)\Lambda_1(b) \\ D_n &= -\frac{4}{b}S_n^2 + 2\left[\frac{1}{b} - 1 + 2(1 + b)\Lambda_1(b)\right]S_n - 4b^2(\Lambda_1^2(b) - \Lambda_n^2(b)) - 2(1 - b^2)\Lambda_1(b) + 1 \end{cases}.$$

From that proposition one can easily see that the kernel of $DG(\Omega, 0, 0)$ is non trivial if and only if

$$\{\exists n \geq 2, \det(M_n) = 0\}$$

Therefore the dimension of the kernel is related to the structure of the eigenvalues and to how they depend on the frequency modes. Observe that $\lambda \mapsto \det(M_n)$ is a second order polynomial and the roots structure depends on the reduced discriminant which is given by

$$\Delta_n = \left(\frac{1}{b} + 1\right)S_n - (1 + b^2)\Lambda_1(b)^2 - 4b^2\Lambda_n^2(b).$$

We shall prove the following proposition.

Proposition 2.5.2. (1) For any $n \in N^*$ we have $\Lambda_n(b) \geq 0$, $n \mapsto S_n$ is a strictly increasing sequence, $n \mapsto \Lambda_n(b)$ is a strictly decreasing sequence and $b \mapsto \Lambda_n(b)$ is a strictly increasing function.

(2) There exists $N \geq 2$ such that for any $n \geq N$ we get $\Delta_n > 0$ and the equation $\det(M_n) = 0$ admits two different real solutions given by

$$\lambda_n^\pm = C_n \pm \sqrt{\Delta_n}.$$

(3) The sequences $(\Delta_n)_{n \geq N}$ and $(\lambda_n^+)_{n \geq N}$ are strictly increasing and $(\lambda_n^-)_{n \geq N}$ is strictly decreasing.

(4) $\forall m > n > N$ we have

$$\lambda_m^- < \lambda_n^- < \lambda_n^+ < \lambda_m^+.$$

Proof. (1) The positivity and the monotonicity of $\Lambda_n(b)$ follow easily from the integral representation

$$\Lambda_n(b) = \frac{b^{n-1}}{\Gamma^2(\frac{1}{2})} \int_0^1 x^{n-\frac{1}{2}}(1-x)^{-\frac{1}{2}}(1-b^2x)^{-\frac{1}{2}} dx, \text{ for } b \in (0, 1).$$

As to the monotonicity of S_n it is obvious.

(2) We write $\Delta_n(b) = E_n(b)F_n(b)$ with

$$\begin{cases} E_n(b) &= \left(\frac{1}{b} + 1\right)S_n - (1 + b^2)\Lambda_1(b) - 2b\Lambda_n(b) \\ F_n(b) &= \left(\frac{1}{b} + 1\right)S_n - (1 + b^2)\Lambda_1(b) + 2b\Lambda_n(b) \end{cases}.$$

We remark that

$$\Delta_n(b) > 0 \text{ if and only if } E_n(b) > 0 \text{ or } F_n(b) < 0.$$

Using the strictly monotonicity of the sequences $(\Lambda_n)_{n \in N^*}$ and $(S_n)_{n \in N^*}$ we get

$$E_{n+1}(b) - E_n(b) = \left(1 + \frac{1}{b}\right)(S_{n+1} - S_n) - 2b(\Lambda_{n+1}(b) - \Lambda_n(b)) > 0.$$

Therefore $(E_n(b))_{n \in N^*}$ is a strictly increasing. As $\lim_{n \mapsto +\infty} E_n(b) = +\infty$ and

$$E_1(b) = -(1 + b)^2\Lambda_1(b),$$

we obtain that

$$\exists N \in \mathbb{N}^* \text{ such that } \forall n \geq N, E_n(b) > 0.$$

This implies the assertion (2).

(3) Straightforward computations yield

$$\begin{aligned} \Delta_{n+1} - \Delta_n &= \left(1 + \frac{1}{b}\right)^2 (S_{n+1}^2 - S_n^2) - 4b^2 (\Lambda_{n+1}^2(b) - \Lambda_n^2(b)) - 2(1+b^2) \left(1 + \frac{1}{b}\right) \Lambda_1(b) (S_{n+1} - S_n) \\ &= \left(1 + \frac{1}{b}\right) (S_{n+1} - S_n) \left[\left(1 + \frac{1}{b}\right) (S_{n+1} + S_n) - 2(1+b^2) \Lambda_1(b) \right] - 4b^2 (\Lambda_{n+1}^2(b) - \Lambda_n^2(b)) \\ &> \left(1 + \frac{1}{b}\right) (S_{n+1} - S_n) \left[\left(1 + \frac{1}{b}\right) (S_{n+1} + S_n) - 2(1+b^2) \Lambda_1(b) \right] \\ &> \left(1 + \frac{1}{b}\right) (S_{n+1} - S_n) \left[\left(1 + \frac{1}{b}\right) (S_{n+1} + S_n) - 2(1+b^2) \Lambda_1(b) - 2b [\Lambda_{n+1}(b) + \Lambda_n(b)] \right] \\ &> \left(1 + \frac{1}{b}\right) (S_{n+1} - S_n) (E_{n+1}(b) + E_n(b)) > 0. \end{aligned}$$

As $(\Delta_n)_{n \geq n}$ and $(S_n)_{n \in \mathbb{N}^*}$ are strictly increasing, $(\lambda_n^+)_{n \geq N}$ is also strictly increasing. We focus now on λ_n^- :

$$\begin{aligned} \lambda_{n+1}^- - \lambda_n^- &= \left(\frac{1}{b} - 1\right) (S_{n+1} - S_n) - [\sqrt{\Delta_{n+1}} - \sqrt{\Delta_n}] \\ &= \left(\frac{1}{b} - 1\right) (S_{n+1} - S_n) - \frac{\Delta_{n+1} - \Delta_n}{\sqrt{\Delta_{n+1}} + \sqrt{\Delta_n}} \\ &= -\frac{1}{\sqrt{\Delta_{n+1}} + \sqrt{\Delta_n}} \left[\left(1 + \frac{1}{b}\right) (S_{n+1} - S_n) \left[\left(1 + \frac{1}{b}\right) (S_{n+1} + S_n) - 2(1+b^2) \Lambda_1(b) \right] \right] \\ &\quad + \frac{4b^2(\Lambda_{n+1}^2(b) - \Lambda_n^2(b))}{\sqrt{\Delta_{n+1}} + \sqrt{\Delta_n}} + \left(\frac{1}{b} - 1\right) (S_{n+1} - S_n) \\ &< -\frac{1}{\sqrt{\Delta_{n+1}} + \sqrt{\Delta_n}} \left[\left(1 + \frac{1}{b}\right) (S_{n+1} - S_n) \left[\left(1 + \frac{1}{b}\right) (S_{n+1} + S_n) - 2(1+b^2) \Lambda_1(b) \right] \right] \\ &\quad + \left(\frac{1}{b} - 1\right) (S_{n+1} - S_n) \\ &< \frac{1}{b} \left[1 - \frac{1}{\sqrt{\Delta_{n+1}} + \sqrt{\Delta_n}} \left[\left(1 + \frac{1}{b}\right) (S_{n+1} + S_n) - 2(1+b^2) \Lambda_1(b) \right] \right] (S_{n+1} - S_n) \\ &\quad - \left[1 + \frac{1}{\sqrt{\Delta_{n+1}} + \sqrt{\Delta_n}} \left[\left(1 + \frac{1}{b}\right) (S_{n+1} + S_n) - 2(1+b^2) \Lambda_1(b) \right] \right] (S_{n+1} - S_n) \\ &< 0 \end{aligned}$$

because $\left[\left(1 + \frac{1}{b}\right) (S_{n+1} + S_n) - 2(1+b^2) \Lambda_1(b)\right] > E_{n+1}(b) + E_n(b) > 0$ and $\sqrt{\Delta_n} < \left(1 + \frac{1}{b}\right) S_n - (1+b^2) \Lambda_1(b)$.

Consequently the sequence $(\lambda_n^-)_{n \geq N}$ is strictly decreasing.

(4) It is obvious and follows from (2) and (3). \square

2.5.3 Proof of Theorem 4.5.1

This section is dedicated to the proof of the main result of this paper which is deeply related to the spectral study developed in the preceding section combined with Crandall-Rabinowitz's theorem. To proceed, fix $b \in (0, 1)$ and $m \geq N$, where N was defined in Proposition 2.5.2. Set,

$$X_m^{k+\log} = X^{k+\log} \cap \mathcal{A}_\varepsilon^m.$$

We define the ball of radius $r \in (0, 1)$ by

$$B_r^m = \left\{ f \in X_m^{k+\log}, \|f\|_{X_m^{k+\log}} \leq r \right\}$$

and we introduce the neighborhood of the trivial solution $(0, 0)$,

$$V_{m,r} \triangleq B_r^m \times B_r^m.$$

The set $V_{m,r}$ is endowed with the induced topology of the product spaces. Take $(f_1, f_2) \in V_{m,r}$ then the expansions of the associated conformal mappings Φ_1, Φ_2 in Δ_ε are given successively by

$$\Phi_1(z) = z + f_1(z) = z \left(1 + \sum_{n=1}^{+\infty} \frac{a_n}{z^{nm}} \right)$$

and

$$\Phi_2(z) = bz + f_2(z) = z \left(b + \sum_{n=1}^{+\infty} \frac{c_n}{z^{nm}} \right).$$

Consequently for any $z \in \Delta_\varepsilon$

$$\Phi_j(e^{\frac{2i\pi}{m}} z) = e^{\frac{2i\pi}{m}} \Phi_j(z), \quad j = 1, 2 \text{ and } |z| > \varepsilon. \quad (2.5.10)$$

From Proposition 2.5.2 recall the definition of the eigenvalues λ_m^\pm and the associated angular velocities are

$$\begin{aligned} \Omega_m^\pm &= \frac{1}{2} - \frac{1}{2} \lambda_m^\pm \\ &= \frac{1}{2} \tilde{C}_m \pm \frac{1}{2} \sqrt{\Delta_m} \end{aligned}$$

with

$$\Delta_m = \left(\left(\frac{1}{b} + 1 \right) S_m - (1 + b^2) \Lambda_1(b) \right)^2 - 4b^2 \Lambda_m^2(b)$$

and

$$\tilde{C}_m = \left(1 - \frac{1}{b} \right) S_m + (1 - b^2) \Lambda_1(b).$$

Note that S_m and $\Lambda_m(b)$ were introduced in Proposition 2.5.1. The V-states equations are described in (2.4.1) and (3.2.3) which we restate here, for $j \in \{1, 2\}$,

$$\tilde{G}(\Omega, \Phi_1, \Phi_2) \triangleq G(\Omega, f_1, f_2) \text{ and } G = (G_1, G_2)$$

with

$$\tilde{G}_j(\Omega, \Phi_1, \Phi_2)(\omega) = \operatorname{Im} \left\{ \left(\Omega \Phi_j(\omega) - \int_{\mathbb{T}} \frac{\tau \Phi'_1(\tau) - \omega \Phi'_j(\omega)}{|\Phi_1(\tau) - \Phi_j(\omega)|} \frac{d\tau}{\tau} + \int_{\mathbb{T}} \frac{\tau \Phi'_2(\tau) - \omega \Phi'_j(\omega)}{|\Phi_2(\tau) - \Phi_j(\omega)|} \frac{d\tau}{\tau} \right) \overline{\Phi'_j(\omega) \bar{\omega}} \right\}.$$

The following result is more precise than Theorem 4.5.1.

Theorem 2.5.3. *Let $k \geq 3, N$ be as in the Proposition 2.5.2, $m \geq N$, and take $\Omega \in \{\Omega_m^\pm\}$. Then, the following assertions hold true.*

- (1) *There exists $r > 0$ such that $G : \mathbb{R} \times V_{m,r} \mapsto Y_m^{k-1} \times Y_m^{k-1}$ is well-defined and is of class C^1 .*
- (2) *The kernel of $DG(\Omega, 0, 0)$ is one dimensional and generated by*

$$v_{0,m} : \omega \in T \mapsto \begin{pmatrix} \Omega + \frac{S_m}{b} - \Lambda_1(b) \\ -\Lambda_m(b) \end{pmatrix} \bar{\omega}^{m-1}.$$

(3) The range of $DG(\Omega, 0, 0)$ is closed and is of co-dimension one in $Y_m^{k-1} \times Y_m^{k-1}$.

(4) Transversality assumption: If Ω is a simple eigenvalue ($\Delta_m > 0$) then

$$\partial_\Omega DG(\Omega_m^\pm, 0, 0)v_{0,m} \notin \text{Im}(DG(\Omega_m^\pm, 0, 0)).$$

Proof. (1) Compared to Propositions 4.6.2 and 2.4.5, we just need to check that $G = (G_1, G_2)$ preserves the m -fold symmetry and maps $X_m^{k+\log} \times X_m^{k+\log}$ into $Y_m^{k-1} \times Y_m^{k-1}$. To this end, it is sufficient to check that for given $(f_1, f_2) \in X_m^{k+\log} \times X_m^{k+\log}$ the Fourier coefficients of $\tilde{G}_j(\Omega, \Phi_1, \Phi_2)$ vanish at frequencies which are not integer multiple of m . This amounts to proving that,

$$\tilde{G}_j(\Omega, \Phi_1, \Phi_2)(e^{i\frac{2\pi}{m}}\omega) = \tilde{G}_j(\Omega, \Phi_1, \Phi_2)(\omega), \forall \omega \in \mathbb{T}, j = 1, 2.$$

As

$$\Phi'_j(e^{\frac{2i\pi}{m}}\omega) = \Phi'_j(\omega), \quad (2.5.11)$$

the property is obvious for the first term $\text{Im}\{\Omega\bar{\omega}\overline{\Phi'_j(\omega)}\Phi_j(\omega)\}$. For the two last terms of \tilde{G}_j it is enough to check the identity,

$$\forall \omega \in \mathbb{T}, S(\Phi_i, \Phi_j)(e^{\frac{2i\pi}{m}}\omega) = e^{\frac{2i\pi}{m}}S(\Phi_i, \Phi_j)(\omega).$$

This follows easily by making the change of variables $\tau = e^{\frac{2i\pi}{m}}\xi$ and from (2.5.10) and (2.5.11),

$$\begin{aligned} S(\Phi_i, \Phi_j)(e^{\frac{2i\pi}{m}}\omega) &= \int_{\mathbb{T}} \frac{e^{\frac{2i\pi}{m}}\xi\Phi'_i(e^{\frac{2i\pi}{m}}\xi) - e^{\frac{2i\pi}{m}}\omega\Phi'_j(e^{\frac{2i\pi}{m}}\omega)}{|\Phi_i(e^{\frac{2i\pi}{m}}\xi) - \Phi_j(e^{\frac{2i\pi}{m}}\omega)|} \frac{d\xi}{\xi} \\ &= e^{\frac{2i\pi}{m}} \int_{\mathbb{T}} \frac{\xi\Phi'_i(\xi) - \omega\Phi'_j(\omega)}{|\Phi_i(\xi) - \Phi_j(\omega)|} \frac{d\xi}{\xi} \\ &= e^{\frac{2i\pi}{m}} S(\Phi_i, \Phi_j)(\omega). \end{aligned}$$

This concludes the proof of the following statement,

$$\forall (f_1, f_2) \in V_{m,r}, \quad G(\Omega, f_1, f_2) \in Y_m^{k-1} \times Y_m^{k-1}.$$

(2) We shall describe the kernel of linear operator $DG(\Omega_m^\pm, 0, 0)$ and show that it is one-dimensional. Let h_1, h_2 be two functions in $X_m^{k+\log}$ such that

$$h_1(\omega) = \sum_{n=1}^{+\infty} a_n \bar{\omega}^{nm-1} \text{ and } h_2(\omega) = \sum_{n=1}^{+\infty} c_n \bar{\omega}^{nm-1}. \quad (2.5.12)$$

Recall from Proposition 2.5.1 the following expression,

$$DG(\Omega, 0, 0)(h_1, h_2) = \frac{i}{2} \sum_{n \geq 1} nm M_{nm} \begin{pmatrix} a_n \\ c_n \end{pmatrix} (\omega^{nm} - \bar{\omega}^{nm}) \quad (2.5.13)$$

where the matrix M_n is given for $n \geq 2$ by :

$$M_n = \begin{pmatrix} \Omega - S_n + b^2 \Lambda_1(b) & -b^2 \Lambda_n(b) \\ b \Lambda_n(b) & b \Omega + S_n - b \Lambda_1(b) \end{pmatrix}.$$

Now if $\Omega \in \{\Omega_m^\pm\}$ then

$$\det(M_m) = 0.$$

Thus, the kernel of $DG(\Omega, 0, 0)$ is non trivial and is one-dimensional if and only if:

$$\det(M_{nm}) \neq 0, \forall n \geq 2.$$

This condition is ensured by Proposition 2.5.2. Hence we have the equivalence:

$$(h_1, h_2) \in \text{Ker}(DG(\Omega, 0, 0)) \quad \text{if and only if} \quad a_n = c_n = 0 \quad \forall n \geq 2 \text{ and } (a_1, c_1) \in \text{Ker}(M_m) \quad (2.5.14)$$

Hence, a generator of $\text{Ker}(DG(\Omega, 0, 0))$ can be chosen as the pair of functions

$$\omega \in \mathbb{T} \mapsto \begin{pmatrix} \Omega + \frac{S_m}{b} - \Lambda_1(b) \\ -\Lambda_m(b) \end{pmatrix} \bar{\omega}^{m-1}.$$

(3) We introduce

$$Z_m = \left\{ g = (g_1, g_2) \in Y_m^{k-1} \times Y_m^{k-1} \mid g(\omega) = \sum_{n \geq 1} \begin{pmatrix} A_n \\ C_n \end{pmatrix} (\omega^{nm} - \bar{\omega}^{nm}), \forall \omega \in \mathbb{T} \right. \\ \left. \text{s.t. } (A_n, C_n) \in \mathbb{R}^2 \quad \forall n \geq 2 \text{ and } \exists (a_1, c_1) \in \mathbb{R}^2 \text{ with } M_m \begin{pmatrix} a_1 \\ c_1 \end{pmatrix} = \begin{pmatrix} A_1 \\ C_1 \end{pmatrix} \right\}.$$

Z_m is closed and of codimension 1 in $Y_m^{k-1} \times Y_m^{k-1}$. The following inclusion is obvious

$$\text{Im}(DG(\Omega, 0, 0)) \subset Z_m.$$

Therefore it remains just to check the converse. Let $(g_1, g_2) \in Z_m$, we shall prove that the equation :

$$DG(\Omega, 0, 0)(h_1, h_2) = (g_1, g_2)$$

admits a solution $(h_1, h_2) \in X_m^{k+\log} \times X_m^{k+\log}$ where the Fourier expansions of these functions are given in (2.5.12). According to (2.4.7), the preceding equation is equivalent to

$$nmM_{nm} \begin{pmatrix} a_n \\ c_n \end{pmatrix} = \begin{pmatrix} A_n \\ C_n \end{pmatrix}, \forall n \in \mathbb{N}^*.$$

For $n = 1$, the existence follows from the condition of space Z_m and therefore we shall only focus on $n \geq 2$. Owing to (2.5.14) the sequences $(a_n)_{n \geq 2}$ and $(c_n)_{n \geq 2}$ are uniquely determined by the formula

$$\begin{pmatrix} a_n \\ c_n \end{pmatrix} = \frac{1}{nm} M_{nm}^{-1} \begin{pmatrix} A_n \\ C_n \end{pmatrix}, \forall n \geq 2.$$

By computing the matrix M_{nm}^{-1} we deduce that for all $n \geq 2$,

$$\begin{cases} a_n &= \frac{b(\Omega + \frac{1}{b} S_{nm} - \Lambda_1(b))}{mn \det(M_{nm})} A_n + \frac{b^2 \Lambda_{nm}(b)}{mn \det(M_{nm})} C_n \\ c_n &= -\frac{b \Lambda_{nm}(b)}{mn \det(M_{nm})} A_n + \frac{(\Omega - b S_{nm} + b^2 \Lambda_1(b))}{mn \det(M_{nm})} C_n \end{cases}.$$

We just need to check that $(h_1, h_2) \in X_m^{k+\log} \times X_m^{k+\log}$. We shall develop the computations only for h_1 since the same analysis can be applied to h_2 . By using the characterization given by Lemma 2.3.2 one writes

$$\begin{aligned} \|h_1\|_{X^{k+\log}}^2 &\approx |a_1|^2 + \sum_{n=2}^{+\infty} \frac{(mn)^{2k}}{\varepsilon^{2(nm+k-1)}} (1 + \log(nm))^2 \left[\frac{b(\Omega + \frac{1}{b} S_{nm} - \Lambda_1(b))}{mn \det(M_{nm})} A_n + \frac{b^2 \Lambda_{nm}(b)}{mn \det(M_{nm})} C_n \right]^2 \\ &\lesssim |a_1|^2 + \sum_{n=2}^{+\infty} \frac{(mn)^{2(k-1)}}{\varepsilon^{2(nm+k-1)}} \frac{(1 + \log(nm))^2}{\det(M_{nm})^2} [S_{nm}^2 A_n^2 + \Lambda_{nm}(b)^2 C_n^2] \\ &\lesssim |a_1|^2 + \sum_{n=2}^{+\infty} \frac{(mn)^{2(k-1)}}{\varepsilon^{2(nm+k-1)}} (A_n^2 + C_n^2) \\ &\lesssim \|g_1\|_{Y_m^{k-1}} + \|g_2\|_{Y_m^{k-1}}. \end{aligned}$$

We have used the asymptotics $S_{nm} \sim \log(nm)$ and $|\det(M_{nm})| \sim S_{nm}^2$.

(4) We have

$$\partial_\Omega DG(\Omega_m^\pm, 0, 0)v_{0,m} = \frac{im}{2} \begin{pmatrix} \Omega + \frac{S_m}{b} - \Lambda_1(b) \\ -b\Lambda_m(b) \end{pmatrix} (\omega^m - \bar{\omega}^m).$$

We resort to reductio ad absurdum and we suppose that

$$\partial_\Omega DG(\Omega_m^\pm, 0, 0)v_{0,m} \in \text{Im}(DG(\Omega_m^\pm, 0, 0)).$$

Then there exists $(a_1, c_1) \in \mathbb{R}^2$ such that

$$\begin{pmatrix} \Omega + \frac{S_m}{b} - \Lambda_1(b) \\ -b\Lambda_m(b) \end{pmatrix} = M_m \begin{pmatrix} a_1 \\ c_1 \end{pmatrix}.$$

As M_m has a one-dimension kernel, $\begin{pmatrix} \Omega + \frac{S_m}{b} - \Lambda_1(b) \\ -b\Lambda_m(b) \end{pmatrix}$ will be a scalar multiple of one column of the matrix M_m which happens if and only if

$$(\Omega + S_m - \Lambda_1(b))^2 - b^2\Lambda_m(b)^2 = 0. \quad (2.5.15)$$

Combining this equation with $\det(M_m) = 0$, we get

$$(\Omega - S_m + b^2\Lambda_1(b)) \left(\Omega + \frac{S_m}{b} - \Lambda_1(b) \right) + \left(\Omega + \frac{S_m}{b} - \Lambda_1(b) \right)^2 = 0.$$

This yields

$$\left(\Omega + \frac{S_m}{b} - \Lambda_1(b) \right) \left(2\Omega + (b^2 - 1)\Lambda_1(b) + \left(-1 + \frac{1}{b} \right) S_m \right) = 0$$

which is equivalent to

$$\Omega + \frac{S_m}{b} - \Lambda_1(b) = 0 \text{ ou } \Omega = \frac{1}{2} \left((1 - b^2)\Lambda_1(b) + \left(1 - \frac{1}{b} \right) S_m \right).$$

This first possibility is excluded by (2.5.15) because $\Lambda_m(b) \neq 0$ and the second one is also impossible because it corresponds to a double eigenvalue which is not also the case here. We obtain an absurdity and this concludes the proof of Theorem 2.5.3. \square

Chapter 3

Existence of small loops in the bifurcation diagram near the degenerate eigenvalues

Injuries are our best teachers.

— *Eat and Run,*
Scott JUREK

This chapter is the subject of the following publication:

Hmidi, Taoufik; Renault, Coralie, *Existence of small loops in the bifurcation diagram near the degenerate eigenvalues.*

Nonlinearity, 30(2017), no.10.

Abstract. In this paper we study for the incompressible Euler equations the global structure of the bifurcation diagram for the rotating doubly connected patches near the degenerate case. We show that the branches with the same symmetry merge forming a small loop provided that they are close enough. This gives an analytical proof for the numerical observations done in the recent work [33].

3.1 Introduction

During the last few decades an intensive research activity has been dedicated to the study in fluid dynamics of relative equilibria, sometimes called steady states or V-states. These vortical structures have the common feature to keep their shape without deformation during the motion and they seem to play a central role in the emergence of coherent structures in turbulent flows at large scales, see for instance [19, 41, 49, 53, 63] and the references therein. Notice that from experimental standpoint, their existence has been revealed in different geophysical phenomena such as the aerodynamic trailing-vortex problem, the two-dimensional shear layers, Saturn's hexagon, the Kármán vortex street, and so on. Several numerical and analytical investigations have been carried out in various configurations depending on the topological structure of the vortices: simply or multiply connected vortices, dipolar or multipolar, see for instance [7, 8, 17, 33, 30, 24, 29, 35, 38, 37, 34].

In this paper we shall be concerned with some refined global structure of the doubly connected rotating patches for the two-dimensional incompressible Euler equations. These equations describe the motion of an ideal fluid and take the form,

$$\begin{cases} \partial_t \omega + v \cdot \nabla \omega = 0, & (t, x) \in \mathbb{R}_+ \times \mathbb{R}^2, \\ v = -\nabla^\perp (-\Delta)^{-1} \omega, \\ \omega|_{t=0} = \omega_0 \end{cases} \quad (3.1.1)$$

where $v = (v_1, v_2)$ refers to the velocity fields and ω being its vorticity which is defined by the scalar $\omega = \partial_1 v_2 - \partial_2 v_1$. Note that one can recover the velocity from the vorticity distribution according to the Biot-Savart law,

$$v(x) = \frac{1}{2\pi} \int_{\mathbb{R}^2} \frac{(x-y)^\perp}{|x-y|^2} \omega(y) dy.$$

The global existence and uniqueness of solutions with initial vorticity lying in the space $L^1 \cap L^\infty$ is a very classical fact established many years ago by Yudovich [72]. This result has the advantage to allow discontinuous vortices taking the form of vortex patches, that is $\omega_0(x) = \chi_D$ the characteristic function of a bounded domain D . The time evolution of this specific structure is preserved and the vorticity $\omega(t)$ is uniformly distributed in bounded domain D_t , which is nothing but the image by the flow mapping of the initial domain. The regularity of this domain is not an easy task and was solved by Chemin in [13] who proved that a $C^{1+\epsilon}$ -boundary keeps this regularity globally in time without any loss. In general the dynamics of the boundary is hard to track and is subject to the nonlinear effects created by the induced velocity. Nonetheless, some special family of rotating patches characterized by uniform rotation without changing the shape are known in the literature and a lot of implicit examples have been discovered in the last few decades. Note that in this setting we have explicitly $D_t = R_{0,\Omega t} D$ where $R_{0,\Omega t}$ is a planar rotation centered at the origin and with angle Ωt ; for the sake of simplicity we have assumed that the center of rotation is the origin of the frame and the parameter Ω denotes the angular velocity of the rotating domains. The first example was discovered very early by Kirchhoff in [43] who showed that an ellipse of semi-axes a and b rotates about its center uniformly with the angular velocity $\Omega = \frac{ab}{(a^2+b^2)}$. Later, Deem and Zabusky gave in [17] numerical evidence of the existence of the V-states with m -fold symmetry for the integers $m \in \{3, 4, 5\}$.

Few years after, Burbea gave in [6] an analytical proof of the existence using complex analysis formulation and bifurcation theory. The regularity of the V-states close to Rankine vortices was discussed quite recently in [8, 37]. We point out that the bifurcation from the ellipses was studied numerically and analytically in [8, 34, 41]. All these results are restricted to simply connected domains and the analytical investigation of doubly connected V-states has been initiated with the works [33, 38]. To fix the terminology, a domain D is said doubly connected if it takes the form $D = D_1 \setminus D_2$ with D_1 and D_2 being two simply connected bounded domains satisfying $\overline{D_2} \subset D_1$. The main result of [33] which is deeply connected to the aim of this paper deals with the bifurcation from the annular patches where $D = \mathbb{A}_b \equiv \{z; b < |z| < 1\}$. For the clarity of the discussion we shall recall the main result of [33].

Theorem 3.1.1. *Given $b \in (0, 1)$ and let m be a positive integer such that,*

$$1 + b^m - \frac{(1 - b^2)}{2}m < 0. \quad (3.1.2)$$

Then there exist two curves of doubly connected rotating patches with m -fold symmetry bifurcating from the annulus \mathbb{A}_b at the angular velocities,

$$\Omega_m^\pm = \frac{1 - b^2}{4} \pm \frac{1}{2m} \sqrt{\Delta_m}$$

with

$$\Delta_m = \left(\frac{1 - b^2}{2}m - 1 \right)^2 - b^{2m}.$$

We emphasize that the condition (3.1.2) is required by the transversality assumption, otherwise the eigenvalues Ω_m^\pm are double and thus the classical theorems in the bifurcation theory such as Crandall-Rabinowitz theorem [16] are out of use. The analysis of the degenerate case corresponding to vanishing discriminant (in which case $\Omega_m^+ = \Omega_m^-$) has been explored very recently in [35]. They proved in particular that for $m \geq 3$ and $b \in (0, 1)$ such that $\Delta_m = 0$ there is no bifurcation to m -fold V-states. However for $b \in (0, 1) \setminus \mathcal{S}$ two-fold V-states still bifurcate from the annulus \mathbb{A}_b where $\mathcal{S} = \{b_m^*, m \geq 3\}$ and b_m^* being the unique solution in the interval $(0, 1)$ of the equation

$$1 + b^m - \frac{(1 - b^2)}{2}m = 0. \quad (3.1.3)$$

The proof of this result is by no means non trivial and based on the local structure of the reduced bifurcation equation obtained through the use of Lyapunov-Schmidt reduction. Note that according to the numerical experiments done in [33] two different scenarios for global bifurcation are conjectured. The first one when the eigenvalues Ω_m^- and Ω_m^+ are far enough in which case each branch ends with a singular V-state and the singularity is a corner of angle $\frac{\pi}{2}$. For more details about the structure of the limiting V-states we refer the reader to the Section 9.3 in [33]. Nevertheless, in the second scenario where the eigenvalues are close enough there is no singularity formation on the boundary and it seems quite evident that there is no spectral gap and the V-states can be constructed for any $\Omega \in [\Omega_m^-, \Omega_m^+]$, see Fig. 3.1 taken from [33]. Moreover, drawing the second Fourier coefficient of each conformal mapping that parametrize each boundary as done in Fig. 3.2 we get a small loop passing through the trivial solution at Ω_m^- and Ω_m^+ . This suggests that the bifurcation curve starting from Ω_m^+ will return back to the trivial solution (annulus) at Ω_m^- .

Our main purpose in this paper is to go further in this study by checking analytically the second scenario and provide for $m \geq 3$ the global structure of the bifurcation curves near the degenerate case. Our result reads as follows.

Theorem 3.1.2. *Let $m \geq 3$ and b_m^* be the unique solution in $(0, 1)$ of the equation (3.1.3). Then there exists $b_m \in (0, b_m^*)$ such that for any b in (b_m, b_m^*) the two curves of m -fold V-states given by Theorem 3.1.1 merge and form a loop.*

Now, we are going to outline the main steps of the proof. Roughly speaking we start with writing down the equations governing the boundary $\partial D_1 \cup \partial D_2$ of the rotating patches and attempt to follow the approach

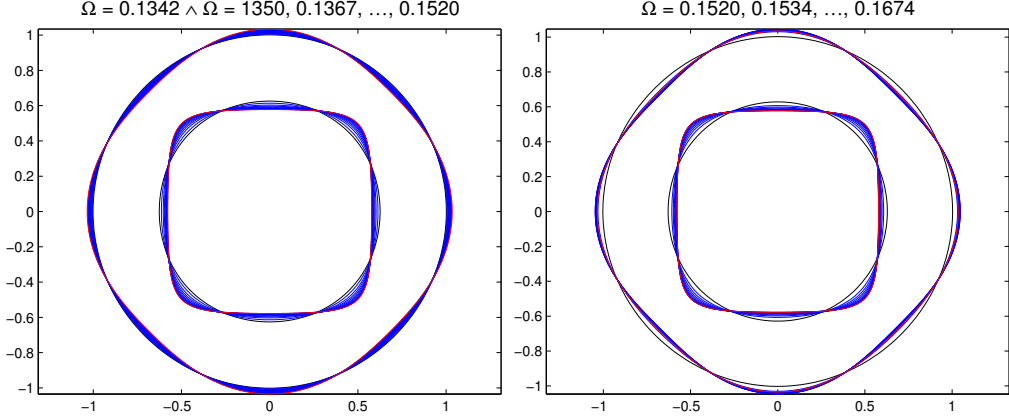


Figure 3.1: Family of 4-fold V -states, for $b = 0.63$ and different Ω . We observe that there is no singularity formation in the boundary.

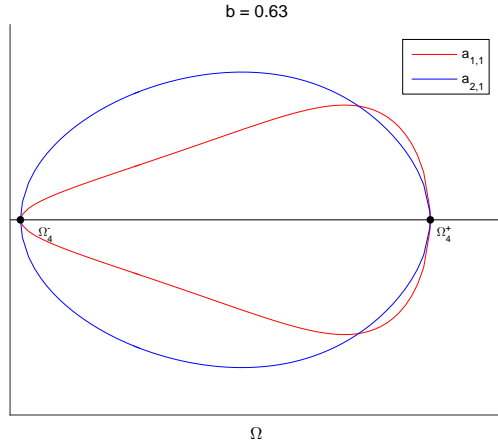


Figure 3.2: Bifurcation curves of the Fourier coefficients $a_{1,1}$ and $a_{2,1}$ in (3.1.4) with respect to Ω .

developed in [33]. For $j \in \{1, 2\}$, let $\Phi_j : \mathbb{D}^c \rightarrow D_j^c$ be the conformal mapping which enjoys the following structure,

$$\forall |z| \geq 1, \Phi_j(z) = b_j z + \sum_{n \in \mathbb{N}} \frac{a_{j,n}}{z^n}, \quad a_{j,n} \in \mathbb{R}, \quad b_1 = 1 \quad \text{and} \quad b_2 = b. \quad (3.1.4)$$

We have denoted by \mathbb{D}^c the complement of the open unit disc \mathbb{D} and we have also assumed that the Fourier coefficients of the conformal mappings are real which means that we look for V -states which have at least one axis of symmetry that can be chosen to be the real axis. It is also important to mention that the domain D is implicitly assumed to be smooth enough, more than C^1 as we shall see in the proof, and therefore each conformal mapping can be extended up to the boundary. According to the subsection 3.2.2 the conformal mappings satisfy the coupled equations: for $j \in \{1, 2\}$

$$G_j(\lambda, f_1, f_2)(w) \triangleq \operatorname{Im} \left\{ \left((1 - \lambda) \overline{\Phi_j(w)} + I(\Phi_j(w)) \right) w \Phi'_j(w) \right\} = 0, \quad \forall w \in \mathbb{T}$$

where

$$\lambda = 1 - 2\Omega, \quad \Phi_j(w) = b_j w + f_j(w)$$

and

$$I(z) = \frac{1}{2i\pi} \int_{\mathbb{T}} \frac{\bar{z} - \overline{\Phi_1(\xi)}}{z - \Phi_1(\xi)} \Phi'_1(\xi) d\xi - \frac{1}{2\pi} \int_{\mathbb{T}} \frac{\bar{z} - \overline{\Phi_2(\xi)}}{z - \Phi_2(\xi)} \Phi'_2(\xi) d\xi.$$

Here $d\xi$ denotes the complex integration over the unit circle \mathbb{T} . The linearized operator around the annulus defined through

$$\mathcal{L}_{\lambda,b}(h) \triangleq \partial_f G(\lambda, 0)h = \frac{d}{dt}[G(\lambda, th)]|_{t=0}$$

plays a significant role in the proof and according to [35] it acts as a matrix Fourier multiplier. Actually, for $h = (h_1, h_2)$ chosen in suitable Banach space with

$$h_j(w) = \sum_{n \geq 1} \frac{a_{j,n}}{w^{nm-1}}, \quad a_{j,n} \in \mathbb{R}$$

we have the expression

$$\mathcal{L}_{\lambda,b}(h) = \sum_{n \geq 1} M_{nm}(\lambda) \begin{pmatrix} a_{1,n} \\ a_{2,n} \end{pmatrix} e_{nm} \quad \text{with} \quad e_n(w) = \text{Im}(\bar{w}^n)$$

where for $n \geq 1$ the matrix M_n is given by

$$M_n(\lambda) = \begin{pmatrix} n\lambda - 1 - nb^2 & b^{n+1} \\ -b^n & b(n\lambda - n + 1) \end{pmatrix}.$$

It is known from [33] that for given $m \geq 3$ the values of b such that $M_m(\lambda)$ is singular, for suitable values of $\lambda = \lambda_m^\pm$, belong to the interval $(0, b_m^*)$ where b_m^* has been introduced in (3.1.3). It is also shown in that paper that the assumptions of Crandall-Rabinowitz theorem are satisfied, especially the transversality assumption which reduces the bifurcation study to some properties of the linearized operator. This latter property is no longer true for $b = b_m^*$ and we have double eigenvalues $\lambda_m^\pm = \frac{1+b_m^*}{2}$. This is a degenerate case and we know from [35] that there is no bifurcation. It seems that the approach implemented in this situation can be carried out for $b \in (0, b_m^*)$ but close enough to b_m^* . In fact, using Lyapunov-Schmidt reduction (through appropriate projections) we transform the infinite-dimensional problem into a two dimensional one. Therefore the V-states equation reduces to the resolution of an equation of the type

$$F_2(\lambda, t) = 0 \quad \text{with} \quad F_2 : \mathbb{R}^2 \rightarrow \mathbb{R},$$

with F_2 being a smooth function and note that when $b = b_m^*$ the point $(\lambda_m^\pm, 0)$ is a critical point for F_2 and for that reason one should expand F_2 to the second order around this point in order to understand the resolvability of the reduced equation. At the order two F_2 is strictly convex and therefore locally the critical point is the only solution for F_2 . Reproducing this approach in the current setting and after long and involved computations we find that for (λ, t) close enough, for example, to the solution $(\lambda_m^+, 0)$

$$F_2(\lambda, t) = a_m(b)(\lambda - \lambda_m^+) + c_m(b)(\lambda - \lambda_m^+)^2 + d_m(b)t^2 + ((\lambda - \lambda_m^+)^2 + t^2)\varepsilon(\lambda, t)$$

with

$$\lim_{(\lambda, t) \rightarrow (\lambda_m^+, 0)} \varepsilon(\lambda, t) = 0.$$

Notice that

$$a_m(b_m^*) = 0, \quad c_m(b_m^*) > 0, \quad d_m(b_m^*) > 0$$

and moreover for b belonging to a small interval (b_m, b_m^*) we get $a_m(b) < 0$. As we can easily check from the preceding facts, the zeros of the associated quadratic form of F_2 is a small ellipse. By implementing perturbation arguments, we show that the structure of solutions of F_2 are actually small perturbation of the ellipse. Furthermore, they can be parametrized by a smooth Jordan curve and the intersection of this curve with the real axis gives rise to two points which are $\{\lambda_m^\pm\}$. Note that the branches emanating from that points describe the bifurcating curves of V-states with exactly m -fold symmetry, which implies the formation of small loops in the bifurcation diagram. More details will be given later in Section 3.4.

The paper is organized as follows. In Section 3.2 we shall introduce some tools, formulate the V-states equations and write down the reduced bifurcation equation using Lyapunov-Schmidt reduction. Section 3.3 is devoted to Taylor expansion at order two of the reduced bifurcation equation and the complete proof of Theorem 3.1.2 will be given in the last section.

3.2 Reminder and preliminaries

We shall recall in this section some tools that we shall frequently use throughout the paper and write down the reduced bifurcation equation which is the first step towards the proof of Theorem 3.1.2. But before that we will fix some notations. The unit disc and its boundary will be denoted respectively by \mathbb{D} and \mathbb{T} . and D_r is the planar disc of radius r and centered at the origin. Given a continuous function $f : \mathbb{T} \rightarrow \mathbb{C}$ we define its mean value by,

$$\int_{\mathbb{T}} f(\tau) d\tau \triangleq \frac{1}{2\pi} \int_{\mathbb{T}} f(\tau) d\tau,$$

where $d\tau$ stands for the complex integration.

3.2.1 Hölder spaces

Now we shall introduce Hölder spaces on the unit circle \mathbb{T} . Let $0 < \gamma < 1$ we denote by $C^\gamma(\mathbb{T})$ the space of continuous functions f such that

$$\|f\|_{C^\gamma(\mathbb{T})} \triangleq \|f\|_{L^\infty(\mathbb{T})} + \sup_{\tau \neq w \in \mathbb{T}} \frac{|f(\tau) - f(w)|}{|\tau - w|^\alpha} < \infty.$$

For any integer n , the space $C^{n+\gamma}(\mathbb{T})$ stands for the set of functions f of class C^n whose n -th order derivatives are Hölder continuous with exponent γ . It is equipped with the usual norm,

$$\|f\|_{C^{n+\gamma}(\mathbb{T})} \triangleq \|f\|_{L^\infty(\mathbb{T})} + \left\| \frac{d^n f}{dw^n} \right\|_{C^\gamma(\mathbb{T})}.$$

Recall that for $n \in \mathbb{N}$, the space $C^n(\mathbb{T})$ is the set of functions f of class C^n such that,

$$\|f\|_{C^n(\mathbb{T})} \triangleq \sum_{k=0}^n \|f^{(k)}\|_{L^\infty(\mathbb{T})} < \infty.$$

3.2.2 Boundary equations

Let $D_2 \Subset D_1$ be two simply connected domains and $D = D_1 \setminus D_2$ be a doubly connected domain. The boundary of D_j will be denoted by Γ_j . Then according to [33], HMdeg we find that that the exterior conformal mappings Φ_1 and Φ_2 associated to D_1 and D_2 satisfy the coupled nonlinear equations. For $j \in \{1, 2\}$,

$$\widehat{G}_j(\lambda, \Phi_1, \Phi_2)(w) = 0, \quad \forall w \in \mathbb{T},$$

with

$$\widehat{G}_j(\lambda, \Phi_1, \Phi_2)(w) \triangleq \text{Im} \left\{ \left((1 - \lambda) \overline{\Phi_j(w)} + I(\Phi_j(w)) \right) w \Phi'_j(w) \right\}. \quad (3.2.1)$$

Note that we have introduced $\lambda \triangleq 1 - 2\Omega$ because it is more convenient for the computations and

$$I(z) = \int_{\mathbb{T}} \frac{\bar{z} - \overline{\Phi_1(\xi)}}{z - \Phi_1(\xi)} \Phi'_1(\xi) d\xi - \int_{\mathbb{T}} \frac{\bar{z} - \overline{\Phi_2(\xi)}}{z - \Phi_2(\xi)} \Phi'_2(\xi) d\xi.$$

The integrals are defined in the complex sense and we shall focus on V-states which are small perturbations of the annulus $\mathbb{A}_b = \{z, b \leq |z| \leq 1\}$ with $b \in (0, 1)$. The conformal mappings Φ_j with $j \in \{1, 2\}$ admit the expansions,

$$\forall |z| \geq 1, \quad \Phi_j(z) = b_j z + f_j(z) = z + \sum_{n=1}^{+\infty} \frac{a_{j,n}}{z^n}$$

with

$$b_1 = 1, b_2 = b.$$

Define

$$G_j(\lambda, f_1, f_2) \triangleq \widehat{G}_j(\lambda, \Phi_1, \Phi_2) \quad (3.2.2)$$

then the equations of the V-states become,

$$\forall w \in \mathbb{T}, G(\lambda, f_1, f_2)(w) = 0$$

with

$$G = (G_1, G_2).$$

Note that the annulus is a solution for any angular velocity, that is,

$$G(\lambda, 0, 0) = 0$$

and the set $\{(\lambda, 0, 0) | \lambda \in \mathbb{R}\}$ will be called the set of trivial solutions.

3.2.3 Reduced bifurcation equation.

For any integer $m \geq 3$, the existence of V-states was proved in [33] provided $b \in (0, b_m^*)$ that guarantee the transversality assumption. The idea is to check that the functional G has non trivial zeros using bifurcation arguments. However, and as we have mentioned before in the Introduction, the knowledge of the linearized operator around the trivial solution is not enough to understand the structure of the bifurcating curves near the degenerate case corresponding to double eigenvalues. To circumvent this difficulty we make an expansion at order two of the reduced bifurcation equation in the spirit of [35], and this will be the subject of the current task. Let us first introduce Banach spaces that we shall use and recall the algebraic structure of the linearized operator.

For $\alpha \in (0, 1)$, we set

$$X_m = \left\{ f = (f_1, f_2) \in (C^{1+\alpha}(\mathbb{T}))^2, f(w) = \sum_{n=1}^{+\infty} A_n \bar{w}^{nm-1}, A_n \in \mathbb{R}^2 \right\}.$$

and

$$Y_m = \left\{ G = (G_1, G_2) \in (C^\alpha(\mathbb{T}))^2, G = \sum_{n=1}^{+\infty} B_n e_{nm}, B_n \in \mathbb{R}^2 \right\}, e_n(w) = \text{Im}(\bar{w}^n).$$

Note that the domains D_j whose conformal mappings Φ_j associated to the perturbations f_j lying in X_m are actually m -fold symmetric. Recall from the subsection 3.2.2 that the equation of m -fold symmetric V-states is given by

$$G(\lambda, f) = 0, \quad f = (f_1, f_2) \in B_r^m \times B_r^m \subset X_m \quad (3.2.3)$$

where B_r^m is the ball given by

$$B_r^m = \left\{ f \in C^{1+\alpha}(\mathbb{T}), f(w) = \sum_{n=1}^{\infty} a_n \bar{w}^{nm-1}, a_n \in \mathbb{R}, \|f\|_{C^{1+\alpha}} \leq r \right\}.$$

We mention that we are looking for solutions close to the trivial solutions and therefore the radius r will be taken small enough. The linearized operator around zero is defined by

$$\partial_f G(\lambda, 0)h = \frac{d}{dt}[G(\lambda, th)]|_{t=0}.$$

As it is proved in [35], for $h = (h_1, h_2) \in X_m$ taking the expansions

$$h_j(w) = \sum_{n \geq 1} \frac{a_{j,n}}{w^{nm-1}},$$

we get the expression

$$\partial_f G(\lambda, 0)h = \sum_{n \geq 1} M_{nm}(\lambda) \begin{pmatrix} a_{1,n} \\ a_{2,n} \end{pmatrix} e_{nm}, \quad (3.2.4)$$

where for $n \geq 1$ the matrix M_n is given by

$$M_n(\lambda) = \begin{pmatrix} n\lambda - 1 - nb^2 & b^{n+1} \\ -b^n & b(n\lambda - n + 1) \end{pmatrix}.$$

We say throughout this paper that λ is an eigenvalue if for some n the matrix $M_n(\lambda)$ is not invertible. Since

$$\det(M_n(\lambda)) = (n\lambda - 1 - nb^2)b(n\lambda - n + 1) + b^{2n+1}$$

is a polynomial of second order on the variable λ , the roots are real if and only if its discriminant is positive. From [?] we remind that the roots take the form,

$$\lambda_n^\pm = \frac{1+b^2}{2} \pm \frac{1}{n} \sqrt{\Delta_n(b)}$$

with the constraint

$$\Delta_n(b) = \left(\frac{1-b^2}{2}n - 1 \right)^2 - b^{2n} \geq 0.$$

According to [33] this condition is equivalent for $n \geq 3$ to

$$n \frac{1-b^2}{2} - 1 \geq b^n. \quad (3.2.5)$$

In addition, it is also proved that for any integer $m \geq 3$ there exists a unique $b_m^* \in (0, 1)$ such that $\Delta_m(b_m^*) = 0$ and $\Delta_m(b) > 0$ for all $b \in [0, b_m^*]$. Moreover,

$$\text{Ker}(\partial_f G(\lambda_m^\pm, 0)) = \langle v_m \rangle$$

with

$$v_m(w) = \begin{pmatrix} \frac{m\lambda_m^\pm - m + 1}{b^{m-1}} \\ 1 \end{pmatrix} \bar{w}^{m-1} \triangleq \begin{pmatrix} v_{1,m} \\ v_{2,m} \end{pmatrix} \bar{w}^{m-1}.$$

In order to be rigorous we could write v_m^\pm but for the sake of simple notations we note simply v_m . Now we shall introduce a complement \mathcal{X}_m of the subspace $\langle v_m \rangle$ in the space X_m ,

$$\mathcal{X}_m = \left\{ h \in (C^{1+\alpha}(\mathbb{T}))^2, h(w) = \sum_{n=2}^{+\infty} A_n \bar{w}^{nm-1} + \alpha \begin{pmatrix} 1 \\ 0 \end{pmatrix} \bar{w}^{m-1}, A_n \in \mathbb{R}^2, \alpha \in \mathbb{R} \right\}.$$

It is easy to prove that the subspace is closed and

$$X_m = \langle v_m \rangle \oplus \mathcal{X}_m.$$

In addition the range \mathcal{Y}_m of $\partial_f G(\lambda_m^\pm, 0)$ in Y_m is given by

$$\mathcal{Y}_m = \left\{ K \in (C^\alpha(\mathbb{T}))^2, K = \sum_{n=2}^{+\infty} B_n e_{nm} + \beta \begin{pmatrix} b^m \\ m\lambda_m^\pm - m + 1 \end{pmatrix} e_m, B_n \in \mathbb{R}^2, \beta \in \mathbb{R} \right\}.$$

The subspace \mathcal{Y}_m is of co-dimension one and its complement is a line generated by

$$\begin{aligned} \mathbb{W}_m &= \frac{1}{\sqrt{(m\lambda_m^\pm - m + 1)^2 + b^{2m}}} \begin{pmatrix} m\lambda_m^\pm - m + 1 \\ -b^m \end{pmatrix} e_m \\ &\triangleq \hat{\mathbb{W}}_m e_m. \end{aligned}$$

Thus we have

$$Y_m = \langle \mathbb{W}_m \rangle \oplus \mathcal{Y}_m.$$

Lyapunov-Schmidt reduction relies on two projections

$$P : X_m \rightarrow \langle v_m \rangle, \quad Q : Y_m \rightarrow \langle \mathbb{W}_m \rangle.$$

For a future use we need the explicit expression of the projection Q . The Euclidian scalar product of \mathbb{R}^2 is denoted by $\langle \cdot, \cdot \rangle$ and for $h \in Y_m$ we have

$$h = \sum_{n=1}^{+\infty} B_n e_{nm}, \quad Qh(w) = \langle B_1, \widehat{\mathbb{W}}_m \rangle \mathbb{W}_m.$$

Moreover, by the definition of Q one has,

$$Q\partial_f G(\lambda_m^\pm, 0) = 0. \quad (3.2.6)$$

Unlike the degenerate case, the transversality assumption holds true

$$\partial_\lambda \partial_f G(\lambda_m^\pm, 0) v_m \notin \text{Im}(\partial_f G(\lambda_m^\pm, 0))$$

and therefore

$$Q\partial_\lambda \partial_f G(\lambda_m^\pm, 0) v_m \neq 0. \quad (3.2.7)$$

For $f \in X_m$ we use the decomposition

$$f = g + k \quad \text{with} \quad g = Pf \quad \text{and} \quad k = (\text{Id} - P)f.$$

Then the V-state equation is equivalent to the system

$$F_1(\lambda, g, k) \triangleq (\text{Id} - Q)G(\lambda, g + k) = 0 \quad \text{and} \quad QG(\lambda, g + k) = 0.$$

Note that $F_1 : \mathbb{R} \times \langle v_m \rangle \times \mathcal{X}_m \rightarrow \mathcal{Y}_m$ is well-defined and smooth. Thus using (3.2.6) we can check the identity,

$$D_k F_1(\lambda_m^\pm, 0, 0) = (\text{Id} - Q)\partial_f G(\lambda_m^\pm, 0) = \partial_f G(\lambda_m^\pm, 0).$$

Consequently

$$D_k F_1(\lambda_m^\pm, 0, 0) : \mathcal{X}_m \rightarrow \mathcal{Y}_m$$

is invertible. The inverse is explicit and is given by the formula

$$\partial_f G(\lambda_m^\pm, 0) h = K \iff \forall n \geq 2, A_n = M_{nm}^{-1} B_n \quad \text{and} \quad \alpha = -\frac{\beta}{b^m} (m\lambda_m^\pm - m + 1). \quad (3.2.8)$$

Thus using the implicit function theorem, the solutions of the equation $F_1(\lambda, g, k) = 0$ are locally described around the point $(\lambda_m^\pm, 0)$ by the parametrization $k = \varphi(\lambda, g)$ with

$$\varphi : \mathbb{R} \times \langle v_m \rangle \rightarrow \mathcal{X}_m.$$

being a smooth function. Remark that in principle φ is locally defined but it can be extended globally to a smooth function still denoted by φ . Moreover, the resolution of the V-state equation near to $(\lambda_m^\pm, 0)$ is equivalent to

$$QG(\lambda, tv_m + \varphi(\lambda, tv_m)) = 0. \quad (3.2.9)$$

As $G(\lambda, 0) = 0, \forall \lambda$ it follows

$$\varphi(\lambda, 0) = 0, \forall \lambda \in \mathcal{V}(\lambda_m^\pm), \quad (3.2.10)$$

where $\mathcal{V}(\lambda_m^\pm)$ is a small neighborhood of λ_m^\pm . Using Taylor expansion at order 1 on the variable t the V-states equation (3.2.9) is equivalent to the *reduced bifurcation equation*,

$$F_2(\lambda, t) \triangleq \int_0^1 Q\partial_f G(\lambda, stv_m + \varphi(\lambda, stv_m))(v_m + \partial_g \varphi(\lambda, stv_m)v_m) ds = 0. \quad (3.2.11)$$

In addition, using (3.2.6) we remark that

$$F_2(\lambda_m^\pm, 0) = 0.$$

3.3 Taylor expansion

The goal of this section is to compute Taylor expansion of F_2 at the second order. This quadratic form will answer about the local structure of the solutions of the equation (3.2.11).

3.3.1 General formulae

The aim of this paragraph is to provide some general results concerning the first and second derivatives of φ and F_2 . First notice that the transversality assumption required for Crandall-Rabinowitz theorem is given by

$$\partial_\lambda F_2(\lambda_m^\pm, 0) = Q\partial_\lambda \partial_f G(\lambda_m^\pm, 0)v_m \neq 0.$$

Thus applying the implicit function theorem to F_2 , we get in a small neighborhood of $(\lambda_m^\pm, 0)$ a unique curve of solutions $t \in [-\varepsilon_0, \varepsilon_0] \mapsto (\lambda(t), t)$. We shall prove that for b close enough to b_m^* this curve is a smooth Jordan curve and for this aim we need to know the full structure of the quadratic form associated to F_2 . The following identities were proved in [35, p 13-14].

$$\partial_\lambda \varphi(\lambda_m^\pm, 0) = \partial_g \varphi(\lambda_m^\pm, 0)v_m = 0. \quad (3.3.1)$$

and

$$\partial_{\lambda\lambda} \varphi(\lambda_m^\pm, 0) = 0. \quad (3.3.2)$$

Now, we give the expressions of the coefficients of the quadratic form associated to F_2 around the point $(\lambda_m^\pm, 0)$. For the proof see [35, Proposition 2].

Proposition 3.3.1. *The following assertions hold true.*

1. *First derivatives:*

$$\partial_\lambda F_2(\lambda_m^\pm, 0) = Q\partial_\lambda \partial_f G(\lambda_m^\pm, 0)(v_m)$$

and

$$\begin{aligned} \partial_t F_2(\lambda_m^\pm, 0) &= \frac{1}{2}Q\partial_{ff}G(\lambda_m^\pm, 0)[v_m, v_m] \\ &= \frac{1}{2}\frac{d^2}{dt^2}[QG(\lambda_m^\pm, tv_m)]|_{t=0}. \end{aligned}$$

2. *Expression of $\partial_{\lambda\lambda} F_2(\lambda_m^\pm, 0)$:*

$$\partial_{\lambda\lambda} F_2(\lambda_m^\pm, 0) = -2Q\partial_\lambda \partial_f G(\lambda_m^\pm, 0)[\partial_f G(\lambda_m^\pm, 0)]^{-1}(\text{Id} - Q)\partial_\lambda \partial_f G(\lambda_m^\pm, 0)v_m$$

3. *Expression of $\partial_{tt} F_2(\lambda_m^\pm, 0)$:*

$$\partial_{tt} F_2(\lambda_m^\pm, 0) = \frac{1}{3}\frac{d^3}{dt^3}[QG(\lambda_m^\pm, tv_m)]|_{t=0} + Q\partial_{ff}G(\lambda_m^\pm, 0)[v_m, \hat{v}_m]$$

with

$$\begin{aligned} \hat{v}_m &\triangleq \frac{d^2}{dt^2} \varphi(\lambda_m^\pm, tv_m)|_{t=0} \\ &= -[\partial_f G(\lambda_m^\pm, 0)]^{-1} \frac{d^2}{dt^2}[(\text{Id} - Q)G(\lambda_m^\pm, tv_m)]|_{t=0} \end{aligned}$$

and

$$Q\partial_{ff}G(\lambda_m^\pm, 0)[v_m, \hat{v}_m] = \partial_t \partial_s [QG(\lambda_m^\pm, tv_m + s\hat{v}_m)]|_{t=0, s=0}.$$

4. Expression of $\partial_\lambda \partial_t F_2(\lambda_m^\pm, 0)$:

$$\begin{aligned}\partial_\lambda \partial_t F_2(\lambda_m^\pm, 0) &= \frac{1}{2} Q \partial_\lambda \partial_{ff} G(\lambda_m^\pm, 0)[v_m, v_m] + \frac{1}{2} Q \partial_\lambda \partial_f G(\lambda_m^\pm, 0)(\hat{v}_m) \\ &\quad + Q \partial_{ff} G(\lambda_m^\pm, 0)[v_m, \partial_\lambda \partial_g \varphi(\lambda_m^\pm, 0)v_m]\end{aligned}$$

with

$$\partial_\lambda \partial_g \varphi(\lambda_m^\pm, 0)v_m = -[\partial_f G(\lambda_m^\pm, 0)]^{-1}(\text{Id} - Q)\partial_\lambda \partial_f G(\lambda_m^\pm, 0)v_m$$

3.3.2 Explicit formulae for the quadratic form

In this section we want to explicit the terms in the Taylor expansion of F_2 at the second order. The main result reads as follows.

Proposition 3.3.2. *Let $m \geq 3$ and $b \in (0, b_m^*)$. Then the following assertions hold true.*

1. Expression of $\partial_t F_2(\lambda_m^\pm, 0)$.

$$\partial_t F_2(\lambda_m^\pm, 0) = 0.$$

2. Expression of $\partial_\lambda F_2(\lambda_m^\pm, 0)$.

$$\partial_\lambda F_2(\lambda_m^\pm, 0) = \frac{m[(m\lambda_m^\pm - m + 1)^2 - b^{2m}]}{b^{m-1}[(m\lambda_m^\pm - m + 1)^2 + b^{2m}]^{\frac{1}{2}}} \mathbb{W}_m.$$

3. Expression of $\partial_{\lambda\lambda} F_2(\lambda_m^\pm, 0)$.

$$\partial_{\lambda\lambda} F_2(\lambda_m^\pm, 0) = \frac{4m^2 b^{1-m} (m\lambda_m^\pm - m + 1)^3}{[(m\lambda_m^\pm - m + 1)^2 + b^{2m}]^{\frac{3}{2}}} \mathbb{W}_m.$$

4. Expression of $\partial_{tt} F_2(\lambda_m^\pm, 0)$.

$$\begin{aligned}\partial_{tt} F_2(\lambda_m^\pm, 0) &= -m(m-1)b^{3-3m} \frac{(b^{2m-2} - (m\lambda_m^\pm - m + 1)^2)^2}{[(m\lambda_m^\pm - m + 1)^2 + b^{2m}]^{\frac{1}{2}}} \mathbb{W}_m \\ &\quad + \tilde{\beta}_m \mathcal{K}_m \mathbb{W}_m\end{aligned}$$

with

$$\begin{aligned}\mathcal{K}_m &\triangleq \frac{b^{1-m} (m\lambda_m^\pm - 1)(m\lambda_m^\pm - m + 1)^2 + (1-2m)(m\lambda_m^\pm - m + 1)b^{m+1} + mb^{3m-1}}{[(m\lambda_m^\pm - m + 1)^2 + b^{2m}]^{\frac{1}{2}}} \\ &\times (2\lambda_m^\pm m - 2m + 1)\end{aligned}$$

and

$$\tilde{\beta}_m = -\frac{2bm(b^m - b^{2-m}(m\lambda_m^\pm - m + 1))^2}{\det(M_{2m}(\lambda_m^\pm))}.$$

5. Expression of $\partial_\lambda \partial_t F_2(\lambda_m^\pm, 0)$.

$$\partial_\lambda \partial_t F_2(\lambda_m^\pm, 0) = 0.$$

Remark 3.3.3. *In [35], all the preceding quantities were computed in the limit case $b = b_m^*$ and our expressions lead to the same thing when we take $b \rightarrow b_m^*$. This can be checked using the identity*

$$m\lambda_m^\pm - m + 1 = -\sqrt{b^{2m} + \Delta_m} \pm \sqrt{\Delta_m}$$

and when $b = b_m^*$ the discriminant Δ_m vanishes.

In what follows we shall establish the formulae of Proposition 3.3.2. As we can observe from Proposition 3.3.1 that most of them are based on the quantities $\frac{d^k}{dt^k}[G(\lambda_m^\pm, tv_m)]_{|t=0}$ for $k \in \{2, 3\}$. We introduce some notations which will be very useful to obtain explicit expressions. We begin with:

$$\Phi_j(t, w) = b^{j-1}w + tv_{j,m}\bar{w}^{m-1}$$

which leads to

$$G_j(\lambda_m^\pm, tv_m) = \operatorname{Im} \left\{ [(1 - \lambda_m^\pm)\overline{\Phi_j(t, w)} + I(\Phi_j(t, w))]w(b^{j-1} + t(1 - m)v_{j,m}\bar{w}^m) \right\}$$

with:

$$I(\Phi_j(t, w)) = I_1(\Phi_j(t, w)) - I_2(\Phi_j(t, w))$$

where:

$$I_i(\Phi_j(t, w)) = \int_{\mathbb{T}} \frac{\overline{\Phi_j(t, w)} - \overline{\Phi_i(t, \tau)}}{\Phi_j(t, w) - \Phi_i(t, \tau)} \Phi'_i(t, \tau) d\tau.$$

We precise that the $\Phi'_i(t, \tau)$ that appears in the preceding formula is the derivative of Φ_i with respect to the second variable τ .

Computation of $\partial_t F_2(\lambda_m^\pm, 0)$

We shall sketch the proof because most of the computations were done in [35]. Note that

$$\partial_t F_2(\lambda_m^\pm, 0) = \frac{1}{2} Q \partial_{ff} G(\lambda_m^\pm, 0)[v_m, v_m] = \frac{1}{2} Q \frac{d^2}{dt^2} [G_j(\lambda_m^\pm, tv_m)]_{|t=0}.$$

To lighten the notations we introduce

$$I_i(\Phi_j(t, w)) = \int_{\mathbb{T}} \frac{\overline{A} + t\overline{B}}{A + tB} (b^{i-1} + tC) d\tau$$

with

$$A = b^{j-1}w - b^{i-1}\tau, \quad B = v_{j,m}\bar{w}^{m-1} - v_{i,m}\bar{\tau}^{m-1} \quad \text{and} \quad C = v_{i,m}(1 - m)\bar{\tau}^m.$$

We can easily find that

$$\begin{aligned} \frac{d^2}{dt^2} [G_j(\lambda_m^\pm, tv_m)]_{|t=0} &= \operatorname{Im} \left\{ b^{j-1}w \frac{d^2}{dt^2} I(\Phi_j(t, w))_{|t=0} + 2(1 - \lambda_m^\pm)(1 - m)v_{j,m}^2 \right. \\ &\quad \left. + 2(1 - m)v_{j,m} \frac{d}{dt} I(\Phi_j(t, w))_{|t=0} \bar{w}^{m-1} \right\} \\ &= \operatorname{Im} \left\{ b^{j-1}w \frac{d^2}{dt^2} I(\Phi_j(t, w))_{|t=0} + 2(1 - m)v_{j,m} \frac{d}{dt} I(\Phi_j(t, w))_{|t=0} \bar{w}^{m-1} \right\}. \end{aligned}$$

Recall from [35, p. 823] that

$$\frac{d}{dt} [I_i(\Phi_j(t, w))]_{|t=0} = \int_{\mathbb{T}} \frac{\overline{A}}{A^2} (AC - b^{i-1}B) d\tau + b^{i-1} \int_{\mathbb{T}} \frac{\overline{B}}{A} d\tau.$$

Moreover, for any $i, j \in \{1, 2\}$, there exist real numbers $\mu_{i,j}, \gamma_{i,j}$ such that

$$\int_{\mathbb{T}} \frac{\overline{B}}{A} d\tau = \mu_{i,j} w^{m-1}$$

and

$$\oint \frac{\bar{A}}{A^2} (AC - b^{i-1}B) d\tau = \gamma_{i,j} \bar{w}^{m+1}.$$

Hence,

$$\frac{d}{dt} [I_i(\Phi_j(t, w))]|_{t=0} = \gamma_{i,j} \bar{w}^{m+1} + b^{i-1} \mu_{i,j} w^{m-1}$$

with

$$\gamma_{i,j} \triangleq v_{i,m}(1-m) \oint \frac{b^{j-1} - b^{i-1}\bar{\tau}}{b^{j-1} - b^{i-1}\tau} \bar{\tau}^m d\tau - b^{i-1} \oint \frac{b^{j-1} - b^{i-1}\bar{\tau}}{(b^{j-1} - b^{i-1}\tau)^2} (v_{j,m} - v_{i,m} \bar{\tau}^{m-1}) d\tau.$$

We also get from (39) of [35],

$$\gamma_{1,2} = 0.$$

For $\gamma_{2,1}$ by writing

$$\gamma_{2,1} = v_{2,m}(1-m) \oint \frac{1 - b\bar{\tau}}{1 - b\tau} \bar{\tau}^m d\tau - b \oint \frac{1 - b\bar{\tau}}{(1 - b\tau)^2} (v_{1,m} - v_{2,m} \bar{\tau}^{m-1}) d\tau.$$

combined with the following identities: for any $m \in \mathbb{N}^*$

$$\oint_{\mathbb{T}} \frac{\bar{\tau}^m}{(1 - b\tau)} d\tau = \oint_{\mathbb{T}} \frac{\tau^{m-1}}{\tau - b} d\tau = b^{m-1} \quad (3.3.3)$$

and

$$\oint_{\mathbb{T}} \frac{\bar{\tau}^m}{(1 - b\tau)^2} d\tau = \oint_{\mathbb{T}} \frac{\tau^m}{(\tau - b)^2} d\tau = mb^{m-1}. \quad (3.3.4)$$

We obtain

$$\begin{aligned} \gamma_{2,1} &= v_{2,m}(1-m)[b^{m-1} - b^{m+1}] + bv_{2,m}[(m-1)b^{m-2} - mb^m] + b^2 v_{1,m} \\ &= -v_{2,m}b^{m+1} + b^2 v_{1,m}. \end{aligned}$$

For $\gamma_{i,i}$ we recall that

$$\gamma_{i,i} = v_{i,m}(1-m) \oint \frac{1 - \bar{\tau}}{1 - \tau} \bar{\tau}^m d\tau - v_{i,m} \oint \frac{1 - \bar{\tau}}{(1 - \tau)^2} (1 - \bar{\tau}^{m-1}) d\tau.$$

Thus using the residue theorem at ∞ we deduce,

$$\gamma_{i,i} = 0.$$

Finally we get,

$$\frac{d}{dt} [I(\Phi_1(t, w))]|_{t=0} = (\mu_{1,1} - b\mu_{2,1}) w^{m-1} + [v_{2,m} b^{m+1} - b^2 v_{1,m}] \bar{w}^{m+1} \quad (3.3.5)$$

and

$$\frac{d}{dt} [I(\Phi_2(t, w))]|_{t=0} = (\mu_{1,2} - b\mu_{2,2}) w^{m-1}. \quad (3.3.6)$$

Now we have to compute $\frac{d^2}{dt^2} [I_i(\Phi_j(t, w))]|_{t=0}$. According to [?, p. 825-826] one has

$$\frac{d^2}{dt^2} [I_i(\Phi_j(t, w))]|_{t=0} = 2 \oint_{\mathbb{T}} \frac{[A\bar{B} - \bar{A}B]}{A^3} [AC - b^{i-1}B] d\tau.$$

Moreover

$$\int_{\mathbb{T}} \frac{\bar{B}}{A^2} [AC - b^{i-1}B] d\tau = \hat{\mu}_{i,j} \bar{w}$$

and

$$-\int_{\mathbb{T}} \frac{\bar{A}B}{A^3} [AC - b^{i-1}B] d\tau = \eta_{i,j} \bar{w}^{2m+1}.$$

Then we have

$$\frac{d^2}{dt^2} [I_i(\Phi_j(t, w))]|_{t=0} = 2\hat{\mu}_{i,j} \bar{w} + 2\eta_{i,j} \bar{w}^{2m+1}$$

with

$$\hat{\mu}_{i,j} = v_{i,m}(1-m) \int_{\mathbb{T}} \frac{(v_{j,m} - v_{i,m}\bar{\tau}^{m-1})}{(b^{j-1} - b^{i-1}\bar{\tau})} \bar{\tau}^m d\tau + \int_{\mathbb{T}} \frac{(v_{j,m} - v_{i,m}\bar{\tau}^{m-1})}{(b^{j-1} - b^{i-1}\bar{\tau})^2} b^{i-1} [v_{i,m}\bar{\tau}^{m-1} - v_{j,m}] d\tau$$

and

$$\begin{aligned} \eta_{i,j} &= \int_{\mathbb{T}} \frac{(b^{j-1} - b^{i-1}\bar{\tau})(v_{j,m} - v_{i,m}\bar{\tau}^{m-1})}{(b^{j-1} - b^{i-1}\bar{\tau})^2} v_{i,m}(m-1)\bar{\tau}^m d\tau \\ &\quad + b^{i-1} \int_{\mathbb{T}} \frac{(b^{j-1} - b^{i-1}\bar{\tau})(v_{j,m} - v_{i,m}\bar{\tau}^{m-1})^2}{(b^{j-1} - b^{i-1}\bar{\tau})^3} d\tau. \end{aligned}$$

For the diagonal terms we get

$$\begin{aligned} \hat{\mu}_{i,i} &= \frac{v_{i,m}^2}{b^{i-1}} (1-m) \int_{\mathbb{T}} \frac{(1 - \bar{\tau}^{m-1})}{(1 - \bar{\tau})} \bar{\tau}^m d\tau + \frac{v_{i,m}^2}{b^{i-1}} \int_{\mathbb{T}} \frac{(1 - \bar{\tau}^{m-1})}{(1 - \bar{\tau})^2} [\bar{\tau}^{m-1} - 1] d\tau \\ &= (m-1) \frac{v_{i,m}^2}{b^{i-1}} \end{aligned}$$

As to the term $\hat{\mu}_{1,2}$, we may write

$$\begin{aligned} \hat{\mu}_{1,2} &= v_{1,m}(1-m) \int_{\mathbb{T}} \frac{(v_{2,m} - v_{1,m}\bar{\tau}^{m-1})}{(b - \bar{\tau})} \bar{\tau}^m d\tau + v_{1,m} \int_{\mathbb{T}} \frac{(v_{2,m} - v_{1,m}\bar{\tau}^{m-1})}{(b - \bar{\tau})^2} \bar{\tau}^{m-1} d\tau \\ &\quad - v_{2,m} \int_{\mathbb{T}} \frac{(v_{2,m} - v_{1,m}\bar{\tau}^{m-1})}{(b - \bar{\tau})^2} d\tau. \end{aligned}$$

The first and the second integrals vanish using the residue theorem at ∞ . Thus we find

$$\hat{\mu}_{1,2} = (m-1)v_{2,m}v_{1,m}b^{m-2}.$$

Concerning the term $\hat{\mu}_{2,1}$ given by

$$\hat{\mu}_{2,1} = v_{2,m}(1-m) \int_{\mathbb{T}} \frac{(v_{1,m} - v_{2,m}\bar{\tau}^{m-1})}{(1 - b\bar{\tau})} \bar{\tau}^m d\tau + \int_{\mathbb{T}} \frac{(v_{1,m} - v_{2,m}\bar{\tau}^{m-1})}{(1 - b\bar{\tau})^2} b[v_{2,m}\bar{\tau}^{m-1} - v_{1,m}] d\tau$$

it can be computed using (3.3.3) and (3.3.4)

$$\begin{aligned} \hat{\mu}_{2,1} &= v_{2,m}(1-m)[v_{1,m}b^{m-1} - v_{2,m}] + bv_{2,m}v_{1,m}(m-1)b^{m-2} \\ &\quad + b \int_{\mathbb{T}} \frac{(-v_{2,m}^2 - v_{1,m}^2 + v_{2,m}v_{1,m}\bar{\tau}^{m-1})}{(1 - b\bar{\tau})^2} d\tau. \end{aligned}$$

The last term vanishes thanks to the residue theorem. Finally we have:

$$\hat{\mu}_{2,1} = v_{2,m}^2(m-1).$$

Now we shall move to the calculation of $\eta_{i,j}$ for $i, j \in \{1, 2\}$. We start with the term,

$$\eta_{1,2} = v_{1,m}(m-1) \int_{\mathbb{T}} \frac{(b-\bar{\tau})(v_{2,m} - v_{1,m}\bar{\tau}^{m-1})}{(b-\tau)^2} \bar{\tau}^m d\tau + \int_{\mathbb{T}} \frac{(b-\bar{\tau})(v_{2,m} - v_{1,m}\bar{\tau}^{m-1})^2}{(b-\tau)^3} d\tau.$$

Using the residue theorem at ∞ we get

$$\eta_{1,2} = 0.$$

Now we focus on the term $\eta_{2,1}$ given by

$$\eta_{2,1} = v_{2,m}(m-1) \int_{\mathbb{T}} \frac{(1-b\bar{\tau})(v_{1,m} - v_{2,m}\bar{\tau}^{m-1})}{(1-b\tau)^2} \bar{\tau}^m d\tau + b \int_{\mathbb{T}} \frac{(1-b\bar{\tau})(v_{1,m} - v_{2,m}\bar{\tau}^{m-1})^2}{(1-b\tau)^3} d\tau.$$

According to (3.3.3) and (3.3.4) we get

$$\begin{aligned} \int_{\mathbb{T}} \frac{(1-b\bar{\tau})(v_{1,m} - v_{2,m}\bar{\tau}^{m-1})}{(1-b\tau)^2} \bar{\tau}^m d\tau &= v_{1,m} \left(mb^{m-1} - (m+1)b^{m+1} \right) \\ &\quad + v_{2,m} \left(2mb^{2m} - (2m-1)b^{2m-2} \right). \end{aligned}$$

Applying the residue theorem, we can easily prove for any $m \in \mathbb{N}^*$,

$$\int_{\mathbb{T}} \frac{\bar{\tau}^m}{(1-b\tau)^3} d\tau = \int_{\mathbb{T}} \frac{\tau^{m+1}}{(\tau-b)^3} d\tau = \frac{m(m+1)}{2} b^{m-1}. \quad (3.3.7)$$

Thus,

$$\begin{aligned} \int_{\mathbb{T}} \frac{(1-b\bar{\tau})(v_{1,m} - v_{2,m}\bar{\tau}^{m-1})^2}{(1-b\tau)^3} d\tau &= v_{1,m} v_{2,m} m \left((m+1)b^m - (m-1)b^{m-2} \right) - bv_{1,m}^2 \\ &\quad + v_{2,m}^2 (2m-1) \left((m-1)b^{2m-3} - mb^{2m-1} \right). \end{aligned}$$

It follows that

$$\eta_{2,1} = -v_{2,m}^2 mb^{2m} - b^2 v_{1,m}^2 + v_{1,m} v_{2,m} (m+1)b^{m+1}.$$

For the diagonal term we write

$$\eta_{i,i} = \frac{v_{i,m}^2}{b^{i-1}} (m-1) \int_{\mathbb{T}} \frac{(1-\bar{\tau})(1-\bar{\tau}^{m-1})}{(1-\tau)^2} \bar{\tau}^m d\tau + \frac{v_{i,m}^2}{b^{i-1}} \int_{\mathbb{T}} \frac{(1-\bar{\tau})(1-\bar{\tau}^{m-1})^2}{(1-\tau)^3} d\tau.$$

By the residue theorem we get

$$\eta_{i,i} = 0.$$

Putting together the preceding estimates yields

$$\begin{aligned} \frac{d^2}{dt^2} [I(\Phi_1(t, w))]|_{t=0} &= 2 \left(v_{2,m}^2 mb^{2m} + b^2 v_{1,m}^2 - v_{1,m} v_{2,m} (m+1)b^{m+1} \right) \bar{w}^{2m+1} \\ &\quad + 2(m-1)(v_{1,m}^2 - v_{2,m}^2) \bar{w} \end{aligned}$$

and

$$\frac{d^2}{dt^2} [I(\Phi_2(t, w))]|_{t=0} = 2(m-1)v_{2,m} \left(v_{1,m} b^{m-2} - \frac{v_{2,m}}{b} \right) \bar{w}.$$

Combining these estimates with (3.3.5) and (3.3.6) we find successively,

$$\begin{aligned} \frac{d^2}{dt^2} [G_1(\lambda_m^\pm, tv_m)]|_{t=0} &= \text{Im} \left\{ w \frac{d^2}{dt^2} I(\Phi_1(t, w))|_{t=0} + 2(1-m)v_{1,m} \frac{d}{dt} I(\Phi_1(t, w))|_{t=0} \bar{w}^{m-1} \right\} \\ &= 2m(v_{2,m} b^m - bv_{1,m})^2 e_{2m} \end{aligned}$$

and

$$\begin{aligned} \frac{d^2}{dt^2}[G_2(\lambda_m^\pm, tv_m)]_{|t=0} &= \operatorname{Im} \left\{ bw \frac{d^2}{dt^2} I(\Phi_2(t, w))_{|t=0} + 2(1-m)v_{2,m} \frac{d}{dt} I(\Phi_2(t, w))_{|t=0} \bar{w}^{m-1} \right\} \\ &= 0. \end{aligned}$$

This can be written in the form,

$$\frac{d^2}{dt^2}[G(\lambda_m^\pm, tv_m)]_{|t=0} = \begin{pmatrix} 2m(v_{2,m}b^m - bv_{1,m})^2 \\ 0 \end{pmatrix} e_{2m}.$$

From the structure of the projector Q we get

$$\begin{aligned} \partial_t F_2(\lambda_m^\pm, 0) &= \frac{1}{2} Q \partial_f G(\lambda_m^\pm, 0)[v_m, v_m] \\ &= \frac{1}{2} Q \frac{d^2}{dt^2}[G(\lambda_m^\pm, tv_m)]_{|t=0} \\ &= 0. \end{aligned}$$

Hence the first point of the Proposition 3.3.2 is proved.

Computation of $\partial_\lambda F_2(\lambda_m^\pm, 0)$

From the explicit expression of $\partial_f G(\lambda_m^\pm, 0)$ it is easy to verify that

$$\partial_\lambda \partial_f G(\lambda_m^\pm, 0)(v_m) = m \begin{pmatrix} v_{1,m} \\ bv_{2,m} \end{pmatrix} e_m. \quad (3.3.8)$$

Thus we have,

$$\begin{aligned} \partial_\lambda F_2(\lambda_m^\pm, 0) &= Q \partial_\lambda \partial_f G(\lambda_m^\pm, 0)(v_m) \\ &= m \left\langle \begin{pmatrix} v_{1,m} \\ bv_{2,m} \end{pmatrix}, \hat{\mathbb{W}}_m \right\rangle \mathbb{W}_m. \end{aligned}$$

Straightforward computations lead to

$$\partial_\lambda F_2(\lambda_m^\pm, 0) = \frac{m[(m\lambda_m^\pm - m + 1)^2 - b^{2m}]}{b^{m-1}[(m\lambda_m^\pm - m + 1)^2 + b^{2m}]} \begin{pmatrix} m\lambda_m^\pm - m + 1 \\ -b^m \end{pmatrix} e_m. \quad (3.3.9)$$

Thus the second point of the Proposition 3.3.2 follows.

Computation of $\partial_{\lambda\lambda} F_2(\lambda_m^\pm, 0)$

Using (3.3.8) and (3.3.9) we obtain

$$\begin{aligned} (\operatorname{Id} - Q) \partial_\lambda \partial_f G(\lambda_m^\pm, 0) v_m &= \frac{2mb(m\lambda_m^\pm - m + 1)}{(m\lambda_m^\pm - m + 1)^2 + b^{2m}} \begin{pmatrix} b^m \\ m\lambda_m^\pm - m + 1 \end{pmatrix} e_m \\ &= \kappa \begin{pmatrix} b^m \\ m\lambda_m^\pm - m + 1 \end{pmatrix} e_m \end{aligned}$$

with

$$\kappa \triangleq \frac{2mb(m\lambda_m^\pm - m + 1)}{(m\lambda_m^\pm - m + 1)^2 + b^{2m}}.$$

Then by (3.2.8) and the expression of $\partial_\lambda \partial_g \varphi(\lambda_m^\pm, 0)$ detailed in Proposition 3.3.1 one gets

$$\begin{aligned}\partial_\lambda \partial_g \varphi(\lambda_m^\pm, 0) &= -[\partial_f G(\lambda_m^\pm, 0)]^{-1} (\text{Id} - Q) \partial_\lambda \partial_f G(\lambda_m^\pm, 0) v_m \\ &= -\kappa [\partial_f G(\lambda_m^\pm, 0)]^{-1} \begin{pmatrix} b^m \\ m\lambda_m^\pm - m + 1 \end{pmatrix} e_m \\ &= \frac{2mb^{1-m}(m\lambda_m^\pm - m + 1)^2}{(m\lambda_m^\pm - m + 1)^2 + b^{2m}} \begin{pmatrix} 1 \\ 0 \end{pmatrix} \bar{w}^{m-1}.\end{aligned}\quad (3.3.10)$$

Consequently,

$$\partial_\lambda \partial_f G(\lambda_m^\pm, 0) [\partial_\lambda \partial_g \varphi(\lambda_m^\pm, 0) v_m] = \frac{2m^2(m\lambda_m^\pm - m + 1)^2}{(m\lambda_m^\pm - m + 1)^2 + b^{2m}} \begin{pmatrix} 1 \\ 0 \end{pmatrix} e_m.$$

Straightforward computations lead to

$$Q \partial_\lambda \partial_f G(\lambda_m^\pm, 0) [\partial_\lambda \partial_g \varphi(\lambda_m^\pm, 0) v_m] = \frac{2m^2b^{1-m}(m\lambda_m^\pm - m + 1)^3}{[(m\lambda_m^\pm - m + 1)^2 + b^{2m}]^2} \begin{pmatrix} m\lambda_m^\pm - m + 1 \\ -b^m \end{pmatrix} e_m.$$

Finally we obtain the following expression

$$\partial_{\lambda\lambda} F_2(\lambda_m^\pm, 0) = \frac{4m^2b^{1-m}(m\lambda_m^\pm - m + 1)^3}{[(m\lambda_m^\pm - m + 1)^2 + b^{2m}]^{\frac{3}{2}}} \mathbb{W}_m.$$

Computation of $\partial_{tt} F_2(\lambda_m^\pm, 0)$

We mention that most of the computations were done in [35] and so we shall just outline the basic steps. Looking to the formula given in Proposition 3.3.1 we need first to compute $\frac{d^3}{dt^3}[G(\lambda_m^\pm, tv_m)]|_{t=0}$. From the identity (60) of [35] we recall that

$$\frac{d^3}{dt^3} G_j(\lambda_m^\pm, tv_m)|_{t=0} = \text{Im} \left\{ b^{j-1} w \frac{d^3}{dt^3} [I(\Phi_j(t, w))]|_{t=0} + 3(1-m)v_{j,m} \bar{w}^{m-1} \left[\frac{d^2}{dt^2} (I(\Phi_j(t, w))) \right]|_{t=0} \right\}.$$

It is also shown in [35, p. 835] that

$$\frac{d^3}{dt^3} [I_i(\Phi_j(t, w))]|_{t=0} = -6 \int_{\mathbb{T}} \frac{[\bar{B}A - \bar{A}B]}{A^4} B [AC - b^{i-1}B] d\tau.$$

One can find real numbers $\hat{\eta}_{i,j}$ such that

$$\frac{1}{6} \frac{d^3}{dt^3} [I_i(\Phi_j(t, w))]|_{t=0} = (m-1)J_{i,j} \bar{w}^{m+1} + b^{i-1}K_{i,j} \bar{w}^{m+1} + \hat{\eta}_{i,j} \bar{w}^{3m+1}$$

where

$$J_{i,j} = v_{i,m} \int_{\mathbb{T}} \frac{(v_{j,m} - v_{i,m}\bar{\tau}^{m-1})(v_{j,m} - v_{i,m}\tau^{m-1})}{(b^{j-1} - b^{i-1}\tau)^2} \bar{\tau}^m d\tau$$

and

$$K_{i,j} = \int_{\mathbb{T}} \frac{(v_{j,m} - v_{i,m}\bar{\tau}^{m-1})^2(v_{j,m} - v_{i,m}\tau^{m-1})}{(b^{j-1} - b^{i-1}\tau)^3} d\tau.$$

To start, we compute $J_{i,j}$. The same proof of (61) of [?] gives

$$J_{1,2} = 0.$$

For $J_{2,1}$ we use (3.3.4),

$$\begin{aligned} J_{2,1} &= v_{2,m} \int_{\mathbb{T}} \frac{(v_{1,m} - v_{2,m}\bar{\tau}^{m-1})(v_{1,m} - v_{2,m}\tau^{m-1})}{(1-b\tau)^2} \bar{\tau}^m d\tau \\ &= v_{2,m}[v_{1,m}^2 + v_{2,m}^2]mb^{m-1} + v_{1,m}v_{2,m}^2[(1-2m)b^{2m-2} - 1]. \end{aligned}$$

As to $J_{i,i}$ we easily get

$$\begin{aligned} J_{i,i} &= \frac{v_{i,m}^3}{b^{2(i-1)}} \int_{\mathbb{T}} \frac{(1-\bar{\tau}^{m-1})(1-\tau^{m-1})}{(1-\tau)^2} \bar{\tau}^m d\tau \\ &= 0. \end{aligned}$$

For $K_{1,2}$ we write

$$\begin{aligned} K_{1,2} &= \int_{\mathbb{T}} \frac{v_{2,m}^3 + v_{1,m}^2 v_{2,m} \bar{\tau}^{2m-2} - 2v_{2,m}^2 v_{1,m} \bar{\tau}^{m-1} - v_{1,m}^3 \bar{\tau}^{m-1} + 2v_{1,m}^2 v_{2,m}}{(b-\tau)^3} d\tau \\ &\quad - v_{1,m} v_{2,m}^2 \int_{\mathbb{T}} \frac{\tau^{m-1}}{(b-\tau)^3} d\tau. \end{aligned}$$

Using the residue theorem at ∞ , we can see that all the terms vanish except the last one that can be computed also with the residue theorem.

$$K_{1,2} = \frac{v_{1,m} v_{2,m}^2 (m-1)(m-2)}{2} b^{m-3}.$$

For $K_{2,1}$ given by

$$K_{2,1} = \int_{\mathbb{T}} \frac{v_{1,m}^3 - v_{1,m}^2 v_{2,m} \tau^{m-1} + 2v_{1,m} v_{2,m}^2 + v_{1,m} v_{2,m}^2 \bar{\tau}^{2m-2} - v_{2,m}^3 \bar{\tau}^{m-1} - 2v_{1,m}^2 v_{2,m} \bar{\tau}^{m-1}}{(1-b\tau)^3} d\tau.$$

we may use the residue theorem combined with (3.3.7)

$$\begin{aligned} K_{2,1} &= \int_{\mathbb{T}} \frac{v_{1,m} v_{2,m}^2 \bar{\tau}^{2m-2} - v_{2,m}^3 \bar{\tau}^{m-1} - 2v_{1,m}^2 v_{2,m} \bar{\tau}^{m-1}}{(1-b\tau)^3} d\tau \\ &= (2v_{1,m}^2 + v_{2,m}^2) v_{2,m} \frac{m(1-m)}{2} b^{m-2} + v_{1,m} v_{2,m}^2 (m-1)(2m-1) b^{2m-3}. \end{aligned}$$

As to the diagonal terms $K_{i,i}$ we use residue theorem leading to

$$\begin{aligned} K_{i,i} &= \frac{v_{i,m}^3}{b^{3(i-1)}} \int_{\mathbb{T}} \frac{(1-\bar{\tau}^{m-1})^2 (1-\tau^{m-1})}{(1-\tau)^3} d\tau \\ &= \frac{v_{i,m}^3}{b^{3(i-1)}} \frac{(m-1)(m-2)}{2} \end{aligned}$$

Summing up we find

$$\begin{aligned} \frac{1}{6} \frac{d^3}{dt^3} [I(\Phi_1(t, w))]|_{t=0} &= (m-1) \left(v_{2,m}^2 v_{1,m} - v_{2,m}^3 \frac{m}{2} b^{m-1} + v_{1,m}^3 \frac{m-2}{2} \right) \bar{w}^{m+1} \\ &\quad + (\hat{\eta}_{1,1} - \hat{\eta}_{2,1}) \bar{w}^{3m+1} \end{aligned}$$

and

$$\begin{aligned} \frac{1}{6} \frac{d^3}{dt^3} [I(\Phi_2(t, w))]_{|t=0} &= \frac{v_{2,m}^2(m-1)(m-2)}{2} \left(v_{1,m} b^{m-3} - \frac{v_{2,m}}{b^2} \right) \bar{w}^{m+1} \\ &\quad + (\widehat{\eta}_{1,2} - \widehat{\eta}_{2,2}) \bar{w}^{3m+1}. \end{aligned}$$

This leads to

$$\begin{aligned} \frac{d^3}{dt^3} [G_1(\lambda_m^\pm, tv_m)]_{|t=0} &= \operatorname{Im} \left\{ 6(m-1) \left(v_{2,m}^2 v_{1,m} - v_{2,m}^3 \frac{m}{2} b^{m-1} + v_{1,m}^3 \frac{m-2}{2} \right) \bar{w}^m \right. \\ &\quad + 6(\widehat{\eta}_{1,1} - \widehat{\eta}_{2,1}) \bar{w}^{3m} + 6(1-m)v_{1,m}(m-1) \left(v_{1,m}^2 - v_{2,m}^2 \right) \bar{w}^m \\ &\quad \left. + 6(1-m)v_{1,m} \left(v_{2,m}^2 m b^{2m} + b^2 v_{1,m}^2 - v_{1,m} v_{2,m} (m+1) b^{m+1} \right) \bar{w}^{3m} \right\} \\ &= 3m(m-1) \left(2v_{2,m}^2 v_{1,m} - v_{2,m}^3 b^{m-1} - v_{1,m}^3 \right) e_m + \gamma_1 e_{3m} \end{aligned}$$

and

$$\begin{aligned} \frac{d^3}{dt^3} [G_2(\lambda_m^\pm, 0)]_{|t=0} &= \operatorname{Im} \left\{ 3v_{2,m}^2(m-1)(m-2) \left(v_{1,m} b^{m-2} - \frac{v_{2,m}}{b} \right) \bar{w}^m + b(\widehat{\eta}_{1,2} - \widehat{\eta}_{2,2}) \bar{w}^{3m} \right. \\ &\quad \left. + 6(1-m)v_{2,m}^2(m-1) \left(v_{1,m} b^{m-2} - \frac{v_{2,m}}{b} \right) \bar{w}^m \right\} \\ &= 3v_{2,m}^2(m-1)m \left(\frac{v_{2,m}}{b} - v_{1,m} b^{m-2} \right) e_m + \gamma_2 e_{3m} \end{aligned}$$

with $\gamma_j \in \mathbb{R}$. In summary,

$$\frac{d^3}{dt^3} [G(\lambda_m^\pm, 0)]_{|t=0} = 3m(m-1) \begin{pmatrix} 2v_{2,m}^2 v_{1,m} - v_{2,m}^3 b^{m-1} - v_{1,m}^3 \\ v_{2,m}^2 \left(\frac{v_{2,m}}{b} - v_{1,m} b^{m-2} \right) \end{pmatrix} e_m + \begin{pmatrix} \gamma_1 \\ \gamma_2 \end{pmatrix} e_{3m}.$$

Using the structure of the projector Q we deduce after algebraic cancellations

$$\frac{1}{3} \frac{d^3}{dt^3} [QG(\lambda_m^\pm, tv_m)]_{|t=0} = -m(m-1)b^{3-3m} \frac{(b^{2m-2} - (m\lambda_m^\pm - m+1)^2)^2}{([m\lambda_m^\pm - m+1]^2 + b^{2m})^{\frac{1}{2}}} \mathbb{W}_m.$$

Now we shall compute the term,

$$Q\partial_{ff}G(\lambda_m^\pm, 0)[v_m, \widehat{v}_m] = Q\partial_t\partial_s[G(\lambda_m^\pm, tv_m + s\widehat{v}_m)]_{|t=0, s=0}.$$

To find an expression of \widehat{v}_m , we recall that

$$\frac{d^2}{dt^2} [G(\lambda_m^\pm, tv_m)]_{|t=0} = \begin{pmatrix} \widehat{\alpha} \\ 0 \end{pmatrix} e_{2m} \quad \text{with} \quad \widehat{\alpha} = 2m(v_{2,m} b^m - b v_{1,m})^2.$$

Thus,

$$\begin{aligned} \widehat{v}_m &= -[\partial_f G(\lambda_m^\pm, 0)]^{-1} \begin{pmatrix} \widehat{\alpha} \\ 0 \end{pmatrix} e_{2m} \\ &= -M_{2m}^{-1} \begin{pmatrix} \widehat{\alpha} \\ 0 \end{pmatrix} \bar{w}^{2m-1} \\ &= \begin{pmatrix} \widehat{v}_{1,m} \\ \widehat{v}_{2,m} \end{pmatrix} \bar{w}^{2m-1} \end{aligned} \tag{3.3.11}$$

with

$$\widehat{v}_{1,m} = -\frac{b\widehat{\alpha}(2m\lambda_m^\pm - 2m+1)}{\det(M_{2m}(\lambda_m^\pm))} \quad \text{and} \quad \widehat{v}_{2,m} = -\frac{b^{2m}\widehat{\alpha}}{\det(M_{2m}(\lambda_m^\pm))}.$$

Finally we can write,

$$\hat{v}_m = \tilde{\beta}_m \tilde{v}_m$$

with

$$\tilde{\beta}_m = -\frac{b\bar{\alpha}}{\det(M_{2m}(\lambda_m^\pm))} \quad (3.3.12)$$

$$\tilde{v}_m = \begin{pmatrix} 2m\lambda_m^\pm - 2m + 1 \\ b^{2m-1} \end{pmatrix} \bar{w}^{2m-1} \triangleq \begin{pmatrix} \beta_1 \\ \beta_2 \end{pmatrix} \bar{w}^{2m-1}.$$

It follows that

$$Q\partial_t\partial_s[G(\lambda_m^\pm, tv_m + s\hat{v}_m)]_{|t=0,s=0} = \tilde{\beta}_m Q\partial_t\partial_s[G(\lambda_m^\pm, tv_m + s\tilde{v}_m)]_{|t=0,s=0}.$$

We shall introduce the functions

$$\varphi_j(t, s, w) = b^{j-1}w + tv_{j,m}w^{1-m} + s\beta_j w^{1-2m}$$

and hence

$$\begin{aligned} G_j(t, s, w) &\triangleq G_j(\lambda, tv_m + s\tilde{v}_m) \\ &= \text{Im} \left\{ \left[(1 - \lambda_m^\pm) \overline{\varphi_j(t, s, w)} + I(\varphi_j(t, s, w)) \right] w \partial_w \varphi_j(t, s, w) \right\}. \end{aligned}$$

The following equality can be easily checked :

$$\begin{aligned} \partial_t\partial_s[G_j(t, s, w)]_{|t=0,s=0} &= \text{Im} \left\{ (1 - \lambda_m^\pm) \beta_j v_{j,m} \left((1 - m)w^m + (1 - 2m)\bar{w}^m \right) \right\} \\ &+ \text{Im} \left\{ wb^{j-1} \frac{d^2}{dt ds} [I(\varphi_j(t, s, w))]_{|t=0,s=0} \right\} \\ &+ \text{Im} \left\{ \beta_j (1 - 2m) \partial_t [I(\varphi_j(t, s, w))]_{|t=0,s=0} \bar{w}^{2m-1} \right\} \\ &+ \text{Im} \left\{ (1 - m) v_{j,m} \bar{w}^{m-1} \partial_s [I(\varphi_j(t, s, w))]_{|t=0,s=0} \right\}. \end{aligned}$$

We write

$$\begin{aligned} I_i(\varphi_j(t, s, w)) &= \int_{\mathbb{T}} \frac{\overline{\varphi_j(t, s, w)} - \overline{\varphi_i(t, s, \tau)}}{\varphi_j(t, s, w) - \varphi_i(t, s, \tau)} \left(b^{i-1} + t(1 - m)v_{i,m}\bar{\tau}^m + s\beta_i(1 - 2m)\bar{\tau}^{2m} \right) d\tau \\ &= \int_{\mathbb{T}} \frac{\bar{A} + t\bar{B} + s\bar{C}}{A + tB + sC} (b^{i-1} + tD + sE) d\tau \end{aligned}$$

with

$$\begin{aligned} A &= b^{j-1}w - b^{i-1}\tau, \quad B = v_{j,m}\bar{w}^{m-1} - v_{i,m}\bar{\tau}^{m-1}, \quad C = \beta_j\bar{w}^{2m-1} - \beta_i\bar{\tau}^{2m-1} \\ D &= (1 - m)v_{i,m}\bar{\tau}^m \quad \text{and} \quad E = (1 - 2m)\beta_i\bar{\tau}^{2m}. \end{aligned}$$

Straightforward computations lead to

$$\begin{aligned} \partial_t[I_i(\varphi_j(t, s, w))]_{|t=0,s=0} &= b^{i-1} \int_{\mathbb{T}} \frac{A\bar{B} - \bar{A}B}{A^2} d\tau + \int_{\mathbb{T}} \frac{\bar{A}D}{A} d\tau \\ &= \tilde{J}_{i,j} w^{m-1} + \theta_{i,j} \bar{w}^{m+1} \end{aligned}$$

with $\theta_{i,j} \in \mathbb{R}$ and

$$\tilde{J}_{i,j} = b^{i-1} \int_{\mathbb{T}} \frac{(v_{j,m} - v_{i,m}\bar{\tau}^{m-1})}{(b^{j-1} - b^{i-1}\tau)} d\tau.$$

For the diagonal tens one has

$$\begin{aligned}\tilde{J}_{i,i} &= v_{i,m} \int_{\mathbb{T}} \frac{(1-\tau^{m-1})}{(1-\tau)} d\tau \\ &= 0\end{aligned}$$

On the other hand

$$\begin{aligned}\tilde{J}_{1,2} &= \int_{\mathbb{T}} \frac{(v_{2,m} - v_{1,m}\tau^{m-1})}{(b-\tau)} d\tau \\ &= v_{1,m}b^{m-1} - v_{2,m}.\end{aligned}$$

Using again the residue theorem it is easy to see that,

$$\tilde{J}_{2,1} = b \int_{\mathbb{T}} \frac{(v_{1,m} - v_{2,m}\tau^{m-1})}{(1-b\tau)} d\tau = 0.$$

Summing up we obtain,

$$\partial_t [I(\varphi_1(t, s, w))]|_{t=0, s=0} = (\theta_{1,1} - \theta_{2,1})\bar{w}^{m+1}$$

and

$$\partial_t [I(\varphi_2(t, s, w))]|_{t=0, s=0} = (\theta_{1,2} - \theta_{2,2})\bar{w}^{m+1} + (v_{1,m}b^{m-1} - v_{2,m})w^{m-1}.$$

For the derivative with respect to s we may write

$$\begin{aligned}\partial_s [I_i(\varphi_j(t, s, w))]|_{t=0, s=0} &= b^{i-1} \int_{\mathbb{T}} \frac{A\bar{C} - \bar{A}C}{A^2} d\tau + \int_{\mathbb{T}} \frac{\bar{A}E}{A} d\tau \\ &= \hat{J}_{i,j}w^{2m-1} + \hat{\theta}_{i,j}\bar{w}^{2m+1}\end{aligned}$$

where

$$\hat{J}_{i,j} = b^{i-1} \int_{\mathbb{T}} \frac{(\beta_j - \beta_i\tau^{2m-1})}{(b^{j-1} - b^{i-1}\tau)} d\tau$$

and

$$\hat{\theta}_{i,j} = \int_{\mathbb{T}} \frac{(b^{j-1} - b^{i-1}\bar{\tau})}{(b^{j-1} - b^{i-1}\tau)} (1-2m)\beta_i\bar{\tau}^{2m} d\tau - b^{i-1} \int_{\mathbb{T}} \frac{(b^{j-1} - b^{i-1}\bar{\tau})(\beta_j - \beta_i\bar{\tau}^{2m-1})}{(b^{j-1} - b^{i-1}\tau)^2} d\tau.$$

It is easy to check that $\hat{\theta}_{i,j} \in \mathbb{R}, \forall i, j \in \{1, 2\}$. Now, we get

$$\hat{J}_{i,i} = \beta_i \int_{\mathbb{T}} \frac{(1-\tau^{2m-1})}{(1-\tau)} d\tau = 0.$$

Using the residue theorem we find

$$\hat{J}_{1,2} = \int_{\mathbb{T}} \frac{(\beta_2 - \beta_1\tau^{2m-1})}{(b-\tau)} d\tau = -\beta_2 + \beta_1 b^{2m-1}.$$

and

$$\hat{J}_{2,1} = b \int_{\mathbb{T}} \frac{(\beta_1 - \beta_2\tau^{2m-1})}{(1-b\tau)} d\tau = 0.$$

To summarize,

$$\partial_s [I(\varphi_1(t, s, w))]|_{t=0, s=0} = (\hat{\theta}_{1,1} - \hat{\theta}_{2,1})\bar{w}^{2m+1}$$

and

$$\partial_s [I(\varphi_2(t, s, w))]_{|t=0, s=0} = (\beta_1 b^{2m-1} - \beta_2) w^{2m-1} + (\widehat{\theta}_{1,2} - \widehat{\theta}_{2,2}) \bar{w}^{2m+1}.$$

Now we shall move to the second derivative with respect to t and s ,

$$\begin{aligned} \frac{d^2}{dsdt} [I_i(\varphi_j(t, s, w))]_{|t=0, s=0} &= -b^{i-1} \int_{\mathbb{T}} \frac{\overline{BC}}{A^2} d\tau + \int_{\mathbb{T}} \frac{\overline{BE}}{A} d\tau - b^{i-1} \int_{\mathbb{T}} \frac{\overline{CB}}{A^2} d\tau + \int_{\mathbb{T}} \frac{\overline{CD}}{A} d\tau \\ &\quad + 2b^{i-1} \int_{\mathbb{T}} \frac{\overline{BC}\overline{A}}{A^3} d\tau - \int_{\mathbb{T}} \frac{\overline{BE}\overline{A}}{A^2} d\tau - \int_{\mathbb{T}} \frac{\overline{DC}\overline{A}}{A^2} d\tau. \end{aligned}$$

By homogeneity, there exist $\varepsilon_{i,j} \in \mathbb{R}$ such that,

$$\frac{d^2}{dsdt} [I_i(\varphi_j(t, s, w))]_{|t=0, s=0} = \varepsilon_{i,j} \bar{w}^{3m+1} - b^{i-1} I_1^{i,j} w^{m-1} - b^{i-1} I_2^{i,j} \bar{w}^{m+1} + I_3^{i,j} \bar{w}^{m+1} + I_4^{i,j} w^{m-1}$$

with

$$\begin{aligned} I_1^{i,j} &= \int_{\mathbb{T}} \frac{(v_{j,m} - v_{i,m} \bar{\tau}^{m-1})(\beta_j - \beta_i \tau^{2m-1})}{(b^{j-1} - b^{i-1} \tau)^2} d\tau, \\ I_2^{i,j} &= \int_{\mathbb{T}} \frac{(v_{j,m} - v_{i,m} \tau^{m-1})(\beta_j - \beta_i \bar{\tau}^{2m-1})}{(b^{j-1} - b^{i-1} \tau)^2} d\tau, \\ I_3^{i,j} &= (1-2m)\beta_i \int_{\mathbb{T}} \frac{(v_{j,m} - v_{i,m} \tau^{m-1})}{(b^{j-1} - b^{i-1} \tau)} \bar{\tau}^{2m} d\tau \end{aligned}$$

and

$$I_4^{i,j} = (1-m)v_{i,m} \int_{\mathbb{T}} \frac{(\beta_j - \beta_i \tau^{2m-1})}{(b^{j-1} - b^{i-1} \tau)} \bar{\tau}^m d\tau.$$

We intend to compute all these terms. For the diagonal terms we write

$$\begin{aligned} I_1^{i,i} &= \frac{v_{i,m}\beta_i}{b^{2(i-1)}} \int_{\mathbb{T}} \frac{(1-\bar{\tau}^{m-1})(1-\tau^{2m-1})}{(1-\tau)^2} d\tau \\ &= (1-m) \frac{v_{i,m}\beta_i}{b^{2(i-1)}}. \end{aligned}$$

As to the term $I_1^{1,2}$ we have

$$I_1^{1,2} = \int_{\mathbb{T}} \frac{v_{2,m}\beta_2}{(b-\tau)^2} d\tau - \int_{\mathbb{T}} \frac{v_{1,m}\beta_2 \bar{\tau}^{m-1}}{(b-\tau)^2} d\tau - \int_{\mathbb{T}} \frac{v_{2,m}\beta_1 \tau^{2m-1}}{(b-\tau)^2} d\tau + \int_{\mathbb{T}} \frac{v_{1,m}\beta_1 \tau^m}{(b-\tau)^2} d\tau.$$

By the residue theorem we get

$$I_1^{1,2} = v_{2,m}\beta_1(1-2m)b^{2m-2} + m\beta_1 v_{1,m} b^{m-1}.$$

Now we move to $I_1^{2,1}$. Residue theorem combined with (3.3.4) implies

$$\begin{aligned} I_1^{2,1} &= \int_{\mathbb{T}} \frac{v_{1,m}\beta_1}{(1-b\tau)^2} d\tau + \int_{\mathbb{T}} \frac{v_{2,m}\beta_2 \tau^m}{(1-b\tau)^2} d\tau - \int_{\mathbb{T}} \frac{v_{1,m}\beta_2 \tau^{2m-1}}{(1-b\tau)^2} d\tau - \int_{\mathbb{T}} \frac{v_{2,m}\beta_1 \bar{\tau}^{m-1}}{(1-b\tau)^2} d\tau \\ &= -v_{2,m}\beta_1(m-1)b^{m-2}. \end{aligned}$$

Moreover,

$$\begin{aligned} I_2^{i,i} &= \frac{v_{i,m}\beta_i}{b^{2(i-1)}} \int_{\mathbb{T}} \frac{(1-\tau^{m-1})(1-\bar{\tau}^{2m-1})}{(1-\tau)^2} d\tau \\ &= (1-m) \frac{v_{i,m}\beta_i}{b^{2(i-1)}}. \end{aligned}$$

For $I_2^{i,j}$ we use the change of variable $\tau \rightarrow \bar{\tau}$

$$\begin{aligned} I_2^{i,j} &= \int_{\mathbb{T}} \frac{(v_{j,m} - v_{i,m}\tau^{m-1})(\beta_j - \beta_i\bar{\tau}^{2m-1})}{(b^{j-1} - b^{i-1}\tau)^2} d\tau \\ &= \int_{\mathbb{T}} \frac{(v_{j,m} - v_{i,m}\bar{\tau}^{m-1})(\beta_j - \beta_i\tau^{2m-1})}{(b^{i-1} - b^{j-1}\tau)^2} d\tau. \end{aligned}$$

Therefore

$$I_2^{1,2} = \int_{\mathbb{T}} \frac{(v_{2,m} - v_{1,m}\bar{\tau}^{m-1})(\beta_2 - \beta_1\tau^{2m-1})}{(1-b\tau)^2} d\tau.$$

Similarly to $I_1^{2,1}$ we find

$$I_2^{1,2} = -v_{1,m}\beta_2(m-1)b^{m-2}.$$

For the term $I_2^{2,1}$ we write

$$I_2^{2,1} = \int_{\mathbb{T}} \frac{(v_{1,m} - v_{2,m}\bar{\tau}^{m-1})(\beta_1 - \beta_2\tau^{2m-1})}{(b-\tau)^2} d\tau.$$

The same computations for $I_1^{1,2}$ yield

$$I_2^{2,1} = v_{1,m}\beta_2(1-2m)b^{2m-2} + m\beta_2v_{2,m}b^{m-1}.$$

For the diagonal term $I_3^{i,i}$ we easily get

$$I_3^{i,i} = (1-2m) \frac{v_{i,m}\beta_i}{b^{i-1}} \int_{\mathbb{T}} \frac{(1-\tau^{m-1})}{(1-\tau)} \bar{\tau}^{2m} d\tau = 0.$$

Moreover,

$$I_3^{1,2} = (1-2m)\beta_2 \int_{\mathbb{T}} \frac{(v_{2,m} - v_{1,m}\bar{\tau}^{m-1})}{(b-\tau)} \bar{\tau}^{2m} d\tau = 0.$$

On the other hand, using (3.3.3) we find

$$\begin{aligned} I_3^{2,1} &= (1-2m)\beta_2 \int_{\mathbb{T}} \frac{(v_{1,m} - v_{2,m}\tau^{m-1})}{(1-b\tau)} \bar{\tau}^{2m} d\tau \\ &= (1-2m)\beta_2(v_{1,m}b^{2m-1} - v_{2,m}b^m). \end{aligned}$$

Now we move to the last terms $I_4^{i,j}$. Concerning the diagonal terms, we may write

$$\begin{aligned} I_4^{i,i} &= (1-m) \frac{v_{i,m}\beta_i}{b^{i-1}} \int_{\mathbb{T}} \frac{(1-\tau^{2m-1})}{(1-\tau)} \bar{\tau}^m d\tau \\ &= (1-m) \frac{v_{i,m}\beta_i}{b^{i-1}}. \end{aligned}$$

For $I_4^{1,2}$ we obtain according to the residue theorem

$$\begin{aligned} I_4^{1,2} &= (1-m)v_{1,m} \int_{\mathbb{T}} \frac{\beta_2 \bar{\tau}^m}{(b-\tau)} d\tau - (1-m)v_{1,m} \int_{\mathbb{T}} \frac{\beta_1 \tau^{m-1}}{(b-\tau)} d\tau \\ &= (1-m)v_{1,m} \beta_1 b^{m-1}. \end{aligned}$$

For the last term, we use (3.3.3) in order to get

$$\begin{aligned} I_4^{2,1} &= (1-m)v_{2,m} \int_{\mathbb{T}} \frac{(\beta_1 - \beta_2 \tau^{2m-1})}{(1-b\tau)} \bar{\tau}^m d\tau \\ &= (1-m)v_{2,m} \beta_1 b^{m-1}. \end{aligned}$$

Putting together the preceding identities we deduce

$$\frac{d^2}{dsdt} [I(\varphi_1(t, s, w))]|_{t=0, s=0} = (\varepsilon_{1,1} - \varepsilon_{2,1}) \bar{w}^{3m+1} + (m-1)(v_{1,m} \beta_1 - \beta_2 v_{2,m} b^m) \bar{w}^{m+1}$$

and

$$\begin{aligned} \frac{d^2}{dsdt} [I(\varphi_2(t, s, w))]|_{t=0, s=0} &= (\varepsilon_{1,2} - \varepsilon_{2,2}) \bar{w}^{3m+1} + (1-2m)\beta_1(v_{1,m} b^{m-1} - v_{2,m} b^{2m-2}) w^{m-1} \\ &\quad + (m-1)\beta_2(v_{1,m} b^{m-2} - \frac{v_{2m}}{b}) \bar{w}^{m+1}. \end{aligned}$$

Finally we get,

$$\begin{aligned} \frac{d^2}{dt ds} [G_1(t, s, w)]|_{t=0, s=0} &= \text{Im} \left\{ (\varepsilon_{1,1} - \varepsilon_{2,1}) \bar{w}^{3m} + (m-1)[v_{1,m} \beta_1 - \beta_2 v_{2,m} b^m] \bar{w}^m \right. \\ &\quad \left. + \beta_1(1-2m)(\theta_{1,1} - \theta_{2,1}) \bar{w}^{3m} \right\} \\ &\quad + \text{Im} \left\{ (\lambda_m^\pm - 1)m \beta_1 v_{1,m} \bar{w}^m + (1-m)v_{1,m}(\hat{\theta}_{1,1} - \hat{\theta}_{2,1}) \bar{w}^{3m} \right\} \\ &= ((m\lambda_m^\pm - 1)v_{1,m} \beta_1 + (1-m)\beta_2 v_{2,m} b^m) e_m + \tilde{\gamma}_1 e_{3m} \\ &= \left((m\lambda_m^\pm - 1)(m\lambda_m^\pm - m + 1)(2m\lambda_m^\pm - 2m + 1)b^{1-m} + (1-m)b^{3m-1} \right) e_m \\ &\quad + \tilde{\gamma}_1 e_{3m} \end{aligned}$$

and

$$\begin{aligned} \frac{d^2}{dt ds} [G_2(t, s, w)]|_{t=0, s=0} &= \text{Im} \left\{ b(\varepsilon_{1,2} - \varepsilon_{2,2}) \bar{w}^{3m} + (1-2m)\beta_1[v_{1,m} b^m - v_{2,m} b^{2m-1}] w^m \right\} \\ &\quad + \text{Im} \left\{ (m-1)\beta_2[v_{1,m} b^{m-1} - v_{2,m}] \bar{w}^m + \beta_2(1-2m)(\theta_{1,2} - \theta_{2,2}) \bar{w}^{3m} \right. \\ &\quad \left. + (1-\lambda_m^\pm)\beta_2 v_{2,m}[(1-m)w^m + (1-2m)\bar{w}^m] + (1-m)v_{2,m}(\beta_1 b^{2m-1} - \beta_2) w^m \right\} \\ &\quad + \text{Im} \left\{ \beta_2(1-2m)(v_{1,m} b^{m-1} - v_{2,m}) \bar{w}^m + (1-m)v_{2,m}(\hat{\theta}_{1,2} - \hat{\theta}_{2,2}) \bar{w}^{3m} \right\} \\ &= \left([(m\lambda_m^\pm - m + 1)\beta_2 - m\beta_1 b^{2m-1}] v_{2,m} + v_{1,m} b^{m-1} [b\beta_1(2m-1) - m\beta_2] \right) e_m \\ &\quad + \tilde{\gamma}_2 e_{3m} \\ &= \left(((1-m)(m\lambda_m^\pm - m + 1) - m(2\lambda_m^\pm m - 2m + 1)) b^{2m-1} \right. \\ &\quad \left. + (m\lambda_m^\pm - m + 1)b(2m\lambda_m^\pm - 2m + 1)(2m-1) \right) e_m + \tilde{\gamma}_2 e_{3m}. \end{aligned}$$

Using the definition of the projector Q , we deduce after some computations

$$Q \frac{d^2}{dt ds} G(t, s, w)|_{t=0, s=0} = \mathcal{K}_m \mathbb{W}_m$$

with

$$\mathcal{K}_m \triangleq (2\lambda_m^\pm m - 2m + 1) \frac{b^{1-m}(m\lambda_m^\pm - 1)(m\lambda_m^\pm - m + 1)^2 + (1 - 2m)(m\lambda_m^\pm - m + 1)b^{m+1} + mb^{3m-1}}{[(m\lambda_m^\pm - m + 1)^2 + b^{2m}]^{\frac{1}{2}}}.$$

Eventually, we find

$$Q\partial_{ff}G(\lambda_m^\pm, 0)[v_m, \partial_\lambda\partial_g\varphi(\lambda_m^\pm, 0)v_m] = \tilde{\beta}_m \mathcal{K}_m \mathbb{W}_m$$

where $\tilde{\beta}_m$ was defined in (3.3.12). This achieves the proof of Proposition 3.3.2-(4).

Computation of $\partial_\lambda\partial_t F_2(\lambda_m^\pm, 0)$

Now we shall prove the last point of Proposition 3.3.2. Recall from Proposition 3.3.1 that

$$\begin{aligned} \partial_\lambda\partial_t F_2(\lambda_m^\pm, 0) &= \frac{1}{2} Q\partial_\lambda\partial_{ff}G(\lambda_m^\pm, 0)[v_m, v_m] + \frac{1}{2} Q\partial_\lambda\partial_f G(\lambda_m^\pm, 0)(\hat{v}_m) \\ &\quad + Q\partial_{ff}G(\lambda_m^\pm, 0)[v_m, \partial_\lambda\partial_g\varphi(\lambda_m^\pm, 0)v_m]. \end{aligned}$$

The first term vanishes since

$$\begin{aligned} \partial_\lambda\partial_{ff}G(\lambda_m^\pm, 0)[v_m, v_m] &= \frac{d^2}{dt^2}[\partial_\lambda G_j(\lambda_m^\pm, tv_m)]|_{\lambda=\lambda_m^\pm, t=0} \\ &= -\frac{d^2}{dt^2}|_{t=0} \operatorname{Im} \left\{ w \overline{\Phi_j(t, w)} \Phi'_j(t, w) \right\} \\ &= 0. \end{aligned}$$

For the second term we combine (3.2.4) with (3.3.11)

$$\partial_\lambda\partial_f G(\lambda_m^\pm, 0)(\hat{v}_m) = 2m \begin{pmatrix} \hat{v}_{1,m} \\ b\hat{v}_{2,m} \end{pmatrix} e_{2m}.$$

Consequently we deduce that

$$Q\partial_\lambda\partial_f G(\lambda_m^\pm, 0)(\hat{v}_m) = 0.$$

Hence we find

$$\partial_\lambda\partial_t F_2(\lambda_m^\pm, 0) = Q\partial_{ff}G(\lambda_m^\pm, 0)[v_m, \partial_\lambda\partial_g\varphi(\lambda_m^\pm, 0)v_m].$$

Now we want to compute

$$Q\partial_{ff}G(\lambda_m^\pm, 0)[v_m, \partial_\lambda\partial_g\varphi(\lambda_m^\pm, 0)v_m] = Q\partial_t\partial_s[G(\lambda_m^\pm, tv_m + s\partial_\lambda\partial_g\varphi(\lambda_m^\pm, 0)v_m)]|_{t=0, s=0}.$$

This was done in [?, Lemma 2-(ii)] combined with (3.3.10) and (3.3.11). We obtain

$$Q\partial_{ff}G(\lambda_m^\pm, 0)[v_m, \partial_\lambda\partial_g\varphi(\lambda_m^\pm, 0)v_m] = 0$$

and this completes the proof of the desired result.

3.4 Proof of the main theorem

This section is devoted to the proof of Theorem 3.1.2. To begin, we choose a small neighborhood of $(\lambda_m^+, 0)$ in the strong topology of $\mathbb{R} \times X_m$ such that the equation

$$F_1(\lambda, tv_m, k) = 0, \quad k \in \mathcal{X}_m$$

admits locally a unique surface of solutions parametrized by

$$(\lambda, t) \in (\lambda_m^+ - \epsilon_0, \lambda_m^+ + \epsilon_0) \times (-\epsilon_0, \epsilon_0) \mapsto k = \varphi(\lambda, tv_m) \in \mathcal{X}_m,$$

with $\epsilon_0 > 0$ and φ being a C^1 function and actually it is of class C^k for any $k \in \mathbb{N}$. This follows from the fact that the functionals defining the V-states are better than C^1 . They are of class C^k and this can be proved by implementing straightforward computations of their successive differentials. In order to alleviate the content of the paper we prefer not to give details because the computations are long and tedious, and do not bring any new difficulties compared to the study of C^1 regularity. For additional materials in this direction we refer to [8, 37] devoted to the boundary regularity of simply connected V-states close to Rankine vortices.

Recall from (3.2.10) that

$$\varphi(\lambda_m^+, 0) = 0.$$

As we have seen in the subsection 3.2.3, the V-states equation is equivalent to,

$$F_2(\lambda, t) = 0 \quad (3.4.1)$$

with (λ, t) being in the neighborhood of $(\lambda_m^+, 0)$ in \mathbb{R}^2 and $F_2 : \mathbb{R}^2 \rightarrow \langle \mathbb{W}_m \rangle$. We intend to prove the following assertion: there exists $b_m \in (0, b_m^*)$ such that for any $b \in (b_m, b_m^*)$ there exists $\varepsilon > 0$ such that the set

$$\mathcal{E}_b \triangleq \{(\lambda, t) \in (\lambda_m^+ - \varepsilon, \lambda_m^+ + \varepsilon) \times (-\varepsilon, \varepsilon), F_2(\lambda, t) = 0\} \quad (3.4.2)$$

is a C^1 -Jordan curve in the complex plane. Taylor expansion of F_2 around the point $(\lambda_m^+, 0)$ at the order two is given by,

$$\begin{aligned} F_2(\lambda, t) &= \partial_\lambda F_2(\lambda_m^+, 0)(\lambda - \lambda_m^+) + \partial_t F_2(\lambda_m^+, 0)t \\ &+ \frac{1}{2} \partial_{\lambda\lambda} F_2(\lambda_m^+, 0)(\lambda - \lambda_m^+)^2 + \frac{1}{2} \partial_{tt} F_2(\lambda_m^+, 0)t^2 \\ &+ ((\lambda - \lambda_m^+)^2 + t^2)\epsilon(\lambda, t)\mathbb{W}_m \end{aligned}$$

where

$$\lim_{(\lambda, t) \rightarrow (\lambda_m^+, 0)} \epsilon(\lambda, t) = 0.$$

Then using Proposition 3.3.2 we get for any $(\lambda, t) \in (\lambda_m^+ - \eta, \lambda_m^+ + \eta) \times (-\eta, \eta)$, with $\eta > 0$,

$$F_2(\lambda, t) = - \left(a_m(b)(\lambda - \lambda_m^+) + c_m(b)(\lambda - \lambda_m^+)^2 + d_m(b)t^2 + ((\lambda - \lambda_m^+)^2 + t^2)\epsilon(\lambda, t) \right) \mathbb{W}_m$$

with

$$\begin{aligned} a_m(b) &= - \frac{m[(m\lambda_m^+ - m + 1)^2 - b^{2m}]}{b^{m-1}[(m\lambda_m^+ - m + 1)^2 + b^{2m}]^{\frac{1}{2}}}, \\ c_m(b) &= - \frac{2m^2 b^{1-m} (m\lambda_m^+ - m + 1)^3}{[(m\lambda_m^+ - m + 1)^2 + b^{2m}]^{\frac{3}{2}}} \end{aligned}$$

and

$$d_m(b) = \frac{m}{2}(m-1)b^{3-3m} \frac{(b^{2m-2} - (m\lambda_m^+ - m + 1)^2)^2}{([m\lambda_m^+ - m + 1]^2 + b^{2m})^{\frac{1}{2}}} - \frac{\tilde{\beta}_m}{2} \mathcal{K}_m.$$

Note that for $b = b_m^*$ we have $\Delta_m = 0$ which implies that

$$\lambda_m^+ = \frac{1 + b^2}{2}, \quad m\lambda_m^+ - m + 1 = -b^m.$$

Thus we get

$$a_m(b_m^*) = 0, c_m(b_m^*) > 0.$$

Moreover we can check that for $b = b_m^*$,

$$\tilde{\beta}_m > 0 \quad \text{and} \quad \mathcal{K}_m < 0$$

which implies in turn that $d_m(b_m^*) > 0$. Those properties on the signs remain true for b close to b_m^* , that is, b belongs to some interval $[b_m, b_m^*]$. In addition we deduce from the identity given in Remark 3.3.3 that for any $b \in (0, b_m^*)$ we have $a_m(b) > 0$. Indeed,

$$\begin{aligned} (m\lambda_m^+ - m + 1)^2 - b^{2m} &= (m\lambda_m^+ - m + 1 - b^m)(m\lambda_m^+ - m + 1 + b^m) \\ &= (\sqrt{\Delta_m} - \sqrt{\Delta_m + b^{2m}} - b^m)(\sqrt{\Delta_m} + b^m - \sqrt{\Delta_m + b^{2m}}) \\ &< 0. \end{aligned}$$

Set $x_0(b) = \frac{a_m(b)}{2c_m(b)}$ and using the change of variables

$$s = \lambda - \lambda_m^+ + x_0(b), \quad \psi(s, t) \triangleq \epsilon(s + \lambda_m^+ - x_0(b), t)$$

then the equation of F_2 becomes

$$c_m(b)s^2 + d_m(b)t^2 - \frac{a_m^2}{4c_m(b)} + ((s - x_0(b))^2 + t^2)\psi(s, t) = 0 \quad (3.4.3)$$

and

$$\lim_{(s,t) \rightarrow (x_0(b), 0)} \psi(s, t) = 0.$$

Note that if we remove ψ from the second term of this equation we get the equation of a small ellipse centered at $(0, 0)$ and of semi-axes $\frac{a_m(b)}{2c_m(b)}$ and $\frac{a_m(b)}{2\sqrt{d_m(b)c_m(b)}}$. Thus taking b close enough to b_m^* one can guarantee that this ellipse is contained in the box $(-\epsilon_0, \epsilon_0)^2$ for which the solutions of the equation F_1 still parametrized by φ . By small perturbation we expect to get a curve of solutions to F_2 which is a small perturbation of the ellipse. To prove rigorously this expectation we start with the change of variable,

$$t = x_0(b)\sqrt{\frac{c_m(b)}{d_m(b)}}x \quad \text{and} \quad s = x_0(b)y.$$

Consequently, the equation (3.4.3) becomes

$$\mathcal{G}(b, x, y) \triangleq x^2 + y^2 - 1 + \frac{1}{c_m(b)} \left((y - 1)^2 + \frac{c_m(b)^2}{d_m(b)} x^2 \right) \hat{\psi}(x_0(b), x, y) = 0 \quad (3.4.4)$$

with

$$\hat{\psi}(\mu, x, y) \triangleq \epsilon \left(\mu y + \lambda_m^+ - \mu, \mu \sqrt{\frac{c_m(b)}{d_m(b)}} x \right).$$

Now we shall characterize the geometric structure of the planar set

$$\hat{\mathcal{E}}_b \triangleq \{(x, y) \in \mathbb{R}^2; \mathcal{G}(b, x, y) = 0\}.$$

Lemma 3.4.1. *There exists $b_m \in (0, b_m^*)$ such that for any $b \in (b_m, b_m^*)$ the set $\hat{\mathcal{E}}_b$ contains a C^1 -Jordan curve and the point $(0, 0)$ is located inside. In addition, this curve is a smooth perturbation of the unit circle \mathbb{T} .*

Proof. We shall look for a curve of solutions lying in the set $\hat{\mathcal{E}}_b$ and that can be parametrized through polar coordinates as follows

$$\theta \in [0, 2\pi] \mapsto (x, y) = R(\theta)e^{i\theta}.$$

Now we fix b and introduce the function

$$\begin{aligned}\mathcal{F}(\mu, R(\theta)) &\triangleq R^2(\theta) - 1 \\ &- \frac{1}{c_m(b)} \left([R(\theta) \sin \theta - 1]^2 + \frac{c_m(b)^2}{d_m(b)} R^2(\theta) \cos^2 \theta \right) \widehat{\psi}(\mu, R(\theta) \cos \theta, R(\theta) \sin \theta).\end{aligned}$$

Then according to (3.4.4) it is enough to solve

$$\mathcal{F}(\mu, R(\theta)) = 0 \quad \text{and} \quad \mu = x_0(b). \quad (3.4.5)$$

Recall that the function ϵ is defined in the box $(\lambda, t) \in (\lambda_m^+ - \eta, \lambda_m^+ + \eta) \times (-\eta, \eta)$ for some given real number $\eta > 0$. Thus it is not hard to find an implicit value $\mu_0 >$ such that

$$\mathcal{F} : (-\mu_0, \mu_0) \times \mathcal{B} \rightarrow C^1(\mathbb{T})$$

is well-defined and is of class C^1 , with \mathcal{B} being the open set of $C^1(\mathbb{T})$ defined by

$$\mathcal{B} = \left\{ R \in C^1(\mathbb{T}); \|1 - R\|_\infty + \|R'\|_\infty < \frac{1}{2} \right\}.$$

In addition

$$\mathcal{F}(0, 1) = 0 \quad \text{and} \quad \partial_R \mathcal{F}(0, 1) h = 2h, \forall h \in C^1(\mathbb{T}).$$

Thus $\partial_R \mathcal{F}(0, 1)$ is an isomorphism and by the implicit function theorem we deduce the existence of $\mu_1 > 0$ such that for any $\mu \in (-\mu_1, \mu_1)$ there exists a unique $R_\mu \in \mathcal{B}$ such that (μ, R_μ) is a solution for $\mathcal{F}(\mu, R_\mu) = 0$. It is worthy to point out that μ_1 can be chosen independent of $b \in [b_m, b_m^*]$ because the coefficients $\frac{1}{c_m(b)}$ and $\frac{d_m(b)}{c_m(b)}$ that appear in the nonlinear contribution of \mathcal{F} are bounded. Now since $\lim_{b \rightarrow b_m^*} x_0(b) = 0$ then we deduce the existence of $b_m \in (0, b_m^*)$ such that for any $b \in (b_m, b_m^*)$ the set of solutions for (3.4.5) is described around the trivial solution $R = 1$ (the circle) by the curve $\theta \in [0, 2\pi] \mapsto R_{x_0(b)}(\theta) e^{i\theta}$. On the other hand from the definition of \mathcal{B} we deduce that this curve of solutions is contained in the annulus centered at the origin and of radii $\frac{1}{2}$ and $\frac{3}{2}$. It should be also non self-intersecting C^1 loop according to the regularity of the polar parametrization. This achieves the proof of the lemma. \square

Now let us see how to use Lemma 3.4.1 to end the proof of Theorem 3.1.2. We have already seen in the subsection 3.2.3 that the vectorial conformal mapping $\Phi \triangleq \begin{pmatrix} \Phi_1 \\ \Phi_2 \end{pmatrix}$ that describes the bifurcation curve from $(\lambda_m^+, 0)$ is decomposed as follows

$$\Phi(w) = \begin{pmatrix} 1 \\ b \end{pmatrix} w + tv_m + \varphi(\lambda, tv_m) \quad \text{with} \quad (t, \lambda) \in \mathcal{E}_b,$$

where \mathcal{E}_b , has been defined in (3.4.2). As the relationship between the sets \mathcal{E}_b and $\widehat{\mathcal{E}}_b$ is given through a non degenerate affine transformations then the set \mathcal{E}_b is also a C^1 -Jordan curve. In addition the point $(\lambda_m^+ - \frac{a_m(b)}{2c_m(b)}, 0)$ is located inside the curve and recall also that the point $(\lambda_m^+, 0)$ belongs to \mathcal{E}_b . This fact implies that the curve intersects necessary the real axis on another point $(\lambda_m, 0) \neq (\lambda_m^+, 0)$. By virtue of (3.2.10) the conformal mappings at those two points coincide which implies in turn that the bifurcation curve bifurcates also from the trivial solution at the point $(\lambda_m, 0)$. Note that looking from the side $(\lambda_m, 0)$ this curve represents V-states with exactly m -fold symmetry and not with more symmetry; to be convinced see the structure of Φ . However from the local bifurcation diagram close to the trivial solution which was studied in [33] we know that the only V-states bifurcating from the trivial solutions with m -fold symmetry bifurcate from the points $(\lambda_m^+, 0)$ and $(\lambda_m^-, 0)$. Consequently we get $\lambda_m = \lambda_m^-$ and this shows that the bifurcation curves of the m -fold V-states merge and form a small loop.

The last point to prove concerns the symmetry of the curve \mathcal{E}_b with respect to the λ axis. This reduces to check that for $(\lambda, t) \in \mathcal{E}_b$ then $(\lambda, -t) \in \mathcal{E}_b$. Indeed, if $D = D_1 \setminus D_2$ is an m -fold doubly-connected V-state, its boundaries are parametrized by the conformal mappings

$$\Phi_j(w) = w \left(b_j + a_{j,1} \bar{w}^m + \sum_{n \geq 2} a_{j,n} \bar{w}^{mn} \right), \quad a_{j,n} \in \mathbb{R}$$

Hence we find that the vectorial conform mapping Φ admits the decomposition

$$\Phi(w) = \begin{pmatrix} 1 \\ b \end{pmatrix} w + \begin{pmatrix} a_{1,1} \\ a_{2,1} \end{pmatrix} \bar{w}^{m-1} + \Psi(w), \quad \Psi \in \mathcal{X}_m$$

Observe that we have a unique t such that

$$\begin{pmatrix} a_{1,1} \\ a_{2,1} \end{pmatrix} \bar{w}^{m-1} = t v_m(w) + \Psi_1(w), \quad \Psi_1 \in \mathcal{X}_m \quad (3.4.6)$$

Now we consider $\widehat{D} = e^{\frac{i\pi}{m}} D$, the rotation of D with the angle $\frac{\pi}{m}$. Then the new domain is also a V-state with a m -fold symmetry rotating with the same angular velocity. Thus it should be associated to a point $(\lambda, \tilde{t}) \in \mathcal{E}_b$. Now the conformal parametrization of \widehat{D} is given by

$$\widehat{\Phi}_j(w) = e^{-\frac{i\pi}{m}} \Phi_j(e^{\frac{i\pi}{m}} w) = w \left(b_j + \sum_{n \geq 1} (-1)^n \frac{a_{j,n}}{w^{mn}} \right), \quad a_{j,n} \in \mathbb{R}.$$

Thus the vectorial conform parametrization $\widehat{\Phi} \triangleq \begin{pmatrix} \widehat{\Phi}_1 \\ \widehat{\Phi}_2 \end{pmatrix}$ admits the decomposition

$$\widehat{\Phi}(w) = \begin{pmatrix} 1 \\ b \end{pmatrix} w - \begin{pmatrix} a_{1,1} \\ a_{2,1} \end{pmatrix} \bar{w}^{m-1} + \widehat{\Psi}(w), \quad \widehat{\Psi} \in \mathcal{X}_m.$$

In view of (3.4.7) we deduce that

$$\widehat{\Phi}(w) = \begin{pmatrix} 1 \\ b \end{pmatrix} w - t v_m(w) + \widehat{\Psi}_1(w), \quad \widehat{\Psi}_1(w) \triangleq -\Psi_1 + \widehat{\Psi} \in \mathcal{X}_m. \quad (3.4.7)$$

This shows that $(\lambda, -t)$ belongs to the curve \mathcal{E}_b and this concludes the desired result.

Acknowledgements. The authors are partially supported by the ANR project Dyficoiti ANR-13-BS01-0003- 01.

Chapter 4

Imperfect bifurcation for the quasi-geostrophic shallow-water equations

Sometimes you just do things!

— *Eat and Run,*
Scott JUREK

We study analytical and numerical aspects of the bifurcation diagram of simply-connected rotating vortex patch equilibria for the quasi-geostrophic shallow-water (QGSW) equations. The QGSW equations are a generalisation of the Euler equations and contain an additional parameter, the Rossby deformation length ε^{-1} , which enters in the relation between streamfunction and (potential) vorticity. The Euler equations are recovered in the limit $\varepsilon \rightarrow 0$. We prove, close to circular (Rankine) vortices, the persistence of the bifurcation diagram for arbitrary Rossby deformation length. However we show that the two-fold branch, corresponding to Kirchhoff ellipses for the Euler equations, is never connected even for small values ε , and indeed is split into a countable set of disjoint connected branches. Accurate numerical calculations of the global structure of the bifurcation diagram and of the limiting equilibrium states are also presented to complement the mathematical analysis.

4.1 Introduction

In this paper we investigate new aspects of simply-connected vortex patch relative equilibria satisfying the quasi-geostrophic shallow water (QGSW) equations. These equations are derived asymptotically from the rotating shallow water equations, in the limit of rapid rotation and weak variations of the free surface [67]. A key property of these equations, and of the parent shallow water equations, is the material conservation of ‘potential vorticity’, q , a quantity which remains unchanged following fluid particles. The QGSW equations are given by

$$\begin{cases} \partial_t q + v \cdot \nabla q = 0, & (t, x) \in \mathbb{R}_+ \times \mathbb{R}^2, \\ v = \nabla^\perp \psi, \\ \psi = (\Delta - \varepsilon^2)^{-1} q, \\ q|_{t=0} = q_0 \end{cases} \quad (4.1.1)$$

where v refers to the velocity field, ψ is the streamfunction, $\nabla^\perp = (-\partial_2, \partial_1)$ and $\varepsilon \in \mathbb{R}$. The parameter ε , when it is positive, is known as the inverse ‘Rossby deformation length’, a natural length scale arising from a balance between rotation and stratification. Small ε physically corresponds to a free surface which is nearly rigid. For $\varepsilon = 0$, we recover the two-dimensional Euler equations.

Historically, substantially more is known about vortex patch relative equilibria for the Euler equations than for the QGSW equations. The most famous example is the exact analytical solution for a rotating ellipse, found by Kirchhoff in 1876 [43]. This is in fact a non-trivial family of solutions bifurcating from Rankine’s vortex, the circular patch (all axisymmetric vorticity distributions are in equilibrium, by symmetry). Kirchhoff’s elliptical vortex is linearly stable when its aspect ratio $\lambda \in [1/3, 1]$, i.e. when it is not strongly deformed from a circle, as was shown in 1893 by Love [48]. Love also discovered that there is a sequence of instabilities, at $\lambda = \lambda_m$ for $m = 3, 4, \dots$, ordered by the elliptical coordinate azimuthal wavenumber m . That is, $\lambda_3 > \lambda_4 > \dots$, with $\lambda_m \rightarrow 0$ as $m \rightarrow \infty$ [19]. Later, it was discovered that new branches of vortex patch equilibria bifurcate from each of these instability points [10, 49], revealing that the equilibrium solutions of Euler’s equations are exceedingly rich and varied. Analytical proofs and results on the boundary regularity were given in [8, 34, 37, 7].

The ellipse is not the only solution which bifurcates from a circle. Deem and Zabusky in 1978 [17] discovered, by numerical methods, m -fold symmetric vortex patch solutions for $m > 2$ which are the generalizations of Kirchhoff’s ellipse. The near-circular solutions resemble small-amplitude boundary waves. Their existence was proved analytically by Burbea [6] using a conformal mapping technique and bifurcation theory. At larger wave amplitudes, the outward protruding crests of the waves sharpen, ultimately limiting in a shape with right-angle corners. These corners coincide with hyperbolic stagnation points in the rotating reference frame in which the patch is steady. From an analytical point of view, this problem is still open and some progress has been recently made in [31].

In the present study, we generalize these vortex patch solutions further by exploring how they are altered for the QGSW equations when $\varepsilon \in \mathbb{R}^*$ (the Euler case corresponds to $\varepsilon = 0$). We focus on $\varepsilon \ll 1$ where

analytical progress can be made, but also present numerical solutions that confirm the analysis and extend it to larger positive ε . A surprising discovery is a new branch of m -fold symmetric solutions which do not bifurcate from the circle (below we exhibit the case $m = 3$). This is an isolated branch and exists even for $\varepsilon = 0$.

Some relevant vortex patch solutions for the QGSW equations are already available in the literature. Polvani (1988) [59] and Polvani, Zabusky and Flierl (1989) [58] computed the generalization of Kirchhoff's ellipse for various values of ε (as well as for doubly-connected patches and for multi-layer flows). Later, Płotka and Dritschel (2012) [56] carried out a more comprehensive analysis of the generalized Kirchhoff ellipse solutions, including linear stability and nonlinear evolution. In these studies, solutions were obtained numerically, starting near the known circular patch solution. In all cases, the limiting states were found to be dumbbell-shaped, specifically two symmetrical teardrop-shaped patches connected at a single point. This is in stark contrast with Kirchhoff's ellipse, which continues as a solution at arbitrarily small aspect ratio λ .

In fact, as shown in this study, there are other two-fold symmetric vortex patch solutions of the QGSW equations. However, these are not on the branch of solutions connected to the circular patch. We demonstrate numerically, then prove mathematically, that the Kirchhoff branch for $\varepsilon = 0$ splits up into many disconnected branches for any $\varepsilon > 0$. The limiting dumbbell state found in the above studies is directly related to the limiting state of just one of the solution branches bifurcating from the Kirchhoff ellipse at $\lambda = \lambda_4$ found by Luzzatto-Fegiz and Williamson (2010) [49] for $\varepsilon = 0$. The other branch lies on a disconnected branch of solutions when $\varepsilon > 0$. The same behavior appears to occur near all other even bifurcations, i.e. near $\lambda = \lambda_6, \lambda_8, \dots$, though we only have numerical evidence for this at present.

The plan of the paper is as follows. In section 4.2, we describe the numerical method employed to compute the vortex patch solutions. Results are then presented in section 4.3, both for the two-fold and the three-fold singly-connected vortex patch solutions. The remainder of the paper is devoted to proving the existence of m -fold solutions (in section 4.5), and proving that the two-fold solution branch splits near $\lambda = \lambda_4$ when $|\varepsilon| \ll 1$ (in section 4.6). We conclude in section 4.7 and suggest ideas for future work.

4.2 Numerical approach

To navigate along equilibrium solution branches up to limiting states having corners on the patch boundaries, it is necessary to employ a robustly convergent numerical method. Here we follow Luzzatto-Fegiz and Williamson (2011) [50], employing a Newton iteration to find corrections to the boundary shape from the exact condition

$$\psi(\mathbf{x}) - \frac{1}{2}\Omega|\mathbf{x}|^2 = C \quad (4.2.1)$$

expressing the fact that the streamfunction is constant in a frame of reference rotating at the angular velocity Ω . Here C is a constant, and in this section only \mathbf{x} refers to the vector position of a point with coordinates (x, y) . For a single patch of uniform (potential) vorticity $q = 2\pi$, the streamfunction ψ is determined from the contour integral

$$\psi(\mathbf{x}) = \oint_{\mathcal{C}} H(\varepsilon r) ((x' - x)dy' - (y' - y)dx') \quad (4.2.2)$$

where \mathcal{C} refers to the boundary of the patch, $r = |\mathbf{x}' - \mathbf{x}|$ is the distance between \mathbf{x}' and \mathbf{x} , and the function H is given by

$$H(z) = \frac{zK_1(z) - 1}{z^2} \quad (4.2.3)$$

where K_1 is the modified Bessel function of order 1 [56]. In the limit $z \rightarrow 0$, relevant to the Euler equations, $H(\varepsilon r)$ reduces to $\frac{1}{4}(\ln r^2 - 1)$ plus an unimportant constant.

We start with a guess $\mathbf{x} = \bar{\mathbf{x}}(\vartheta)$ for the shape of \mathcal{C} . Here, following [21], we use a special coordinate ϑ proportional to the travel time of a fluid particle around \mathcal{C} from some pre-assigned starting point. This

coordinate simplifies the equations which must be solved at each step of the iterative procedure correcting the boundary shape. The travel time t is computed from

$$t = \int_0^s \frac{ds'}{|\tilde{\mathbf{u}}(s')|} \quad (4.2.4)$$

where s is arc length measured from the starting point, and $\tilde{\mathbf{u}} = \nabla^\perp(\psi - \frac{1}{2}\Omega|\mathbf{x}|^2)$ is the velocity in the rotating frame of reference (here $\nabla^\perp = (-\partial/\partial y, \partial/\partial x)$ is the skewed gradient operator). The integral around the entire boundary, T_p , gives the particle orbital period, from which we define the particle frequency $\Omega_p = 2\pi/T_p$, a particularly useful diagnostic in which to characterize the equilibrium patch solutions. From Ω_p , we define the travel-time coordinate as $\vartheta = \Omega_p t$, where t is given in (4.2.4). Notably, at equilibrium, $\tilde{\mathbf{u}}$ is tangent to \mathcal{C} . During the iteration to find an equilibrium, this will not be exactly true, but the small discrepancy has no significant effect on the convergence of the numerical procedure.

We correct the previous guess $\bar{\mathbf{x}}$ at each step of the iteration by taking

$$\mathbf{x} = \bar{\mathbf{x}} + \frac{\hat{\eta}(\vartheta)(\bar{y}_\vartheta, -\bar{x}_\vartheta)}{|\bar{\mathbf{x}}_\vartheta|^2} \quad (4.2.5)$$

where a ϑ subscript denotes differentiation with respect to ϑ . This represents a normal perturbation to the previous boundary, though the scalar function $\hat{\eta}$ has units of area. This choice of perturbation leads to the simplest form for the linearized approximation to (4.2.1) and (4.2.2),

$$\Omega_p \hat{\eta}(\vartheta) - \int_0^{2\pi} \hat{\eta}(\vartheta') K_0(\varepsilon|\bar{\mathbf{x}}(\vartheta') - \bar{\mathbf{x}}(\vartheta)|) d\vartheta' - \frac{1}{2} \hat{\Omega} |\bar{\mathbf{x}}(\vartheta)|^2 = C - \bar{\psi}(\vartheta) + \frac{1}{2} \bar{\Omega} |\bar{\mathbf{x}}(\vartheta)|^2 \equiv R(\vartheta) \quad (4.2.6)$$

where terms only up to first order in $\hat{\eta}$ have been retained, and we have additionally included a perturbation $\hat{\Omega}$ in the rotation rate $\Omega = \bar{\Omega} + \hat{\Omega}$. Above, K_0 is the modified Bessel function of order 0, and notably $K_0(\varepsilon r)$ reduces to $-\ln r$ plus an unimportant constant in the limit $\varepsilon \rightarrow 0$. On the right hand side of (4.2.6), $\bar{\psi}$ refers to the streamfunction evaluated using the previous guess $\bar{\mathbf{x}}$, i.e. using $\bar{\mathbf{x}}$ in place of \mathbf{x} in (4.2.2). This is a linear integral equation for $\hat{\eta}$ and possibly $\hat{\Omega}$, but its solution requires additional constraints. First of all, we require that the vortex patch area A remains constant, and without loss of generality we may take $A = \pi$. This constraint gives rise to an additional equation after linearising the expression for area

$$A = \frac{1}{2} \oint_C x dy - y dx \quad (4.2.7)$$

leading to

$$\int_0^{2\pi} \hat{\eta}(\vartheta) d\vartheta = A - \bar{A} \quad (4.2.8)$$

where \bar{A} is the area of the previous guess found by using $\bar{\mathbf{x}}$ in place of \mathbf{x} in (4.2.7). If Ω is held fixed during the iteration ($\hat{\Omega} = 0$), no further constraints are necessary. However, holding Ω fixed does not allow one to negotiate turning points in the equilibrium solution branches [50]. If we let Ω vary (and thus be determined as part of the solution), we need to impose a further constraint. The most natural is angular impulse:

$$J = \frac{1}{4} \oint_C |\mathbf{x}|^2 (x dy - y dx) \quad (4.2.9)$$

whose linearisation leads to the additional equation

$$\int_0^{2\pi} |\bar{\mathbf{x}}(\vartheta)|^2 \hat{\eta}(\vartheta) d\vartheta = J - \bar{J} \quad (4.2.10)$$

where \bar{J} is the angular impulse of the previous guess found by using $\bar{\mathbf{x}}$ in place of \mathbf{x} in (4.2.9).

Numerically, the vortex patch boundary for an m -fold equilibrium is represented by $n = 400m$ boundary nodes, approximately equally spaced in ϑ . Upon each iteration, the travel time coordinate is recomputed and the nodes are redistributed to be equally-spaced in ϑ , to within numerical discretisation error. The algorithm for node redistribution is otherwise the same as that introduced in [20] and uses local cubic splines for high accuracy. Also, the calculation of the streamfunction ψ and velocity $\mathbf{u} = \nabla^\perp \psi$ by contour integration is described in [20], and further in [18] for the QGSW equations (as used by [56] to determine the branch of 2-fold QGSW equilibria bifurcating from the Rankine vortex).

The perturbation function $\hat{\eta}(\vartheta)$ is represented as the truncated Fourier series

$$\hat{\eta}(\vartheta) = \sum_{j=0}^N a_j \cos(jm\vartheta) \quad (4.2.11)$$

which imposes even symmetry. The same symmetry is imposed for the node redistribution, so only 201 boundary nodes are unique. Not all vortex patch equilibria have such symmetry [50], but we restrict attention to symmetric equilibria in this study. A truncation of $N = 32$ was found sufficient to produce results accurate to within the plotted line widths below. Accuracy is not significantly improved when using larger N because ultimately the highest modes $\cos(jm\vartheta)$ for j near N are poorly represented by the boundary nodes. In general, we find $N \sim 0.08n/m$ ensures the highest modes are adequately resolved, as judged by the decay of the Fourier coefficients a_j for j large.

Note the coefficient a_0 is directly determined by area conservation. From (4.2.8), we find

$$a_0 = \frac{A - \bar{A}}{2\pi}. \quad (4.2.12)$$

This means that the streamfunction constant C is determined by averaging (4.2.6) over ϑ , and thus C is generally determined from all of the a_n and $\hat{\Omega}$. However, C is not needed to find an equilibrium, so this calculation need not be done.

We solve (4.2.6) for a_n ($n > 0$) — together with (4.2.10) for $\hat{\Omega}$ when Ω is allowed to vary — by substituting (4.2.11) into (4.2.6), then multiplying both sides by $\pi^{-1} \cos(im\vartheta)$, and finally integrating over ϑ . This results in the linear system

$$\sum_{j=1}^N A_{ij} a_j - B_i \hat{\Omega} = C_i, \quad i = 1, 2, \dots, N \quad (4.2.13)$$

where the matrix elements A_{ij} and vector components B_i and C_i are given by

$$\begin{aligned} A_{ij} &= \Omega_p \delta_{ij} - \frac{1}{\pi} \int_0^{2\pi} \int_0^{2\pi} \cos(im\vartheta) \cos(jm\vartheta') K_0(\varepsilon |\bar{\mathbf{x}}(\vartheta') - \bar{\mathbf{x}}(\vartheta)|) d\vartheta' d\vartheta \\ B_i &= \frac{1}{2\pi} \int_0^{2\pi} |\bar{\mathbf{x}}(\vartheta)|^2 \cos(im\vartheta) d\vartheta \\ C_i &= \frac{1}{\pi} \int_0^{2\pi} R(\vartheta) \cos(im\vartheta) d\vartheta \end{aligned} \quad (4.2.14)$$

where δ_{ij} is the Kronecker delta. Notably, $A_{ij} = A_{ji}$. Care is taken to avoid the logarithmic singularity in $K_0(\varepsilon r)$ by separating this function into a singular part $S = -\ln(1 - \cos(\vartheta' - \vartheta))$, which can be integrated analytically (and contributes $-\pi \delta_{ij}/(im)$ to A_{ij}), and a non-singular remainder $K_0 - S$ which is integrated by two-point Gaussian quadrature. The same numerical quadrature is used to compute B_i (if $\hat{\Omega} \neq 0$) and C_i . The area constant a_0 from (4.2.12) is ignored at this stage and is added after the linear system (4.2.13) is solved.

When Ω is held fixed, we have $\hat{\Omega} = 0$ in (4.2.13) above, and then (4.2.13) may be directly solved for the coefficients a_j , $j = 1, 2, \dots, N$. Otherwise, we need to add another equation in order to also obtain $\hat{\Omega}$. We do this by fixing the angular impulse and thus use (4.2.10). Inserting (4.2.11) into (4.2.10) and dividing by 2π results in the further linear equation

$$\sum_{j=1}^N B_j a_j = \frac{J - \bar{J}}{2\pi} \quad (4.2.15)$$

(again ignoring the area constant a_0). If we tag $-\hat{\Omega}$ to the end of the vector of coefficients (a_1, a_2, \dots, a_N) , we obtain a symmetric linear system for this vector, which is easily solved by standard numerical linear algebra packages. Only at this stage do we add a_0 from (4.2.12) and fully determine $\hat{\eta}(\vartheta)$ from the sum in (4.2.11). We then obtain a new guess for the vortex boundary shape from (4.2.5), and accept this as the converged solution if the maximum value in $|\mathbf{x} - \bar{\mathbf{x}}| < 10^{-7}$. Otherwise, we use \mathbf{x} as the next guess $\bar{\mathbf{x}}$ and repeat the above procedure.

The above explains how we obtain a single equilibrium state for either fixed rotation rate Ω or fixed angular impulse J . To obtain a whole family of states or solutions, after convergence to one state, we slightly change either Ω or J and search for the next state using the same iterative procedure described above.

This approach fails when we reach a turning point in either Ω or J . When this happens, we switch the control parameter (e.g. instead of changing Ω we change J) and continue to the next turning point. Fortunately, the turning points for Ω and J are almost never coincident, so this is an effective strategy. A more elaborate strategy was followed in [50], but the proposed strategy has been found to be highly effective. We always reach limiting states containing near corners on their boundaries, beyond which there are no other states with the same topology.

We note for completeness that the above procedure is readily generalized to study multiply-connected vortex patch equilibria. The primary change is that the constant C and all functions of ϑ in (4.2.6) acquire a k subscript (denoting the k th patch boundary or contour), while all functions of ϑ' acquire an ℓ subscript. Furthermore, the integral is now summed over all contours ℓ and multiplied by the uniform potential vorticity q_ℓ . Each contour must also satisfy an area constraint like (4.2.8), with η and A supplemented by k subscripts. If angular impulse is fixed, additionally (4.2.10) must be satisfied. Here again all functions of ϑ acquire a k subscript, and the integral must be summed over k and multiplied by the uniform potential vorticity q_k . The impulse is an invariant of the entire vortex system.

The procedure also generalizes to cases in which the vortex patches steadily translate rather than rotate. In this case, without loss of generality, we may suppose that the patches translate in the x direction at speed U . The only changes then required in the procedure described above is to replace $\frac{1}{2}\Omega|\bar{\mathbf{x}}|^2$ by $-U\bar{y}$ and to impose linear impulse conservation,

$$I = \frac{1}{3} \sum_k q_k \oint_{C_k} y_k (x_k dy_k - y_k dx_k). \quad (4.2.16)$$

When searching for equilibria of a fixed linear impulse I , an additional equation is required to determine the perturbation \hat{U} to the speed U . This is found by linearising (4.2.16) after substituting (4.2.5), supplemented by k subscripts, yielding

$$\sum_k q_k \int_0^{2\pi} \bar{y}_k(\vartheta) \hat{\eta}_k(\vartheta) d\vartheta = I - \bar{I} \quad (4.2.17)$$

where \bar{I} is the linear impulse of the previous guess found by using $\bar{\mathbf{x}}_k$ in place of \mathbf{x}_k in (4.2.16).

Various diagnostics may be used to characterize the equilibrium vortex patch solutions. For the symmetric m -fold solutions studied here, the only other non-zero invariant besides angular impulse is the ‘excess’ energy

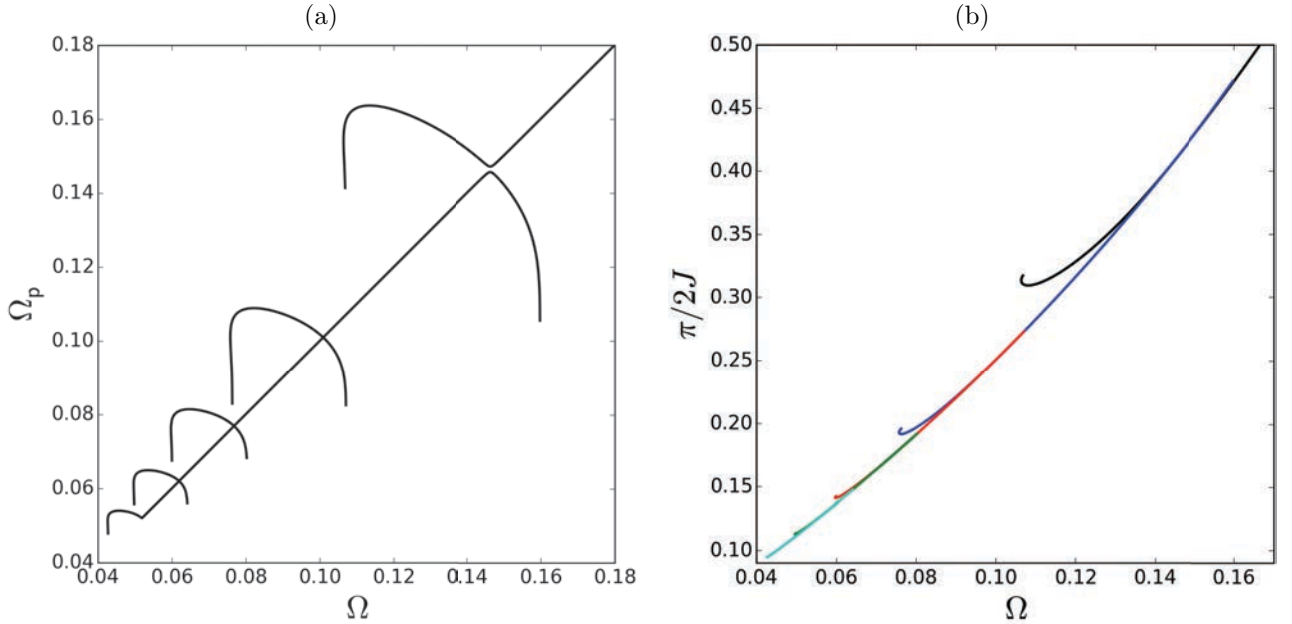


Figure 4.1: Solution branch structure for 2-fold vortex patch equilibria when $\varepsilon = 0.01$. In (a), we show the particle frequency Ω_p versus rotation rate Ω , while in (b) we show $\pi/2J$ versus Ω and render separate branches in different colours. Note, for a circular vortex patch, $J = \pi/2$. The upper right branch is not shown in its entirety; it begins at the circular patch with $\Omega \approx \frac{1}{4}$ and $\Omega_p \approx \frac{1}{4}$. Also, only the first five branches of an infinite set of them converging on $\Omega = \Omega_p = 0$ are shown.

E , as defined in [56]. For a single patch of area $A = \pi$, this is determined from

$$E = \frac{\pi}{4}(\ln(\varepsilon/2) + \gamma) - \frac{1}{4\pi} \oint_C \oint_C H(\varepsilon r)[(\mathbf{x}' - \mathbf{x}) \cdot d\mathbf{x}'][(\mathbf{x}' - \mathbf{x}) \cdot d\mathbf{x}] \quad (4.2.18)$$

where $\gamma = 0.5772\dots$ is Euler's constant, $r = |\mathbf{x} - \mathbf{x}'|$, and $H(z)$ is defined in (4.2.3). This expression for E has a finite limit as $\varepsilon \rightarrow 0$, and equals the excess energy for the Euler equations (see discussion in appendix B of [56]). For a circular patch, $E = \pi/16$ when $\varepsilon = 0$.

The energy and angular impulse are important since minima or maxima of these quantities, as a function of a control parameter like Ω , generally indicate changes in stability. In the results below, we have confirmed this by a direct linear stability analysis outlined in [21] and used previously in [56].

4.3 Numerical results

4.3.1 2-fold vortex patch equilibria

We begin by discussing 2-fold symmetric vortex patch equilibria, in particular the structure of the solution branches for small ε . This structure is illustrated in two ways for $\varepsilon = 0.01$ in figure 4.1.

This figure shows the difficulty in distinguishing solution branches when a conserved quantity like J or E is plotted versus the control parameter Ω . On the other hand, Ω_p versus Ω fully opens the branching structure, enabling one to see the separation in the branch stemming from the circular vortex (upper right)

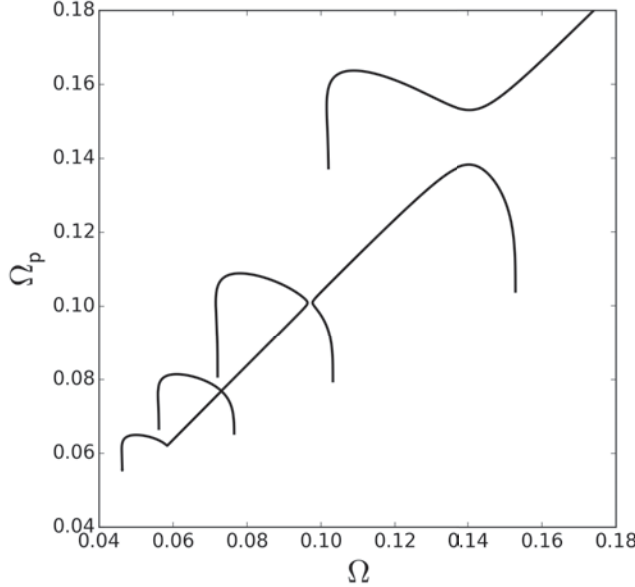


Figure 4.2: Solution branch structure for 2-fold vortex patch equilibria when $\varepsilon = 0.1$. Here, only Ω_p versus Ω is shown.

from the next branch. In panel (b), the separate branches are coloured, with the primary one being black, the second one blue (partly overlaid by the third one in red), etc. The blue, red, green and cyan branches all have the same general form. They rise at larger Ω from small Ω_p , reach a maximum in Ω_p , then fall at smaller Ω . If we could reach the limiting states having one or more stagnation points on the vortex boundary (where the boundary exhibits a corner), we would find $\Omega_p = 0$ since it would take an infinite time for a particle to circulate around the boundary.

The separation of these branches becomes increasingly difficult to see as Ω decreases; however, at the larger value of $\varepsilon = 0.1$ (shown in figure 4.2), we can clearly see the second branch separating from the third. We believe this is a generic feature for all $\varepsilon > 0$: all branches separate.

The uppermost branch of solutions stemming from the circular vortex was computed previously by [56], and at that time was thought to be the only branch of 2-fold solutions. The limiting state is a dumbbell shaped vortex touching at a single point at the origin. On the second branch, there are two limiting states. The one having the largest Ω has a rugby-ball shape with right-angled corners at the outermost tips. The other limiting state has the form of an array of three vortices connected at two stagnation points. This pattern continues for the other branches, with the vortex become increasingly elongated. The (near) limiting states are illustrated in figures 4.3 and 4.4 together with the streamfunction in the co-rotating frame of reference.

Key properties of the two-fold limiting states for $\varepsilon = 0.01$ are provided in Table 1.

4.3.2 3-fold vortex patch equilibria

We next turn to 3-fold symmetric vortex patch equilibria, first studied by Deem and Zabusky in 1978 [17] for the Euler equations ($\varepsilon = 0$). Here we discuss the structure of the solution branches for a wide range of ε .

The most surprising result is that there is a disconnected branch of solutions, not terminating at either

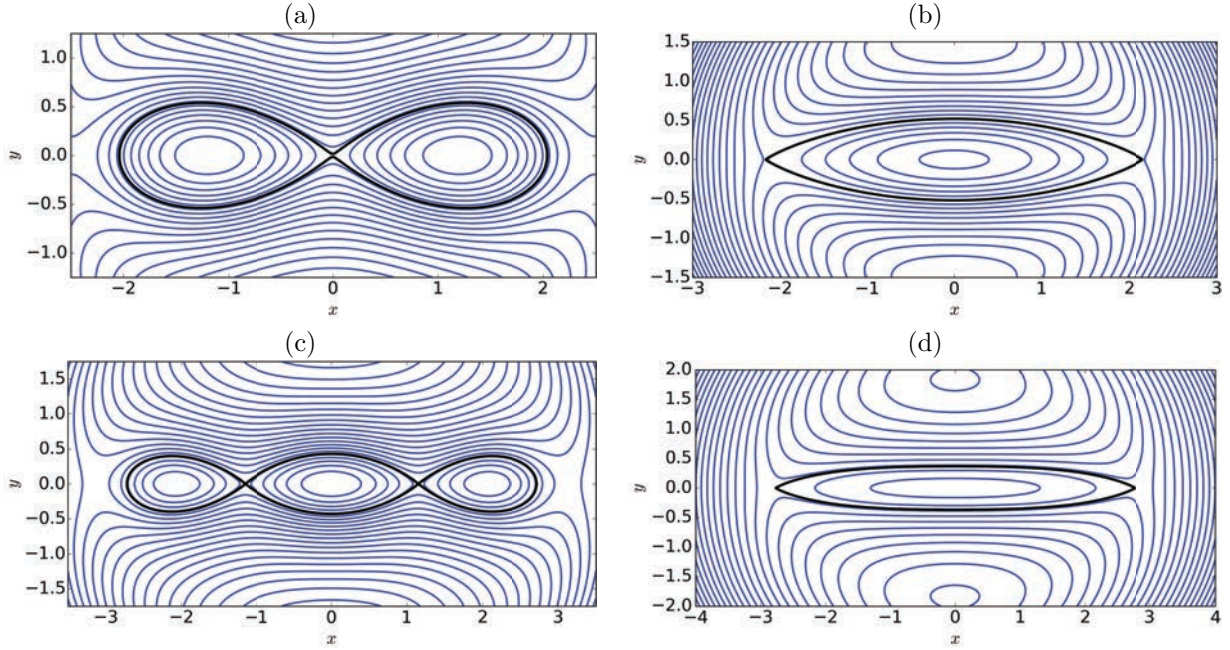


Figure 4.3: Form of the (near) limiting solutions (black contours) and the co-rotating streamfunction (blue) for (a) the end of the first branch, (b) the start of the second branch, (c) the end of the second branch, and (d) the start of the third branch.

Branch	Ω	$\pi/2J$	$16E/\pi$
1a	0.250000	1.000000	1.000000
1b	0.106827	0.317246	-0.456852
2a	0.159754	0.471293	0.110399
2b	0.076297	0.195486	-1.231673
3a	0.107035	0.272772	-0.692599
3b	0.059980	0.142097	-1.777402
4a	0.080209	0.191364	-1.268668
4b	0.049782	0.113129	-2.181805
5a	0.064135	0.147404	-1.714846
5b	0.042700	0.094682	-2.504112

Table 4.1: Key properties of the (near) limiting states for $\varepsilon = 0.01$ for the first 5 branches shown in figure 1. In the first column, ‘a’ denotes the start of a branch while ‘b’ denotes the end of it.

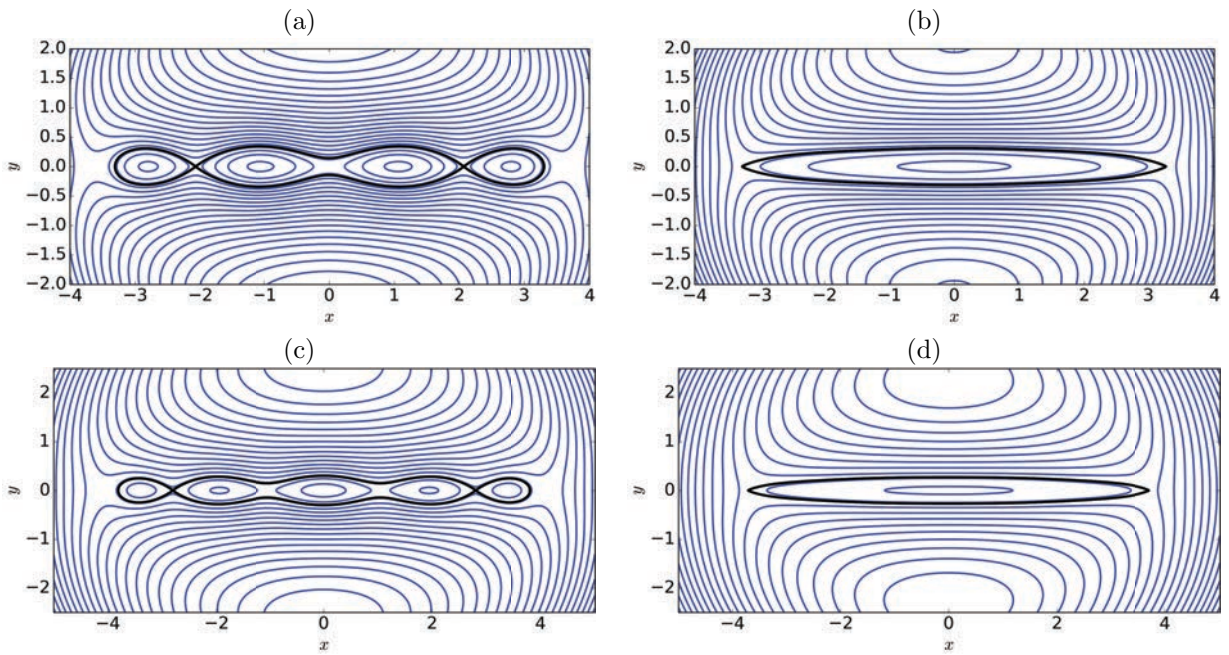


Figure 4.4: Form of the (near) limiting solutions (black contours) and the co-rotating streamfunction (blue) for (a) the end of the third branch, (b) the start of the fourth branch, (c) the end of the fourth branch, and (d) the start of the fifth branch.

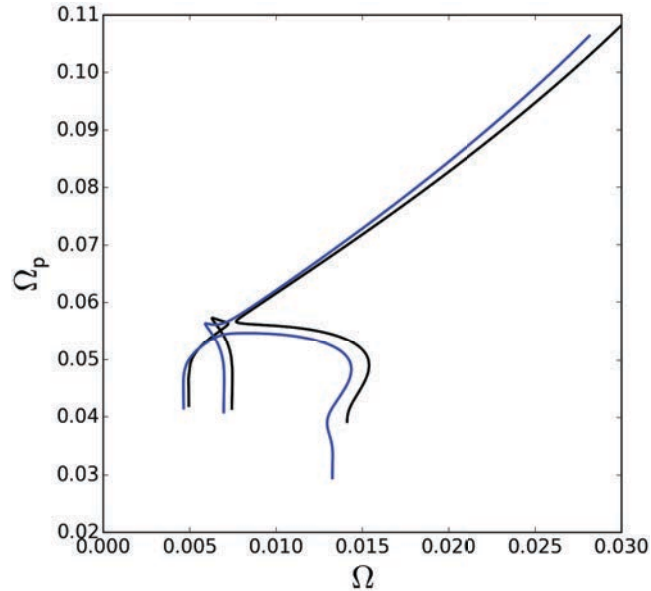


Figure 4.5: Solution branch structure for 3-fold vortex patch equilibria when $\varepsilon = 3.5$ (black) and $\varepsilon = 3.6$ (blue). The branches start at the circular vortex patch solution in the upper right portion of the graph.

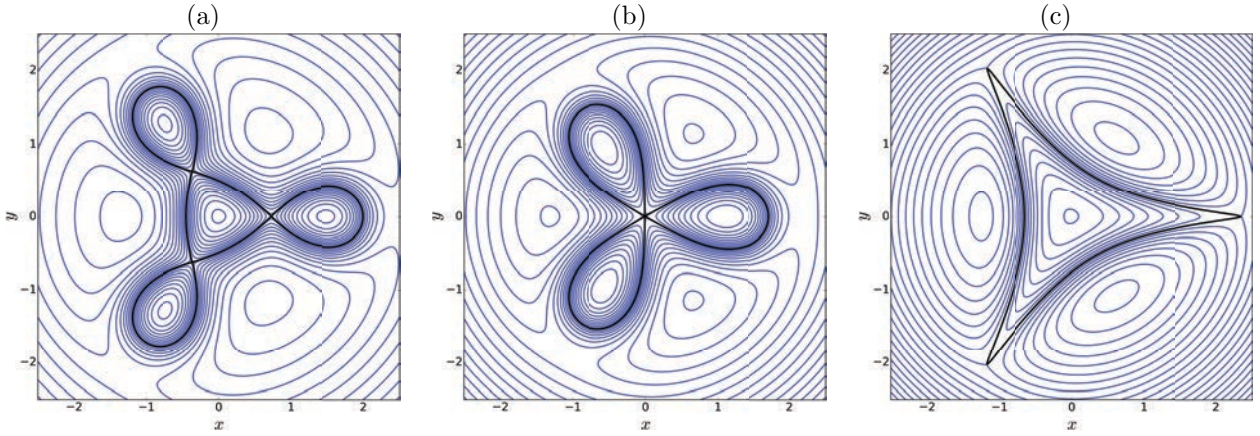


Figure 4.6: Form of the (near) limiting solutions (black contours) and the co-rotating streamfunction (blue) for the state with (a) the smallest Ω , (b) the intermediate value of Ω , and (c) the largest Ω . Here $\varepsilon = 3.6$, corresponding to the blue curves in figure 4.5.

end at the circular Rankine vortex. This was discovered by increasing ε and finding a change in the topology of the limiting states between $\varepsilon = 3.5$ and 3.6 . This is associated with a bifurcation in the structure of the solution branches, as shown in figure 4.5. For $\varepsilon = 3.5$ (black curves), the branch starting from the circular patch in the upper right corner reaches a minimum in Ω at $\Omega = 0.007704627$, then increases and finally decreases approaching the limiting state. (In fact $d\Omega/d\Omega_p$ likely changes sign an infinite number of times before reaching the limiting state at $\Omega_p = 0$.) This limiting state is triangular (albeit with curved sides), and has the same form as found for the Euler equations ($\varepsilon = 0$) in [17] (see below). For $\varepsilon = 3.6$ (blue curves), the branch starting from the circular patch in the upper right corner also reaches a minimum in Ω , but then Ω increases and limits to a significantly smaller value as $\Omega_p \rightarrow 0$. This limiting state resembles three petal-like vortices connected at a single point at the origin. This state is also the limiting state of three identical co-rotating vortex patches, first studies in [21]. Having determined that there is a bifurcation in the solution branch structure between $\varepsilon = 3.5$ and 3.6 , a new branch was discovered by taking the near limiting solution for $\varepsilon = 3.6$ and gradually decreasing ε to $\varepsilon = 3.5$, holding the angular impulse fixed (Ω must be allowed to vary). In this way, we could find a solution on the black separated branch next to the blue one (the middle pair of curves in the lower part of the figure with $\Omega \approx 0.007$). Having found one solution, we could then continue in both directions to find the limiting states on this separated branch. (The blue separated branch can be found similarly by jumping from the black separated branch at small Ω .) One of these limiting states is the petal-like state just described. The other, at the smallest Ω , is a new state consisting of a triangular central vortex attached to three petals — a four vortex state. These limiting solutions are illustrated for $\varepsilon = 3.6$ in figure 4.6.

By continuing to jump branches from one value of ε to another, we were able to determine that separated branches exist over a wide range of ε , and likely for all ε . As $\varepsilon \rightarrow 0$, the separated branch moves far from the primary branch stemming from the circular patch, as shown in figure 7. The limiting states are qualitatively similar to those for $\varepsilon = 3.6$ and are shown in figure 4.8. Key properties of the three-fold limiting states for $\varepsilon = 0$ are provided in Table 2.

A more complete picture of the bifurcation structure of the three-fold patch solutions for various values of ε is provided in figure 4.9. Each value of ε is seen to have a separated branch which exists at values of Ω smaller than that of the limiting circular patch solution. In all cases, this separated branch is linearly

Ω	$\pi/2J$	$16E/\pi$
0.333333	1.000000	1.000000
0.301234	0.885055	0.835043
0.122420	0.290564	-1.002261
0.113192	0.272230	-1.110795

Table 4.2: Key properties of the three-fold (near) limiting states for $\varepsilon = 0$.

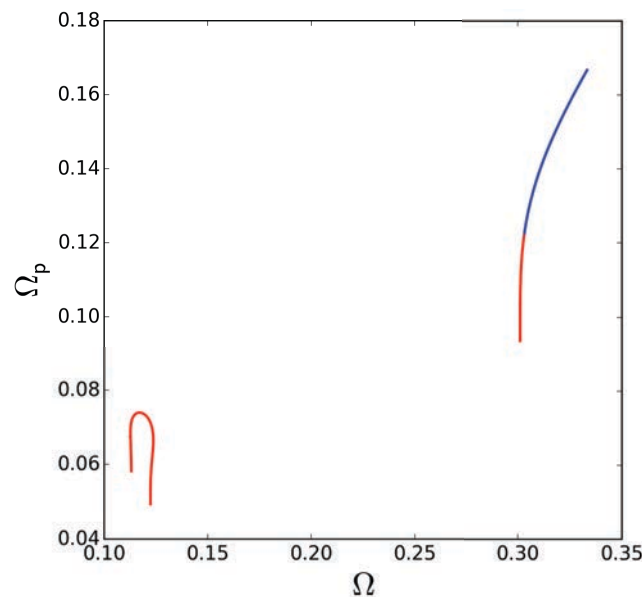


Figure 4.7: Solution branch structure for 3-fold vortex patch equilibria when $\varepsilon = 0$ (the Euler equations). The primary branch starts at the circular vortex patch solution in the upper right portion of the graph. There, $\Omega = \frac{1}{3}$ and $\Omega_p = \frac{1}{6}$. The separated branch is new. The blue portion of the primary branch is linearly stable while the red portion and the entire separated branch is linearly unstable.

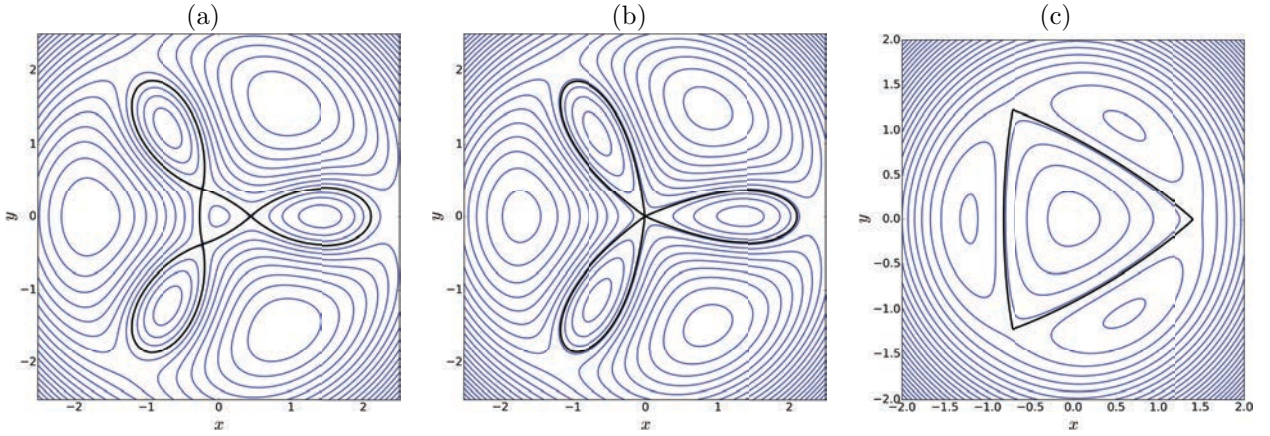


Figure 4.8: Form of the (near) limiting solutions (black contours) and the co-rotating streamfunction (blue) for the state with (a) the smallest Ω , (b) the intermediate value of Ω , and (c) the largest Ω . Here $\varepsilon = 0$, corresponding to the Euler equations. The state in (c) at the end of the primary branch of solutions was discovered in [17]; the state in (b) was discovered in [21], while that in (a) is new.

unstable. Portions of the primary branch are also unstable, though there is a window of stability for all $\varepsilon > 0$. The nonlinear evolution of the unstable states is deferred to another study, but the instabilities often leave a time-dependent pulsating state.

4.4 Tools used for the mathematical analysis

The purpose of this section is to review and collect some technical tools that are used throughout the remainder of this paper. We first recall some simple facts about Hölder spaces on the unit circle. Second, we discuss basic properties of modified Bessel functions. Last we state the classical Crandall-Rabinowitz theorem and give a generalized version with a parameter.

4.4.1 Notation

Here we introduce some notation that is used in the forthcoming sections.

- The unit disc of the plane and its boundary will be denoted by \mathbb{D} and \mathbb{T} , respectively.
- We denote by C any positive constant that may change from line to line.
- For a given continuous function $f : \mathbb{T} \rightarrow \mathbb{C}$, we define its mean value by

$$\int_{\mathbb{T}} f(\tau) d\tau \triangleq \frac{1}{2i\pi} \int_{\mathbb{T}} f(\tau) d\tau,$$

where $d\tau$ stands for the complex integration.

- Let X and Y be two normed spaces. We denote by $\mathcal{L}(X, Y)$ the vector space of all the continuous linear maps endowed with its usual strong topology.
- Let Y be a vector space and R be a subspace, then Y/R denotes the quotient space.

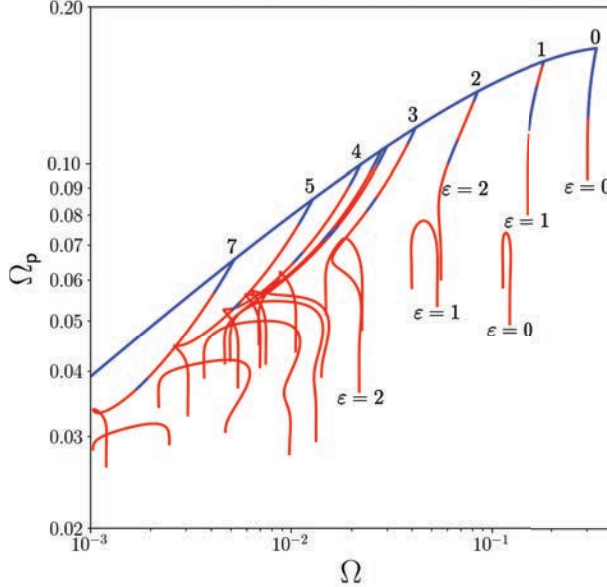


Figure 4.9: Solution branch structure for 3-fold vortex patch equilibria for various ε , as labelled. Blue portions of the curves are linearly stable while red portions are linearly unstable, as determined by a full linear stability analysis (following [21] and [56]). The uppermost blue curve connects the limiting circular patch solutions continuously as a function of ε .

4.4.2 Modified Bessel functions

This section is devoted to some classical properties of Bessel functions of imaginary argument. We start with the Bessel function of the first kind and order ν given by the expansion

$$J_\nu(z) = \sum_{m=0}^{+\infty} \frac{(-1)^m \left(\frac{z}{2}\right)^{\nu+2m}}{m! \Gamma(\nu + m + 1)}, \quad |\arg(z)| < \pi.$$

Note that this sum converges in a classical way provided that $\Gamma(\nu + m + 1)$ exists for any positive integer. In addition, for $\nu = n \in \mathbb{Z}$ it is known that Bessel functions admit the following integral representation:

$$\forall z \in \mathbb{C}, \quad J_n(z) = \frac{1}{\pi} \int_0^\pi \cos(n\theta - z \sin \theta) d\theta.$$

Bessel functions of imaginary argument, denoted by I_ν and K_ν , are given by

$$I_\nu(z) = \sum_{m=0}^{+\infty} \frac{\left(\frac{z}{2}\right)^{\nu+2m}}{m! \Gamma(\nu + m + 1)}, \quad |\arg(z)| < \pi$$

and

$$K_\nu(z) = \frac{\pi}{2} \frac{I_{-\nu}(z) - I_\nu(z)}{\sin(\nu\pi)}, \quad \nu \in \mathbb{C} \setminus \mathbb{Z} \quad |\arg(z)| < \pi.$$

However, for $\nu = n \in \mathbb{Z}$ we set $K_n(z) = \lim_{\nu \rightarrow n} K_\nu(z)$. At this stage we recall useful expansions for K_n that can be found for instance in [69, p. 79-80],

$$K_0(z) = -\log\left(\frac{z}{2}\right) I_0(z) + \sum_{m=0}^{\infty} \frac{(\frac{z}{2})^{2m}}{(m!)^2} \psi(m+1), \quad K'_0(z) = -K_1(z), \quad (4.4.1)$$

where

$$\psi(1) = -\gamma \quad \text{and} \quad \forall m \in \mathbb{N}^*, \quad \psi(m+1) = \sum_{k=1}^m \frac{1}{k} - \gamma.$$

In addition, for $n \in \mathbb{N}^*$

$$\begin{aligned} K_n(z) &= (-1)^{n+1} \sum_{m=0}^{+\infty} \frac{\left(\frac{z}{2}\right)^{n+2m}}{m!(n+m)!} \left(\log\left(\frac{z}{2}\right) - \frac{1}{2}\psi(m+1) - \frac{1}{2}\psi(n+m+1) \right) \\ &\quad + \frac{1}{2} \sum_{m=0}^{n-1} \frac{(-1)^m (n-m-1)!}{m! \left(\frac{z}{2}\right)^{n-2m}}. \end{aligned}$$

Another useful property is the positivity of I_n and K_n . In fact, for any $n \in \mathbb{N}$ we have

$$\forall x > 0, I_n(x) > 0 \quad \text{and} \quad K_n(x) > 0. \quad (4.4.2)$$

The first one is obvious from the definition since each term in the sum is strictly positive. As for the second one, it can be deduced from the following integral representation found in e.g. [69, p. 181],

$$K_\nu(z) = \int_0^{+\infty} e^{-z \cosh t} \cosh(\nu t) dt. \quad (4.4.3)$$

Another useful identity found in [69, p. 441] deals with Nicholson's integral representation of $I_n(z)K_n(z)$: for $n \in \mathbb{N}$

$$I_n(z)K_n(z) = \frac{2(-1)^n}{\pi} \int_0^{\frac{\pi}{2}} K_0(2z \cos \theta) \cos(2n\theta) d\theta. \quad (4.4.4)$$

For the convenience of the reader, we next describe the relationship between K_0 and the Green function associated with Helmholtz's operator in two-dimensional space. Let $\varepsilon \in \mathbb{R}^*$ and consider in the distribution sense the equation

$$(-\Delta + \varepsilon^2)G_\varepsilon = \delta_0, \text{ in } \mathcal{S}'(\mathbb{R}^2).$$

Then using a Fourier transform we obtain

$$\widehat{G}_\varepsilon(\xi) = \frac{1}{|\xi|^2 + \varepsilon^2}, \quad \forall \xi \in \mathbb{R}^2.$$

Thus by a scaling argument, we have

$$G_\varepsilon(x) = G_1(\varepsilon x), \quad \text{with} \quad G_1(x) = \frac{1}{4\pi^2} \int_{\mathbb{R}^2} \frac{e^{ix \cdot \xi}}{1 + |\xi|^2} d\xi.$$

Hence, a change of variables using polar coordinates yields

$$\begin{aligned} G_1(x) &= \frac{1}{4\pi^2} \int_0^{+\infty} \frac{r}{1+r^2} \int_0^{2\pi} \cos(|x|r \cos \theta) d\theta dr \\ &= \frac{1}{2\pi} \int_0^{+\infty} \frac{r J_0(|x|r)}{1+r^2} dr \\ &= \frac{1}{2\pi} K_0(|x|), \end{aligned}$$

where in the last line we have used an identity from [69, p. 425]. As an application we show how to recover the velocity from the domain of the patch in (4.1.1). In fact, if D is a smooth bounded simply-connected domain and $q = \mathbf{1}_D$, then from the foregoing results the streamfunction ψ , which is the solution of the elliptic equation

$$(\Delta - \varepsilon^2)\psi = \mathbf{1}_D$$

is given explicitly by

$$\psi(x) = -\frac{1}{2\pi} \int_{\mathbb{R}^2} K_0(|\varepsilon||x-y|) \mathbf{1}_D(y) dA(y)$$

where dA denotes the planar Lebesgue measure. It follows that the velocity induced by the patch $v = \nabla^\perp \psi$ takes the form

$$v(x) = \frac{1}{2\pi} \int_{\partial D} K_0(|\varepsilon||x-\xi|) d\xi, \quad (4.4.5)$$

where the integration should be understood in the complex sense.

4.4.3 Boundary equations

In what follows we state the boundary equation of a rotating patch. First, the initial data $q_0 = \mathbf{1}_D$ generate a rotating patch about the origin with uniform angular velocity $\Omega \in \mathbb{R}$ if

$$q(t) = \mathbf{1}_{D_t} \quad \text{with} \quad D_t = e^{it\Omega} D.$$

We may check that this is equivalent to

$$(v(x) - \Omega x^\perp) \cdot \vec{n}(x) = 0, \quad \forall x \in \partial D$$

with $\vec{n}(x)$ being the unit outward normal vector to the boundary at the point x . The velocity v induced by q_0 is given by (4.4.5). Using complex notation we find that

$$\forall w \in \mathbb{T}, G(\varepsilon, \Omega, \Phi)(w) = 0,$$

with

$$G(\varepsilon, \Omega, \Phi)(w) = \operatorname{Im} \left\{ \Omega \Phi(w) \overline{\Phi'(w)} \bar{w} - \overline{\Phi'(w)} \bar{w} \oint_{\mathbb{T}} \Phi'(\tau) K_0(|\varepsilon||\Phi(w) - \Phi(\tau)|) d\tau \right\}$$

and $\Phi : \mathbb{T} \rightarrow \mathbb{C}$ is at least a C^1 parametrization of the boundary. Actually, we may add a constant term in the kernel K_0 without changing the equation. Thus according to the singularity structure of K_0 near the origin detailed in (4.4.1) the suitable constant to add is $\log\left(\frac{|\varepsilon|}{2}\right)$. Therefore

$$G(\varepsilon, \Omega, \Phi)(w) = \operatorname{Im} \left\{ \Omega \Phi(w) \overline{\Phi'(w)} \bar{w} - \overline{\Phi'(w)} \bar{w} \oint_{\mathbb{T}} \Phi'(\tau) K_0^\varepsilon(|\Phi(w) - \Phi(\tau)|) d\tau \right\} \quad (4.4.6)$$

with

$$K_0^\varepsilon(x) \triangleq K_0(|\varepsilon|x|) + \log\left(\frac{|\varepsilon|}{2}\right).$$

If we let $\varepsilon \rightarrow 0$, then without surprise we get the vortex patch equation associated with the Euler equations described for example in [?]:

$$G_E(\Omega, \Phi(w)) = \operatorname{Im} \left\{ \left(\Omega \overline{\Phi(w)} + \frac{1}{2} \oint_{\mathbb{T}} \frac{\overline{\Phi(\tau)} - \overline{\Phi(w)}}{\Phi(\tau) - \Phi(w)} \Phi'(\tau) d\tau \right) w \Phi'(w) \right\}.$$

One may notice that

$$G(0, \Omega, \Phi(w)) = -G_E(\Omega, \Phi(w)). \quad (4.4.7)$$

Indeed, starting from the general formula

$$\oint_{\partial D} \log |z - \xi| d\xi = -\frac{1}{2} \overline{\oint_{\partial D} \frac{\bar{\xi} - \bar{z}}{\xi - z} d\xi}$$

we find by a change of variables

$$\oint_{\mathbb{T}} \log(|\Phi(w) - \Phi(\tau)|) \Phi'(\tau) d\tau = -\frac{1}{2} \overline{\int_{\mathbb{T}} \frac{\overline{\Phi(\tau)} - \overline{\Phi(w)}}{\Phi(\tau) - \Phi(w)} \Phi'(\tau) d\tau}. \quad (4.4.8)$$

Thus

$$G_E(\Omega, \Phi(w)) = -\text{Im} \left\{ \left(\Omega \Phi(w) + \oint_{\mathbb{T}} \log(|\Phi(w) - \Phi(\tau)|) \Phi'(\tau) d\tau \right) \bar{w} \overline{\Phi'(w)} \right\}.$$

It suffices now to use the expansion (4.4.1) to deduce that

$$\forall x \neq 0, \quad \lim_{\varepsilon \rightarrow 0} K_0^\varepsilon(x) = -\log(x/2)$$

and thus we find (4.4.7).

4.5 Bifurcation to m -fold symmetric vortex patch equilibria

The main task of this section is to prove the existence of rotating m -fold vortex patch (relative) equilibria, or ‘V-states’ [17], for the QGSW model given by (4.1.1). In the first section we state our main result. The proof is carried out in several steps and is detailed in different sections. The basic tool is the classical Crandall–Rabinowitz’s theorem, and for the study of the imperfect bifurcation we need a slight generalization of this theorem.

4.5.1 Main result

We first state our principal result concerning the existence of a countable family of bifurcating curves with m -fold symmetry from Rankine (circular) vortices. More precisely, we obtain the following result.

Theorem 4.5.1. *Let $\varepsilon \in \mathbb{R}$, then for each integer $m \geq 1$ there exists a curve (or branch) of m -fold rotating vortex patches bifurcating from the unit disc at the angular velocity*

$$\Omega_m(\varepsilon) = I_1(|\varepsilon|)K_1(|\varepsilon|) - I_m(|\varepsilon|)K_m(|\varepsilon|).$$

Moreover, the existence is uniform for vanishing ε . More precisely, there exists $a > 0$ and continuous functions $\varphi : (-a, a)^2 \rightarrow \mathbb{R}$, $\psi : (-a, a)^2 \rightarrow C^{1+\alpha}(\mathbb{T})$ satisfying

$$\varphi(0, 0) = \Omega_m(0) = \frac{m-1}{2m}, \quad \psi(0, 0) = 0$$

such that

$$\Omega = \varphi(\varepsilon, s), \quad \psi(\varepsilon, s, w) = \sum_{n \geq 2} a_{nm-1}(\varepsilon, s) \bar{w}^{nm-1}$$

and

$$G(\varepsilon, \varphi(\varepsilon, s), w + s\bar{w}^{m-1} + s\psi(\varepsilon, s, w)) = 0, \quad \forall (\varepsilon, s) \in (-a, a)^2, \quad \forall w \in \mathbb{T}.$$

Recall that the function G defining the vortex patch equation is given by (4.4.6).

Remark 4.5.2. On the one hand, the case $m = 1$ is trivial. It corresponds simply to the translation of the unit disc, and with the notation of the theorem we have $\psi(\varepsilon, s, w) = 0$. On the other hand, the regularity of the boundary is not at all optimal; like for the Euler equations we guess that it must be analytic, see [8, 37].

Remark 4.5.3. It is known that for the Euler equations the bifurcation diagram of simply connected vortex patches is organized around Rankine vortices through a countable collection of pitchfork curves (one for each symmetry). Theorem 4.5.1 shows that locally this structure is preserved for any perturbation size of ε and therefore there is no symmetry breakdown. This is not the case however for the bifurcation diagram close to Kirchhoff’s ellipse, as discussed below in Section 4.6.

The proof of Theorem 4.5.1 is a consequence of the materials developed in next sections. Actually, the first part of Theorem 4.5.1 follows from Theorem 4.5.4, Proposition 4.5.7, and Proposition 4.5.9. However for the second part dealing with the stability of Eulerian branches under small perturbation on ε , we need to make use of Theorem 4.5.5.

4.5.2 Crandall-Rabinowitz's Theorem with a parameter

The main objective of this section is to formulate suitable conditions for the bifurcation from the trivial solutions of a general nonlinear equation of the type

$$F(\varepsilon, \lambda, x) = 0, \quad F : \mathbb{R} \times \mathbb{R} \times V \rightarrow Y$$

with Y a Banach space and V a neighborhood of 0 in some Banach space X . We assume that F is smooth enough and

$$\forall \lambda, F(0, \lambda, 0) = 0.$$

The starting point is that for $\varepsilon = 0$ we know the structure of the bifurcation diagram near the trivial solutions and it is of interest to understand how its geometric structure varies with respect to an arbitrary perturbation in ε . This is called an imperfect bifurcation. This subject is well developed in the literature starting with the pioneering work of Golubitsky and Schaeffer [28], who classify the bifurcation diagram in a general setting using tools from the theory of singularities. Various particular studies related to the present study have been carried out over the last few decades, and one may consult for instance [47, 65] and the references therein. In what follows we formulate some results dealing with imperfect bifurcations with symmetry persistence. This phenomenon occurs especially when the trivial solutions do not vary with respect to the parameter ε , that is

$$\forall \lambda, \forall \varepsilon, F(\varepsilon, \lambda, 0) = 0.$$

For the steadily-rotating vortex patch solutions of (4.1.1), these are precisely the suitable conditions enabling a detailed study of the bifurcations from the unit disc. Next we recall the classical theorem of Crandall-Rabinowitz [16] concerning bifurcations from trivial solutions. This will be applied to get the first part of Theorem 4.5.1 when ε is fixed at an arbitrary value.

Theorem 4.5.4. *Let X, Y be two Banach spaces, V be a neighborhood of 0 in X and let*

$$F : \mathbb{R} \times V \rightarrow Y$$

with the following properties:

1. $F(\lambda, 0) = 0$ for any $\lambda \in \mathbb{R}$.
2. The partial derivatives F_λ , F_x and $F_{\lambda x}$ exist and are continuous.
3. $\text{Ker}(\partial_x F(0, 0)) = \langle x_0 \rangle$ and $Y/R(\partial_x F(0, 0))$ are one-dimensional.
4. Transversality assumption: $\partial_\lambda \partial_x F(0, 0)x_0 \notin R(\partial_x F(0, 0))$.

If \mathcal{X} is any complement of $\text{Ker}(\partial_x F(0, 0))$ in X , then there is a neighborhood U of $(0, 0)$ in $\mathbb{R} \times X$, an interval $(-a, a)$, and continuous functions $\psi : (-a, a) \rightarrow \mathbb{R}$, $\phi : (-a, a) \rightarrow Z$ such that $\psi(0) = 0$, $\phi(0) = 0$ and

$$\{(\lambda, x) \in U, F(\lambda, x) = 0\} = \{(\psi(s), sx_0 + s\phi(s)) ; |s| < a\} \cup \{(\lambda, 0) ; (\lambda, 0) \in U\}.$$

The next result deals with a slight generalization of the preceding Crandall-Rabinowitz's theorem to include a parameter. This allows us to treat the stability of the bifurcation diagram under a small perturbation. This will be the cornerstone of the proof of the second part of Theorem 4.5.1.

Theorem 4.5.5. *Let X, Y be two Banach spaces, V a neighbourhood of 0 in X and let*

$$F : (-1, 1) \times \mathbb{R} \times V \rightarrow Y$$

be a function of class C^1 with the following properties:

1. $F(\varepsilon, \lambda, 0) = 0$ for any $\varepsilon \in \mathbb{R}$ and $\lambda \in \mathbb{R}$.

2. The partial derivatives F_ε , F_λ , F_x and $F_{\lambda x}$ exist and are continuous.
3. $\text{Ker}(\partial_x F(0, 0, 0)) = \langle x_0 \rangle$ and $Y/R(\partial_x F(0, 0, 0))$ are one-dimensional.
4. Transversality assumption: $\partial_\lambda \partial_x F(0, 0, 0)x_0 \notin R(\partial_x F(0, 0, 0))$.

If \mathcal{X} is any complement of $\text{Ker}(\partial_x F(0, 0, 0))$ in X , then there is a neighborhood U of $(0, 0, 0)$, an interval $(-a, a)$, with $a > 0$, and continuous functions

$$\psi : (-a, a)^2 \rightarrow \mathbb{R}, \quad \phi : (-a, a)^2 \rightarrow \mathcal{X}$$

such that $\varphi(0, 0) = 0$, $\psi(0, 0) = 0$ and

$$\left\{ (\varepsilon, \lambda, x) \in U, F(\varepsilon, \lambda, x) = 0 \right\} = \left\{ (\varepsilon, \psi(\varepsilon, s), sx_0 + s\phi(\varepsilon, s)) ; |\varepsilon|, |s| < a \right\} \cup \left\{ (\varepsilon, \lambda, 0) ; (\varepsilon, \lambda, 0) \in U \right\}.$$

Proof. The proof is a simple adaptation of [16]. Let $\langle w_0 \rangle$ be a complement of $\mathcal{Y} \triangleq \mathcal{R}(\partial_x F(0, 0, 0))$ in Y . Then

$$X = \langle x_0 \rangle \oplus \mathcal{X} \quad \text{and} \quad Y = \langle w_0 \rangle \oplus \mathcal{Y}.$$

Consider the projection $P : X \mapsto \langle x_0 \rangle$ on $\langle x_0 \rangle$ along \mathcal{X} given by

$$x = sx_0 + z, z \in \mathcal{X} \implies Px = sx_0$$

and similarly define the projection $Q : Y \mapsto \langle w_0 \rangle$ on $\langle w_0 \rangle$ along \mathcal{Y} . Then the equation $F(\varepsilon, \lambda, x) = 0$ is equivalent to the system

$$F_1(\varepsilon, \lambda, s, z) \triangleq (\text{Id} - Q)F(\varepsilon, \lambda, sx_0 + z) = 0 \quad \text{and} \quad QF(\varepsilon, \lambda, sx_0 + z) = 0.$$

It is clear that for some $\eta > 0$, the function

$$F_1 : (-1, 1) \times \mathbb{R} \times (-\eta, \eta) \times \mathcal{U} \rightarrow \mathcal{Y}_m$$

is C^1 with \mathcal{U} a small neighbourhood of 0 in \mathcal{X} . Moreover, it is not difficult to check that

$$\partial_z F_1(0, 0, 0, 0) = (\text{Id} - Q)\partial_x F(0, 0, 0) : \mathcal{X} \rightarrow \mathcal{Y}$$

is an isomorphism. By the implicit function theorem, the solutions of the equation $F_1(\varepsilon, \lambda, s, z) = 0$ are described near the point $(0, 0, 0, 0)$ by the parametrization $z = \varphi(\varepsilon, \lambda, s)$ with

$$\varphi : (-\delta, \delta)^3 \rightarrow \mathcal{X}, \quad \delta > 0$$

being a C^1 function. Therefore we obtain

$$(\text{Id} - Q)F(\varepsilon, \lambda, sx_0 + \varphi(\varepsilon, \lambda, s)) = 0, \forall |\varepsilon|, |\lambda|, |s| < \delta. \quad (4.5.1)$$

Consequently, solving the equation $F(\varepsilon, \lambda, x) = 0$ close to $(0, 0, 0)$ is equivalent to

$$F_2(\varepsilon, \lambda, s) \triangleq QF(\varepsilon, \lambda, sx_0 + \varphi(\varepsilon, \lambda, s)) = 0, \quad \forall |\varepsilon|, |\lambda|, |s| < \delta.$$

Using the assumption $F(\varepsilon, \lambda, 0) = 0$, for any $\varepsilon \in \mathbb{R}$ and $\lambda \in \mathbb{R}$, one deduces by uniqueness that

$$\varphi(\varepsilon, \lambda, 0) = 0, \quad \forall |\varepsilon|, |\lambda| < \delta. \quad (4.5.2)$$

Now differentiating equation (4.5.1) with respect to s we get

$$\partial_s \left((\text{Id} - Q)F(\varepsilon, \lambda, sx_0 + \varphi(\varepsilon, \lambda, s)) \right) = 0, \forall |\varepsilon|, |\lambda|, |s| < \delta.$$

In particular we deduce for $s = 0$

$$(\text{Id} - Q)\partial_x F(\varepsilon, \lambda, \varphi(\varepsilon, \lambda, 0))(x_0 + \partial_s \varphi(\varepsilon, \lambda, 0)) = 0,$$

which implies, in view of (4.5.2), that

$$\partial_x F(0, 0, 0)(\partial_s \varphi(0, 0, 0)) = 0.$$

This gives $\partial_s \varphi(0, 0, 0) \in \langle x_0 \rangle$, but from the definition one has $\partial_s \varphi(0, 0, 0) \in \mathcal{X}$ and consequently

$$\partial_s \varphi(0, 0, 0) = 0. \quad (4.5.3)$$

Hence there exists a continuous function $\varphi_1 : (-\delta, \delta)^3 \rightarrow \mathcal{X}$ such that

$$\varphi(\varepsilon, \lambda, s) = s\varphi_1(\varepsilon, \lambda, s) \text{ and } \varphi_1(0, 0, 0) = 0.$$

Set

$$g(\varepsilon, \lambda, s) \triangleq \begin{cases} QF(\varepsilon, \lambda, sx_0 + \varphi(\varepsilon, \lambda, s))/s, & s \neq 0 \\ Q\partial_x F(\varepsilon, \lambda, 0)[x_0 + \partial_s \varphi(\varepsilon, \lambda, 0)], & s = 0. \end{cases} \quad (4.5.4)$$

Note that g is continuous and

$$g(0, 0, 0) = Q\partial_x F(0, 0, 0)x_0 = 0.$$

Moreover, thanks to (4.5.2) one may easily check that

$$\partial_\lambda \varphi(\varepsilon, \lambda, 0) = 0, \forall |\varepsilon|, |\lambda| < \delta.$$

Consequently, the partial derivative $\partial_\lambda g$ exists, it is continuous and satisfies

$$\partial_\lambda g(0, 0, 0) = Q\partial_\lambda \partial_x F(0, 0, 0)x_0.$$

From the transversality assumption we find

$$\partial_\lambda g(0, 0, 0) \neq 0.$$

Hence we can use a weak version of the implicit function theorem, see Appendix A in [16], and thus find that the solutions of $g(\varepsilon, \lambda, s) = 0$ near the origin are parametrized by a C^1 surface $\psi : (-a, a)^2 \rightarrow \mathbb{R}$ such that $\lambda = \psi(\varepsilon, s)$ and

$$g(\varepsilon, \psi(\varepsilon, s), s) = 0, \forall |\varepsilon|, |s| < a, a > 0.$$

Therefore the non-trivial solutions of the equation $F(\varepsilon, \lambda, x) = 0$ near the origin are parametrized by

$$\lambda = \psi(\varepsilon, s), \quad x = sx_0 + s\varphi_1(\varepsilon, \psi(\varepsilon, s), s) \triangleq sx_0 + s\phi(\varepsilon, s), \quad \forall |s|, |\varepsilon| < a.$$

This completes the proof of the desired result. \square

4.5.3 Function spaces I

In this section we introduce the function spaces used below in studying the bifurcation from the unit disc. For $\alpha \in (0, 1)$, we set

$$X = \left\{ f \in C^{1+\alpha}(\mathbb{T}), \text{s.t. } \forall w \in \mathbb{T}, f(w) = \sum_{n=0}^{+\infty} f_n \bar{w}^n, f_n \in \mathbb{R} \right\}$$

and

$$Y = \left\{ g \in C^\alpha(\mathbb{T}), \text{s.t. } \forall w \in \mathbb{T}, g(w) = \sum_{n=1}^{+\infty} g_n e_n(w), g_n \in \mathbb{R} \right\}, \text{ with } e_n(w) = \text{Im}(w^n).$$

As discussed below, the m -fold symmetric vortex patch solutions are essentially arising from bifurcations in the more restrictive function spaces

$$X_m = \left\{ f \in X, \text{s.t. } \forall w \in \mathbb{T}, f(w) = \sum_{n=1}^{+\infty} f_{nm-1} \bar{w}^{nm-1} \right\}$$

and

$$Y_m = \left\{ g \in Y, \text{s.t. } \forall w \in \mathbb{T}, g(w) = \sum_{n=1}^{+\infty} g_n e_{nm}(w) \right\}.$$

Of course, the spaces X and X_m are equipped with the strong topology of $C^{1+\alpha}$ whereas Y and Y_m are equipped with the strong topology of C^α .

Next we recall the following lemma (see e.g. [37, 29]).

Lemma 4.5.6. *Let $\Delta = \{(w, w), w \in \mathbb{T}\}$ and let $K : \mathbb{T} \times \mathbb{T} \setminus \Delta \mapsto \mathbb{C}$ be a measurable function with the following properties. There exists $C > 0$ such that,*

$$|K(w, \tau)| \leq C, \quad \forall (w, \tau) \notin \Delta$$

and that for each $\tau \in \mathbb{T}$, the function $w \in \mathbb{T} \setminus \{\tau\} \mapsto K(w, \tau)$ is differentiable and

$$\left| \partial_w K(w, \tau) \right| \leq \frac{C}{|w - \tau|}.$$

Then the operator

$$T\varphi(w) = \int_{\mathbb{T}} K(w, \tau) \varphi(\tau) d\tau,$$

sends $C^\alpha(\mathbb{T})$ to $L^\infty(\mathbb{T})$ for any $\alpha \in (0, 1)$ with

$$\|T\varphi\|_\alpha \leq C_\alpha C \|\varphi\|_\infty, \quad \varphi \in L^\infty(\mathbb{T}),$$

where C_α depends only on α .

4.5.4 Regularity of the functional I

The main goal of this section is to study the regularity properties required by Theorem 4.5.4 and Theorem 4.5.5 for the functional G introduced in (4.4.6). Denote by B_r the ball of center Id and radius r in the space X and B_r^m the same ball in the space X_m .

Proposition 4.5.7. *There exists $r \in (0, 1)$ such that for any $\alpha \in (0, 1)$ the following holds true.*

1. $G : \mathbb{R} \times \mathbb{R} \times B_r \rightarrow Y$ is of class C^1 . It is at least of class C^3 .
2. The restriction $G : \mathbb{R} \times \mathbb{R} \times B_r^m \rightarrow Y_m$ is well-defined.

Proof. The proofs are classical and can be performed in a similar way to those of [29, 37], using Lemma 4.5.6 in particular. Some details will be given later in the subsection 4.6.3. Thus we only sketch the proof of the symmetry given in point (2). The spaces that used are described in subsection 4.5.3. Recall that

$$B_r^m = \{\Phi \in X_m, \|\Phi - \text{Id}\|_{C^{1+\alpha}(\mathbb{T})} \leq r\}, \quad \Phi(w) = w + \sum_{n=1}^{+\infty} f_{nm-1} \bar{w}^{nm-1}$$

and

$$G(\varepsilon, \Omega, \Phi) = \text{Im} \left\{ \left(\Omega \Phi(w) - I(\varepsilon, \Phi)(w) \right) \overline{\Phi'(w)} \bar{w} \right\}$$

with

$$I(\varepsilon, \Phi)(w) = \int_{\mathbb{T}} \Phi'(\tau) K_0(|\varepsilon| |\Phi(w) - \Phi(\tau)|) d\tau.$$

We begin by checking that $G(\varepsilon, \Omega, f)$ belongs to Y_m . It is enough for that purpose to prove that

$$G(\varepsilon, \Omega, \Phi)\left(e^{\frac{2i\pi}{m}} w\right) = G(\varepsilon, \Omega, \Phi)(w), \quad \forall w \in \mathbb{T}.$$

Note that

$$\Phi\left(e^{\frac{2i\pi}{m}} w\right) = e^{\frac{2i\pi}{m}} \Phi(w), \quad \Phi'\left(e^{\frac{2i\pi}{m}} w\right) = \Phi'(w) \tag{4.5.5}$$

and thus the property is obvious for the first term $\text{Im}\left\{\Omega \Phi(w) \overline{\Phi'(w)} \bar{w}\right\}$. For the last term of G , it is enough to check the identity,

$$I(\varepsilon, \Phi)\left(e^{\frac{2i\pi}{m}} w\right) = e^{\frac{2i\pi}{m}} I(\varepsilon, \Phi)(w), \quad \forall w \in \mathbb{T}.$$

This follows simply by making the change of variable $\tau = e^{\frac{2i\pi}{m}} \xi$:

$$\begin{aligned} I(\varepsilon, \Phi)\left(e^{\frac{2i\pi}{m}} w\right) &= \int_{\mathbb{T}} e^{\frac{2i\pi}{m}} \Phi'\left(e^{\frac{2i\pi}{m}} \tau\right) K_0\left(|\varepsilon| |\Phi\left(e^{\frac{2i\pi}{m}} w\right) - \Phi\left(e^{\frac{2i\pi}{m}} \tau\right)|\right) d\tau \\ &= e^{\frac{2i\pi}{m}} \int_{\mathbb{T}} \Phi'(\tau) K_0\left(|\varepsilon| |\Phi(w) - \Phi(\tau)|\right) d\tau \\ &= e^{\frac{2i\pi}{m}} I(\varepsilon, \Phi)(w). \end{aligned}$$

This ends the proof. \square

4.5.5 Spectral study

In this section we compute the linearized operator at the trivial solution of the functional G introduced in (4.4.6). We prove that it acts as a Fourier multiplier with symbol related to modified Bessel functions. This allows us to describe the full range of Ω corresponding to non-trivial kernels. Finally, we check that for these values of Ω all the assumptions of Crandall-Rabinowitz's theorem are satisfied.

Structure of the linearized operator

We prove the following result.

Proposition 4.5.8. *Let $h : w \mapsto \sum_{n=0}^{+\infty} a_n \bar{w}^n \in X$, then*

$$D_f G(\varepsilon, \Omega, \text{Id})(h)(w) = \sum_{n=0}^{+\infty} a_n (n+1) (\Omega_{n+1}(\varepsilon) - \Omega) e_{n+1}(w), \quad \text{with } e_n(w) = \text{Im}(w^n)$$

and

$$\Omega_m(\varepsilon) = I_1(|\varepsilon|) K_1(|\varepsilon|) - I_m(|\varepsilon|) K_m(|\varepsilon|).$$

Proof. Without loss of generality, we may assume that $\varepsilon > 0$. Now, for given $h \in X$, one may deduce from straightforward computations that

$$D_f G(\varepsilon, \Omega, \text{Id})(h)(w) = \mathcal{L}_0(h)(w) + \mathcal{L}_1(h)(w) + \mathcal{L}_2(h)(w) \tag{4.5.6}$$

with

$$\mathcal{L}_0(h)(w) = \Omega \text{Im} \left\{ h(w) \bar{w} + \overline{h'(w)} \right\},$$

$$\mathcal{L}_1(h)(w) = \operatorname{Im} \left\{ -\overline{h'(w)} \overline{w} \int_{\mathbb{T}} K_0(\varepsilon|w-\tau|) d\tau - \overline{w} \int_{\mathbb{T}} h'(\tau) K_0(\varepsilon|w-\tau|) d\tau \right\}$$

and

$$\mathcal{L}_2(h)(w) = \varepsilon \operatorname{Im} \left\{ -\overline{w} \int_{\mathbb{T}} \frac{\operatorname{Re}((h(w) - h(\tau))(\overline{w} - \bar{\tau}))}{|w - \tau|} K'_0(\varepsilon|w - \tau|) d\tau \right\}.$$

We begin with the easier term $\mathcal{L}_0(h)(w)$ whose computation is straightforward:

$$\mathcal{L}_0(h)(w) = - \sum_{n=0}^{+\infty} a_n \Omega(n+1) e_{n+1}. \quad (4.5.7)$$

For $\mathcal{L}_1(h)$ we first use the change of variable $\tau \mapsto w\tau$

$$\mathcal{L}_1(h)(w) = \operatorname{Im} \left\{ -\overline{h'(w)} \int_{\mathbb{T}} K_0(\varepsilon|1 - \tau|) d\tau - \int_{\mathbb{T}} h'(\tau w) K_0(\varepsilon|1 - \tau|) d\tau \right\}$$

which implies that

$$\mathcal{L}_1(h)(w) = - \sum_{n=1}^{+\infty} n a_n \left[\int_{\mathbb{T}} K_0(\varepsilon|1 - \tau|) (\bar{\tau}^{n+1} - 1) d\tau \right] e_{n+1}.$$

We focus on the integral term involving in $\mathcal{L}_1(h)(w)$. By symmetry arguments we obtain

$$\begin{aligned} \int_{\mathbb{T}} K_0(\varepsilon|1 - \tau|) (\bar{\tau}^{n+1} - 1) d\tau &= \frac{1}{2\pi} \int_0^{2\pi} K_0(2\varepsilon \sin(\theta/2)) (\cos(n\theta) - \cos\theta) d\theta \\ &= \frac{2}{\pi} \int_0^{\frac{\pi}{2}} K_0(2\varepsilon \sin\theta) (\cos(2n\theta) - \cos(2\theta)) d\theta \\ &= \frac{2}{\pi} \int_0^{\frac{\pi}{2}} K_0(2\varepsilon \cos\theta) ((-1)^n \cos(2n\theta) + \cos(2\theta)) d\theta. \end{aligned}$$

Using (4.4.4) we deduce that

$$\int_{\mathbb{T}} K_0(\varepsilon|1 - \tau|) (\bar{\tau}^{n+1} - 1) d\tau = I_n(\varepsilon) K_n(\varepsilon) - I_1(\varepsilon) K_1(\varepsilon).$$

Therefore

$$\mathcal{L}_1(h)(w) = \sum_{n=1}^{+\infty} n a_n (I_1(\varepsilon) K_1(\varepsilon) - I_n(\varepsilon) K_n(\varepsilon)) e_{n+1}. \quad (4.5.8)$$

For the computation of $\mathcal{L}_2(h)(w)$, we write

$$\mathcal{L}_2(h)(w) = - \sum_{n=1}^{+\infty} \frac{\varepsilon a_n}{2} \left(\int_{\mathbb{T}} \left[\frac{(\tau^n - 1)(\tau - 1)}{|1 - \tau|} - \frac{(\bar{\tau}^n - 1)(\bar{\tau} - 1)}{|1 - \tau|} \right] K'_0(\varepsilon|1 - \tau|) d\tau \right) e_{n+1}.$$

Now we compute the following integral term which is more delicate

$$d_n \triangleq \frac{\varepsilon}{2} \int_{\mathbb{T}} \left[\frac{(\tau^n - 1)(\tau - 1)}{|1 - \tau|} - \frac{(\bar{\tau}^n - 1)(\bar{\tau} - 1)}{|1 - \tau|} \right] K'_0(\varepsilon|1 - \tau|) d\tau.$$

First we use the following trigonometric identity: for $\tau = e^{i\theta}, \theta \in [0, 2\pi]$, one has

$$\operatorname{Re} \left\{ \left(\frac{(\tau^n - 1)(\tau - 1)}{|1 - \tau|} - \frac{(\bar{\tau}^n - 1)(\bar{\tau} - 1)}{|1 - \tau|} \right) \frac{d\tau}{2i\pi} \right\} = \frac{1}{\pi} \cos(\theta/2) \left(\sin\theta + \sin(n\theta) - \sin((n+1)\theta) \right) d\theta.$$

Thus integration by parts yields

$$\begin{aligned} d_n &= \frac{1}{2\pi} \int_0^{2\pi} (\varepsilon \cos(\theta/2)) K'_0(2\varepsilon \sin(\theta/2)) (\sin \theta + \sin(n\theta) - \sin((n+1)\theta)) d\theta \\ &= -\frac{1}{2\pi} \int_0^{2\pi} K_0(2\varepsilon \sin(\theta/2)) (\cos \theta + n \cos(n\theta) - (n+1) \cos((n+1)\theta)) d\theta. \end{aligned}$$

Performing a change of variables and invoking symmetry arguments imply

$$\begin{aligned} d_n &= -\frac{2}{\pi} \int_0^{\frac{\pi}{2}} K_0(2\varepsilon \sin(\theta)) (\cos(2\theta) + n \cos(2n\theta) - (n+1) \cos(2(n+1)\theta)) d\theta \\ &= \frac{2}{\pi} \int_0^{\frac{\pi}{2}} K_0(2\varepsilon \cos(\theta)) (\cos(2\theta) - n(-1)^n \cos(2n\theta) - (n+1)(-1)^n \cos(2(n+1)\theta)) d\theta. \end{aligned}$$

Using (4.4.4) we obtain

$$d_n = -I_1(\varepsilon)K_1(\varepsilon) - nI_n(\varepsilon)K_n(\varepsilon) + (n+1)I_{n+1}(\varepsilon)K_{n+1}(\varepsilon). \quad (4.5.9)$$

Combined with (4.5.8) we find that

$$\mathcal{L}_1(h)(w) + \mathcal{L}_2(h)(w) = \sum_{n=0}^{+\infty} (n+1)a_n (I_1(\varepsilon)K_1(\varepsilon) - I_{n+1}(\varepsilon)K_{n+1}(\varepsilon)) e_{n+1}.$$

Putting together this identity with (4.5.7) gives the desired result. \square

Bifurcation assumptions

Next we check the assumptions on the linearized operator required by Theorem 4.5.4 and Theorem 4.5.5. For this purpose, we introduce the countable dispersion set

$$\mathbb{S} = \left\{ \Omega_m(\varepsilon) \triangleq I_1(|\varepsilon|)K_1(|\varepsilon|) - I_m(|\varepsilon|)K_m(|\varepsilon|), \quad m \geq 1 \right\}. \quad (4.5.10)$$

The main result reads as follows.

Proposition 4.5.9. *Let $\varepsilon \in \mathbb{R}$ be a fixed real number and G be the functional defined in (4.4.6); note that some of its properties are detailed in Proposition 4.5.7. Then the following assertions hold.*

1. *The sequence $m \mapsto \Omega_m(\varepsilon)$ is strictly increasing and converges to $I_1(|\varepsilon|)K_1(|\varepsilon|)$.*
2. *The kernel of $D_f G(\varepsilon, \Omega, \text{Id})$ is non-trivial if and only if $\Omega = \Omega_m(\varepsilon) \in \mathbb{S}$. In this case, it is one-dimensional and generated by*

$$v_m : w \in \mathbb{T} \mapsto \overline{w}^{m-1}.$$

3. *The range of $D_f G(\varepsilon, \Omega_m(\varepsilon), \text{Id})$ is closed in Y and is of co-dimension one. It is given by*

$$\mathcal{R}(D_f G(\varepsilon, \Omega_m(\varepsilon), \text{Id})) = \left\{ g \in C^\alpha(\mathbb{T}), g = \sum_{\substack{n=1 \\ n \neq m}}^{+\infty} g_n e_n, g_n \in \mathbb{R} \right\}.$$

4. *Transversality assumption:*

$$\partial_\Omega D_f G(\varepsilon, \Omega_m, \text{Id}) v_m \notin \mathcal{R}(D_f G(\varepsilon, \Omega_m, \text{Id})).$$

Proof. (1) We use the following inequality (see [64]). For $\nu \geq 0$ and $x > 0$

$$\frac{I_{\nu+\frac{1}{2}}(x)}{I_{\nu-\frac{1}{2}}(x)} < \frac{x}{\nu + \sqrt{\nu^2 + x^2}} \leq \frac{K_{\nu-\frac{1}{2}}(x)}{K_{\nu+\frac{1}{2}}(x)}. \quad (4.5.11)$$

Thus using the positivity of I_n and K_n mentioned in (4.4.2), we find that the sequence $n \mapsto I_n(|\varepsilon|)K_n(|\varepsilon|)$ is strictly decreasing. It remains to check that $\lim_{n \rightarrow \infty} I_n(|\varepsilon|)K_n(|\varepsilon|) = 0$. For this, we establish a precise result on the convergence rate used below: there exists $C > 0$ such that for any real number ε ,

$$\forall n \in \mathbb{N}^*, \quad 0 < I_n(|\varepsilon|)K_n(|\varepsilon|) \leq C \frac{\ln(n+1)}{n}. \quad (4.5.12)$$

Indeed, using integration by parts in (4.4.4) we find

$$I_n(|\varepsilon|)K_n(|\varepsilon|) = -\frac{2(-1)^n \varepsilon}{\pi n} \int_0^{\frac{\pi}{2}} \sin \theta K_1(2|\varepsilon| \cos \theta) \sin(2n\theta) d\theta.$$

Thus

$$0 < I_n(|\varepsilon|)K_n(|\varepsilon|) \leq \frac{2|\varepsilon|}{\pi n} \int_0^{\frac{\pi}{2}} |\sin \theta| K_1(2|\varepsilon| \cos \theta) |\sin(2n\theta)| d\theta.$$

On the other hand using (4.4.3) we deduce by the change of variable $\theta = \cosh t$ that for $x > 0$

$$\begin{aligned} K_1(x) &= \int_1^{+\infty} e^{-x\theta} \frac{\theta}{\sqrt{\theta^2 + 1}} d\theta \\ &= \int_1^2 e^{-x\theta} \frac{\theta}{\sqrt{\theta^2 + 1}} d\theta + \int_2^{+\infty} e^{-x\theta} \frac{\theta}{\sqrt{\theta^2 + 1}} d\theta \\ &\leq e^{-x} + \int_2^{+\infty} e^{-x\theta} d\theta \\ &\leq e^{-x} + \frac{1}{x} e^{-2x}. \end{aligned}$$

Consequently there exists $C > 0$ such that for any $x > 0$,

$$K_1(x) \leq \frac{C}{x}$$

which implies after straightforward computations related to Dirichlet kernel,

$$\begin{aligned} \forall n \in \mathbb{N}^*, \quad I_n(\varepsilon)K_n(\varepsilon) &\leq \frac{C}{n} \int_0^{\frac{\pi}{2}} \frac{|\sin(2n\theta)|}{\cos \theta} d\theta \\ &\leq \frac{C}{n} \int_0^{\frac{\pi}{2}} \frac{|\sin(2n\theta)|}{\sin \theta} d\theta \\ &\leq C \frac{\ln(n+1)}{n}. \end{aligned}$$

(2) The result follows from the structure of the linearized operator stated in Proposition 4.5.8 and the strict monotonicity of the eigenvalues $(\Omega_m(\varepsilon))_{m \geq 1}$.

(3) We want to prove that for any $m \geq 1$ the range of $D_f G(\varepsilon, \Omega_m(\varepsilon), \text{Id})$ coincides with

$$Z_m \triangleq \left\{ g \in C^\alpha(\mathbb{T}), g(w) = \sum_{n=1}^{+\infty} g_n e_n, g_n \in \mathbb{R} \right\}.$$

As Z_m is closed in Y and of co-dimension one, it is enough to check that the range is Z_m . First, it is obvious that

$$\mathcal{R}(D_f G(\varepsilon, \Omega_m(\varepsilon), \text{Id}) \subset Z_m$$

and it thus remains to check the reverse inclusion. Let $g = \sum_{n \geq 1} g_n e_n \in Z_m$; we want to find $h \in X$ such that

$$D_f G(\varepsilon, \Omega_m(\varepsilon), \text{Id})(h) = g.$$

Set $h(w) = \sum_{n \geq 0} h_n \bar{w}^n$, then the equation

$$D_f G(\varepsilon, \Omega_m(\varepsilon), \text{Id})h = g$$

admits an explicit solution such that

$$h_n = \frac{g_{n+1}}{(n+1)(\Omega_{n+1}(\varepsilon) - \Omega_m(\varepsilon))}, \quad n \neq m-1$$

and

$$h_{m-1} = 0.$$

We next check that $h \in C^{1+\alpha}(\mathbb{T})$. Since

$$h(w) = \sum_{\substack{n \neq m-1 \\ n \geq 0}} \frac{g_{n+1}}{(n+1)(\Omega_{n+1}(\varepsilon) - \Omega_m(\varepsilon))} \bar{w}^n$$

then it follows from Cauchy-Schwarz inequality and the Bessel identity that

$$\begin{aligned} \|h\|_{L^\infty(\mathbb{T})} &\leq C_0 \sum_{n \geq 1} \frac{|g_{n+1}|}{n+1} \\ &\leq C \|g\|_{L^2(\mathbb{T})} \\ &\leq C \|g\|_{C^\alpha(\mathbb{T})} \end{aligned}$$

where C_0 is the inverse of the distance between $\Omega_m(\varepsilon)$ and $\mathbb{S} \setminus \{\Omega_m(\varepsilon)\}$. C_0 is finite due to the monotonicity of the eigenvalues. We now prove that the derivative h' belongs to C^α . It is obvious that

$$h'(w) = \sum_{\substack{n \neq m-1 \\ n=1}}^{+\infty} \frac{n g_{n+1}}{(n+1)(\Omega_m(\varepsilon) - \Omega_{n+1}(\varepsilon))} \bar{w}^{n+1},$$

which can be split as follows

$$\begin{aligned} h'(w) &= \sum_{\substack{n \neq m \\ n=2}}^{+\infty} \frac{g_n}{\Omega_m(\varepsilon) - \Omega_n(\varepsilon)} \bar{w}^n + \sum_{\substack{n \neq m \\ n=2}}^{+\infty} \frac{g_n}{n(\Omega_n(\varepsilon) - \Omega_m(\varepsilon))} \bar{w}^n \\ &= - \sum_{\substack{n \neq m \\ n=2}}^{+\infty} \frac{g_n}{K_m(\varepsilon) I_m(\varepsilon)} \bar{w}^n - \sum_{\substack{n \neq m \\ n=2}}^{+\infty} g_n \left[\frac{1}{\Omega_n(\varepsilon) - \Omega_m(\varepsilon)} - \frac{1}{K_m(|\varepsilon|) I_m(|\varepsilon|)} \right] \bar{w}^n \\ &\quad + \sum_{\substack{n \neq m \\ n=2}}^{+\infty} \frac{g_n}{n K_m(|\varepsilon|) I_m(|\varepsilon|)} \bar{w}^n + \sum_{\substack{n \neq m \\ n=2}}^{+\infty} \frac{g_n}{n} \left[\frac{1}{\Omega_n(\varepsilon) - \Omega_m(\varepsilon)} - \frac{1}{K_m(|\varepsilon|) I_m(|\varepsilon|)} \right] \bar{w}^n. \end{aligned}$$

Set

$$\chi(w) = \sum_{\substack{n \neq m \\ n=2}}^{+\infty} g_n \bar{w}^n, \quad H_1(w) = \sum_{\substack{n \neq m \\ n=2}}^{+\infty} \left[\frac{1}{\Omega_n(\varepsilon) - \Omega_m(\varepsilon)} - \frac{1}{K_m(|\varepsilon|) I_m(|\varepsilon|)} \right] \bar{w}^n, \quad H_2(w) = \sum_{\substack{n \neq m \\ n=2}}^{+\infty} \frac{\bar{w}^n}{n}$$

and

$$H_3(w) = \sum_{\substack{n \neq m \\ n=2}}^{+\infty} \frac{1}{n} \left[\frac{1}{\Omega_n(\varepsilon) - \Omega_m(\varepsilon)} - \frac{1}{K_m(|\varepsilon|) I_m(|\varepsilon|)} \right] \bar{w}^n.$$

Then

$$h'(w) = -\frac{1}{K_m(|\varepsilon|) I_m(|\varepsilon|)} \chi(w) - \chi * H_1(w) + \frac{1}{K_m(|\varepsilon|) I_m(|\varepsilon|)} \chi * H_2(w) + \chi * H_3(w).$$

As $\chi(w) = \Pi_+(2ig(w)) - 2ig(w)$, with Π_+ being the Szegö projection that sends continuously $C^\alpha(\mathbb{T})$ to itself, we deduce that $\chi \in C^\alpha(\mathbb{T})$. Hence in order to ensure $h' \in C^\alpha(\mathbb{T})$ it is enough to prove that $H_j \in L^1(\mathbb{T})$, $j \in \{1, 2, 3\}$. Let us start with H_1 . It is obvious that

$$\left| \frac{1}{\Omega_n(\varepsilon) - \Omega_m(\varepsilon)} - \frac{1}{K_m(|\varepsilon|) I_m(|\varepsilon|)} \right| = \left| \frac{K_n(|\varepsilon|) I_n(|\varepsilon|)}{K_m(|\varepsilon|) I_m(|\varepsilon|) (K_m(|\varepsilon|) I_m(l\varepsilon) - K_n(|\varepsilon|) I_n(|\varepsilon|)))} \right|.$$

Hence using (4.5.12) we find a constant C depending on m and ε such that for any $n \neq m$

$$\begin{aligned} \left| \frac{1}{\Omega_n(\varepsilon) - \Omega_m(\varepsilon)} - \frac{1}{K_m(|\varepsilon|) I_m(|\varepsilon|)} \right| &\leq C K_n(|\varepsilon|) I_n(|\varepsilon|) \\ &\leq C \frac{\ln(n+1)}{n}. \end{aligned}$$

According to the Parseval identity, this proves that $H_1 \in L^2(\mathbb{T})$ and by the usual embedding we find $H_1 \in L^1(\mathbb{T})$. It is simple to check that H_2, H_3 belong to $L^2(\mathbb{T})$ and so to $L^1(\mathbb{T})$ which completes the desired result.

(4) For the transversality assumption, it is obvious that for any $h \in X$

$$\partial_\Omega D_f G(\varepsilon, \Omega_m(\varepsilon), \text{Id}) h = \text{Im} \left\{ h(w) \bar{w} + \overline{h'(w)} \right\}.$$

Therefore, for $v_m(w) = \bar{w}^{m-1}$

$$\partial_\Omega D_f G(\varepsilon, \Omega_m(\varepsilon), \text{Id}) v_m = -m e_m \notin \mathcal{R}(D_f G(\varepsilon, \Omega_m(\varepsilon), \text{Id}))$$

and consequently the transversality condition is verified. □

4.6 Imperfect bifurcation close to the branch of Kirchhoff ellipses

This section is devoted to the study of the global structure of the two-fold branch. According to Theorem 4.5.1 we know there exists a local branch close to Rankine vortices that bifurcates at the point $\Omega_2(\varepsilon)$. For $\varepsilon = 0$ the full branch is explicitly described by Kirchhoff ellipses, and according to [8, 34, 41, 49] we known that from this branch a countable family of bifurcating curves emerges at the Love instability points [48]. Notice that these new curves model alternating one/two-fold V-states and the two-fold V-states are characterized by an odd frequency perturbation of the conformal mapping of the ellipse $w \in \mathbb{T} \mapsto w + Q\bar{w}$.

We investigate below the ‘imperfect’ bifurcation, that is, the behavior of the solution branch structure subject to a small perturbation in ε . We prove that the scenarios of persistence/breakdown symmetry occur

simultaneously close to the Kirchhoff ellipse branch. Indeed, we prove by using perturbation theory, see Theorem 4.6.3, that far from the second bifurcating point the local structure of the two-fold branch persists and varies continuously with respect to a small perturbation in ε . However around the singularity set the issue depends on the symmetry of the V-states. In fact, we show in Theorem 4.6.3 that the diagram structure around the one-fold bifurcating curves is not destroyed and is similar to the Euler one. However, and this is only proved for the $m = 4$ Love instability point, the symmetry is broken down around the first bifurcating curve of the two-fold V-states (see Theorem 4.6.5). This is a kind of resonance phenomenon between the two branches with the same symmetry leading to a separation of the singularity and a loss of the connectedness. Numerically, in Section 4.3 this behavior is observed for the first two-fold branches emerging from the ellipse, but from an analytical standpoint the problem is difficult due to the cumbersome computations required for higher elliptical azimuthal wavenumbers.

4.6.1 Function spaces II

We first introduce the function spaces suitable for studying the bifurcation from the two-fold branch. We draw attention to the fact that we use the same notation as in the Section 4.5 dealing with the m -folds structure but with a different meaning. For $\alpha \in (0, 1)$, we set

$$X = \left\{ f \in C^{1+\alpha}(\mathbb{T}), f(w) = \sum_{n=2}^{+\infty} f_n w^n, f_n \in \mathbb{R} \right\} \quad (4.6.1)$$

and

$$Y = \left\{ g \in C^\alpha(\mathbb{T}), g(w) = \sum_{n=1}^{+\infty} g_n e_n(w), g_n \in \mathbb{R} \right\}, \text{ with } e_n(w) = \operatorname{Im}(w^n). \quad (4.6.2)$$

4.6.2 Summary of the bifurcations from Kirchhoff ellipses

The results of this section were obtained in [34] and for the commodity of the presentation we briefly recall them. Since ellipses are explicit rotating solutions for the Euler equations, then from [34] one finds that

$$G(0, \frac{1-Q^2}{4}, \alpha_Q) = 0, \quad \forall Q \in (0, 1)$$

with $\alpha_Q: w \in \mathbb{T} \mapsto w + Q\bar{w}$ being the conformal parametrization of the ellipse centered at the origin and with semi-axes $1 \pm Q$ and $Q \in [0, 1)$. Notice that Kirchhoff discovered that such ellipses rotate at the angular velocity $\frac{1-Q^2}{4}$. Introducing

$$F(\varepsilon, Q, f) = G\left(\varepsilon, \frac{1-Q^2}{4}, \alpha_Q + f\right), \quad f \in X \quad (4.6.3)$$

where the space X is described in (4.6.1), it is plain that

$$F(0, Q, 0) = 0, \quad \forall Q \in [0, 1).$$

From (4.4.7) one obtains

$$\mathcal{L}_Q \triangleq D_f F(0, Q, 0) = -D_f G_E\left(\frac{1-Q^2}{2}, \alpha_Q\right). \quad (4.6.4)$$

Let $m \geq 3$ be an integer and denote by Q_m the unique solution in $[0, 1)$ of the equation

$$1 + Q^m - \frac{1-Q^2}{2} m = 0, \quad (4.6.5)$$

and set

$$\mathcal{S} \triangleq \{Q_m, m \geq 3\}.$$

At various points in the argument, we need to distinguish between the following two subsets of \mathcal{S} :

$$\mathcal{S}_{\text{reso}} \triangleq \{Q_{2m}, m \geq 2\} \quad \text{and} \quad \mathcal{S}_{\text{Nreso}} \triangleq \{Q_{2m+1}, m \geq 1\}. \quad (4.6.6)$$

The first one is called the ‘resonant set’ and the second is the ‘non-resonant set’. Note that from [34] we know that the sequence $(Q_m)_{m \geq 3}$ is strictly increasing with

$$\lim_{m \rightarrow +\infty} Q_m = 1.$$

The following result dealing with the structure of the linearized operator \mathcal{L}_Q was proved in [34]. This was used to prove the existence of bifurcations from Kirchhoff ellipses using the Crandall-Rabinowitz theorem.

Proposition 4.6.1. *Let X and Y be the spaces introduced in (4.6.1) and (4.6.2). Then the following assertions hold true.*

1. Let $h(w) = \sum_{n \geq 2} a_n w^n \in X$, then

$$\mathcal{L}_Q h = \frac{1}{2} \sum_{n \geq 1} g_{n+1} e_n; \quad e_n(w) = \text{Im}(w^n),$$

with

$$\begin{aligned} g_2 &= \frac{1}{2}(1+Q)^2 a_2, \\ g_3 &= 2Q^2 a_3, \\ g_{n+1} &= \left(1+Q^n - \frac{1-Q^2}{2} n\right)(a_{n+1} - Q a_{n-1}), \quad \forall n \geq 3. \end{aligned}$$

2. The kernel of \mathcal{L}_Q is non-trivial if and only if $Q = Q_m \in \mathcal{S}$ and it is a one-dimensional vector space generated by

$$v_m(w) = \frac{w^{m+1}}{1-Qw^2}.$$

3. The range of \mathcal{L}_Q is of co-dimension one in Y and it is given by

$$R(\mathcal{L}_Q) = \left\{ g \in C^\alpha(\mathbb{T}), g = \sum_{\substack{n \geq 1 \\ n \neq m}} g_{n+1} e_n, \quad g_n \in \mathbb{R} \right\}.$$

4. Transversality assumption: for any $Q = Q_m \in \mathcal{S}$,

$$\partial_Q \mathcal{L}_Q v_m \notin R(\mathcal{L}_Q).$$

4.6.3 Regularity of the functional II

The main goal of this section is to study the regularity properties required by Theorem 4.5.4 for the functional F introduced in (4.6.3).

Proposition 4.6.2. *Let $\alpha \in (0, 1)$, $\mu \in (0, 1)$ and set $r_\mu = \frac{1-\mu}{2}$. Then we have*

$$\begin{array}{ccc} F : (-1, 1) \times (0, \mu) \times B_{r_\mu} & \longrightarrow & Y \\ (\varepsilon, Q, f) & \longmapsto & F(\varepsilon, \Omega, f) \end{array}$$

is well-defined and of class C^1 , and $\partial_Q \partial_f F$ exists and is continuous on $(-1, 1) \times (0, \mu) \times B_{r_\mu}$, where $B_{r_\mu} = \{f \in X, \|f\|_{C^{1+\alpha}} \leq r_\mu\}$. Moreover for any $i, j \in \mathbb{N}, i+j \leq 3$ the function $\partial_Q^i \partial_f^j F(\varepsilon, ., .)$ is continuous.

Proof. We only sketch the basic steps of the proof which closely parallels the proof developed in [34]. For more details we refer the reader to this reference. First, we write

$$\begin{aligned} F(\varepsilon, Q, f(w)) &= \operatorname{Im} \left\{ \frac{1-Q^2}{4} \left(1 + Q\bar{w}^2 + \bar{w}f(w) \right) \left(1 - Qw^2 + \overline{f'(w)} \right) \right. \\ &\quad \left. - \overline{\Phi'(w)}\bar{w} \int_{\mathbb{T}} \Phi'(\tau) K_0^\varepsilon(|\Phi(w) - \Phi(\tau)|) d\tau \right\} \end{aligned}$$

with the notation $\Phi(w) = \alpha_q(w) + f(w)$ and

$$K_0^\varepsilon(x) = K_0(|\varepsilon|x) + \log\left(\frac{|\varepsilon|}{2}\right).$$

Since C^α is an algebra, $f \in C^{1+\alpha}$ and $f' \in C^\alpha$, then the first function

$$w \in \mathbb{T} \mapsto \frac{1-Q^2}{4} \operatorname{Im} \left\{ [1 + Q\bar{w}^2 + \bar{w}f(w)][1 - Qw^2 + \overline{f'(w)}] \right\}$$

belongs to C^α and its Fourier coefficients are all real; therefore, it belongs to the space Y . The C^1 regularity with respect to (Q, f) is elementary and was discussed in [34]. For the second term, using the results in subsection 4.4.2, one may write

$$K_0^\varepsilon(x) = -\log(x) - \left(\log\left(\frac{|\varepsilon|}{2}\right) + \log(x) \right) \frac{\varepsilon^2 x^2}{4} \mathcal{K}_1(\varepsilon^2 x^2) + \mathcal{K}_2(\varepsilon^2 x^2) \quad (4.6.7)$$

where

$$\mathcal{K}_1(z) = \sum_{m=1}^{+\infty} \frac{\left(\frac{z}{4}\right)^{m-1}}{(m!)^2}$$

and

$$\mathcal{K}_2(z) = \sum_{m=0}^{+\infty} \left(\frac{z}{4}\right)^m \frac{\psi(m+1)}{(m!)^2}.$$

Consequently,

$$-\int_{\mathbb{T}} \Phi'(\tau) K_0^\varepsilon(|\Phi(w) - \Phi(\tau)|) d\tau = T_0 \Phi'(w) + T_1 \Phi'(w) + T_2 \Phi'(w)$$

where

$$T_0 \varphi(w) = \int_{\mathbb{T}} \log(|\Phi(w) - \Phi(\tau)|) \varphi(\tau) d\tau,$$

$$T_1 \varphi(w) \triangleq \int_{\mathbb{T}} \widehat{K}_1(\tau, w, \varepsilon) \varphi(\tau) d\tau$$

and

$$T_2 \varphi(w) \triangleq -\int_{\mathbb{T}} \mathcal{K}_2(\varepsilon^2 |\Phi(w) - \Phi(\tau)|^2) \varphi(\tau) d\tau$$

with

$$\widehat{K}_1(\tau, w, \varepsilon) \triangleq \frac{\varepsilon^2}{4} \left(\log\left(\frac{|\varepsilon|}{2}\right) + \log(|\Phi(w) - \Phi(\tau)|) \right) |\Phi(w) - \Phi(\tau)|^2 \mathcal{K}_1(\varepsilon^2 |\Phi(w) - \Phi(\tau)|^2)$$

Moreover, we have seen in (4.4.8) that

$$T_0 \Phi'(w) = \overline{\widehat{T}_0 \Phi'(w)}$$

with

$$\widehat{T}_0 \varphi(w) = -\frac{1}{2} \int_{\mathbb{T}} \frac{\overline{\Phi(w)} - \overline{\Phi(\tau)}}{\Phi(w) - \Phi(\tau)} \varphi(\tau) d\tau.$$

Let $Q \in (0, \mu)$ and take $r_\mu = \frac{1-\mu}{2}$. By the mean value theorem, there exists a constant C_μ such that for all $f \in B_{r_\mu}$

$$\frac{1-\mu}{2} |\tau - w| \leq |\Phi(w) - \Phi(\tau)| \leq C_\mu |\tau - w|, \quad \forall \tau, w \in \mathbb{T}.$$

In addition, we may easily check that the kernel $K(\tau, w) = \frac{\overline{\Phi(w)} - \overline{\Phi(\tau)}}{\Phi(w) - \Phi(\tau)}$ satisfies the assumptions of Lemma 4.5.6 and thus

$$\|T_0\Phi'\|_{C^\alpha(\mathbb{T})} \leq C \|\Phi'\|_{L^\infty} \leq C_0.$$

Note that according to [34] we also have that $(\varepsilon, Q, f) \mapsto T_0\Phi'$ is of class C^1 from $(-1, 1) \times (0, \mu) \times B_{r_\mu}$ to $C^\alpha(\mathbb{T})$. As for T_2 , the kernel is not singular and one may easily check that

$$|\widehat{K}_1(\tau, w, \varepsilon)| + |\partial_w \widehat{K}_1(\tau, w, \varepsilon)| \leq C_0, \quad \forall \tau, w \in \mathbb{T}.$$

Consequently we may use once again Lemma 4.5.6 and deduce that $(\varepsilon, Q, f) \mapsto T_1\Phi'$ is well-defined. Moreover the Fourier coefficients of $T_1\Phi'$ are real which follows from the general fact

$$\overline{T_1\varphi(w)} = T_1\varphi(\bar{w}), \quad \forall \varphi \in X, \forall w \in \mathbb{T}.$$

By straightforward arguments we can also prove that $(\varepsilon, Q, f) \mapsto T_1\Phi'$ is of class C^1 . Observe that the regularity with respect to ε comes in particular from the fact that the function $\varepsilon \in (-1, 1) \mapsto \varepsilon^2 \log \varepsilon$ is C^1 . The same analysis can be implemented for the last term $T_2\Phi'$ and this concludes the C^1 regularity of $(\varepsilon, Q, f) \mapsto F(\varepsilon, Q, f)$. Concerning the existence and the regularity of $\partial_Q \partial_f F$ it can be proved similarly to the case $\varepsilon = 0$ discussed in [34]. \square

4.6.4 Bifurcation diagram far from the resonant set

The main goal of this section is study the structure of the bifurcation diagram far from the resonant set S_{reso} defined in (4.6.6). We prove its persistence for small perturbations. This is done in two different subsections. First we prove the stability of the Kirchhoff ellipse branch under small perturbations, leading to the existence of a two-fold branch for (4.1.1) living close to the ellipse branch. Second we explore the bifurcation of one-fold curves from the two-fold branch close to the non-resonant set. This proves the persistence of the bifurcation diagram of the Euler equations under small perturbations in ε but far from the resonant set.

Structure of the two-fold curve

The aim in this subsection is to construct two-fold V-states close to Kirchhoff ellipses \mathcal{E}_Q parametrized by $w \in \mathbb{T} \mapsto w + Q\bar{w}$, with $Q \in [0, 1)$. We first study the case where Q is far from the resonant set $S_{\text{reso}} = \{Q_{2m}, m \in \mathbb{N}^*\}$. We prove that a one-dimensional continuous curve can be constructed away from this set and which remains close to Kirchhoff ellipses for small values of ε . For this purpose we introduce the spaces

$$X_2 = \left\{ f \in C^{1+\alpha}(\mathbb{T}), f(w) = \sum_{n \in \mathbb{N}^*} f_n w^{2n+1}, f_n \in \mathbb{R} \right\} \quad (4.6.8)$$

and

$$Y_2 = \left\{ g \in C^\alpha(\mathbb{T}), g(w) = \sum_{n \in \mathbb{N}^*} g_n e_{2n}, g_n \in \mathbb{R} \right\}, \quad \text{with } e_n(w) = \text{Im}(w^n). \quad (4.6.9)$$

Note that a domain whose boundary is parametrized by $\Phi(w) = w + Q\bar{w} + f(w), w \in \mathbb{T}$ with $f \in X_2$ is two-fold. The main goal is to prove the following.

Theorem 4.6.3. *Consider the V-state equation (4.6.3) and let $m \in \mathbb{N}^*$, $\delta < \frac{Q_{2m+2} - Q_{2m}}{2}$. Define $I_{m,\delta} = [Q_{2m} + \delta, Q_{2m+2} - \delta]$. Then there exists $\varepsilon_0 >$ and a function*

$$\begin{aligned} f: [-\varepsilon_0, \varepsilon_0] \times I_{m,\delta} &\longrightarrow X_2 \\ (\varepsilon, Q) &\longmapsto f(\varepsilon, Q). \end{aligned}$$

of class C^1 such that

$$F(\varepsilon, Q, f(\varepsilon, Q)) = 0, \quad \forall (\varepsilon, Q) \in [-\varepsilon_0, \varepsilon_0] \times I_{m,\delta}.$$

In particular the curve $Q \in I_{m,\delta} \mapsto \alpha_Q + f(\varepsilon, Q)$ describes rotating patches with two-fold symmetry living close to Kirchhoff ellipses.

Proof. The proof relies on the use of the implicit function theorem. First notice from Proposition 4.6.2 that for any $\mu \in (0, 1)$, the functional

$$\begin{aligned} F: (-1, 1) \times (0, \mu) \times B_{r_\mu}^2 &\longrightarrow Y_2 \\ (\varepsilon, Q, f) &\longmapsto F(\varepsilon, Q, f) \end{aligned}$$

is well-defined and of class C^1 , where

$$B_{r_\mu}^2 = \{f \in X_2, \|f\|_{C^{1+\alpha}} \leq r_\mu\} \quad \text{and} \quad r_\mu = \frac{1-\mu}{2}. \quad (4.6.10)$$

We point out that the persistence of two-fold symmetry follows from Proposition 4.6.2. In addition, $D_f F(0, Q, 0)$ is given by the restriction of the operator \mathcal{L}_Q described by (4.6.4) on the sub-space X_2 . As we have seen in Proposition 4.6.1, the kernel of \mathcal{L}_Q is non-trivial if and only if $Q \in \mathcal{S}$. Since $Q \in I_{m,\delta}$ then $\text{Ker } D_f F(0, Q, 0)$ is trivial for any $Q \neq Q_{2m+1}$, and for $Q = Q_{2m+1}$ the kernel is one-dimensional and generated by the vector $v_{2m+1}(w) = \frac{w^{2m+2}}{1-Qw^2}$. However this vector does not belong to X_2 and consequently $\text{Ker } D_f F(0, Q_{2m+1}, 0)$ is also trivial. Therefore for any $Q \in I_{m,\delta}$ the linear operator $D_f F(0, Q, 0) \in \mathcal{L}(X_2, Y_2)$ is one-to-one. We check that it is also onto. Let $g = \sum_{n \geq 1} g_n e_{2n} \in Y_2$ and consider finding the pre-image by $D_f F(0, Q, 0)$. Then according to Proposition 4.6.1, $h(w) = \sum_{n \geq 1} h_n w^{2n+1}$ satisfies $D_f F(0, Q, 0)h = g$ if and only if

$$g_1 = 2Q^2 h_1 \quad \text{and} \quad g_n = (1 + Q^{2n} - (1 - Q^2)n)(h_n - Qh_{n-1}), \forall n \geq 2. \quad (4.6.11)$$

Note that for each n the number $((1 - Q^2)n - 1 - Q^{2n})$ vanishes if and only if $Q = Q_{2n}$, and thus for $Q \in I_{m,\delta}$ this coefficient does not vanish uniformly in n . One can see from the recursion relation that

$$h(w) = \frac{h_1 w^3 + G(w)}{1 - Qw^2} \quad \text{with} \quad G(w) = \sum_{n \geq 2} \frac{g_n}{1 + Q^{2n} - (1 - Q^2)n} w^{2n+1}.$$

Since $Q \in (0, 1)$ and $\frac{1}{1-Qw^2}$ is $C^\infty(\mathbb{T})$, then $h \in X_2$ if and only if $G \in C^{1+\alpha}(\mathbb{T})$. Thus it suffices to establish $G' \in C^\alpha(\mathbb{T})$ or equivalently

$$\chi : w \in \mathbb{T} \mapsto \sum_{n \geq 2} \frac{n(1 - Q^2) g_n}{1 + Q^{2n} - (1 - Q^2)n} w^{2n} \in C^\alpha(\mathbb{T}).$$

It is plain that

$$\begin{aligned} \chi(w) &= - \sum_{n \geq 2} g_n w^{2n} + \sum_{n \geq 1} \frac{1 + Q^{2n}}{1 + Q^{2n} - (1 - Q^2)n} g_n w^{2n} \\ &= -\Pi^+(2ig(w) - g_1 w^2) + K \star \Pi^+(2ig(w) - g_1 w^2) \end{aligned}$$

with Π^+ being the Szegő projection and

$$K(w) = \sum_{n \geq 2} \frac{1 + Q^{2n}}{1 + Q^{2n} - (1 - Q^2)n} w^{2n}.$$

It is easy to prove the existence of a constant $C > 0$ such that for any $Q \in I_{m,\delta}$

$$\left| \frac{1 + Q^{2n}}{1 + Q^{2n} - (1 - Q^2)n} \right| \leq \frac{C}{n}.$$

Therefore $K \in L^2(\mathbb{T}) \subset L^1(\mathbb{T})$, combined with the fact $\Pi^+ g \in C^\alpha(\mathbb{T})$, implies that $\chi \in C^\alpha(\mathbb{T})$. Finally we see that $D_f F(0, Q, 0)$ is onto and thus it is an isomorphism from X_2 to Y_2 . By the implicit function theorem and a standard compactness argument we conclude the existence of a unique surface of solutions

$$F(\varepsilon, Q, f(\varepsilon, Q)) = 0, \quad \forall (\varepsilon, Q) \in [-\varepsilon_0, \varepsilon_0] \times I_{m,\delta}.$$

This achieves the proof of Theorem 4.6.3. \square

Bifurcation from the two-fold curve

In this subsection we prove the bifurcation of countable family of one-dimensional curves of V-states from the curve constructed in Theorem 4.6.3 at some points which are close to the points of the non-resonant set $S_{\text{Nreso}} = \{Q_{2m+1}, m \geq 1\}$.

The main result may be stated as follows.

Theorem 4.6.4. *Let $m \geq 3$ be an odd number. There exists $\varepsilon_0 > 0$ such that for any $\varepsilon \in [-\varepsilon_0, \varepsilon_0]$, there exists a one-dimensional curve of one-fold V-states bifurcating from the two-fold branch constructed in Theorem 4.6.3 at a point $Q_{\varepsilon,m}$ close to Q_m .*

Proof. The proof follows the same lines of Theorem 4.5.5 with slight modifications using the Lyapunov-Schmidt reduction in an important way. First recall from Proposition 4.6.2 that the functional $F : (-1, 1) \times (0, \mu) \times B_{r_\mu} \rightarrow Y$ is well-defined and is of class C^1 , with

$$B_{r_\mu} = \{f \in X, \|f\|_{C^{1+\alpha}} \leq r_\mu\} \quad \text{and} \quad r_\mu = \frac{1-\mu}{2}.$$

According to Proposition 4.6.1, for $Q = Q_m$ the kernel of \mathcal{L}_{Q_m} is generated by the vector $v_m(w) = \frac{w^{m+1}}{1-Qw^2}$. Denote by \mathcal{X} a complement of v_m in X such that

$$X_2 \subset \mathcal{X}.$$

This last fact follows since m is odd and therefore the function v_m is even; consequently, we can choose a complement containing odd functions which is exactly the space X_2 . Recall that the spaces X and X_2 were introduced in (4.6.1) and (4.6.8). The range of \mathcal{L}_{Q_m} , denoted by \mathcal{Y} , is of co-dimension one and we may choose a complement generated by the vector $w_m = e_m$. Then

$$X = \langle v_m \rangle \oplus \mathcal{X} \quad \text{and} \quad Y = \langle w_m \rangle \oplus \mathcal{Y}.$$

Let $\Pi_1 : X \mapsto \langle v_m \rangle$ be the projection along \mathcal{X} onto $\langle v_m \rangle$. Thus

$$f = sv_m + g, \quad g \in \mathcal{X} \implies \Pi_1 f = sv_m,$$

and similarly define the projection $\Pi_2 : Y \mapsto \langle w_m \rangle$ along \mathcal{Y} onto $\langle w_m \rangle$. The V-state equation $F(\varepsilon, Q, f) = 0$ is then equivalent to the system

$$F_1(\varepsilon, Q, s, g) \triangleq (\text{Id} - \Pi_2)F(\varepsilon, Q, sv_m + g) = 0$$

and

$$F_2(\varepsilon, Q, s, g) \triangleq \Pi_2 F(\varepsilon, Q, sv_m + g) = 0.$$

The function $F_1 : (-1, 1) \times (0, \mu) \times (-\eta, \eta) \times B_r \rightarrow \mathcal{Y}$ is C^1 , with B_r a small ball in \mathcal{X} centered at 0, and $\eta > 0$ such that for any $s \in (-\eta, \eta)$ and for any $g \in B_r$ we have $sv_m + g \in B_{r_\mu}$. Moreover,

$$F_1(0, Q_m, 0, 0) = 0$$

and it is not difficult to check that

$$\partial_g F_1(0, Q_m, 0, 0) = (\text{Id} - \Pi_2) \partial_f F(0, Q_m, 0) : \mathcal{X} \rightarrow \mathcal{Y}$$

is an isomorphism. By the implicit function theorem the solutions of the equation $F_1(\varepsilon, Q, s, g) = 0$ are described near the point $(0, Q_m, 0, 0)$ by the parametrization $g = \varphi(\varepsilon, Q, s)$ with

$$\varphi: (-\delta, \delta) \times (Q_m - \delta, Q_m + \delta) \times (-\delta, \delta) \rightarrow \mathcal{X}, \quad \delta > 0$$

being a C^1 function. By virtue of Theorem 4.6.3, we know the existence of a function

$$(\varepsilon, Q) \mapsto f(\varepsilon, Q) \in X_2 \subset \mathcal{X}$$

such that

$$F(\varepsilon, Q, f(\varepsilon, Q)) = 0 \tag{4.6.12}$$

and so in particular

$$F_1(\varepsilon, Q, 0, f(\varepsilon, Q)) = 0.$$

Thus by uniqueness we get

$$\varphi(\varepsilon, Q, 0) = f(\varepsilon, Q), \quad \forall (\varepsilon, Q) \in (-\delta, \delta) \times (Q_m - \delta, Q_m + \delta). \tag{4.6.13}$$

As Kirchhoff ellipses are exact solutions for $\varepsilon = 0$, we obtain

$$\varphi(0, Q, 0) = 0, \quad \forall Q \in (Q_m - \delta, Q_m + \delta). \tag{4.6.14}$$

The equation of F_2 in a neighbourhood of $(0, Q_m, 0, 0)$ takes the form

$$\widehat{F}_2(\varepsilon, Q, s) \triangleq \Pi_2 F(\varepsilon, Q, sv_m + \varphi(\varepsilon, Q, s)) = 0, \quad \forall |\varepsilon|, |Q - Q_m|, |s| < \delta.$$

From the relations (4.6.12) and (4.6.13) we deduce that

$$\widehat{F}_2(\varepsilon, Q, 0) = 0, \quad \forall |\varepsilon| \leq \delta, \forall |Q - Q_m| \leq \delta.$$

Set

$$\widehat{g}(\varepsilon, Q, s) \triangleq \begin{cases} \frac{\widehat{F}_2(\varepsilon, Q, s)}{s}, & s \neq 0 \\ \Pi_2 \partial_f F(\varepsilon, Q, \varphi(\varepsilon, Q, 0))(v_m + \partial_s \varphi(\varepsilon, Q, 0)), & s = 0. \end{cases} \tag{4.6.15}$$

Then the function \widehat{g} is continuous and

$$\begin{aligned} \widehat{g}(0, Q_m, 0) &= \Pi_2 \partial_f F(0, Q_m, 0)(v_m + \partial_s \varphi(0, Q_m, 0)) \\ &= 0. \end{aligned}$$

Indeed, by differentiating with respect to s the following equation

$$F_1(\varepsilon, Q, s, \varphi(\varepsilon, Q, s)) = 0, \quad \forall |\varepsilon|, |Q - Q_m|, |s| \leq \delta$$

at the point $(0, Q_m, 0)$, we find

$$(\text{Id} - \Pi_2) \partial_f F(0, Q_m, 0)(v_m + \partial_s \varphi(0, Q_m, 0)) = 0.$$

Consequently, $\partial_s \varphi(0, Q_m, 0) \in \text{Ker}(\mathcal{L}_{Q_m}) \cap \mathcal{X}$, and therefore

$$\partial_s \varphi(0, Q_m, 0) = 0.$$

Thanks to (4.6.14), we obtain

$$\partial_Q \varphi(0, Q_m, 0) = 0.$$

Moreover, \widehat{g} is differentiable with respect to Q and

$$\begin{aligned}\partial_Q \widehat{g}(0, Q_m, 0) &= \Pi_2 \partial_Q \partial_f F(0, Q_m, 0)(v_m + \partial_s \varphi(0, Q_m, 0)) \\ &+ \Pi_2 \partial_f F(0, Q_m, 0)(\partial_Q v_m|_{Q=Q_m} + \partial_Q \partial_s \varphi(0, Q_m, 0)) \\ &+ \Pi_2 \partial_f^2 F(0, Q_m, 0)(v_m + \partial_s \varphi(0, Q_m, 0), \partial_Q \varphi(0, Q_m, 0)) \\ &= \Pi_2 \partial_Q \partial_f F(0, Q_m, 0)(v_m).\end{aligned}$$

From the transversality assumption proved in Proposition (4.6.1), we obtain

$$\partial_Q \widehat{g}(0, Q_m, 0) \neq 0.$$

Hence using a weak version of the implicit function theorem, see [16], we deduce that the solutions of $\widehat{g}(\varepsilon, Q, s) = 0$ near the point $(0, Q_m, 0)$ are parametrized by a continuous surface $\gamma : (-\varepsilon_0, \varepsilon_0)^2 \rightarrow \mathbb{R}$ such that $Q = \gamma(\varepsilon, s)$ and

$$\widehat{g}(\varepsilon, \gamma(\varepsilon, s), s) = 0, \forall |\varepsilon| \leq \varepsilon_0, \forall |s| \leq \varepsilon_0, \quad \text{with } \varepsilon_0 > 0.$$

Therefore the solutions of the equation $F(\varepsilon, Q, f) = 0$ near the point $(0, Q_m, 0)$ are given by the union $\mathcal{C}_1 \cup \mathcal{C}_2$ where

$$\mathcal{C}_1 = \left\{ (\varepsilon, Q, \varphi(\varepsilon, Q, 0)), |\varepsilon| \leq \varepsilon_0, |Q - Q_m| \leq \varepsilon_0 \right\}$$

corresponding to the two-fold V-states constructed in Theorem 4.6.3 and

$$\mathcal{C}_2 = \left\{ (\varepsilon, \gamma(\varepsilon, s), sv_m + \varphi(\varepsilon, \gamma(\varepsilon, s), s)), |\varepsilon| \leq \varepsilon_0, |s| \leq \varepsilon_0 \right\}.$$

Note that the curve \mathcal{C}_2 is different from \mathcal{C}_1 since for $s \neq 0$ the V-state parametrized by

$$w \in \mathbb{T} \mapsto w + Q\bar{w} + sv_m(w) + \varphi(\varepsilon, \gamma(\varepsilon, s), s)$$

is not two-fold because m is odd and therefore v_m is a non-vanishing even function. In addition the curve \mathcal{C}_2 intersects \mathcal{C}_1 at $s = 0$. This achieves the proof. \square

4.6.5 Breakdown of the bifurcation diagram close to the resonant set

The numerical study conducted in Section 4.3 shows that, contrary to what occurs in the Euler equations, the two-fold branch is never connected for small ε and is split into countable disjoint connected components or branches. The separation of the singularity set seems to happen around the resonant set $\mathcal{S}_{\text{reso}} = \{Q_{2m}, m \geq 2\}$ due to the resonance between branches with the same symmetry. We provide an analytical confirmation of this behavior only around the point Q_4 which is more tractable than the remaining cases $Q_{2m}, m \geq 3$. We point out that the separation of the two-fold branch around Q_4 is only proved locally in the bifurcation diagram. The global structure of this separation is much more complicated and may require more elaborate tools.

More precisely, we prove the following result.

Theorem 4.6.5. *Consider the V-state equation (4.6.3). There exists $\varepsilon_0 > 0$ such that for any $\varepsilon \in (-\varepsilon_0, \varepsilon_0) \setminus \{0\}$ there exists $r_\varepsilon > 0$ such that the set*

$$\left\{ F(\varepsilon, Q, f) = 0, |Q - Q_4| < r_\varepsilon, f \in X_2, \|f\|_{C^{1+\alpha}} < r_\varepsilon \right\}$$

is given by the union of two disjoint one-dimensional curves.

Proof. The proof is based on studying the local structure of the V-state equation (4.4.6) through the associated quadratic form. At first sight there is a logarithmic singularity in ε at second order which could present difficulties for understanding the local structure. However, as shown below, this term may be combined with

the rotation term and therefore it does not contribute at the nonlinear level. To show this, we first make some transformations using new unknowns. From (4.6.7) we may write for $x > 0$ the expansion

$$K_0^\varepsilon(x) = \psi(1) - \log(x) - \frac{\varepsilon^2}{4}x^2 \log(x) + \frac{\varepsilon^2}{4}(\psi(2) - \log(|\varepsilon|/2))x^2 + \varepsilon^4 \log \varepsilon \mathcal{R}^\varepsilon(x)$$

where \mathcal{R}^ε is at least of class C^3 in the variable x and analytic in the variable ε . It follows that

$$\begin{aligned} \int_{\mathbb{T}} \Phi'(\tau) K_0^\varepsilon(|\Phi(\tau) - \Phi(w)|) d\tau &= - \int_{\mathbb{T}} \Phi'(\tau) \log(|\Phi(\tau) - \Phi(w)|) d\tau \\ &+ \frac{\varepsilon^2}{4} (\psi(2) - \log(|\varepsilon|/2)) \int_{\mathbb{T}} \Phi'(\tau) |\Phi(\tau) - \Phi(w)|^2 d\tau \\ &- \frac{\varepsilon^2}{4} \int_{\mathbb{T}} \Phi'(\tau) \log(|\Phi(\tau) - \Phi(w)|) |\Phi(\tau) - \Phi(w)|^2 d\tau \\ &+ \varepsilon^4 \log |\varepsilon| \int_{\mathbb{T}} \Phi'(\tau) \mathcal{R}^\varepsilon(|\Phi(\tau) - \Phi(w)|) d\tau. \end{aligned}$$

Denote $\Gamma = \Phi(\mathbb{T})$; then it is simple to obtain, by a change of variables and the residue theorem,

$$\begin{aligned} \int_{\mathbb{T}} \Phi'(\tau) |\Phi(\tau) - \Phi(w)|^2 d\tau &= \int_{\Gamma} |\xi - \Phi(w)|^2 d\xi \\ &= \int_{\Gamma} (|\xi|^2 - \Phi(w)\bar{\xi}) d\xi. \end{aligned}$$

From Cauchy-Pompeiu's formula we find

$$\int_{\Gamma} |\xi|^2 d\xi = \frac{1}{\pi} \int_D \xi dA,$$

and since the domain D delimited by the curve Γ is two-fold and centered at the origin then

$$\int_{\Gamma} |\xi|^2 d\xi = 0.$$

Hence

$$\int_{\mathbb{T}} |\Phi(\tau) - \Phi(w)|^2 \Phi'(\tau) d\tau = -\Phi(w) \int_{\mathbb{T}} \overline{\Phi(\tau)} \Phi'(\tau) d\tau.$$

Thus we obtain

$$\begin{aligned} \int_{\mathbb{T}} K_0^\varepsilon(|\Phi(\tau) - \Phi(w)|) \Phi'(\tau) d\tau &= - \int_{\mathbb{T}} \log(|\Phi(\tau) - \Phi(w)|) \Phi'(\tau) d\tau \\ &- \frac{\varepsilon^2}{4} (\psi(2) - \log(|\varepsilon|/2)) \Phi(w) \int_{\mathbb{T}} \overline{\Phi(\tau)} \Phi'(\tau) d\tau \\ &- \frac{\varepsilon^2}{4} \int_{\mathbb{T}} \log(|\Phi(\tau) - \Phi(w)|) |\Phi(\tau) - \Phi(w)|^2 \Phi'(\tau) d\tau \\ &+ \varepsilon^4 \log |\varepsilon| \int_{\mathbb{T}} \mathcal{R}^\varepsilon(|\Phi(\tau) - \Phi(w)|) \Phi'(\tau) d\tau. \end{aligned}$$

Inserting this identity into (4.4.6) and using (4.4.7) we find

$$G(\varepsilon, \Omega, \Phi) = -G_E(\Omega_\varepsilon, \Phi) + \frac{\varepsilon^2}{4} \operatorname{Im}\{G_1(\Phi)\} + \varepsilon^4 \log |\varepsilon| \operatorname{Im}\{G_2(\varepsilon, \Phi)\}$$

with

$$\begin{aligned}\Omega_\varepsilon &\triangleq \Omega + \frac{\varepsilon^2}{4} (\psi(2) - \log(|\varepsilon|/2)) \int_{\mathbb{T}} \overline{\Phi(\tau)} \Phi'(\tau) d\tau, \\ G_1(\Phi) &\triangleq \overline{w} \overline{\Phi'(w)} \int_{\mathbb{T}} \log(|\Phi(\tau) - \Phi(w)|) |\Phi(\tau) - \Phi(w)|^2 \Phi'(\tau) d\tau\end{aligned}$$

and

$$G_2(\varepsilon, \Phi) \triangleq -\overline{w} \overline{\Phi'(w)} \int_{\mathbb{T}} \Phi'(\tau) \mathcal{R}^\varepsilon(|\Phi(\tau) - \Phi(w)|) d\tau.$$

As before we look for solutions of the form

$$\Phi = \alpha_Q + f, \quad f \in X_2.$$

Note that the space X_2 was introduced previously in (4.6.8). We now impose the constraint

$$\Omega_\varepsilon = \frac{1 - Q^2}{4}.$$

Set

$$F_E(Q, f) \triangleq -G_E((1 - Q^2)/4, \alpha_Q + f), \quad F_1(Q, f) \triangleq G_1(\alpha_Q + f)$$

and

$$F_2(\varepsilon, Q, f) \triangleq G_2(\varepsilon, \alpha_Q + f).$$

Then the V-state equation is equivalent to

$$\widehat{F}(\varepsilon, Q, f) \triangleq F_E(Q, f) + \frac{\varepsilon^2}{4} \operatorname{Im}\{F_1(Q, f)\} + \varepsilon^4 \log(|\varepsilon|) \operatorname{Im}\{F_2(\varepsilon, Q, f)\} = 0. \quad (4.6.16)$$

Following the same lines of Proposition 4.6.2 we can check that

$$\begin{aligned}\widehat{F}: (-1, 1) \times (0, \mu) \times B_{r_\mu} &\longrightarrow Y_2 \\ (\varepsilon, Q, f) &\longmapsto \widehat{F}(\varepsilon, Q, f)\end{aligned}$$

is well-defined and of class C^1 , where the ball B_{r_μ} was previously defined in (4.6.10). In fact, we can easily check that \widehat{F} is at least C^3 . Moreover, $\partial_Q \widehat{F}$ and $D_f \widehat{F}$ are also C^3 . Note that from (4.6.3) we have

$$D_f \widehat{F}(0, Q, 0) = D_f F_E(Q, 0) = \mathcal{L}_Q,$$

and the full structure of \mathcal{L}_Q was previously detailed in Proposition 4.6.1. Recall in particular that for $Q = Q_4$ one has

$$\operatorname{Ker} \mathcal{L}_{Q_4} = \langle v_4 \rangle, \quad v_4(w) = \frac{w^5}{1 - Q_4 w^2}$$

and

$$R(\mathcal{L}_{Q_4}) = \left\{ g \in C^\alpha(\mathbb{T}), g = \sum_{\substack{n \geq 1 \\ n \neq 2}} g_n e_{2n}, \quad g_n \in \mathbb{R} \right\}.$$

Let \widehat{X}_2 be a complement of v_4 in X_2 , that is,

$$X_2 = \widehat{X}_2 \oplus \langle v_4 \rangle.$$

Thus any $f \in X_2$ admits a unique decomposition in the form $f = sv_4 + g$ with $g \in \widehat{X}_2$ and $s \in \mathbb{R}$. Denote by \widehat{Y}_2 the space $R(\mathcal{L}_{Q_4})$, then

$$Y_2 = \widehat{Y}_2 \oplus \langle e_4 \rangle,$$

and let $\Pi : Y_2 \rightarrow \langle e_4 \rangle$ be the canonical projection along \widehat{Y}_2 . Thus equation (4.6.16) is equivalent to

$$H_1(\varepsilon, Q, s, g) \triangleq (\text{Id} - \Pi)\widehat{F}(\varepsilon, Q, sv_4 + g) = 0 \quad \text{and} \quad H_2(\varepsilon, Q, s, g) \triangleq \Pi\widehat{F}(\varepsilon, Q, sv_4 + g) = 0. \quad (4.6.17)$$

Now we can directly observe that

$$\partial_g H_1(0, Q_4, 0, 0) = (\text{Id} - \Pi)\mathcal{L}_{Q_4},$$

and that $\partial_g H_1(0, Q_4, 0, 0) : \widehat{X}_2 \rightarrow \widehat{Y}_2$ is an isomorphism. Thus, by the implicit function theorem, the solutions of the equation $H_1(\varepsilon, Q, s, g) = 0$ are described near the point $(0, Q_4, 0, 0)$ by the parametrization $g = \varphi(\varepsilon, Q, s)$ with

$$\varphi : (-\delta, \delta) \times (Q_4 - \delta, Q_4 + \delta) \times (-\delta, \delta) \rightarrow \widehat{X}_2, \quad \delta > 0 \quad (4.6.18)$$

being a C^1 function. As the functions defining the V-states are smooth enough, φ is in fact at least of class C^3 . Notice that the defect of regularity comes only from the variable ε and thus one gets more smoothness in the remaining variables. Indeed, we have the following.

Remark 4.6.6. *The functions $\partial_Q \varphi$ and $\partial_s \varphi$ are at least C^3 . To prove this, we just differentiate the equation*

$$(\text{Id} - \Pi)\widehat{F}(\varepsilon, Q, sv_4 + \varphi(\varepsilon, Q, s)) = 0, \quad \forall (\varepsilon, Q, s) \in (-\delta, \delta) \times (Q_4 - \delta, Q_4 + \delta) \times (-\delta, \delta)$$

and argue by induction.

Now since the ellipses are solutions, then by uniqueness we obtain

$$\varphi(0, Q, 0) = 0, \quad \forall Q \in (Q_4 - \delta, Q_4 + \delta). \quad (4.6.19)$$

This implies that for any $k \in \{1, 2, 3\}$

$$\partial_Q^k \varphi(0, Q, 0) = 0, \quad \forall Q \in (Q_4 - \delta, Q_4 + \delta). \quad (4.6.20)$$

On the other hand differentiating the first equation in (4.6.17) with respect to s we obtain

$$(\text{Id} - \Pi)(\mathcal{L}_{Q_4}(v_4 + \partial_s \varphi(0, Q_4, 0))) = 0$$

and as $\partial_s \varphi(0, Q_4, 0) \in \widehat{X}_2$ we deduce

$$\partial_s \varphi(0, Q_4, 0) = 0. \quad (4.6.21)$$

Similarly, differentiating the first equation of (4.6.17) with respect to ε , we obtain (due to (4.6.16))

$$(\text{Id} - \Pi)\mathcal{L}_{Q_4}\partial_\varepsilon \varphi(0, Q_4, 0) = 0$$

which implies that

$$\partial_\varepsilon \varphi(0, Q_4, 0) = 0. \quad (4.6.22)$$

Now the V-state equation reduces in this small neighbourhood to the finite-dimensional equation

$$\psi(\varepsilon, Q, s) \triangleq H_2(\varepsilon, Q, s, \varphi(\varepsilon, Q, s)) = 0. \quad (4.6.23)$$

It is obvious from (4.6.16) that

$$\psi(\varepsilon, Q, s) = \psi_E(\varepsilon, Q, s) + \frac{\varepsilon^2}{4}\psi_1(\varepsilon, Q, s) + \varepsilon^4 \log |\varepsilon| \psi_2(\varepsilon, Q, s) \quad (4.6.24)$$

with

$$\psi_E(\varepsilon, Q, s) \triangleq \Pi F_E(Q, sv_4 + \varphi(\varepsilon, s, Q)), \quad \psi_1(\varepsilon, Q, s) \triangleq \Pi \text{Im}\{F_1(Q, sv_4 + \varphi(\varepsilon, Q, s))\}$$

and

$$\psi_2(\varepsilon, Q, s) \triangleq \Pi \text{Im}\{F_2(Q, sv_4 + \varphi(\varepsilon, Q, s))\}.$$

Moreover,

$$\psi(0, Q, 0) = 0, \forall Q \in (Q_4 - \delta, Q_4 + \delta)$$

which implies that for any $k \in \{1, 2, 3, 4\}$

$$\partial_Q^k \psi(0, Q, 0) = 0, \forall Q \in (Q_4 - \delta, Q_4 + \delta). \quad (4.6.25)$$

Moreover straightforward computations yield, in view of (4.6.22) and the structures of Π and \mathcal{L}_{Q_4} ,

$$\partial_\varepsilon \psi_E(0, Q_4, 0) = \Pi \mathcal{L}_{Q_4} \partial_\varepsilon \varphi(0, Q_4, 0) = 0.$$

Using once again (4.6.22) we find

$$\begin{aligned} \partial_\varepsilon^2 \psi_E(0, Q_4, 0) &= \Pi \partial_f^2 F_E(Q_4, 0) (\partial_\varepsilon \varphi(0, Q_4, 0), \partial_\varepsilon \varphi(0, Q_4, 0)) + \Pi \mathcal{L}_{Q_4} \partial_\varepsilon^2 \varphi(0, Q_4, 0) \\ &= 0. \end{aligned}$$

Hence we obtain

$$\begin{aligned} \partial_\varepsilon^2 \psi(0, Q_4, 0) &= \frac{1}{2} \psi_1(0, Q_4, 0) \\ &= \frac{1}{2} \Pi \operatorname{Im}\{F_1(Q_4, 0)\}. \end{aligned}$$

To compute the projection, we need to calculate the coefficients of w^4 and \bar{w}^4 in the Fourier expansion of $F_1(Q_4, 0)$. First we have

$$\begin{aligned} F_1(Q_4, 0) &= \bar{w} \overline{\alpha'_{Q_4}(w)} I(w) \\ &= (\bar{w} - Q_4 w) I(w) \end{aligned}$$

with

$$I(w) \triangleq \int_{\mathbb{T}} \log(|\alpha_{Q_4}(\tau) - \alpha_{Q_4}(w)|) |\alpha_{Q_4}(\tau) - \alpha_{Q_4}(w)|^2 \alpha'_{Q_4}(\tau) d\tau.$$

Using the identity

$$|\alpha_{Q_4}(\tau) - \alpha_{Q_4}(w)| = |\tau - w| |1 - Q_4 \tau w|, \quad \forall \tau, w \in \mathbb{T}$$

we find after straightforward computations

$$|\alpha_{Q_4}(\tau) - \alpha_{Q_4}(w)|^2 \alpha'_{Q_4}(\tau) = \sum_{k=0}^2 \alpha_k(w) \tau^k + \sum_{k=1}^4 \beta_k(w) \bar{\tau}^k \quad (4.6.26)$$

with

$$\alpha_0(w) \triangleq 2 + Q_4^2 + Q_4(w^2 + \bar{w}^2), \quad \alpha_1(w) \triangleq -2Q_4 w - (1 + Q_4^2) \bar{w}, \quad \alpha_2(w) \triangleq Q_4,$$

$$\beta_1(w) \triangleq (Q_4^2 - 1)(Q_4 \bar{w} + w), \quad \beta_2(w) \triangleq -Q_4(2Q_4^2 + 1) - Q_4^2 w^2 - Q_4^2 \bar{w}^2,$$

$$\beta_3(w) \triangleq 2Q_4^2 \bar{w} + Q_4(1 + Q_4^2)w \quad \text{and} \quad \beta_4(w) \triangleq -Q_4^2.$$

Now we compute for $n \in \mathbb{Z}$

$$\begin{aligned} \int_{\mathbb{T}} \log(|\alpha_{Q_4}(\tau) - \alpha_{Q_4}(w)|) \tau^n d\tau &= \int_{\mathbb{T}} \log(|\tau - w|) \tau^n d\tau + \int_{\mathbb{T}} \log(|1 - Q_4 \tau w|) \tau^n d\tau \\ &\triangleq I_n(w) + J_n(w). \end{aligned}$$

First note that by a change of variables

$$I_n(w) = w^{n+1} \frac{1}{2\pi} \int_0^{2\pi} \log |1 - e^{i\theta}| e^{i(n+1)\theta} d\theta.$$

From elementary trigonometric identities we write

$$I_n(w) = w^{n+1} \frac{1}{4\pi} \int_0^{2\pi} \log (4 \sin^2(\theta/2)) e^{i(n+1)\theta} d\theta.$$

Using Lemma A.3 of [8] we get

$$I_n(w) = \begin{cases} -\frac{1}{2|n+1|} w^{n+1}, & \text{if } n \in \mathbb{Z} \setminus \{-1\} \\ 0, & \text{if } n = -1. \end{cases}$$

In addition

$$\begin{aligned} J_n(w) &= \bar{w}^{n+1} \frac{1}{2\pi} \int_0^{2\pi} \log |1 - Q_4 e^{i\theta}| e^{i(n+1)\theta} d\theta \\ &= \bar{w}^{n+1} \frac{1}{4\pi} \int_0^{2\pi} \log |1 + Q_4^2 - 2Q_4 \cos(\theta)| e^{i(n+1)\theta} d\theta. \end{aligned}$$

Again from Lemma A.4 [8] we obtain

$$J_n(w) = \begin{cases} -\frac{1}{2|n+1|} Q_4^{|n+1|} \bar{w}^{n+1}, & \text{if } n \in \mathbb{Z} \setminus \{-1\} \\ 0, & \text{if } n = -1. \end{cases}$$

Putting together the preceding identities one finds

$$\oint_{\mathbb{T}} \log(|\alpha_{Q_4}(\tau) - \alpha_{Q_4}(w)| \tau^n d\tau = \begin{cases} -\frac{1}{2|n+1|} (w^{n+1} + Q_4^{|n+1|} \bar{w}^{n+1}), & \text{if } n \in \mathbb{Z} \setminus \{-1\} \\ 0, & \text{if } n = -1. \end{cases} \quad (4.6.27)$$

Using (4.6.26) we find

$$\begin{aligned} I(w) &= \sum_{k=0}^2 \alpha_k(w) (I_k(w) + J_k(w)) + \sum_{k=1}^4 \beta_k(w) (I_{-k}(w) + J_{-k}(w)) \\ &= \sum_{k=0}^2 \alpha_k(w) (I_k(w) + J_k(w)) + \sum_{k=2}^4 \beta_k(w) (I_{-k}(w) + J_{-k}(w)). \end{aligned}$$

From straightforward calculation, and using the fact that Q_4 is a solution of (4.6.5) with $m = 4$, we obtain

$$\Pi \operatorname{Im} \left\{ \bar{w} \overline{\alpha'_{Q_4}(w)} \sum_{k=0}^2 \alpha_k (I_k + J_k) \right\} = \frac{Q_4^2}{12} (5 - Q_4^2) e_4.$$

Similarly we obtain

$$\Pi \operatorname{Im} \left\{ \bar{w} \overline{\alpha'_{Q_4}(w)} \sum_{k=2}^4 \beta_k (I_{-k} + J_{-k}) \right\} = \frac{Q_4^6 - 3Q_4^4 - 2Q_4^2}{12} e_4.$$

Consequently

$$\Pi \operatorname{Im} \left\{ F_1(Q_4, 0) \right\} = \frac{Q_4^2}{12} (Q_4^4 - 4Q_4^2 + 3) e_4.$$

Therefore

$$\partial_\varepsilon^2 \psi(0, Q_4, t) = \frac{Q_4^2}{24} (Q_4^4 - 4Q_4^2 + 3) e_4. \quad (4.6.28)$$

We next compute $\partial_s \partial_\varepsilon \psi(0, Q_4, 0)$. From (4.6.24) we write

$$\begin{aligned}\partial_s \partial_\varepsilon \psi(0, Q_4, 0) &= \Pi \partial_f^2 F_E(Q_4, 0)[\partial_\varepsilon \varphi(0, Q_4, 0), v_4 + \partial_s \varphi(0, Q_4, 0)] \\ &\quad + \Pi \mathcal{L}_{Q_4} \partial_\varepsilon \partial_s \varphi(0, Q_4, 0).\end{aligned}$$

From (4.6.22) and the structure of Π we find

$$\partial_s \partial_\varepsilon \psi(0, Q_4, 0) = 0. \quad (4.6.29)$$

Similarly we find

$$\begin{aligned}\partial_Q \partial_s \psi(0, Q_4, 0) &= \Pi \partial_Q \partial_s F_E(0, Q_4, 0) \\ &= \partial_Q \{\Pi \partial_f F_E(Q, \varphi(0, Q, 0))(v_4 + \partial_s \varphi(0, Q, 0))\}_{Q=Q_4}.\end{aligned}$$

Using (4.6.19) and (4.6.20) we deduce that

$$\partial_Q \partial_s \psi(0, Q_4, 0) = \Pi \{\partial_Q \mathcal{L}_Q v_4\}_{Q=Q_4}.$$

This is the transversality assumption in the Crandall-Rabinowitz theorem. According to [?] we have

$$\Pi \{\partial_Q \mathcal{L}_Q v_4\}_{Q=Q_4} = 4(Q_4 + Q_4^3)e_4$$

and thus

$$\partial_Q \partial_s \psi(0, Q_4, 0) = 4(Q_4 + Q_4^3)e_4. \quad (4.6.30)$$

To compute $\partial_Q \partial_\varepsilon \psi(0, Q_4, 0)$ we note from (4.6.19), (4.6.22) and the identity $\Pi \mathcal{L}_{Q_4} = 0$ that

$$\begin{aligned}\partial_Q \partial_\varepsilon \psi(0, Q_4, 0) &= \Pi \partial_Q \{\partial_f F_E(Q, \varphi(0, Q, 0)) \partial_\varepsilon \varphi(0, Q, 0)\}_{Q=Q_4} \\ &= 0.\end{aligned} \quad (4.6.31)$$

The computations of $\partial_s^2 \psi(0, Q_4, 0)$ can be performed using the formula

$$\begin{aligned}\partial_s^2 \psi(0, Q_4, 0) &= \partial_f^2 F_E(Q_4, 0)[v_4, v_4] \\ &= \left\{ \frac{d^2}{ds^2} F_E(Q_4, sv_4) \right\}_{s=0}.\end{aligned}$$

Observe from (4.4.7) that

$$\begin{aligned}F_E(Q_4, sv_4) &= G(0, (1 - Q_4^2)/4, \alpha_{Q_4} + sv_4) \\ &= -G_E((1 - Q_4^2)/4, \alpha_{Q_4} + sv_4)\end{aligned}$$

with

$$\begin{aligned}G_E(1 - Q_4^2/4, \alpha_{Q_4} + sv_4) &= \text{Im} \left\{ \left(\frac{1 - Q_4^2}{4} (\overline{\alpha_{Q_4}(w)} + \overline{sv_4(w)}) + I(s) \right) w (\alpha'_{Q_4}(w) + sv'_4(w)) \right\}, \\ I(s) &\triangleq \frac{1}{2} \int_{\mathbb{T}} \frac{\overline{A} + s\overline{B}}{A + sB} (\alpha'_{Q_4}(\tau) + sv'_4(\tau)) d\tau\end{aligned}$$

and

$$\begin{aligned}A &= \alpha_{Q_4}(\tau) - \alpha_{Q_4}(w) \\ B &= v_4(\tau) - v_4(w).\end{aligned}$$

It is easy to obtain

$$\begin{aligned} \left\{ \frac{d^2}{ds^2} G_E(1 - Q_4^2/4, \alpha_{Q_4} + sv_4) \right\}_{s=0} &= \frac{1 - Q_4^2}{2} \operatorname{Im} \left\{ \overline{v_4(w)} w v'_4(w) \right\} + \operatorname{Im} \left\{ 2I'(0) w v'_4(w) + I''(0) w \alpha'_{Q_4}(w) \right\} \\ &\triangleq \frac{1 - Q_4^2}{2} \operatorname{Im} \{ I_1(w) \} + \operatorname{Im} \{ I_2(w) \} + \operatorname{Im} \{ I_3(w) \}. \end{aligned}$$

We start by computing $\Pi \operatorname{Im} \{ I_1(w) \}$. It is straightforward to show

$$\overline{v_4(w)} w v'_4(w) = \frac{w^2}{w^2 - Q_4} \frac{-3Q_4 w^2 + 5}{(1 - Q_4 w^2)^2}.$$

Set $z = w^2$. Then

$$\overline{v_4(w)} w v'_4(w) = \frac{z}{z - Q_4} \frac{-3Q_4 z + 5}{(1 - Q_4 z)^2}.$$

Note that $z \mapsto \frac{z}{z - Q_4} \frac{-3Q_4 z + 5}{(1 - Q_4 z)^2}$ is holomorphic in the annulus of small radius Q_4 and large radius $\frac{1}{Q_4}$, and therefore it admits a Laurent expansion in this domain. To evaluate $\Pi \operatorname{Im} \{ I_1(w) \}$ it suffices to compute the coefficients of z^2 and $\frac{1}{z^2}$ in that expansion using the residue theorem. The coefficient of z^2 is given by

$$a \triangleq \int_{\mathbb{T}} \frac{1}{z - Q_4} \frac{-3Q_4 z + 5}{(1 - Q_4 z)^2} \frac{dz}{z^2}.$$

Using the change of variable $z \mapsto \frac{1}{z}$ we obtain

$$\begin{aligned} a &= \int_{\mathbb{T}} \frac{z^2}{1 - Q_4 z} \frac{5z - 3Q_4}{(z - Q_4)^2} dz \\ &\triangleq \int_{\mathbb{T}} \frac{g(z)}{(z - Q_4)^2} dz \\ &= g'(Q_4) \end{aligned}$$

with

$$g(z) \triangleq \frac{z^2(5z - 3Q_4)}{1 - Q_4 z}.$$

Thus we obtain,

$$a = \frac{-7Q_4^4 + 9Q_4^2}{(1 - Q_4^2)^2}.$$

Now we move on to the coefficient of $\frac{1}{z^2}$ given by the formula

$$b \triangleq \int_{\mathbb{T}} \frac{z^2}{z - Q_4} \frac{-3Q_4 z + 5}{(1 - Q_4 z)^2} dz.$$

Using the residue theorem we obtain

$$b = Q_4^2 \frac{-3Q_4^2 + 5}{(1 - Q_4^2)^2}.$$

Consequently

$$\begin{aligned} \frac{1 - Q_4^2}{2} \Pi \operatorname{Im} \{ I_1(w) \} &= \frac{1 - Q_4^2}{2} (a - b) e_4 \\ &= 2Q_4^2 e_4. \end{aligned} \tag{4.6.32}$$

Next we compute $\Pi \operatorname{Im} \{ I_2(w) \}$. First notice that

$$2I'(0) = \int_{\mathbb{T}} \frac{\bar{A}}{A} v'_4(\tau) d\tau + \int_{\mathbb{T}} \frac{A\bar{B} - B\bar{A}}{A^2} \alpha'_{Q_4}(\tau) d\tau.$$

We rewrite $I_2(w)$ as follows,

$$I_2(w) = I_{21}(w) + I_{22}(w) + I_{23}(w),$$

where

$$I_{21}(w) = wv'_4(w) \oint_{\mathbb{T}} \frac{\bar{A}}{A} v'_4(\tau) d\tau$$

$$I_{22}(w) = wv'_4(w) \oint_{\mathbb{T}} \frac{\bar{B}}{A} \alpha'_{Q_4}(\tau) d\tau$$

and

$$I_{23}(w) = -wv'_4(w) \oint_{\mathbb{T}} \frac{B\bar{A}}{A^2} \alpha'_{Q_4}(\tau) d\tau.$$

Straightforward computations imply

$$\oint_{\mathbb{T}} \frac{\bar{A}}{A} v'_4(\tau) d\tau = \bar{w} \oint_{\mathbb{T}} \frac{Q_4 w\tau - 1}{\tau - Q_4 \bar{w}} \frac{-3Q_4 \tau^6 + 5\tau^4}{(1 - Q_4 \tau^2)^2} d\tau.$$

Hence by the residue theorem we obtain

$$\oint_{\mathbb{T}} \frac{\bar{A}}{A} v'_4(\tau) d\tau = \bar{w}^5 (Q_4^2 - 1) \frac{-3Q_4^7 \bar{w}^2 + 5Q_4^4}{(1 - Q_4^3 \bar{w}^2)^2}.$$

Since we can extend $z \mapsto I_{21}(z)$ to a holomorphic function in the annulus of small radius Q and large radius $\frac{1}{Q_4}$, then I_{21} admits a Laurent expansion in this domain. As before, to evaluate $\text{II Im}\{I_{21}(w)\}$ it suffices to compute the coefficients of z^4 and $\frac{1}{z^4}$ in that expansion using the residue theorem. The coefficient of z^4 is given by

$$\tilde{a} = \oint_{\mathbb{T}} wv'_4(w) \bar{w}^5 (Q_4^2 - 1) \frac{-3Q_4^7 \bar{w}^2 + 5Q_4^4}{(1 - Q_4^3 \bar{w}^2)^2} \frac{dw}{w^5}.$$

Moreover, the coefficient of $\frac{1}{z^4}$ is given by

$$\tilde{b} = \oint_{\mathbb{T}} wv'_4(w) \bar{w}^5 (Q_4^2 - 1) \frac{-3Q_4^7 \bar{w}^2 + 5Q_4^4}{(1 - Q_4^3 \bar{w}^2)^2} w^3 dw.$$

One may thus deduce the following equality,

$$\begin{aligned} \text{II Im}\{I_{21}(w)\} &= (\tilde{a} - \tilde{b}) e_4 \\ &= \frac{Q_4^6 (45 - 58 Q_4^4 + 21 Q_4^8)}{(Q_4^4 - 1)(Q_4^2 + 1)} e_4. \end{aligned} \tag{4.6.33}$$

As for I_{22} , using the change of variable $\tau \mapsto \bar{\tau}$, we obtain by the residue theorem

$$\begin{aligned} \oint_{\mathbb{T}} \frac{\bar{B}}{A} \alpha'_{Q_4}(\tau) d\tau &= -\bar{w} \oint_{\mathbb{T}} \frac{v_4(\tau) - v_4(\bar{w})}{\tau - \bar{w}} \frac{1 - Q_4 \tau^2}{1 - Q_4 \bar{w}} \frac{d\tau}{\tau} \\ &= -v_4(\bar{w}). \end{aligned}$$

Again, we can extend $z \mapsto I_{21}(z)$ to a holomorphic function in the same annulus and thus we just need to compute the coefficients of z^4 and $\frac{1}{z^4}$ denoted by \tilde{c} and \tilde{d} , respectively:

$$\tilde{c} = -\oint_{\mathbb{T}} wv'_4(w) v_4(\bar{w}) \frac{dw}{w^5}$$

and

$$\tilde{d} = -\oint_{\mathbb{T}} wv'_4(w) v_4(\bar{w}) w^3 dw.$$

According to the residue theorem we obtain

$$\begin{aligned}\Pi \operatorname{Im}\{I_{22}(w)\} &= (\tilde{c} - \tilde{d})e_4 \\ &= \frac{4Q_4^2}{(Q_4^2 - 1)}e_4.\end{aligned}\quad (4.6.34)$$

Now we move on to the last term $I_{23}(w)$. The computations are very tedious and we use the Maple symbolic manipulation package to obtain the following expressions

$$-\oint_{\mathbb{T}} \frac{B\bar{A}}{A^2} \alpha'_{Q_4}(\tau) d\tau = \frac{\sum_{i=0}^5 \tilde{\alpha}_{2i}(Q_4) w^{2i}}{\omega^3(\omega^2 - Q_4^3)(Q_4^3 + Q_4\omega^4 - (1 + Q_4^4)\omega^2)}$$

where

$$\begin{aligned}\tilde{\alpha}_0(Q_4) &\triangleq 3Q_4^7 - 4Q_4^9, \quad \tilde{\alpha}_2(Q_4) \triangleq 4Q_4^{10} - 4Q_4^8 + 7Q_4^6 - 5Q_4^4, \\ \tilde{\alpha}_4(Q_4) &\triangleq Q_4^9 - 8Q_4^7 + 7Q_4^5 - Q_4^3, \quad \tilde{\alpha}_6(Q_4) \triangleq Q_4^8 - 3Q_4^6 + 3Q_4^4 - Q_4^2, \\ \tilde{\alpha}_8(Q_4) &\triangleq 3Q_4^3 - 2Q_4^5 - Q_4 \quad \text{and} \quad \tilde{\alpha}_{10}(Q_4) \triangleq Q_4^2 - 1.\end{aligned}$$

Let \tilde{e} and \tilde{f} be the coefficient of z^4 and $\frac{1}{z^4}$ in the Laurent expansion of $I_{23}(z)$. Again using Maple, we obtain

$$\begin{aligned}\Pi \operatorname{Im}\{I_{23}(w)\} &= (\tilde{e} - \tilde{f})e_4 \\ &= -\frac{Q_4^2 (21Q_4^{12} - 65Q_4^8 - 12Q_4^6 + 47Q_4^4 + 12Q_4^2 + 5)}{(Q_4^4 - 1)(Q_4^2 + 1)}e_4.\end{aligned}\quad (4.6.35)$$

Now using (4.6.33), (4.6.34) and (4.6.35) we find

$$\Pi \operatorname{Im}\{I_2(w)\} = \frac{1}{2} \frac{Q_4^2 (7Q_4^4 - 2Q_4^2 - 1)}{(Q_4^2 - 1)} e_4. \quad (4.6.36)$$

Now we compute $\operatorname{Im}\{I_3(w)\}$. First we notice that

$$I''(0) = \oint_{\mathbb{T}} \frac{B^2\bar{A} - B\bar{B}A}{A^3} \alpha'_{Q_4}(\tau) d\tau + \oint_{\mathbb{T}} \frac{\bar{B}A - B\bar{A}}{A^2} v'_4(\tau) d\tau.$$

Consequently, we can split I_3 as follows,

$$I_3(w) = I_{31}(w) + I_{32}(w) + I_{33}(w) + I_{34}(w)$$

where

$$\begin{aligned}I_{31}(w) &= w\alpha'_{Q_4}(w) \oint_{\mathbb{T}} \frac{B^2\bar{A}}{A^3} \alpha'_{Q_4}(\tau) d\tau, \\ I_{32}(w) &= w\alpha'_{Q_4}(w) \oint_{\mathbb{T}} \frac{\bar{B}}{A} v'_4(\tau) d\tau, \\ I_{33}(w) &= -w\alpha'_{Q_4}(w) \oint_{\mathbb{T}} \frac{B\bar{A}}{A^2} v'_4(\tau) d\tau\end{aligned}$$

and

$$I_{34}(w) = -w\alpha'_{Q_4}(w) \oint_{\mathbb{T}} \frac{B\bar{B}}{A^2} \alpha'_{Q_4}(\tau) d\tau.$$

In the following, we denote by a_{3i} and b_{3i} the coefficient in front of z^4 and $\frac{1}{z^4}$ in the Laurent expansion of $I_{3i}(z)$ on the same annulus as before. We obtain the following expressions using Maple,

$$a_{31} = -\frac{Q_4^2 (-12Q_4^6 + 8Q_4^2 + 26Q_4^4 + 3 + 12Q_4^{12} + 4Q_4^{10} - 33Q_4^8)}{(Q_4^4 - 1)^2 (Q_4^2 + 1)}$$

and

$$b_{31} = -\frac{Q_4^6 (78 Q_4^4 + 8 Q_4^2 + 3 + 56 Q_4^{12} - 129 Q_4^8 - 20 Q_4^6 + 12 Q_4^{10})}{(Q_4^4 - 1)^2 (Q_4^2 + 1)}.$$

Therefore,

$$\begin{aligned} \text{II Im}\{I_{31}(w)\} &= (a_{31} - b_{31})e_4 \\ &= \frac{(56 Q_4^{12} + 12 Q_4^{10} - 85 Q_4^8 - 12 Q_4^6 + 26 Q_4^4 + 8 Q_4^2 + 3) Q_4^2}{(Q_4^2 + 1) (-1 + Q_4^4)} e_4. \end{aligned} \quad (4.6.37)$$

Similarly we obtain using Maple,

$$\int_{\mathbb{T}} \frac{\bar{B}}{A} v'_4(\tau) d\tau = \frac{\sum_{i=0}^5 \beta_{2i}(Q_4) w^{2i}}{w^5 (w^2 - Q_4^3)^2 (w^2 - Q_4) (Q_4^2 - 1)^2}$$

where

$$\begin{aligned} \beta_0(Q_4) &:= -6Q_4^9 + 3Q_4^7 + 3Q_4^{11}, & \beta_2(Q_4) &:= 3Q_4^{10} - 11Q_4^8 + 13Q_4^6 - 5Q_4^4, \\ \beta_4(Q_4) &:= 3Q_4^9 - 11Q_4^7 + 13Q_4^5 - 5Q_4^3, & \beta_6(Q_4) &:= -6Q_4^6 + 13Q_4^4 - 5Q_4^2, \\ \beta_8(Q_4) &:= -Q_4^5 + 6Q_4^3 - 5Q_4 \quad \text{and} \quad \beta_{10}(Q_4) &:= 3Q_4^2 - 5. \end{aligned}$$

The coefficients in the Laurent expansion have the following expressions,

$$a_{32} = 0$$

and

$$b_{32} = \frac{(7 Q_4^6 - 9 Q_4^4 + 3 Q_4^2 - 5) Q_4^2}{(Q_4^2 - 1)^2}.$$

Consequently,

$$\begin{aligned} \text{IIIIm}\{I_{32}(w)\} &= (a_{32} - b_{32})e_4 \\ &= -\frac{(7 Q_4^6 - 9 Q_4^4 + 3 Q_4^2 - 5) Q_4^2}{(Q_4^2 - 1)^2} e_4. \end{aligned} \quad (4.6.38)$$

Thanks to Maple, one may find the following expression

$$I_{33}(w) = \frac{(w^2 - Q_4) Q_4^4 (\sum_{i=0}^6 \gamma_{2i}(Q_4) w^{2i})}{w^6 (w^2 - Q_4^3) (-Q_4^{10} + 3Q_4^6) w^2 + 3Q_4^3 (Q_4^4 + 1) w^4 - (3Q_4^4 + 1) w^6 + Q_4^9 + Q_4 w^8}$$

where

$$\begin{aligned} \gamma_0(Q_4) &= 18Q_4^{12} - 15Q_4^{10}, & \gamma_2(Q_4) &= 30Q_4^{11} - 68Q_4^9 + 48Q_4^7 - 18Q_4^{13}, \\ \gamma_4(Q_4) &= -15Q_4^{12} - 105Q_4^8 + 90Q_4^6 + 80Q_4^{10} - 45Q_4^4, & \gamma_6(Q_4) &= -12Q_4^{11} - 136Q_4^7 + 122Q_4^5 + 66Q_4^9 - 40Q_4^3, \\ \gamma_8(Q_4) &= -35Q_4^2 + 104Q_4^4 + 46Q_4^8 - 112Q_4^6, & \gamma_{10}(Q_4) &= -30Q_4 - 64Q_4^5 + 86Q_4^3, \end{aligned}$$

and

$$\gamma_{12}(Q_4) = 30Q_4^2 - 25.$$

This allows one to obtain

$$a_{33} = \frac{Q_4^6 (9 Q_4^8 - 26 Q_4^4 + 25)}{(Q_4^2 + 1) (-1 + Q_4^4)^2}$$

and

$$b_{33} = \frac{Q_4^6 (-131 Q_4^8 + 56 Q_4^{12} + 78 Q_4^4 + 5 + 12 Q_4^2 - 24 Q_4^6 + 12 Q_4^{10})}{(Q_4^2 + 1) (-1 + Q_4^4)^2}.$$

Finally we obtain

$$\begin{aligned} \Pi \operatorname{Im}\{I_{33}(w)\} &= (a_{33} - b_{33})e_4 \\ &= -4 \frac{Q_4^6 (14 Q_4^8 + 3 Q_4^6 - 21 Q_4^4 - 3 Q_4^2 + 5)}{(Q_4^2 + 1) (-1 + Q_4^4)} e_4. \end{aligned} \quad (4.6.39)$$

For the last term, we use Maple to obtain

$$-\int_{\mathbb{T}} \frac{B\bar{B}}{A^2} \alpha'_{Q_4}(\tau) d\tau = -\frac{\sum_{i=0}^5 \xi_{2i}(Q_4) w^{2i}}{w^5(w^2 - Q_4^3)((Q_4^4 + Q_4^2 + 1)w^2(Q_4 - w^2) + Q_4(w^6 - Q_4^3))}$$

where

$$\begin{aligned} \xi_0(Q_4) &= -3Q_4^7, & \xi_2(Q_4) &= 3Q_4^8 - 3Q_4^6 + 5Q_4^4, \\ \xi_4(Q_4) &= 3Q_4^7 - 8Q_4^5 + 5Q_4^3, & \xi_6(Q_4) &= 3Q_4^6 - 8Q_4^4 + 5Q_4^2, \\ \xi_8(Q_4) &= -6Q_4^3 + 5Q_4 \text{ and } \xi_{10}(Q_4) &= 2Q_4^2 + 5. \end{aligned}$$

Thus we deduce using Maple once again

$$a_{34} = -\frac{Q_4^2(3Q_4^2 - 5)}{(Q_4^2 - 1)^2}$$

and

$$b_{34} = -\frac{Q_4^2(4Q_4^6 - 4Q_4^4 + 3Q_4^2 - 5)}{(Q_4^2 - 1)^2}.$$

Therefore we find

$$\begin{aligned} \Pi \operatorname{Im}\{I_{34}(w)\} &= (a_{34} - b_{34})e_4 \\ &= \frac{4Q_4^6}{(Q_4^2 - 1)} e_4. \end{aligned} \quad (4.6.40)$$

Finally, using (4.6.37), (4.6.38), (4.6.39) and (4.6.40) one finds

$$\Pi \operatorname{Im}\{I_3(w)\} = -2 \frac{Q_4^2 (2 Q_4^6 - 4 Q_4^4 + Q_4^2 - 1)}{(-1 + Q_4^2)^2} e_4. \quad (4.6.41)$$

Now combining (4.6.32), (4.6.36) with (4.6.41) and simplifying the polynomial equation of Q_4 , we obtain

$$\partial_t^2 \psi(0, Q_4, 0) = -\frac{Q_4^2 (3 Q_4^6 + Q_4^4 - 5 Q_4^2 + 5)}{(-1 + Q_4^2)^2} e_4$$

To summarize, up to this point we have proved that the V-state equation (4.6.24) reduces in the small neighbourhood $I_\delta \triangleq (-\delta, \delta) \times (-\delta + Q_4, Q_4 + \delta) \times (-\delta, \delta)$ to the finite-dimensional equation

$$\psi(\varepsilon, Q, s) = 0. \quad (4.6.42)$$

As ψ is at least \mathcal{C}^3 , we can use a Taylor expansion with the integral form for the remainder around the point $(0, Q_4, 0)$,

$$\begin{aligned} \psi(\varepsilon, Q, s) &= \psi(0, Q_4, 0) + s \partial_s \psi(0, Q_4, 0) + \varepsilon \partial_\varepsilon \psi(0, Q_4, 0) + (Q - Q_4) \partial_Q \psi(0, Q_4, 0) + \frac{s^2}{2} \partial_{ss}^2 \psi(0, Q_4, 0) \\ &+ \frac{\varepsilon^2}{2} \partial_\varepsilon^2 \psi(0, Q_4, 0) + \frac{(Q - Q_4)^2}{2} \partial_Q^2 \psi(0, Q_4, 0) + \varepsilon (Q - Q_4) \partial_{\varepsilon Q}^2 \psi(0, Q_4, 0) + \varepsilon s \partial_{\varepsilon s}^2 \psi(0, Q_4, 0) \\ &+ (Q - Q_4) s \partial_{Qs}^2 \psi(0, Q_4, 0) + \tilde{\varepsilon}(\varepsilon, Q, s) e_4 \end{aligned}$$

where

$$\tilde{\varepsilon}(\varepsilon, Q, s)e_4 = \int_0^1 \frac{(1-\theta)^2}{2!} D^3\psi(\theta\varepsilon, Q_4 + \theta(Q - Q_4), \theta s)(\varepsilon, Q - Q_4, s)^3 d\theta.$$

For a given vector h we use the notation h^3 to denote (h, h, h) . Consequently, using the preceding computations concerning the quadratic expansion, we obtain for any $(\varepsilon, Q, s) \in I_\delta$

$$\psi(\varepsilon, Q, s) = [a\varepsilon^2 + b s(Q - Q_4) + c s^2 + \tilde{\varepsilon}(\varepsilon, Q, s)]e_4$$

with

$$a = \frac{Q_4^2(Q_4^4 - 4Q_4^2 + 3)}{48}, \quad b = 4Q_4(Q_4^2 + 1)$$

and

$$c = -\frac{Q_4^2(3Q_4^6 + Q_4^4 - 5Q_4^2 + 5)}{(-1 + Q_4^2)^2}.$$

Since $Q_4 = \sqrt{\sqrt{2} - 1}$, one may easily check that

$$a > 0, \quad b > 0 \text{ and } c < 0.$$

We introduce the parameters $\tilde{c} = -c$, $\tilde{b} = -\frac{b^2}{4c}$ and $d = -\frac{b}{2c}$, which are three positive constants, and write equation (4.6.42) in the new variables $\mathbf{Q} = Q - Q_4$ and $X = s - d\mathbf{Q}$. In this way, we find in a small neighbourhood of zero,

$$\hat{\psi}(\varepsilon, \mathbf{Q}, X) \triangleq [a\varepsilon^2 - \tilde{c}X^2 + \tilde{b}\mathbf{Q}^2 + \hat{\varepsilon}(\varepsilon, \mathbf{Q}, X)]e_4 = 0 \quad (4.6.43)$$

where

$$\hat{\varepsilon}(\varepsilon, \mathbf{Q}, X) = \tilde{\varepsilon}(\varepsilon, Q, s).$$

For the quadratic equation

$$a\varepsilon^2 - \tilde{c}X^2 + \tilde{b}\mathbf{Q}^2 = 0$$

we find for given $\varepsilon \neq 0$ two disjoint curves

$$X = \pm \sqrt{\frac{a}{\tilde{c}}\varepsilon^2 + \frac{\tilde{b}}{\tilde{c}}\mathbf{Q}^2}.$$

We prove that this structure persists for the full equation,

$$a\varepsilon^2 - \tilde{c}X^2 + \tilde{b}^2\mathbf{Q}^2 + \hat{\varepsilon}(\varepsilon, \mathbf{Q}, X) = 0. \quad (4.6.44)$$

To this end, we check that the solutions have the form

$$X = \sqrt{\frac{a}{\tilde{c}}\varepsilon^2 + \frac{\tilde{b}}{\tilde{c}}\mathbf{Q}^2 + y}$$

where y is a small correction described shortly below. From (4.6.44) we deduce that y satisfies the equation

$$G(\mathbf{Q}, y) = y,$$

with

$$G(\mathbf{Q}, y) = -\frac{y^2}{2\sqrt{\frac{a}{\tilde{c}}\varepsilon^2 + \frac{\tilde{b}}{\tilde{c}}\mathbf{Q}^2}} + \frac{\hat{\varepsilon}(\varepsilon, \mathbf{Q}, \sqrt{\frac{a}{\tilde{c}}\varepsilon^2 + \frac{\tilde{b}}{\tilde{c}}\mathbf{Q}^2} + y)}{2\tilde{c}\sqrt{\frac{a}{\tilde{c}}\varepsilon^2 + \frac{\tilde{b}}{\tilde{c}}\mathbf{Q}^2}}.$$

We prove the following lemma,

Lemma 4.6.7. *There exist two strictly positive constants η and $\varepsilon_0 < 1$ such that for any $0 < \varepsilon \leq \varepsilon_0$*

$$G : \begin{aligned} \overline{B}_{\eta\varepsilon^{\frac{5}{6}}} \times \overline{B}_{\eta\varepsilon^{\frac{3}{2}}} &\longrightarrow \overline{B}_{\eta\varepsilon^{\frac{3}{2}}} \\ (\mathbf{Q}, y) &\longmapsto G(\mathbf{Q}, y) \end{aligned}$$

is well-defined. Moreover, for any $\mathbf{Q} \in \overline{B}_{\eta\varepsilon^{\frac{5}{6}}}$, G admits a unique fixed point $y(\mathbf{Q})$ which depends continuously on \mathbf{Q} .

Proof. We begin with the simple inequality,

$$|G(\mathbf{Q}, y)| \leq \frac{y^2}{2\sqrt{\frac{a}{c}\varepsilon^2 + \frac{b}{c}\mathbf{Q}^2}} + \left| \frac{\hat{\varepsilon}(\varepsilon, \mathbf{Q}, \sqrt{\frac{a}{c}\varepsilon^2 + \frac{b}{c}\mathbf{Q}^2} + y)}{2\sqrt{\frac{a}{c}\varepsilon^2 + \frac{b}{c}\mathbf{Q}^2}} \right|.$$

It is plain that there exists $C > 0$ such that,

$$\frac{y^2}{2\tilde{c}\sqrt{\frac{a}{c}\varepsilon^2 + \frac{b}{c}\mathbf{Q}^2}} \leq C\eta^2\varepsilon^2.$$

For the second term we use the cubic form of the remainder and its continuity,

$$\left| \hat{\varepsilon}(\varepsilon, \mathbf{Q}, \sqrt{\frac{a}{c}\varepsilon^2 + \frac{b}{c}\mathbf{Q}^2} + y) \right| \leq C\eta^3\varepsilon^{\frac{5}{2}}.$$

It follows that,

$$|G(\mathbf{Q}, y)| \leq C\eta^2\varepsilon^2 + C\eta^3\varepsilon^{\frac{3}{2}}.$$

Choosing η such that

$$C\eta + C\eta^2 \leq 1 \quad (4.6.45)$$

we guarantee that G is well-defined. In order to apply the Banach fixed point theorem with a parameter, we need only check that G is a contraction. Let y and \tilde{y} be two elements of $\overline{B}_{\eta\varepsilon^{\frac{3}{2}}}$, then we have

$$\begin{aligned} |G(\mathbf{Q}, y) - G(\mathbf{Q}, \tilde{y})| &\leq \left| \frac{(y + \tilde{y})(\tilde{y} - y)}{2\sqrt{\frac{a}{c}\varepsilon^2 + \frac{b}{c}\mathbf{Q}^2}} \right| \\ &+ \left| \frac{\hat{\varepsilon}(\varepsilon, \mathbf{Q}, \sqrt{\frac{a}{c}\varepsilon^2 + \frac{b}{c}\mathbf{Q}^2} + y) - \hat{\varepsilon}(\varepsilon, \mathbf{Q}, \sqrt{\frac{a}{c}\varepsilon^2 + \frac{b}{c}\mathbf{Q}^2} + \tilde{y})}{2\tilde{c}\sqrt{\frac{a}{c}\varepsilon^2 + \frac{b}{c}\mathbf{Q}^2}} \right|. \end{aligned}$$

For the first term we write

$$\left| \frac{(y + \tilde{y})(\tilde{y} - y)}{2\sqrt{\frac{a}{c}\varepsilon^2 + \frac{b}{c}\mathbf{Q}^2}} \right| \leq C\eta\varepsilon^{\frac{1}{2}}|\tilde{y} - y|.$$

As for the second term we split it into two parts

$$\hat{\varepsilon}(\varepsilon, \mathbf{Q}, \sqrt{\frac{a}{c}\varepsilon^2 + \frac{b}{c}\mathbf{Q}^2} + y) - \hat{\varepsilon}(\varepsilon, \mathbf{Q}, \sqrt{\frac{a}{c}\varepsilon^2 + \frac{b}{c}\mathbf{Q}^2} + \tilde{y}) = T_1(\varepsilon, \mathbf{Q}, \tilde{y}, y) + T_2(\varepsilon, \mathbf{Q}, \tilde{y}, y)$$

with

$$T_1(\varepsilon, \mathbf{Q}, \tilde{y}, y) = \int_0^1 \frac{(1-\theta)^2}{2!} \left[D^3\psi(\beta(\theta, \varepsilon, \mathbf{Q}, y)) - D^3\psi(\beta(\theta, \varepsilon, \mathbf{Q}, \tilde{y})) \right] [v(\varepsilon, \mathbf{Q}, y)]^3 d\theta$$

where

$$\beta(\theta, \varepsilon, \mathbf{Q}, y) = \left(\theta \varepsilon, Q_4 + \theta \mathbf{Q}, \theta \left(\sqrt{\frac{a}{\varepsilon} \varepsilon^2 + \frac{\tilde{b}}{\varepsilon} \mathbf{Q}^2} + y + d \mathbf{Q} \right) \right), \quad v(\varepsilon, \mathbf{Q}, y) = \begin{pmatrix} \varepsilon \\ \mathbf{Q} \\ \sqrt{\frac{a}{\varepsilon} \varepsilon^2 + \frac{\tilde{b}}{\varepsilon} \mathbf{Q}^2 + y + d \mathbf{Q}} \end{pmatrix}$$

and

$$T_2(\varepsilon, \mathbf{Q}, \tilde{y}, y) = \int_0^1 \frac{(1-\theta)^2}{2!} \left(D^3 \psi_{\beta(\theta, \varepsilon, \mathbf{Q}, \tilde{y})} [v(\varepsilon, \mathbf{Q}, y)]^3 d\theta - D^3 \psi_{\beta(\theta, \varepsilon, \mathbf{Q}, \tilde{y})} [v(\varepsilon, \mathbf{Q}, \tilde{y})]^3 \right) d\theta.$$

According to Remark 4.6.6 and (4.6.23) one has that $\partial_y D^3 \psi$ is continuous. This implies by virtue of the mean value theorem that

$$\begin{aligned} |T_1(\varepsilon, Q, \tilde{y}, y)| &\leq C|y - \tilde{y}|(\varepsilon^3 + |\mathbf{Q}|^3 + |y|^3) \\ &\leq C|y - \tilde{y}|(\varepsilon^3 + \eta^3 \varepsilon^{\frac{5}{2}} + \eta^3 \varepsilon^{\frac{9}{2}}) \\ &\leq C|y - \tilde{y}|(\varepsilon^3 + \eta^3 \varepsilon^{\frac{5}{2}}). \end{aligned}$$

For the term T_2 we use the multi-linear structure of $D^3 \psi$ which gives

$$\begin{aligned} |T_2(\varepsilon, Q, \tilde{y}, y)| &\leq C(\varepsilon^2 + \mathbf{Q}^2 + y^2)|y - \tilde{y}| \\ &\leq C(\varepsilon^2 + \eta^2 \varepsilon^{\frac{5}{3}})|y - \tilde{y}|. \end{aligned}$$

Finally, we have the following inequality, since $\varepsilon, \eta \in [0, 1]$,

$$\begin{aligned} |G(Q, y) - G(Q, \tilde{y})| &\leq C|y - \tilde{y}|(\varepsilon^3 + \eta^3 \varepsilon^{\frac{5}{2}} + \eta^2 \varepsilon^{\frac{5}{3}}) \\ &\leq C|y - \tilde{y}|(\varepsilon^3 + \eta^2 \varepsilon^{\frac{5}{3}}). \end{aligned}$$

For the choice of η made before in (4.6.45), it suffices to fix ε_0 such that

$$C(\varepsilon_0^3 + \eta^2 \varepsilon_0^{\frac{5}{3}}) < 1$$

in order to guarantee that G is a contraction and hence admits a unique fixed point $y(\mathbf{Q}) \in \overline{B}_{\eta \varepsilon^{\frac{3}{2}}}$. The continuity dependence with respect to \mathbf{Q} is classical and follows from the fixed point theorem with a parameter. This achieves the proof of the lemma. \square

Therefore equation (4.6.43) admits a solution in the form

$$X = X_+(\mathbf{Q}) = \sqrt{\frac{a}{\tilde{c}} \varepsilon^2 + \frac{\tilde{b}}{\tilde{c}} \mathbf{Q}^2 + y(\mathbf{Q})}.$$

Reproducing the same analysis we can prove that the equation (4.6.43) admits another solution of the form

$$X_-(\mathbf{Q}) = -\sqrt{\frac{a}{\tilde{c}} \varepsilon^2 + \frac{\tilde{b}}{\tilde{c}} \mathbf{Q}^2 + \hat{y}(\mathbf{Q})}, \quad \hat{y}(\mathbf{Q}) \in \overline{B}_{\eta \varepsilon^{\frac{3}{2}}}.$$

It remains only to check that the curves $\mathbf{Q} \in \overline{B}_{\eta \varepsilon^{\frac{5}{6}}} \mapsto X_{\pm}$ are disjoint graphs. For this we write, by the triangular inequality,

$$\begin{aligned} |X_+(\mathbf{Q}) - X_-(\mathbf{Q})| &\geq 2\sqrt{\frac{a}{\tilde{c}} \varepsilon^2 + \frac{\tilde{b}}{\tilde{c}} \mathbf{Q}^2} - (|y(\mathbf{Q})| + |\hat{y}(\mathbf{Q})|) \\ &\geq C(|\varepsilon| - 2\eta|\varepsilon|^{\frac{3}{2}}) \\ &> C\varepsilon \end{aligned}$$

if ε is small enough. Coming back to the initial unknowns, we find two disjoint curves of solutions to equation (4.6.42). The proof of Theorem 4.6.5 is now complete. \square

4.7 Conclusions

In this paper we have described both numerically and analytically the bifurcation structure of two-fold and three-fold symmetric singly-connected vortex patch equilibria for the Quasi-Geostrophic Shallow-Water equations. The numerical results reveal that the branch of solutions for two-fold symmetric equilibria, consisting of a main branch of Kirchhoff elliptical vortices and secondary branches bifurcating at the Love instability points for the Euler equations, likely separates into an infinite set of disjoint branches for any finite value of the Rossby deformation length ε^{-1} . This is confirmed for $\varepsilon \ll 1$ by mathematical analysis for the first separation near the Love instability point for elliptical azimuthal wavenumber $m = 4$.

The numerical results for the three-fold symmetric equilibria also reveal a separated branch, in this case existing for all ε . The mathematical analysis confirms that solutions exist for small ε near the Euler limit ($\varepsilon = 0$); these solutions are near circular in form. The separated solutions are beyond the scope of this analysis. In a future work, we will report on the stability and nonlinear evolution of these solutions.

Acknowledgements. DGD received support for this research from the UK Engineering and Physical Sciences Research Council (grant number EP/H001794/1). TH is partially supported by the the ANR project Dyficolti ANR-13-BS01-0003- 01.

Bibliography

- [1] H. Aref. Point vortex dynamics: A classical mathematics playground. *Journal of Mathematical Physics*, 48(6):065401, 2007.
- [2] H. Aref and R. Hansen. Relative equilibria of point vortices. 2008.
- [3] H. Aref, P. K. Newton, M.A. Stremler, T. Tokieda, and D.L. Vainchtein. Vortex crystals. volume 39 of *Advances in Applied Mechanics*, pages 1 – 79. Elsevier, 2003.
- [4] A. Bertozzi and A. Majda. Vorticity and incompressible flow. 2002.
- [5] Tristan Buckmaster, Steve Shkoller, and Vlad Vicol. Nonuniqueness of weak solutions to the sqg equation. 10 2016.
- [6] J. Burbea. Motions of vortex patches. *Lett. Math. Phys.*, 6(1):1–16, 1982.
- [7] A. Castro, D. Córdoba, and J. Gomez-Serrano. Existence and regularity of rotating global solutions for the generalized surface quasi-geostrophic equations. *Duke Math. J.*, 165(5):935–984, 2016.
- [8] A. Castro, D. Córdoba, and J. Gomez-Serrano. Uniformly rotating analytic global patch solutions for active scalars. *Ann. PDE*, 2(1):Art.1, 34pp, 2016.
- [9] A. Castro, D. Córdoba, and J. Gómez-Serrano. Uniformly rotating smooth solutions for the incompressible 2D Euler equations. *ArXiv e-prints*, 2016.
- [10] C. CERRETELLI and C. H. K. WILLIAMSON. A new family of uniform vortices related to vortex configurations before merging. *Journal of Fluid Mechanics*, 493:219–229, 2003.
- [11] D. Chae, P. Constantin, D. Córdoba, F. Gancedo, and J. Wu. Generalized surface quasi- geostrophic equations with singular velocities. *Comm. Pure Appl. Math.*, 65(8):1037–1066, 2012.
- [12] E. Charpentier and E. Ghys. *L'héritage scientifique de Poincaré*. Échelles. Humensis, 2015.
- [13] J-Y. Chemin. Perfect incompressible fluids. 1998.
- [14] P. Constantin, A.J. Majda, and E Tabak. Formation of strong fronts in the 2-d quasigeostrophic thermal active scalar. *Nonlinearity*, 7(6):1495–1533, 1994.
- [15] D. Córdoba, M.A. Fontelos, A.M. Mancho, and J.L. Rodrigo. *Evidences of singularities for a family of contour dynamics equations*, volume 102. 2005.
- [16] M.G. Crandall and P.H. Rabinowitz. Bifurcation from simple eigenvalues. *J. of Func. Analysis*, 8:321–340, 1971.
- [17] G.S. Deem and N.J. Zabusky. Vortex waves: Stationnary "v-states", interactions, recurrence, and breaking. *Phys. Rev. Lett.*, 40(13):859–862, 1978.

- [18] David Dritschel. Contour dynamics and contour surgery: Numerical algorithms for extended, high-resolution modelling of vortex dynamics in two-dimensional, inviscid, incompressible flows. 10:77–146, 08 1989.
- [19] David G. Dritschel. The nonlinear evolution of rotating configurations of uniform vorticity. *Journal of Fluid Mechanics*, 172:157–182, 1986.
- [20] David G Dritschel. Contour surgery: A topological reconnection scheme for extended integrations using contour dynamics. *Journal of Computational Physics*, 77(1):240 – 266, 1988.
- [21] David G. Dritschel. A general theory for two-dimensional vortex interactions. *Journal of Fluid Mechanics*, 293:269–303, 1995.
- [22] D Durkin and J Fajans. Experiments on two-dimensional vortex patterns. 12:289–293, 02 2000.
- [23] T.M. Elgindi and I.-J. Jeong. Symmetries and Critical Phenomena in Fluids. *ArXiv e-prints*, 2016.
- [24] G.R. Flierl and L.M. Polvani. Generalized kirchhoff vortices. *Phys. Fluids*, 29:2376– 2379, 1986.
- [25] T.H. Havelock F.R.S. Lii. the stability of motion of rectilinear vortices in ring formation. *The London, Edinburgh, and Dublin Philosophical Magazine and Journal of Science*, 11(70):617–633, 1931.
- [26] F. Gancedo. Existence for the α -patch model and the qg sharp front in sobolev spaces. *Adv. MATH*, 217(6):2569–2598, 2008.
- [27] S. Garner, I. Held, R. Pierrehumbert, and K. Swanson. Surfaces quasi-geostrophic dynamics. *J. Fluid Mech.*, 282(120), 1995.
- [28] M. Golubitsky and D. Schaeffer. Imperfect bifurcation in the presence of symmetry. *Comm. Math. Phys.*, 67(3):205–232, 1979.
- [29] Z. Hassainia and T. Hmidi. On the v -states for the generalized quasi-geostrophic equations. *Comm. Math. Phys.*, 337(1):321–377, 2015.
- [30] Z. Hassainia, T. Hmidi, and F. de la Hoz. Doubly connected v -states for the generalized quasi-geostrophic equations. *Arch. Ration. Mech. Anal.*, 220(3):1209–1281, 2016.
- [31] Z. Hassainia, N. Masmoudi, and M.H. Wheeler. Uniformly rotating smooth solutions for the incompressible 2D Euler equations. *ArXiv e-prints*, 2016.
- [32] H. Helmholtz. Lxiii. on integrals of the hydrodynamical equations, which express vortex-motion. *The London, Edinburgh, and Dublin Philosophical Magazine and Journal of Science*, 33(226):485–512, 1867.
- [33] T. Hmidi, F. de la Hoz, J. Mateu, and J. Verdera. Doubly connected v -states for the planar euler equations. *SIAM J. Math. Anal.*, 48(3):1892–1928, 2016.
- [34] T. Hmidi and J. Mateu. Bifurcation of rotating patches from Kirchhoff vortices. *Discrete and Continuous Dynamical Systems - Series A*, 36(10):5401–5422, 2016. 21 pages.
- [35] Taoufik Hmidi and Joan Mateu. Degenerate bifurcation of the rotating patches. *Advances in Mathematics*, 302:799–850, 2016.
- [36] Taoufik Hmidi and Joan Mateu. Existence of corotating and counter-rotating vortex pairs for active scalar equations. *Communications in Mathematical Physics*, 350(2):699–747, Mar 2017.
- [37] Taoufik Hmidi, Joan Mateu, and Joan Verdera. Boundary regularity of rotating vortex patches. *Archive for Rational Mechanics and Analysis*, 209(1):171–208, 2013. 31 pages.

- [38] Taoufik Hmidi, Joan Mateu, and Joan Verdera. On rotating doubly connected vortices. *Journal of Differential Equations*, 258(4):1395–1429, 2015. 30 pages.
- [39] M. Juckes. Quasigeostrophic dynamics of the tropopause. *J. Atmos. Sci.*, pages 2756–2768, 1994.
- [40] J.R. Kamm. Shape and stability of two-dimensional uniform vorticity regions. 1987.
- [41] J.R. Kamm. Shape and stability of two-dimensional uniform vorticity regions. 1987.
- [42] H. Kielhofer. *Bifurcation Theory : An introduction with Applications to Partial Differential Equations*. Springer, 2011.
- [43] G. Kirchhoff. *Vorlesungen über mathematische Physik*. 1874.
- [44] A. Kiselev, L. Ryzhik, Y. Yao, and A. Zlatoš. Finite time singularity for the modified sqg patch equation. *Annals of mathematics*, 184:909–948, 2016.
- [45] P. Klein and G. Lapeyre. Dynamics of upper oceanic layers in terms of surface quasigeostrophic theory. *J. Phys. Oceanogr.*, 36:165–176, 2006.
- [46] H. Lamb. *Hydrodynamics*. Dover Publications, 1945.
- [47] Ping Liu, Junping Shi, and Yuwen Wang. Imperfect transcritical and pitchfork bifurcations. *Journal of Functional Analysis*, 251(2):573 – 600, 2007.
- [48] A. E. H. Love. On the stability of certain vortex motions. *Proceedings of the London Mathematical Society*, s1-25(1):18–43, 1893.
- [49] Paolo Luzzatto-Fegiz and Charles H. K. Williamson. Stability of elliptical vortices from “imperfect–velocity–impulse” diagrams. 24:181–188, 03 2010.
- [50] Paolo Luzzatto-Fegiz and Charles H.K. Williamson. An efficient and general numerical method to compute steady uniform vortices. *Journal of Computational Physics*, 230(17):6495 – 6511, 2011.
- [51] Fabien Marchand. Existence and regularity of weak solutions to the quasi-geostrophic equations in the spaces L^p or $\dot{H}^{-\frac{1}{2}}$. *Communications in Mathematical Physics*, 277(1):45–67, Jan 2008.
- [52] PK Newton. The n-vortex problem: Analytical techniques. vol. 145 of *appl. Math. Sci. Series*. Springer-Verlag, Berlin-Heidelberg-New York, 2001.
- [53] E.A. Overman. Steady-state solutions of the euler equations in two dimensions. ii. local analysis of limiting v-states. *SIAM J. Appl. Math.*, 46:765– 800, 1986.
- [54] J. Pedlosky. *Geophysical Fluid Dynamics*. Springer study edition. Springer New York, 1992.
- [55] Hanna Plotka and David G. Dritschel. Quasi-geostrophic shallow-water doubly-connected vortex equilibria and their stability. *Journal of Fluid Mechanics*, 723:40–68, 2013.
- [56] Hanna Plotka and David G. Dritschel. Quasi-geostrophic shallow-water doubly-connected vortex equilibria and their stability. *Journal of Fluid Mechanics*, 723:40–68, 2013.
- [57] L. M. Polvani, N. J. Zabusky, and G. R. Flierl. Two-layer geostrophic vortex dynamics. part 1. upper-layer v-states and merger. *Journal of Fluid Mechanics*, 205:215–242, 1989.
- [58] L. M. Polvani, N. J. Zabusky, and G. R. Flierl. Two-layer geostrophic vortex dynamics. part 1. upper-layer v-states and merger. *Journal of Fluid Mechanics*, 205:215–242, 1989.
- [59] Lorenzo Polvani. Geostrophic vortex dynamics. page 225, 10 1988.

- [60] Christian Pommerenke. Boundary Behaviour of Conformal Maps (Grundlehren der mathematischen Wissenschaften). Springer, 2010.
- [61] S.G. Resnick. Dynamical Problems in Non-linear Advection Partial Differential Equations. University of Chicago, Department of Mathematics, 1995.
- [62] José Luis Rodrigo. On the evolution of sharp fronts for the quasi-geostrophic equation. Communications on Pure and Applied Mathematics, 58(6):821–866, 2005.
- [63] P. G. Saffman. Vortex Dynamics (Cambridge Monographs on Mechanics). Cambridge University Press, 2012.
- [64] Javier Segura. Bounds for ratios of modified bessel functions and associated turán-type inequalities. Journal of Mathematical Analysis and Applications, 374(2):516 – 528, 2011.
- [65] Junping Shi. Persistence and bifurcation of degenerate solutions. Journal of Functional Analysis, 169(2):494 – 531, 1999.
- [66] Joseph John Thomson. A Treatise on the Motion of Vortex Rings: an essay to which the Adams prize was adjudged in 1882, in the University of Cambridge. Macmillan, 1883.
- [67] G. K. Vallis. Atmospheric and Oceanic Fluid Dynamics. Cambridge University Press, Cambridge, U.K., 2006.
- [68] Stefan E. Warschawski. On the higher derivatives at the boundary in conformal mapping. Transactions of the American Mathematical Society, 38(2):310–340, 1935.
- [69] G. N. Watson. A Treatise on the Theory of Bessel Functions (Cambridge Mathematical Library). Cambridge University Press, 1995.
- [70] Jiahong Wu. Solutions of the 2d quasi-geostrophic equation in holder spaces. Nonlinear Analysis: Theory, Methods Applications, 62(4):579 – 594, 2005.
- [71] E. J. Yarmchuk, M. J. V. Gordon, and R. E. Packard. Observation of stationary vortex arrays in rotating superfluid helium. Phys. Rev. Lett., 43:214–217, Jul 1979.
- [72] V.I. Yudovich. Non-stationary flow of an ideal incompressible liquid. USSR Computational Mathematics and Mathematical Physics, 3(6):1407 – 1456, 1963.

RÉSUMÉ

Dans cette thèse, on s'est intéressé à la dynamique des poches de tourbillon pour des équations issues de la mécanique des fluides posées dans le plan. La thèse est composée de trois partie indépendantes. Un des objectifs est d'établir l'existence des tourbillons uniformément concentrés et rigides, c-à-d, qui ne se déforment pas lors de l'évolution. Nous analysons deux configurations liées à la nature topologique du support: poches simplement et doublement connexes. Nos solutions sont obtenues via des techniques de bifurcations et d'analyse complexe. Le deuxième objectif est d'obtenir des précisions sur la structure globale du diagramme de bifurcation et sa réponse vis-à-vis des petites perturbations dans le modèle.

Plus précisément, dans le deuxième chapitre on prouve l'existence de V-states doublement connexes dans un voisinage de l'anneau pour le modèle des surfaces quasi-géostrophique. On montre que l'on peut construire des branches de solutions qui sont des anneaux perturbés pour certaines valeurs explicites de vitesses angulaires qui sont liées aux fonctions hypergéométriques de Gauss et aux fonctions de Bessel.

Le troisième chapitre porte sur l'étude de la structure du diagramme de bifurcation dans le cas doublement connexes pour l'équation d'Euler. Numériquement, près d'un cas dégénéré, les deux branches issues des deux vitesses angulaires possibles semblaient se rejoindre pour former un lacet. Nous avons prouvé analytiquement ce résultat.

Le quatrième chapitre porte sur le modèle shallow water quasi-géostrophique. Dans une première partie, on prouve l'existence de V-states simplement connexes dans un voisinage du tourbillon de Rankine pour un nombre dénombrable de vitesses angulaires liées aux fonctions de Bessels modifiées. La deuxième partie porte sur la réponse du diagramme de bifurcation lorsque l'on fait varier un paramètre du modèle. On montre en particulier qu'une singularité présente lors d'un cas limite est éclatée. Notre étude analytique a été complétée par des simulations numériques portant sur les V-states limites pour les symétries deux et trois.

ABSTRACT

In this dissertation, we are concerned with the vortex dynamics for some equations arising in fluid mechanics. We distinguish three independent parts. One of the objectives is to prove the existence of uniformly concentrated rigid vortices, they do not change their shapes during the motion. We examine two configurations related to the topological nature of the support: simply and doubly connected vortex patches. Our solutions are obtained using bifurcation arguments and complex analysis tools. The second objective is to obtain some precisions on the global structure of the bifurcation diagram and "its response to small perturbations.

More precisely, in the second chapter we prove the existence of doubly connected V-states in a neighborhood of the annulus for the surface quasi-geostrophic model. We check that we can construct some branches of solutions which are perturbated annulus at some angular velocities related to hypergeometric Gauss functions and Bessel functions.

The goal of the third chapter is to study the structure of the bifurcation diagram in the doubly connected case for Euler equations. Numerically, close to a degenerate case, the two branches of solutions come from the two angular velocities seems to merge to form a loop. We prove analytically this result.

In the last chapter, we focus on the shallow quasi-geostrophic model. In the first part, we prove the existence of the simply V-states in a neighborhood of the Rankine Vortices for a countable number of angular velocities related to modified Bessel functions. In the second part, we study the reaction of the diagram bifurcation for small perturbations of the parameter. In particular, we prove that some singularities are broken due to a resonance phenomenon. Our analytical study is completed by numerical simulations on the limiting V-states for the two and three fold symmetries.